

SCIENTIFIC REPORTS



OPEN

Synthetic small molecule GLP-1 secretagogues prepared by means of a three-component indole annulation strategy

Received: 11 January 2016

Accepted: 13 June 2016

Published: 29 June 2016

Oleg G. Chepurny¹, Colin A. Leech¹, Martin Tomanik², Maria C. DiPoto², Hui Li², Xinping Han^{2,†}, Qinghe Meng³, Robert N. Cooney³, Jimmy Wu² & George G. Holz^{1,4}

Rational assembly of small molecule libraries for purposes of drug discovery requires an efficient approach in which the synthesis of bioactive compounds is enabled so that numerous structurally related compounds of a similar basic formulation can be derived. Here, we describe (4 + 3) and (3 + 2) indole annulation strategies that quickly generate complex indole heterocycle libraries that contain novel cyclohepta- and cyclopenta[*b*]indoles, respectively. Screening of one such library comprised of these indoles identifies JWU-A021 to be an especially potent stimulator of glucagon-like peptide-1 (GLP-1) secretion *in vitro*. Surprisingly, JWU-A021 is also a potent stimulator of Ca²⁺ influx through TRPA1 cation channels (EC₅₀ ca. 200 nM), thereby explaining its ability to stimulate GLP-1 release. Of additional importance, the available evidence indicates that JWU-A021 is one of the most potent non-electrophilic TRPA-1 channel agonists yet to be reported in the literature.

The indole heterocycle is among the most important nitrogen-containing heterocycles in both medicine and the broader spectrum of biologically active compounds. Indeed, it prominently occupies a spot in the top 10 most frequently occurring nitrogen heterocycles of FDA approved drugs in the US¹. The significance of indole is further underscored by the fact that it is also the side-chain of L-tryptophan, one of only 21 proteinogenic amino acids found in eukaryotes. It is perhaps not surprising then that a subset of the indole motif, cycloalka[*b*]indoles, has garnered considerable attention from pharmaceutical and biotechnology companies as a promising pharmacophore for new drugs. In 2012, our group reported a novel (4 + 3) strategy for preparing cyclohepta[*b*]indoles in a single chemical transformation by means of a three-component annulation reaction beginning with an indole, a carbonyl, and a diene². Because each of the starting materials can be independently varied, it was possible to quickly produce a large library of these compounds. Density functional theory (DFT) calculations suggested that the reaction proceeds through a step-wise mechanism, rather than a concerted, pericyclic 6πe⁻ process. No longer constrained by the Woodward-Hoffmann selection rules that govern pericyclic transformations, we then extended the methodology to include (3 + 2) annulation reactions in which the dienes were substituted by styrenyl substrates (total 4πe⁻) to furnish cyclopenta[*b*]indoles.

These theoretical considerations prompted us to investigate if cyclohepta[*b*]indole libraries could be screened to allow the identification of small molecules with biologically significant properties. To achieve proof of concept, we evaluated the capacity of cyclohepta[*b*]indoles to act as glucagon-like peptide-1 (GLP-1) secretagogues. GLP-1 is synthesized and secreted from intestinal L-cells, and it is the prototype of a new class of blood glucose-lowering agents that are now in use for the treatment of type 2 diabetes mellitus (T2DM)³. In this manuscript we report: **1)** for the first time our findings on the (3 + 2) methodology, **2)** expanded substrate scope for the (4 + 3) annulation, **3)** the identification of one of these compounds, JWU-A021, as a potent GLP-1 secretagogue, and **4)** experimental evidence indicating that JWU-A021 likely operates in the intestinal L-cells by elevating the intracellular [Ca²⁺] by means of activating the Transient Receptor Potential Ankyrin 1 channel (TRPA1)⁴.

¹Department of Medicine, State University of New York (SUNY), Upstate Medical University, Syracuse, New York, USA. ²Department of Chemistry, Dartmouth College, Hanover, New Hampshire, USA. ³Department of Surgery, State University of New York (SUNY), Upstate Medical University, Syracuse, New York, USA. ⁴Department of Pharmacology, State University of New York (SUNY), Upstate Medical University, Syracuse, New York, USA. [†]Present address: Department of Biochemistry, UT Southwestern, Dallas TX 75390, USA. Correspondence and requests for materials should be addressed to J.W. (email: jimmy.wu@dartmouth.edu) or G.G.H. (email: holzg@upstate.edu)

Cycloalka[b]indoles

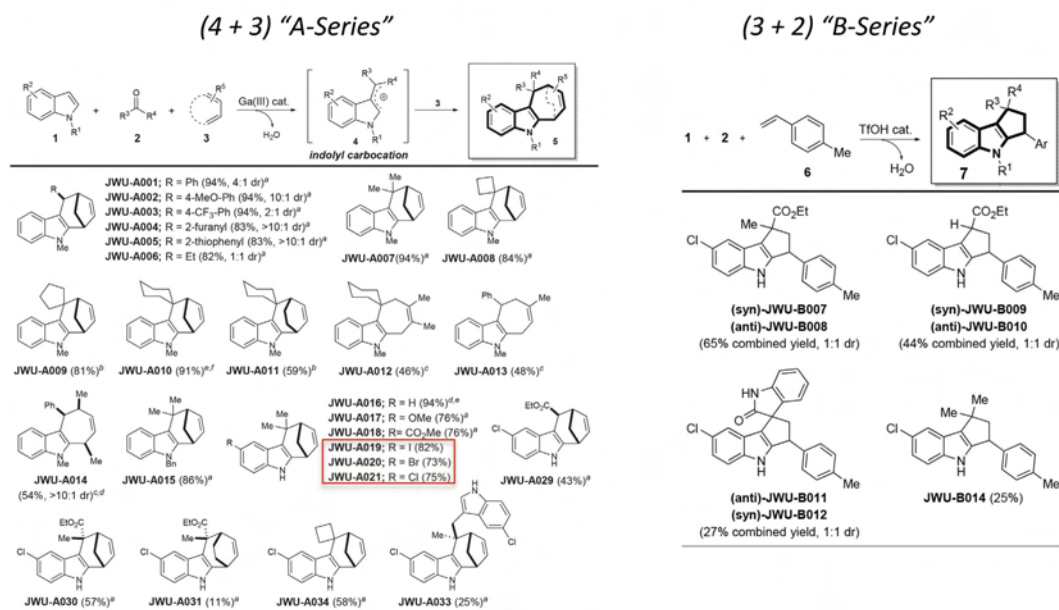


Figure 1. Cyclohepta[b]indole synthesis by (4 + 3) and (3 + 2) cycloaddition reactions. (Left panel)

"A-Series" heterocyclics generated by (4 + 3) cycloaddition reactions. ^aindole (1 equiv), carbonyl (2 equiv), diene (5 equiv), GaBr₃ (10 mol%), rt. ^bindole (1 equiv), carbonyl (2 equiv), diene (5 equiv), Ga(OTf)₃ (10 mol%), rt. ^cindole (1 equiv), carbonyl (1.1 equiv), diene (5 equiv), Ga(OTf)₃ (20 mol%), rt. ^dSingle-crystal X-ray analysis. ^e2 mmol scale. **(Right panel)** "B-Series" heterocyclics generated by (3 + 2) cycloaddition reactions. ^aindole (1 equiv), carbonyl (2 equiv), diene (1.5 equiv), TfOH (20 mol%), rt.

Results

Identification of cyclohepta[b]indoles with GLP-1 releasing actions.

Using a three-component (4 + 3) annulation methodology developed by one of our groups (see Supplemental Material)², we generated a library of cyclohepta[b]indoles (Fig. 1, left panel). These products were screened for their capacity to stimulate GLP-1 release from mouse STC-1 intestinal enteroendocrine cells⁵⁻⁷. Three cyclohepta[b]indoles with GLP-1 releasing properties were identified, each of which contain either I, Br, or Cl substitutions that append an identical core structure. These "A-Series" compounds include JWU-A019, JWU-A020, and JWU-A021 (red box, Fig. 1, left panel), each of which dose-dependently stimulated GLP-1 release by ca. 2-fold over baseline (Fig. 2a-c), with JWU-A021 being the most potent (EC₅₀ 1.9 μM). Surprisingly, the GLP-1 secretagogue action of JWU-A021 was reduced by the selective TRPA1 cation channel blockers A967079, AP-18, and HC030031 (Fig. 2d-g). This finding indicated that JWU-A021 might be a TRPA1 cation channel activator. In fact, JWU-A021 raised the [Ca²⁺]_i in fura-2 loaded STC-1 cell monolayers (Fig. 3a). Furthermore, this Ca²⁺-elevating action of JWU-A021 (EC₅₀ ca. 200 nM) was abrogated by the TRPA1 channel blockers A967079 and HC030031 (Fig. 3b,c). Consistent with prior reports that TRPA1 channels are expressed in STC-1 cells^{8,9}, and that TRPA1 channel activation leads to GLP-1 secretion from this cell line⁹, the established TRPA1 channel activator allyl isothiocyanate (AITC) raised the [Ca²⁺]_i, and this effect was abrogated by A967079 (Fig. 3d). Since an increase of [Ca²⁺]_i triggers GLP-1 release from intestinal L-cells¹⁰, and since L-cells express TRPA1 channels⁹, these findings indicated that JWU-A021 might serve as the prototype of a new class of small molecule GLP-1 secretagogues with TRPA1 channel activating properties.

Structure-function properties of the A-Series of cyclohepta[b]indoles.

Although JWU-A021 contains a chlorine substitution (Fig. 1, left panel), this halogenation was not essential to its biological activity since the non-halogenated indole JWU-A016 also exerted a dose-dependent stimulatory effect to raise the [Ca²⁺]_i (Fig. 3e). Other compounds of the A-series designated as JWU A029 through A034 (see Fig. 1, left panel) were considerably less potent (EC₅₀ > 3 μM) in this assay (Fig. 3f) despite their structural similarity to JWU-A021. Furthermore, for JWU-A021, the dextrorotatory enantiomer (+)-(6R,9S)-JWU-A021¹¹ stimulated a larger increase of [Ca²⁺]_i in comparison to the levorotatory enantiomer (-)-(6S,9R)-JWU-A021¹¹ (Fig. 4a,b), whereas racemic JWU-A021 exerted a stimulatory effect that was intermediate between that of the dextrorotatory and levorotatory enantiomers (Fig. 4c,d).

The A-Series of cyclohepta[b]indoles derived by the (4 + 3) annulation methodology (Fig. 1, left panel) were then compared with a B-series of cyclopenta[b]indoles derived by a (3 + 2) annulation methodology (see Fig. 1, right panel). These B-series compounds (JWU B007 through B014) were obtained by modifying the annulation reaction so that the Lewis acid catalyst GaBr₃ was replaced with 20 mol% of TfOH (see Supplemental Material). When the B-series compounds were evaluated in the fura-2 assay using STC-1 cells, they were established to

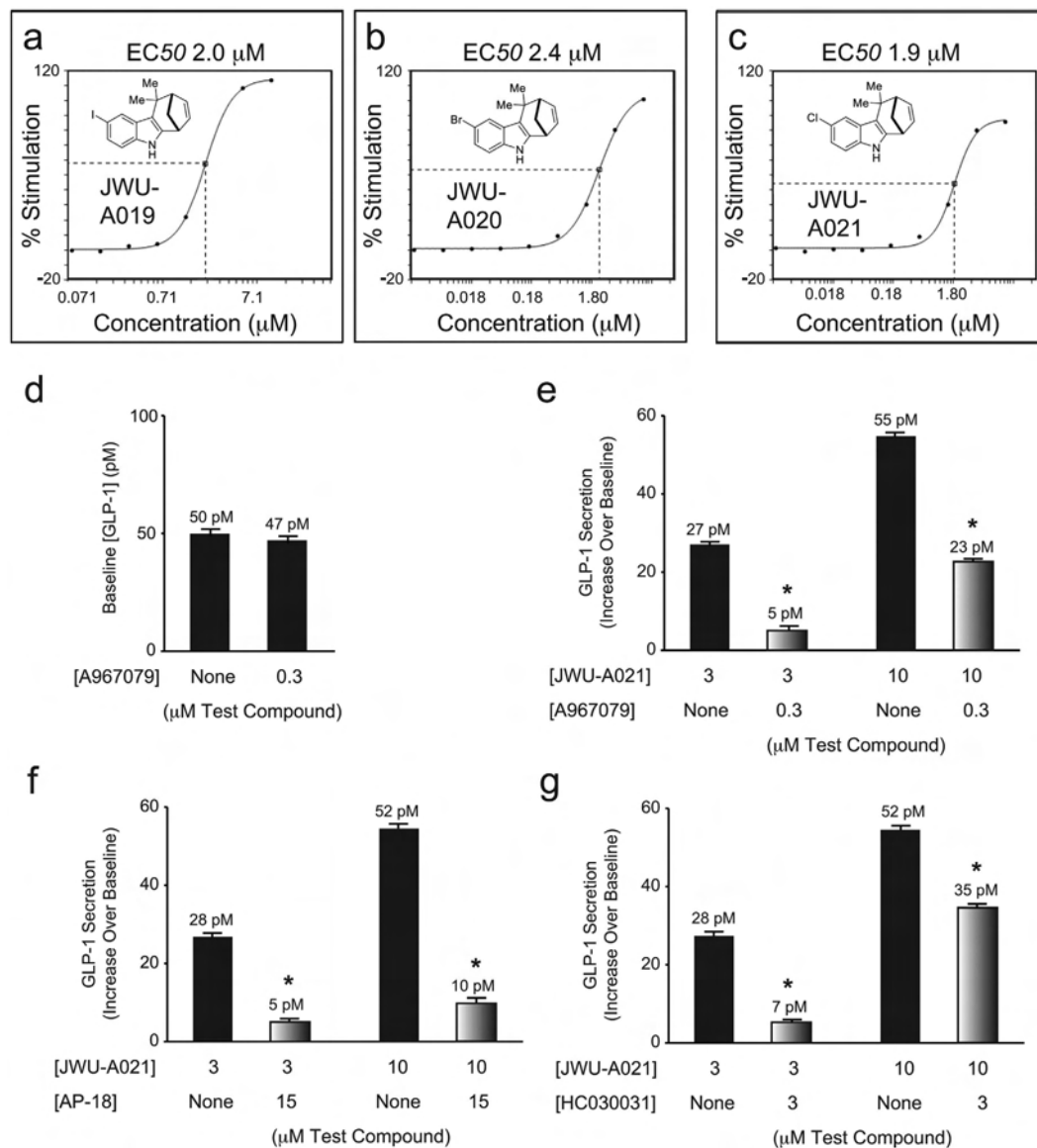


Figure 2. Cyclohepta[b]indole-stimulated GLP-1 release: effects of TRPA1 channel blockers. (a–c) JWU-A019, JWU-A020, and JWU-A021 stimulated GLP-1 secretion from STC-1 cells. (d) Basal GLP-1 secretion was not significantly altered by A967079. (e–g) GLP-1 secretion stimulated by JWU-A021 was reduced by A967079, AP-18, and HC030031. Data are the mean + s.d. of $N = 3$ independent experiments (* $p < 0.05$; paired t test).

be especially weak Ca^{2+} elevating agents such that a test concentration of $10 \mu\text{M}$ was necessary to detect any increase of $[\text{Ca}^{2+}]_i$ (data not shown). In summary, these findings demonstrated that there existed a clear structural specificity for cycloalka[b]indoles as Ca^{2+} -elevating agents in STC-1 cells. The A-Series cyclohepta[b]indole JWU-A021 was bioactive at nM concentrations, whereas all B-series cyclopenta[b]indoles were ineffective.

JWU-A021 activates TRPA1 channels to promote Ca^{2+} influx. We next sought to identify the molecular target that mediates the action of JWU-A021 to stimulate an increase of $[\text{Ca}^{2+}]_i$ in STC-1 cells. Initially, we found that the Ca^{2+} -elevating action of JWU-A021 was blocked by inclusion of La^{3+} in the standard extracellular saline (SES) (Fig. 5a). This finding is significant because La^{3+} blocks Ca^{2+} entry through non-selective cation channels (NSCCs) and voltage-dependent Ca^{2+} channels (VDCCs)^{4,12}. We also found that JWU-A021 failed to stimulate an increase of the $[\text{Ca}^{2+}]_i$ when the extracellular $[\text{Ca}^{2+}]$ was lowered from 2.6 mM to 100 nM (Fig. 5b). This finding is expected if JWU-A021 promotes Ca^{2+} influx rather than Ca^{2+} mobilization from intracellular Ca^{2+} stores. Since it might be argued that Ca^{2+} stores were simply depleted under conditions in which the SES contained 100 nM Ca^{2+} , we compared the Ca^{2+} mobilizing properties of a purinergic receptor agonist (ATP) under conditions in which the SES contained 2.6 mM Ca^{2+} or 100 nM Ca^{2+} . This control experiment revealed that ATP retained its ability to mobilize Ca^{2+} even when the extracellular Ca^{2+} was set to 100 nM (c.f., Fig. 5c,d). Thus, a depletion of Ca^{2+} stores did not explain why JWU-A021 failed to raise the $[\text{Ca}^{2+}]_i$ when the SES contained

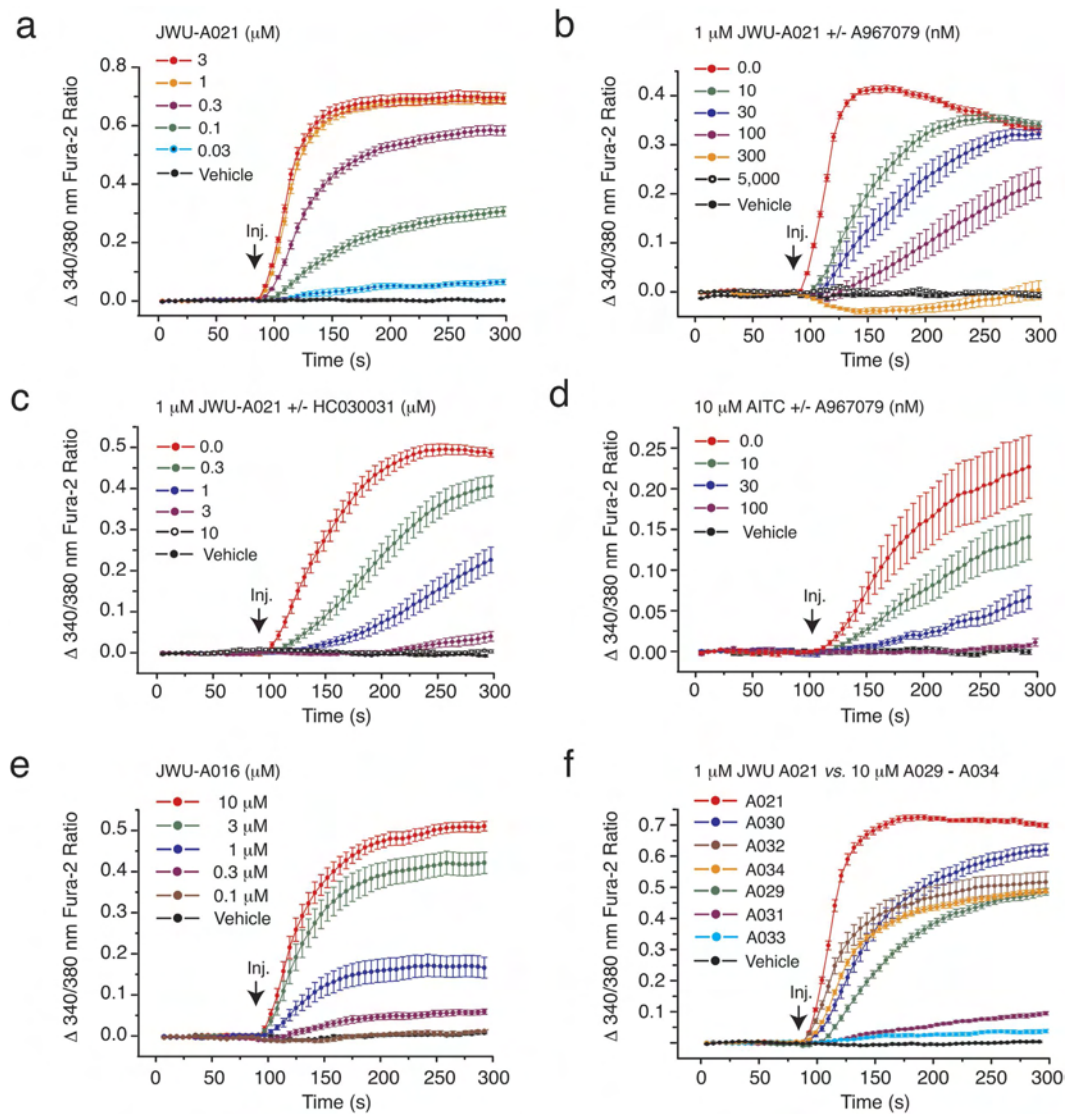


Figure 3. Actions of JWU-A021 and other A-series compounds to increase $[Ca^{2+}]_i$. (a) Fura-2 assays of STC-1 cell monolayers demonstrated the concentration-dependent action of JWU-A021 to increase $[Ca^{2+}]_i$. (b,c) A967079 and HC030031 each exerted concentration-dependent actions to counteract the stimulatory effect of JWU-A021 (1 μ M) in STC-1 cells. (d) The TRPA1 channel activator AITC (10 μ M) increased $[Ca^{2+}]_i$, and this action of AITC was also reduced by A967079 and HC030031 in STC-1 cells. For these panels and subsequent figures, JWU-A021 was administered by bolus injection (Inj.). (e,f) Ca^{2+} -elevating actions of JWU-A016 (e) and the A029-A034 series of test agents (f). For all examples depicted here, the findings are representative of a single experiment repeated a minimum of five times on five different occasions with similar results.

100 nM Ca^{2+} . Instead, the SES containing 100 nM Ca^{2+} failed to support the action of JWU-A021 to promote Ca^{2+} influx.

Ca^{2+} influx stimulated by JWU-A021 might result solely from TRPA1 channel activation since GLP-1 secretion stimulated by JWU-A021 was reduced by TRPA1 channel blockers (Fig. 2d–g). In fact, TRPA1 channels are NSCCs that allow Ca^{2+} permeation⁴. However, it is important to take into account the possibility that binding of JWU-A021 to TRPA1 channels leads to membrane depolarization and action potential generation, thereby stimulating additional Ca^{2+} influx through VDCCs. Therefore, a systematic analysis was performed to evaluate potential effects of selective VDCC blockers¹². Nimodipine, a blocker of L-type VDCCs, slowed the initial increase of $[Ca^{2+}]_i$ measured in response to JWU-A021 (Fig. 5e), but the sustained increase of $[Ca^{2+}]_i$ occurring at the assay's end-point was unaffected (Fig. 5e). As a positive control, we confirmed the ability of nimodipine to suppress the increase of $[Ca^{2+}]_i$ that resulted from 28 mM KCl-induced membrane depolarization (Fig. 5f). Thus, L-type VDCCs played a minor role as mediators of sustained Ca^{2+} influx stimulated by JWU-A021. Since the selective TRPA1 channel blockers A967079 and HC030031 fully abolished all Ca^{2+} -elevating actions of JWU-A021

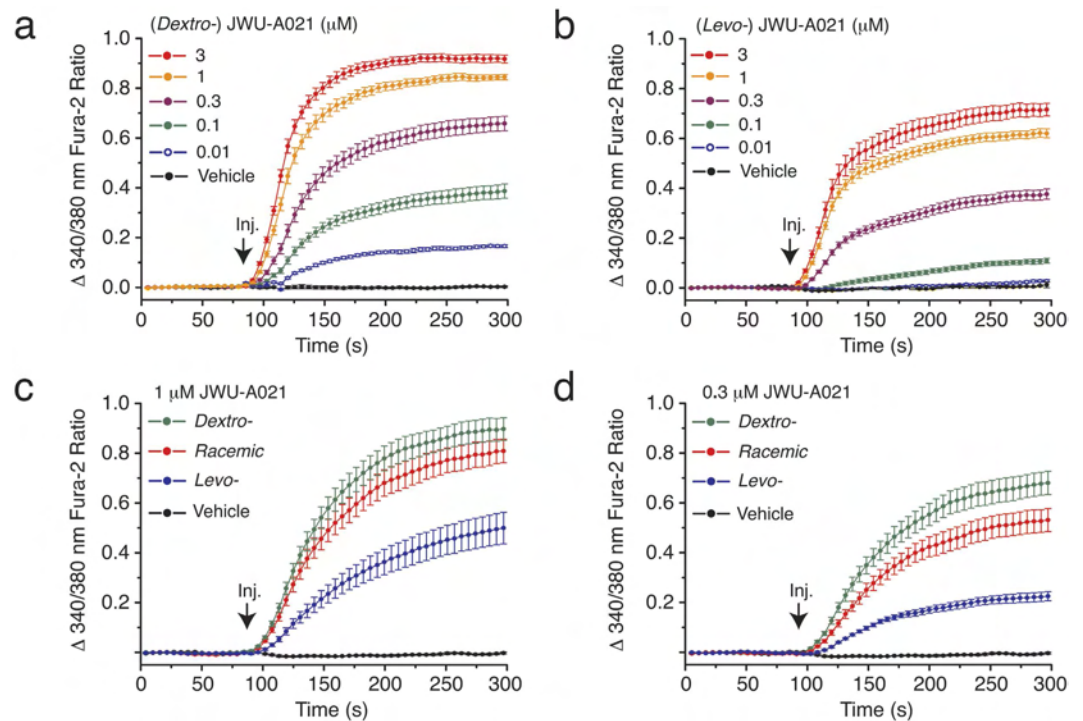


Figure 4. Differential actions of JWU-A021 enantiomers to increase $[Ca^{2+}]_i$. (a,b) The dextrorotatory (*Dextro-*) enantiomer (+)-(6*R*,9*S*)-JWU-A021 exerted a more powerful stimulatory effect in comparison to the levorotatory (*Levo-*) enantiomer (+)-(6*S*,9*R*)-JWU-A021 when it was tested in the fura-2 assay using monolayers of STC-1 cells. (c,d) Differential stimulation of an increase of $[Ca^{2+}]_i$ by the dextrorotatory, levorotatory, and racemic forms of either 1 μ M or 0.3 μ M JWU-A021. For all examples depicted here, the findings are representative of a single experiment that was repeated a minimum of three times on three different occasions with similar results.

(Fig. 3b,c), the increase of $[Ca^{2+}]_i$ measured at the end-point was instead explained by TRPA1 channel activation in response to JWU-A021.

We also tested T-type (kurtoxin, mibefradil), N-type (omega-conotoxin GVIA), and P/Q-type (omega-agatoxin IVA) blockers of VDCCs. None of these agents altered the end-point increase of $[Ca^{2+}]_i$ measured in response to JWU-A021 (data not shown). Using whole-cell patch clamp analysis in the voltage-clamp mode, we then demonstrated that brief focal application of JWU-A021 to STC-1 cells led to the appearance of an inward current when the membrane potential was set to -60 mV (Fig. 6a). By using a ramp stimulus protocol to vary the holding potential, it was established that the current activated by JWU-A021 exhibited outward rectification (Fig. 6a, inset), as is expected for TRPA1 channels⁴. Using RT-PCR analysis, the expression of TRPA1 mRNA in STC-1 cells was confirmed (Fig. 6b). Finally, live-cell imaging demonstrated reversible actions of JWU-A021 to raise the $[Ca^{2+}]_i$ in STC-1 cells (Fig. 6c). This was also the case for HEK-293 cells transfected with a rat TRPA1 cDNA (Fig. 6d). Thus, target validation was achieved in which JWU-A021 was established to be a TRPA1 channel activator.

JWU-A021 retains its ability to activate mutant C622S TRPA1. Electrophiles such as AITC activate TRPA1 channels by covalently modifying cysteine residues located near the cytosolic N-terminus of the channel^{4,13}. Although the structure of JWU-A021 indicates that it is unlikely to act as an electrophile, we sought experimental evidence that this is the case. Thus, the action of JWU-A021 was evaluated in HEK-293 cells transfected with a wild-type (WT) TRPA1, an empty vector (EV), or a mutant (MT) C622S TRPA1 channel that has reduced sensitivity to electrophiles¹⁴. For cells transfected with the WT TRPA1 channel, JWU-A021 stimulated an increase of $[Ca^{2+}]_i$, and this effect was blocked by A967079 (Fig. 7a). However, for cells transfected with the EV, there was no effect of JWU-A021 (Fig. 7b). As a control, we verified that AITC also increased the $[Ca^{2+}]_i$ in cells transfected with the WT TRPA1 channel, but not the EV (Fig. 7c,d), and that this effect of AITC was inhibited by A967079 (Fig. 7c).

Further analysis revealed that the C622S TRPA1 channel was activated by JWU-A021 in a manner nearly identical to that of the WT (Fig. 7e,f). However, the C622S TRPA1 channel responded poorly to AITC (Fig. 7g,h). The reduced AITC sensitivity of the mutant channel is expected since the cysteine 622 residue that is implicated in the control of channel activity, by covalent modification with AITC, is missing in the mutant channel¹⁴. Collectively, such findings provide support for a model in which JWU-A021 acts independently of covalent cysteine modification to activate TRPA1 channels. This model is supported by our single cell imaging studies in which it was demonstrated that the Ca^{2+} -elevating action of JWU-A021 was repeatable and rapidly reversible following wash

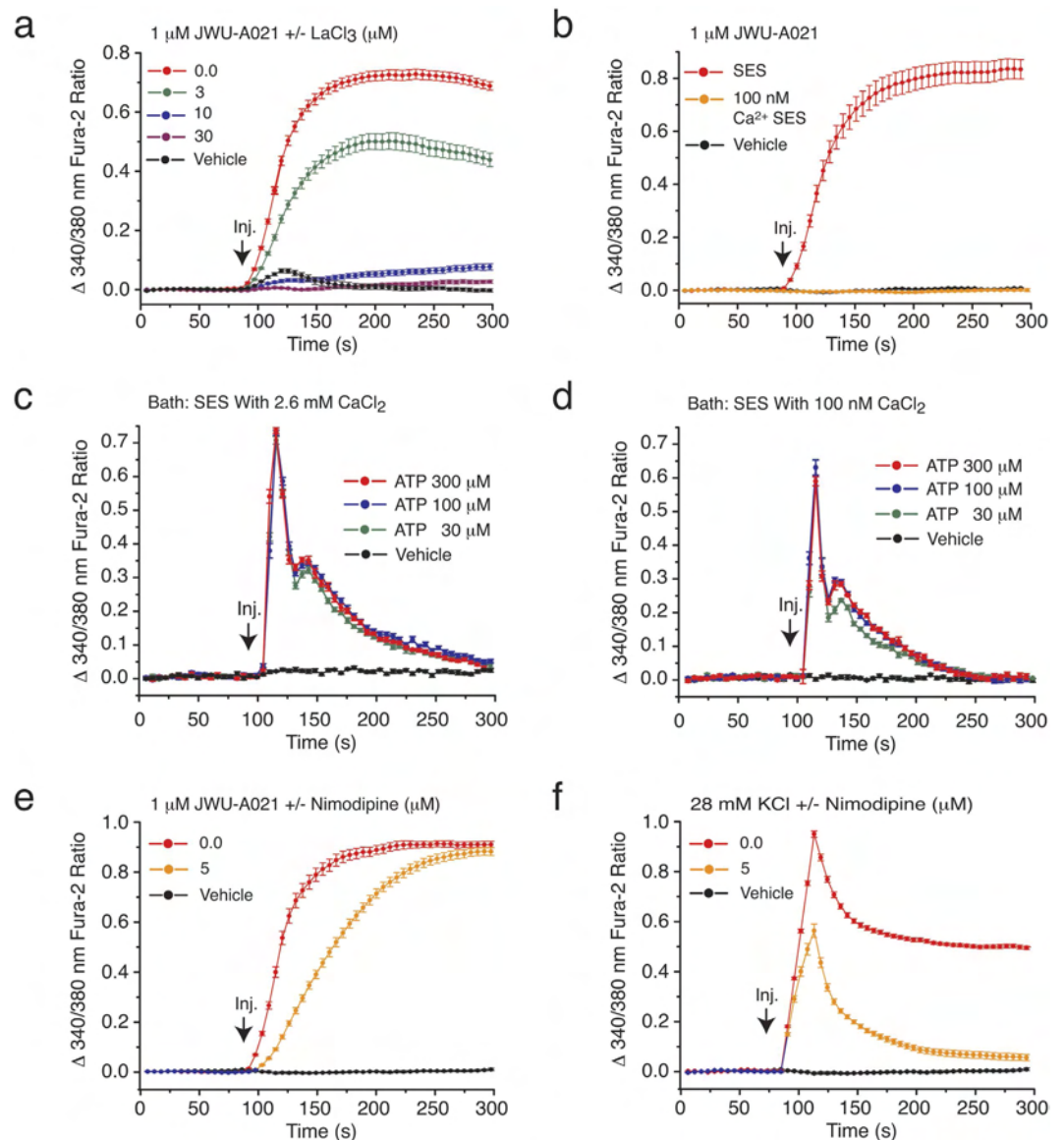


Figure 5. JWU-A021 promotes Ca^{2+} influx rather than Ca^{2+} mobilization. (a) The Ca^{2+} channel blocker La^{3+} exerted a concentration-dependent action to abrogate the increase of $[\text{Ca}^{2+}]_i$ stimulated by JWU-A021 ($1 \mu\text{M}$). (b) The action of JWU-A021 ($1 \mu\text{M}$) to increase $[\text{Ca}^{2+}]_i$ was abrogated when the Ca^{2+} concentration of the SES was reduced to 100 nM . (c,d) ATP dose-dependently increased the $[\text{Ca}^{2+}]_i$ measured under conditions in which the SES contained either 2.6 mM CaCl_2 (c) or 100 nM CaCl_2 (d). (e) The L-type Ca^{2+} channel blocker nimodipine ($5 \mu\text{M}$) slowed the rate of onset but failed to reduce the end-point increase of $[\text{Ca}^{2+}]_i$ measured in response to JWU-A021 ($1 \mu\text{M}$). (f) The effectiveness of nimodipine ($5 \mu\text{M}$) as an inhibitor of Ca^{2+} influx was demonstrated by its ability to fully block the end-point increase of $[\text{Ca}^{2+}]_i$ measured in response to 28 mM KCl -induced depolarization. For all examples depicted here, the findings are representative of a single experiment repeated a minimum of three times on three different occasions with similar results.

out of JWU-A021 (Fig. 6c,d). Thus, JWU-A021 might activate TRPA1 channels through reversible binding to a receptor that corresponds to the channel, itself.

JWU-A021 stimulates GLP-1 release from primary intestinal cell cultures. The GLP-1 secretagogue action of JWU-A021 was also tested using mouse intestine primary cell cultures enriched in L-cells. These cultures exhibited glucose-stimulated GLP-1 release (Fig. 8a), and they also released GLP-1 in response to JWU-A021 and AITC (Fig. 8b). Furthermore, the GLP-1 secretagogue actions of JWU-A021 and AITC were inhibited by the TRPA1 channel blocker HC030031 (Fig. 8b). Immunocytochemical analysis using a GLP-1 specific monoclonal antibody in combination with a horseradish peroxidase (HRP) conjugated secondary antiserum revealed that ca. 20% of the cells comprising these cultures contained GLP-1 (Fig. 8c, top panel). However, a negative control demonstrated that GLP-1 immunoreactivity was not measurable using the secondary antiserum alone (Fig. 8c, bottom panel). Interestingly, quantitative reverse transcriptase polymerase chain reaction

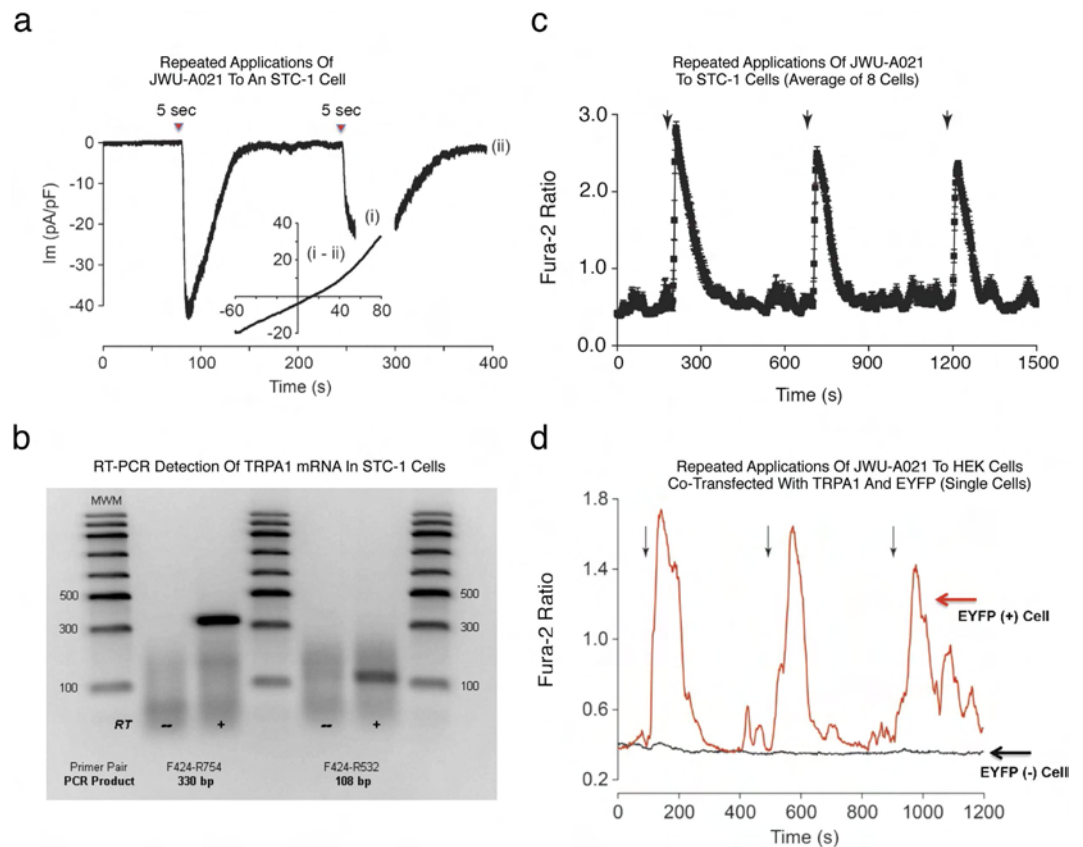


Figure 6. Membrane currents and Ca^{2+} transients activated by JWU-A021. (a) Whole-cell patch clamp analysis ($V_h -60$ mV) demonstrated inward membrane currents activated by repeated 5 sec focal applications of JWU-A021 ($3 \mu\text{M}$; red triangles) to a single STC-1 cell. The inset provides a current-voltage (I-V) relationship for the current activated by JWU-A021 (I_m , membrane current in pA normalized to membrane capacitance in pF). It is the difference current obtained by subtracting the IV relationships measured during (time point “i”) and after recovery (time point “ii”) of the response. Findings are representative of a single patch clamp experiment that was repeated with similar results using $N = 10$ cells. (b) RT-PCR validation that STC-1 cells express TRPA1 channel mRNA, as detected using two different primer pairs (RT, reverse transcriptase; MWM, molecular weight markers). Findings are representative of a single experiment repeated twice with similar results. (c) Averaged Ca^{2+} transients obtained from STC-1 cells stimulated by focal application (arrows) of JWU-A021 ($3 \mu\text{M}$) to $N = 8$ cells. (d) Ca^{2+} transients stimulated by focal application (arrows) of JWU-A021 ($3 \mu\text{M}$) to a single HEK-293 cell transfected with rat TRPA1 cDNA fused to EYFP cDNA (red trace), or a HEK-293 cell transfected with EYFP cDNA but not rat TRPA1 cDNA (black trace). EYFP fluorescence was used as a marker to positively identify cells that were transfected so that fura-2 based assays of $[\text{Ca}^{2+}]_i$ could be performed using these cells. Findings are representative of a single experiment repeated a minimum of three times on three different occasions with similar results.

(qRT-PCR) analysis revealed that JWU-A021 significantly increased levels of TRPA1 channel mRNA by ca. 40% in these cultures (Fig. 8d). Furthermore, this action of JWU-A021 was inhibited by HC030031 (Fig. 8d). Thus, Ca^{2+} entry through TRPA1 channels seems to exert a positive feedback effect on TRPA1 channel mRNA expression. Collectively, such findings are in agreement with the report of Emery and co-workers that TRPA1 channel activation by AITC leads to GLP-1 release from mouse L-cells⁹. In summary, the new method of cycloalka[b] indole library construction reported here has identified JWU-A021 to be a GLP-1 secretagogue with potent TRPA1 activating properties, not only in STC-1 cells, but also in mouse L-cells.

Discussion

Rational assembly of small molecule libraries for purposes of drug discovery requires an efficient approach in which the synthesis of bioactive compounds is enabled so that numerous structurally related compounds of a similar basic formulation can be derived. Here, we describe (4 + 3) and (3 + 2) annulation strategies that quickly generate complex indole heterocycle libraries that contain novel cyclohepta and cyclopenta [b]indoles, respectively. We demonstrate that these indole heterocycle libraries are amenable to screening so that new GLP-1 secretagogues can be identified. Thus, the primary outcome of this study is that the cyclohepta[b]indole JWU-A021 is revealed to be a novel stimulator of GLP-1 release from STC-1 cells and mouse intestinal L-cells. These findings

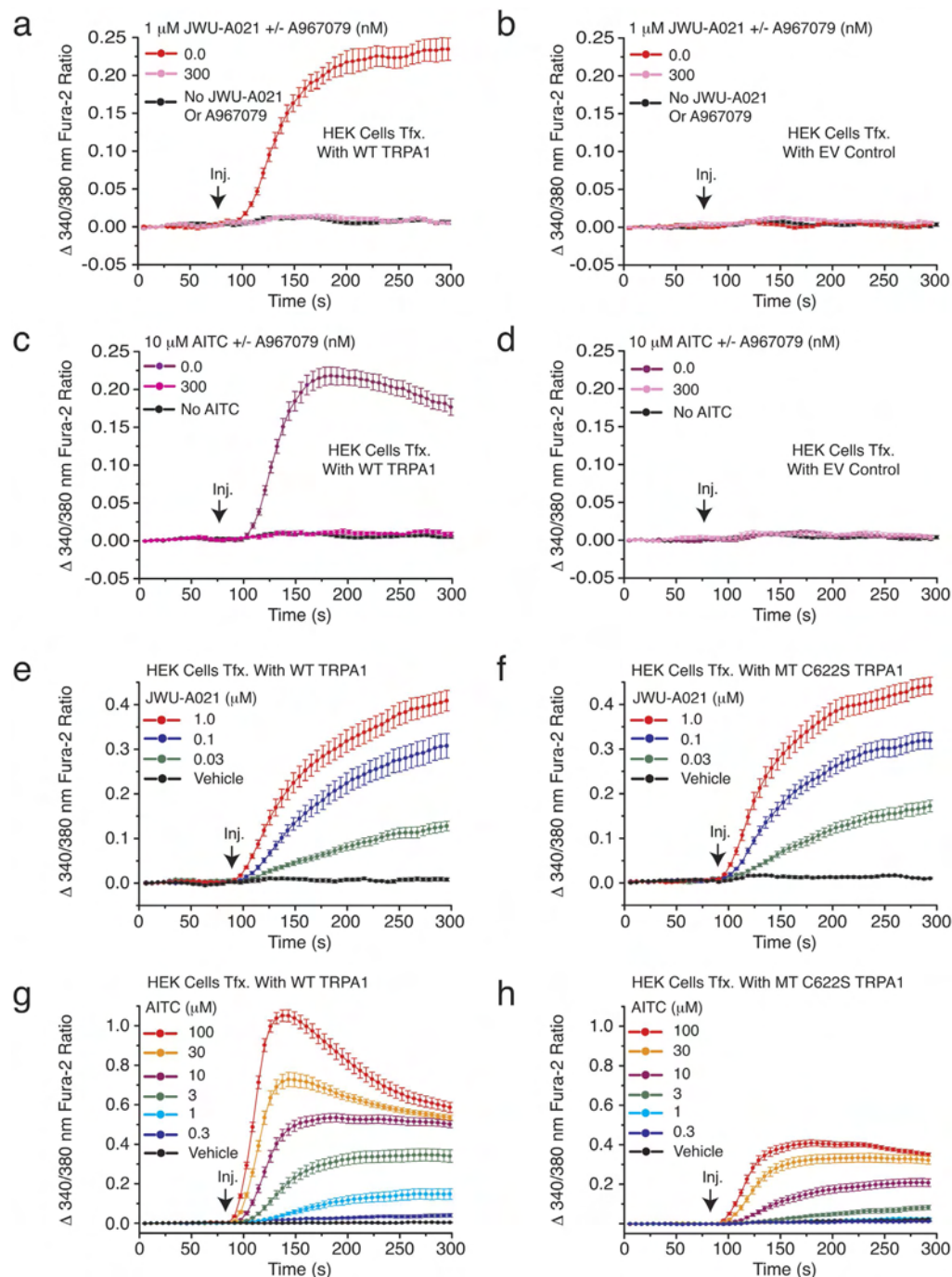


Figure 7. Studies with HEK-293 cells transfected with recombinant TRPA1. (a,b) HEK-293 cell monolayers transfected with wild-type (WT) rat TRPA1 cDNA, but not a negative control empty vector (EV), exhibited an increase of $[\text{Ca}^{2+}]_i$ in response to JWU-A021 (1 μM), and this action of JWU-A021 was abrogated by the TRPA1 channel blocker A967079. (c,d) HEK-293 cells transfected with WT rat TRPA1 cDNA, but not a negative control EV, exhibited an increase of $[\text{Ca}^{2+}]_i$ in response to AITC (10 μM), and this action of AITC was abrogated by the TRPA1 channel blocker A967079. This experiment confirmed the expected failure of HEK-293 cells to express endogenous TRPA1 channels. (e) A concentration-dependent action of JWU-A021 to increase $[\text{Ca}^{2+}]_i$ was measured in HEK-293 cell monolayers transfected with wild-type (WT) rat TRPA1 cDNA. (f) HEK-293 cell monolayers transfected with mutant C622S rat TRPA1 cDNA responded to JWU-A021 in a manner nearly identical to that of cells transfected with WT TRPA1 (compare panels e,f). Thus, the non-electrophile JWU-A021 acted independently of C622 covalent modification. (g,h) The TRPA1 activator AITC stimulated an increase of $[\text{Ca}^{2+}]_i$ in HEK-293 cell monolayers transfected with WT rat TRPA1, and this action of AITC to increase $[\text{Ca}^{2+}]_i$ was greatly diminished in HEK-293 cells transfected with mutant C622S TRPA1 cDNA (compare panels g,h). Thus, the electrophile AITC must covalently modify C622 in order to fully activate the channel. For all examples depicted here, the findings are representative of a single experiment repeated a minimum of three times on three different occasions with similar results.

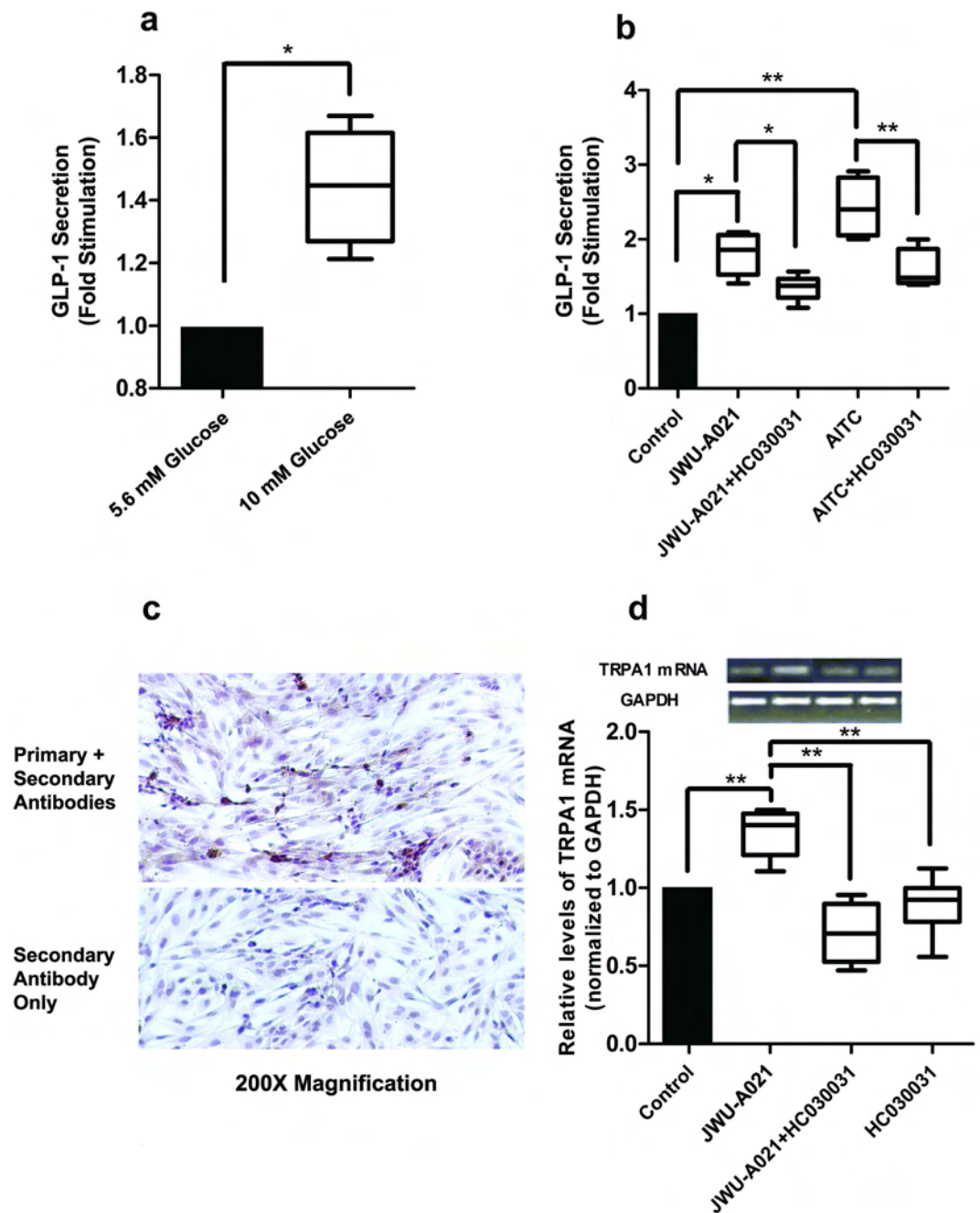


Figure 8. JWU-A021 stimulates GLP-1 release from mouse intestinal cells. (a) Primary cultures were stimulated for 30 min using serum-free DMEM assay buffer containing either 5.6 or 10 mM glucose so that glucose-stimulated GLP-1 secretion could be measured. Data are the mean + s.d. of 4 independent assays (* $p < 0.05$; paired t test) and are expressed as the fold-stimulation of GLP-1 release, so that a value of 1.0 corresponds to GLP-1 release measured for buffer containing 5.6 mM glucose. (b) HC030031 ($10 \mu\text{M}$) inhibited the actions of JWU-A021 ($3 \mu\text{M}$) and AITC ($100 \mu\text{M}$) to stimulate GLP-1 secretion from primary cultures. HC030031 was administered 15 minutes prior to addition of JWU-A021 or AITC, and it was also present during the 30 minutes test interval during which cells were exposed to JWU-A021 or AITC dissolved in serum free DMEM assay buffer containing 5.6 mM glucose. Data are the mean + s.d. of 4–6 independent assays (* $p < 0.05$; ** $p < 0.01$; ANOVA with Bonferroni post test). (c) Immunocytochemical detection of GLP-1 in primary cell cultures. The top panel illustrates specific GLP-1 immunoreactivity (brown), as detected using the anti-GLP-1 monoclonal primary antibody in combination with an HRP conjugated secondary antiserum. The bottom panel illustrates negative control non-specific labeling obtained when using the secondary antiserum only. (d) qRT-PCR analysis demonstrated that JWU-A021 ($3 \mu\text{M}$) increased the relative abundance of TRPA1 channel mRNA in primary cell cultures, and that this effect was reduced by HC030031 ($10 \mu\text{M}$). For this analysis, cultures were maintained for 30 minutes in serum-free DMEM assay buffer containing 5.6 mM glucose and the test compounds. Data are the mean + s.d. of 6 independent assays (** $p < 0.01$; ANOVA with Bonferroni post test). The top inset illustrates qRT-PCR products detected by agarose gel electrophoresis.

are of potential medical importance due to the fact that small molecule GLP-1 secretagogues are now under investigation for use in the treatment of T2DM³.

It is intriguing that JWU-A021 exerts its GLP-1 secretagogue action by stimulating Ca²⁺ influx through TRPA1 channels. This finding expands on the already established role of TRPA1 channels in peripheral sensory neuron function¹³, and it is consistent with the new view that members of the *Trp* ion channel family participate in the control of multiple intestinal cell functions^{15,16}. Since Ca²⁺-dependent exocytosis of GLP-1 from L-cells is stimulated by ingested nutrients^{17–19}, orally administered JWU-A021 might activate intestinal TRPA1 channels so that it replicates the GLP-1 secretagogue effect of such nutrients. If so, synthetic small molecule TRPA1 channel activators might constitute a new class of blood glucose-lowering agents. This general line of thinking is consistent with an emerging field of investigation in which TRPA1 channel-targeted drug discovery is applied for disease processes unrelated to sensory neuron function²⁰.

When considering a possible use of JWU-A021 in therapeutics, it is noteworthy that the TRPA1 channel activator cinnamaldehyde exerts blood glucose-lowering and weight-reducing actions in mice²¹. However, cinnamaldehyde is an electrophile that is not a specific TRPA1 channel activator owing to its promiscuous alkylating properties. JWU-A021 avoids such non-specificity since it is not an electrophile and most likely acts independently of covalent TRPA1 channel modification. While a few non-electrophilic, non-covalent TRPA1 activators are reported (e.g., carvacrol)⁴, only one (PF-4840154) is especially potent²². Unfortunately, PF-4840154 is a hERG K⁺ channel inhibitor and it has the predicted adverse side effect to induce cardiac arrhythmia²².

One prior *in vivo* study failed to detect elevated levels of GLP-1 in the blood after oral administration of the TRPA1 channels activators cinnamaldehyde and methyl syringate to mice²³. However, levels of the intestinal hormone peptide YY (PYY) were elevated in the blood, and this effect was suppressed by a TRPA1 channel blocker²³. Since GLP-1 and PYY are co-secreted from L-cells²⁴, the failure of cinnamaldehyde and methyl syringate to raise circulating levels of GLP-1 seems paradoxical. However, detection of circulating GLP-1 is complicated owing to its rapid degradation and inactivation by dipeptidylpeptidase-4 (DPP-4), as well as its quick clearance from the systemic circulation²⁵. Ideally, quantification of secreted GLP-1 must be based on its concentration immediately at the site of its release in the intestine where it exerts a local effect to activate vagal sensory neurons within the intestinal wall so that vasovagal reflexes important to global metabolic homeostasis can be initiated^{26,27}. Although prior studies were performed using mice, a rationale exists for future studies examining TRPA1 channel-dependent regulation of GLP-1 secretion from human L-cells.

Although not a focus of the report here, we recently found that JWU-A021 failed to stimulate GLP-1 release from GLUTag cells, a mouse L-cell line²⁸. Furthermore, JWU-A021 failed to increase the [Ca²⁺]_i in GLUTag cells, whereas AITC exerted only a weak effect (data not shown). Such findings are consistent with one prior report documenting low level expression of TRPA1 mRNA in GLUTag cells, whereas higher levels exist in STC-1 cells and mouse L-cells⁹. Evidently, GLUTag cells do not recapitulate the TRPA1 channel expression that is characteristic of mouse L-cells. For these reasons, species-specific and cell line-specific actions of TRPA1 channel activators such as JWU-A021 must be taken into account when planning high throughput screening approaches targeted at the identification of new GLP-1 secretagogues.

Conclusion

Summarized here are (4 + 3) and (3 + 2) annulation strategies that we believe will be generally applicable to the synthesis of small molecule cycloalka[*b*]indole libraries that are useful for drug screening purposes. The feasibility of this approach is established herein by demonstrating the rapid synthesis, purification, identification, and characterization of cyclohepta[*b*]indoles with potent GLP-1 releasing properties. The power of this approach is further emphasized in that the (4 + 3) annulation strategy is revealed to be an effective means with which to generate novel TRPA1 channel activators. Therefore, findings presented here validate a new strategy for small molecule combinatorial library construction. Although *in vivo* testing to determine the safety and efficacy of JWU-A021 still remains to be achieved, cyclohepta[*b*]indoles based on the structure of JWU-A021 might find a role in therapeutics as a new class of GLP-1 secretagogues.

Methods

STC-1 and HEK-293 cell culture. STC-1 and HEK-293 cells were obtained from the ATCC (Manassas, VA). Culture medium was comprised of Dulbecco's Modified Eagle Medium (DMEM) containing 25 mM glucose, 10% fetal bovine serum (FBS), 100 units ml⁻¹ penicillin G, and 100 µg/ml streptomycin. Cultures were passaged once a week while maintained at 37 °C in a humidified incubator gassed with 5% CO₂. Cultures harvested by trypsinization were plated at a density of 40,000–50,000 cells per well on rat tail collagen (RTC) coated 96-well Costar 3904 plates two days prior to each experiment. Cultures were 85–95% confluent on the day of the experiment. Culture media, additives, Costar plates, and RTC were from Gibco/Thermo Fisher Scientific (Waltham, MA).

Fura-2 based assays of [Ca²⁺]_i. The fura-2 loading solution for all assays was comprised of a standard extracellular solution (SES; 295 milliosmoles/L) containing (in mM): 138 NaCl, 5.6 KCl, 2.6 CaCl₂, 1.2 MgCl₂, 10 HEPES (adjusted to pH 7.4 with NaOH), and supplemented with 11.1 mM glucose, 20 µl ml⁻¹ FBS, 1 µl ml⁻¹ Pluronic F-127, and 1 µM fura-2 acetoxymethyl ester (fura 2-AM; Thermo Fisher Sci.)²⁹. Measurements of [Ca²⁺]_i from monolayers of fura-2 loaded cells were performed at 25 °C using a FlexStation 3 microplate reader under the control of SoftMaxPro v5.4 software (Molecular Devices, Sunnyvale, CA)²⁹. Spectrofluorimetry was performed using excitation light at 335/9 and 375/9 nm (center/bandpass wavelengths) delivered using a 455 nm dichroic mirror. Emitted light was detected at 505/15 nm and the ratio of emission light intensities due to excitation at 335 and 375 nm was calculated. Raw data were exported to Origin v7.5 (Origin Lab., Northampton, MA)

for processing. Fura-2 based single cell measurements of $[Ca^{2+}]_i$ were performed with minor modifications, as described previously^{30–32}.

Patch clamp electrophysiology. Membrane currents were recorded in the whole-cell configuration under conditions of voltage clamp in which cells were bathed in SES^{33,34}. The patch pipette solution contained (in mM): 140 Cs-glutamate, 10 NaCl, 1 MgCl₂, 0.2 EGTA, 2 MgATP, and 5 HEPES adjusted to pH 7.4 with CsOH. Test compounds were added to SES as indicated in the text. Patch pipettes were pulled from thin walled glass capillaries (G85150T-4, Warner Instruments, Hamden, CT) using a P-97 pipette puller (Sutter Inst., Novato, CA) and had resistances of 2–5 MΩ when filled with the pipette solution. Measurements of membrane currents were obtained using an EPC-9 amplifier controlled using PatchMaster software (HEKA Elektronik, Lambrecht/Pfalz, Germany). Test solutions containing JWU-A021 were applied to single cells from a puffer pipette using a PicoSpritzer III pressure ejection system (Parker Hannifin, Hollis, NH). TRPA1 current-voltage relationships were obtained by subtracting the background membrane current from the activated TRPA1 current under conditions in which there was a 1 V/s shift of the holding potential, applied as a linear voltage ramp. Whole-cell currents were digitally sampled at a frequency of 10 kHz after filtering at 1–3 kHz. Current amplitudes were normalized to cell capacitance.

Expression of recombinant TRPA1. JM109 competent *E. coli* (Promega, Madison, WI) were transformed with plasmid DNA, and antibiotic resistance selection was used to obtain single bacterial colonies expressing the indicated rat TRPA1 plasmid DNAs. These plasmids were isolated from bacteria using a HiSpeed Midi Kit (Qiagen, Valencia, CA). Transient transfection of HEK-293 cells with these plasmids was performed using Lipofectamine and Plus reagent according to the manufacturer's protocol (Thermo Fisher Scientific).

Sources of plasmids, channel blockers, and activators. A mutant rat C622S TRPA1 construct, and also the wild-type TRPA1 coding sequence (GenBank No. AY496961.1) fused at its 5' terminus to the yellow fluorescent protein (YFP), were provided by Prof. Emily Liman (University of Southern California, USA)^{14,35}. A967079, AP-18, and HC030031 were from Tocris Biosci. (Minneapolis, MN). AITC, ATP, and nimodipine were from Sigma-Aldrich (St. Louis, MO).

STC-1 cell GLP-1 secretion assay. STC-1 cells were maintained in RTC-coated 96-well cell culture plates and were allowed to reach 85–95% confluence. On the day of the experiment, the culture medium was replaced with DMEM containing 5.6 mM glucose and 0.1% bovine serum albumin (BSA) and the cells were then serum starved for 3 hours while equilibrated in a tissue culture incubator. The medium was then replaced with the fresh DMEM containing 5.6 mM glucose and 0.1% BSA with or without the indicated test solutions so that there were four wells per each experimental condition. STC-1 cells were exposed to these test solutions for 30 min while again being equilibrated in a cell culture incubator. Medium from each of the four wells was collected and stored at –80 °C prior to immunoassays. GLP-1 in these samples was detected using a GLP-1 Total ELISA kit (Cat. No. EZGLP1T-36K; EMD Millipore, Billerica, MA) according to the manufacturer's instructions. O.D. values for ELISA assay samples were measured using a Benchmark Plus plate-reading spectrophotometer under the control of Microplate Manager software (Bio-Rad Laboratories, Hercules, CA). Each experiment was repeated 3 times so that the data are the average of $N = 3$ experiments. Data were evaluated for statistical significance by a paired *t* test. A *p*-value of <0.05 was considered to be statistically significant.

Ethical use of vertebrate animals. All experiments using mice were performed in accordance with relevant guidelines and regulations specified in the Animal Welfare Act (AWA) (7 U.S.C. § 2131) per United States of America federal government law. Ethical use of mice for the experiments reported here were also in accordance with an animal use protocol (IACUC #338) that was approved by the Institutional Animal Care and Use Committee of SUNY Upstate Medical University.

Neonatal mouse intestinal cell culture. Newborn mice (C57BL/6) from Charles River Laboratories (Wilmington, MA) were used for preparation of mixed primary intestinal cell cultures enriched with L-cells using a modification of previously published techniques^{36–38}.

Step #1. Newborn mice (C57BL/6) from Charles River Laboratories (Wilmington, MA) were euthanized according to a SUNY Upstate Medical University animal use protocol (IACUC #338, mice for a separate project donated by Dr. Li-Ru Zhao). The entire intestine was removed, rinsed, and chopped into 1–2 mm pieces in ice-cold Ca²⁺-free Hank's balanced salt solution containing 0.65 mM dithiothreitol, 1% BSA, penicillin, streptomycin, 9.05 mM NaHCO₃, and 20 mM HEPES. The tissue was then digested for 15 min in a 37 °C shaking water bath incubator using 5 ml of 100 U/ml collagenase type I (Sigma) in Basal Medium Eagle (Thermo Fisher Scientific) and supplemented with 1% BSA, 26.4 mM NaHCO₃, and 10 mM HEPES (pH 6.9). Digested tissue was centrifuged at 120 × *g* and the resulting pellet was re-suspended in DMEM containing 5.6 mM glucose (Cat. #11885, Gibco/Thermo Fisher), penicillin, streptomycin, and 5% FBS.

Step #2. The re-suspended tissue digest derived by centrifugation was filtered through an 80 μm nylon filter (Merk Millipore, Darmstadt, Germany). The filtered eluent containing intestinal cells was subjected to two rounds of centrifugation at 120 × *g* for 3 min each cycle in DMEM containing 2% sorbitol. The final pellet was re-suspended in DMEM containing penicillin, streptomycin, 10% FBS, 1 μg/ml insulin (Sigma), and 20 ng/ml epidermal growth factor (EGF, Sigma). Cells were added to culture plates (Cat. No. 10062-892, VWR International, LLC, Radnor, PA) for culture at 37 °C in DMEM containing 5.6 mM glucose, penicillin, streptomycin, and 5% FBS.

GLP-1 release assay. Primary cell cultures enriched with mouse L-cells were allowed to achieve 70–90% confluence in a humidified incubator gassed with 5% CO₂. On the day of the experiment, they were equilibrated for 3 hours in serum-free DMEM containing 5.6 mM glucose, penicillin, streptomycin, and 0.1% BSA. After washing the cultures three times with serum-free DMEM, GLP-1 release assays were performed for 30 minutes during which the cells were exposed to test compounds dissolved in serum-free DMEM containing 5.6 mM glucose and 0.1% BSA. An EIA-GLP-1 ELISA kit (RayBio, Norcross, GA) was used to detect GLP-1 released into the assay medium. All samples were assayed in duplicate.

RT-PCR for TRPA1 mRNA. RNA was isolated from STC-1 cells using RNeasy kits (Qiagen). Quantitect Reverse Transcriptase (RT) kits (Qiagen) were used to generate cDNA per kit instructions with control reactions performed without RT. The PCR primers were designed against a mouse sequence for TRPA1 (GenBank NM_177781.4) and had the following sequences: Sense primer [ATGTCACCCCTTCACATAGC]; Anti-sense primer #1 [CGTGTTCCTTCTCTCCTT]; Anti-sense primer #2 [GGCTGGCTTTCTTGTGATTC]. Both anti-sense primers were used with the same sense primer. PCR products spanned one or two exons and had predicted product sizes of 109 and 331 bp, respectively. PCR reactions were performed using a Mini-Opticon cycler (Bio-Rad, Hercules, CA) and a QuantiTect SYBR-Green PCR kit (Qiagen). The thermal cycle parameters were: 95 °C for 15 min followed by 35 cycles of 95 °C for 15 s, 57 °C for 30 s and 72 °C for 30 s. A melting curve analysis was performed from 60 °C to 85 °C, and products were run on 2% agar gels to test product specificity using GelRed loading buffer and a pre-stained DNA marker (GenScript, Piscataway, NJ). PCR products were extracted from these gels using a QIAquick Gel Extraction kit (Qiagen).

qRT-PCR for TRPA1 mRNA. Quantitative real-time polymerase chain reaction (qRT-PCR) analysis was used to detect TRPA1 mRNA expression in mixed primary L-cell cultures. Cells were lysed in Trizol (Invitrogen) and total RNA was extracted. First-strand cDNA synthesis was performed with 1 µg of total RNA in 20 µl reactions using an iScript cDNA Synthesis Kit (Bio-Rad, Hercules, CA). qRT-PCR was then performed using iQ SYBR Green Mix (Bio-Rad, Hercules, CA). Relative gene expression was determined by the CT method, and TRPA1 mRNA levels were normalized relative to the levels of glyceraldehyde phosphodehydrogenase (GAPDH) mRNA. Primers used for TRPA1 were: sense 5'-CCATGACCTGGCAGAATACC-3' and antisense 5'-TGGAGAGCGTCTTCAGAAT-3'. Primers used for GAPDH were: sense 5'-CAATGTGTC CGTGGA-3' and antisense 5'-GATGCCTGCTTCACCACC-3'.

Immunocytochemistry for detection of GLP-1. Cultures of mouse intestinal cells were fixed for 10 min at room temperature in PBS containing 4% paraformaldehyde, and were then permeabilized by incubation for 10 min in PBS containing 0.25% Triton X-100. The blocking buffer was PBS-Tween containing 1% BSA. Cells were exposed at 4 °C overnight to PBS-Tween containing a 1:50 dilution of a mouse monoclonal anti-GLP-1 antibody (Cat. No. AB23468, Abcam, Cambridge, MA). A goat anti-mouse polyclonal antiserum conjugated to horseradish peroxidase (HRP) served as the secondary antibody (Cat. No. 1706516, Bio-Rad, Hercules, CA). A DAB Stain kit (Vector, CA) was used to detect the HRP reaction product that signified GLP-1 immunoreactivity, whereas hematoxylin was used to detect nuclei. Photomicrographs were taken with an Eclipse TE 2000-U microscope (Nikon).

Primary and secondary screens of a cycloalka[b]indole library. The ELISA-based primary screen to identify JWU-A021 as a GLP-1 secretagogue was performed as part of the Open Innovation Drug Discovery Program (OID) of Eli Lilly and Company. Subsequent identification of JWU-A021 as a TRPA1 channel activator was achieved at the Holz laboratory in a fura-2-based secondary screen that used a panel of calcium channel blockers or activators. OIID screening data presented in Fig. 2a–c was supplied courtesy of Eli Lilly and Company-used with Lilly's permission. To learn more about the Lilly Open Innovation Drug Discovery Program, please visit the program website at <https://openinnovation.lilly.com> (last accessed on 05-04-2016).

Statistical analyses. The repeatability of findings was confirmed by performing all experiments a minimum of three times. GLP-1 secretion assay data and qRT-PCR data were evaluated for statistical significance by Student's paired *t* test or by ANOVA analysis followed by a Bonferroni post test, as indicated in the figure legends. For all assays, a *p*-value of <0.05 was considered to be statistically significant. Appropriate sample size was determined post-hoc so that the sample size could be increased, if necessary, so that statistical significance would be achieved if it existed.

References

- Vitaku, E., Smith, D. T. & Njardarson, J. T. Analysis of the structural diversity, substitution patterns, and frequency of nitrogen heterocycles among U.S. FDA approved pharmaceuticals: miniperspective. *J. Med. Chem.* **57**, 10257–10274 (2014).
- Han, X., Li, H., Hughes, R. P. & Wu, J. Gallium(III)-catalyzed three-component (4 + 3) cycloaddition reactions. *Angew. Chem. Int. Ed.* **51**, 10390–10393 (2012).
- Nadkarni, P., Chepurny, O. G. & Holz, G. G. Regulation of glucose homeostasis by GLP-1. *Prog. Molec. Biol. Trans. Res.* **12**, 23–65 (2014).
- Nilius, B., Appendino, G. & Owsianik, G. The transient receptor potential channel TRPA1: from gene to pathophysiology. *Pflugers Arch.* **464**, 425–458 (2012).
- Rindi, G. *et al.* Development of neuroendocrine tumors in the gastrointestinal tract of transgenic mice. Heterogeneity of hormone expression. *Am. J. Pathol.* **136**, 1349–1363 (1990).
- Grant, S. G. N., Seidman, I., Hanahan, D. & Bautch, V. L. Early invasiveness characterizes metastatic carcinoid tumors in transgenic mice. *Cancer Res.* **51**, 4917–4923 (1991).
- Abello, J. *et al.* Stimulation of glucagon-like peptide-1 secretion by muscarinic agonist in a murine intestinal endocrine cell line. *Endocrinology* **134**, 2011–2017 (1994).

8. Purhonen, A. K., Louhivuori, L. M., Kiehne, K., Akerman, K. E. O. & Herzig, K. H. TRPA1 channel activation induces cholecystokinin release via extracellular calcium. *FEBS Lett.* **582**, 229–232 (2008).
9. Emery, E. C. *et al.* Stimulation of GLP-1 secretion downstream of the ligand-gated ion channel TRPA1. *Diabetes* **64**, 1202–1210 (2014).
10. Rogers, G. J. *et al.* Electrical activity-triggered glucagon-like peptide-1 secretion from primary murine L-cells. *J. Physiol.* **589**, 1081–1093 (2011).
11. Flack, H. D. & Bernardinelli, G. The use of X-ray crystallography to determine absolute configuration. *Chirality* **20**, 681–690 (2008).
12. Caterall, W. A. Voltage-gated calcium channels. *Cold Spring Harb. Perspect. Biol.* **3**(8), a003947 (2011).
13. Julius, D. TRP channels and pain. *Ann. Rev. Cell. Develop. Biol.* **29**, 355–384 (2013).
14. Wang, Y. Y., Chang, R. B., Allgood, S. D., Silver, W. L. & Liman, E. R. A TRPA1-dependent mechanism for the pungent sensation of weak acids. *J. Gen. Physiol.* **137**, 493–505 (2011).
15. Boesmans, W., Owsianik, G., Tack, J., Voets, T. & Berghe, P. V. TRP channels in neurogastroenterology: opportunities for therapeutic intervention. *British J. Pharmacol.* **162**, 18–37 (2011).
16. Fernandes, E. S., Fernandes, M. A. & Keeble, J. E. The functions of TRPA1 and TRPV1: moving away from sensory neurons. *British J. Pharmacol.* **166**, 510–521 (2012).
17. Lim, G. E. & Brubaker, P. L. Glucagon-like peptide-1 secretion by the L-cell: the view from within. *Diabetes* **55**(S2), S70–S77 (2006).
18. Diakogiannaki, E., Gribble, F. M. & Reimann, F. Nutrient detection by incretin hormone secreting cells. *Physiol. & Behavior* **106**, 387–393 (2012).
19. Psichas, A., Reimann, F. & Gribble, F. M. Gut chemosensing mechanisms. *J. Clin. Invest.* **125**, 908–917 (2015).
20. Chen, J. & Hackos, D. H. TRPA1 as a drug target-promise and challenges. *Naunyn-Schmiedeberg's Arch. Pharmacol.* **388**, 451–463 (2015).
21. Camacho, S. *et al.* Anti-obesity and anti-hyperglycemic effects of cinnamaldehyde via altered ghrelin secretion and functional impact on food intake and gastric emptying. *Sci. Rep.* **5**, 7919 (2015).
22. Ryckmans, T. *et al.* Design and pharmacological evaluation of PF-4840157, a non-electrophilic reference agonist of the TRPA1 channel. *Bioorg. Med. Chem. Lett.* **21**, 4857–4859 (2011).
23. Kim, M. J. *et al.* The TRPA1 agonist, methyl syringate suppresses food intake and gastric emptying. *PLoS One* **8**(8), e71603 (2013).
24. De Silva, A. & Bloom, S. R. Gut hormones and appetite control: a focus on PYY and GLP-1 as therapeutic targets in obesity. *Gut Liver* **6**, 10–20 (2012).
25. Holst, J. J. The physiology of glucagon-like peptide-1. *Physiol. Rev.* **87**, 1409–1439 (2007).
26. D'Allesio, D. A. What if gut hormones aren't really hormones: DPP-4 inhibition and local action of GLP-1 in the gastrointestinal tract. *Endocrinology* **152**, 2925–2926 (2011).
27. D'Alessio, D. A. Is GLP-1 a hormone: whether and when? *J. Diabetes Investig.* **7**, 50–55 (2016).
28. Drucker, D. J., Jin, T., Asa, T. L., Young, T. A. & Brubaker, P. L. Activation of proglucagon gene transcription by protein kinase A in a novel mouse enteroendocrine cell line. *Mol. Endocrinol.* **8**, 1646–1655 (1994).
29. Chepurny, O. G., Holz, G. G., Roe, M. W. & Leech, C. A. GPR119 agonist AS1269574 activates TRPA1 cation channels to stimulate GLP-1 secretion. *Mol. Endocrinol.* **30**, 614–29 doi: <http://dx.doi.org/10.1210/me.2015-1306>, in press (2016).
30. Leech, C. A., Holz, G. G. & Habener, J. F. Pituitary adenylyl cyclase-activating protein induces the voltage-independent activation of inward membrane currents and elevation of intracellular calcium in HIT-T15 insulinoma cells. *Endocrinol.* **136**, 1530–1536 (1995).
31. Holz, G. G. & Habener, J. F. Black widow spider alpha-latrotoxin: a presynaptic neurotoxin that shares structural homology with the glucagon-like peptide-1 family of insulin secretagogic hormones. *Comp. Biochem. Physiol. B Biochem. Mol. Biol.* **121**, 177–184 (1998).
32. Kopp, R. F., Leech, C. A. & Roe, M. W. Resveratrol interferes with fura-2 intracellular calcium measurements. *J. Fluoresc.* **24**, 279–284 (2014).
33. Leech, C. A. & Holz, G. G. Application of patch clamp methods to the study of calcium currents and calcium channels. *Methods Cell. Biol.* **40**, 135–151 (1994).
34. Leech, C. A., Holz, G. G. & Habener, J. F. Voltage-independent calcium channels mediate slow oscillations of cytosolic calcium that are glucose-dependent in pancreatic beta-cells. *Endocrinol.* **135**, 365–372 (1994).
35. Wang, Y. Y., Chang, R. B., Waters, H. N., McKemy, D. D. & Liman, E. R. The nociceptor ion channel TRPA1 is potentiated and inactivated by permeating calcium ions. *J. Biol. Chem.* **283**, 32691–703 (2008).
36. Evans, G. S., Flint, N., Somers, A. S., Eyden, B. & Potten, C. S. The development of a method for the preparation of rat intestinal epithelial cell primary cultures. *J. Cell Sci.* **101**, 219–231 (1992).
37. Damholt, A. B., Buchan, A. M. & Kodfod, H. Glucagon-like peptide-1 secretion from canine L-cells is increased by glucose-dependent insulinotropic peptide but unaffected by glucose. *Endocrinology* **139**, 2085–2091 (1998).
38. Reimann, F., Habib, A. M., Tolhurst, G., Rogers, G. J. & Gribble, F. M. Glucose sensing in L cells: a primary cell study. *Cell. Metab.* **8**, 532–539 (2008).

Acknowledgements

J.W., G.G.H., C.A.L. and M.C.D. acknowledge the support of NIH R01-GM111638. G.G.H., C.A.L. and O.G.C. were supported, in part, by NIH R01-DK069575. M.C.D. was supported, in part, by a GAANN fellowship provided by the United States Department of Education. G.G.H. acknowledges the support of the Holz Laboratory Diabetes Research Fund of the Health Science Center Foundation of SUNY Upstate Medical University. Additional support was provided by American Diabetes Association Basic Research Awards 7-12-BS-077 (G.G.H) and 1-12-BS-109 (C.A.L.).

Author Contributions

J.W. invented the chemistry for cycloalka[b]indole library construction. M.T., M.C.D., H.L. and X.H. participated in cycloalka[b]indole synthesis, purification, and characterization. O.G.C. performed STC-1 cell Flexstation 3 assays for Ca²⁺ and GLP-1 release. C.A.L. performed STC-1 cell RT-PCR, single-cell imaging, and patch clamp assays. Q.M. performed qRT-PCR, immunocytochemistry, and GLP-1 release assays using intestinal cell cultures. G.G.H., O.G.C., C.A.L., Q.M. and R.N.C. designed the experiments. O.G.C., C.A.L., M.C.D. and H.L. edited the paper. G.G.H. and J.W. conceived of the project and wrote the paper.

Additional Information

Supplementary information accompanies this paper at <http://www.nature.com/srep>

Competing financial interests: The authors declare no competing financial interests.

How to cite this article: Chepurny, O. G. *et al.* Synthetic small molecule GLP-1 secretagogues prepared by means of a three-component indole annulation strategy. *Sci. Rep.* **6**, 28934; doi: 10.1038/srep28934 (2016).



This work is licensed under a Creative Commons Attribution 4.0 International License. The images or other third party material in this article are included in the article's Creative Commons license, unless indicated otherwise in the credit line; if the material is not included under the Creative Commons license, users will need to obtain permission from the license holder to reproduce the material. To view a copy of this license, visit <http://creativecommons.org/licenses/by/4.0/>

Synthetic small molecule GLP-1 secretagogues prepared by means of a three-component indole annulation strategy

Oleg G. Chepurny¹, Colin A. Leech¹, Martin Tomanik², Maria C. DiPoto², Hui Li², Xinping Han^{2,†}, Qinghe Meng³, Robert N. Cooney³, Jimmy Wu^{2*}, George G. Holz^{1,4*}

Departments of Medicine¹, Surgery³, and Pharmacology⁴, State University of New York (SUNY), Upstate Medical University, Syracuse, New York, USA

Department of Chemistry², Dartmouth College, Hanover, New Hampshire, USA

[†]Current Address: Department of Biochemistry, UT Southwestern, Dallas TX 75390

Table of Contents

General Information.....	S2
Synthetic Experimental Procedures	S3
Characterization of Cyclohepta[<i>b</i>]indole products	S4
Characterization of Cyclopenta[<i>b</i>]indole products	S7
References.....	S11
NMR Spectra	
JWU-A029	S12
JWU-A030	S18
JWU-A031	S24
JWU-A033	S30
JWU-A034	S36
(syn)-JWU-B007.....	S42
(anti)-JWU-B008	S47
(syn)-JWU-B009.....	S53
(anti)-JWU-B010	S59
(anti)-JWU-B011	S65
(syn)-JWU-B012.....	S71
JWU-B014	S77
X-Ray Crystallography Data for (-)-JWU-A021	S82

General Information

¹H NMR data were recorded on a Bruker Avance III 500 MHz spectrometer (TBI probe) and Bruker Avance III 600 MHz (BBFO probe) with calibration spectra to CHCl₃ (7.26 ppm) and CH₂Cl₂ (5.32 ppm) at ambient temperature. Multiplicities are indicated as s (singlet), d (doublet), t (triplet), and m (multiplet). ¹³C NMR data were recorded at 125 MHz on Bruker Avance III 600 MHz spectrometer (BBFO probe) at ambient temperature and expressed in ppm using solvent as the internal standard CD₂Cl₂ (53.84 ppm) and CDCl₃ (77.16 ppm). IR spectra were recorded on Jasco FT-IR 4100 Series spectrophotometer, ν_{\max} (cm⁻¹) are partially reported. Analytical thin layer chromatography (TLC) was performed on SILICYCLE pre-coated TLC plates (silica gel 60 F-254, 0.25mm). Flush column chromatography was performed on silica gel 60 (SILICYCLE 230–400 mesh). Visualization was accomplished with UV light and ceric ammonium molybdate (CAM). High-resolution mass spectroscopy data were acquired from Mass Spectrometry Laboratory of the University of Illinois (Urbana-Champaign, IL).

All reactions were carried out in oven-dried glassware with magnetic stirring. Solvents were freshly distilled. All reagents and starting materials were purchased from commercial vendors and used without further purification.

Experimental Procedures

General Procedure A for the Synthesis of Cyclohepta[b]indoles

A round-bottom flask was charged with indole (0.66 mmol, 1 equiv), aldehyde or ketone (1.32 mmol, 2 equiv), and diene (3.30 mmol, 5 equiv). Then, CH₂Cl₂ (2.0 mL) was added followed by GaBr₃ (0.07 mmol, 0.1 equiv). The reaction was stirred at room temperature until it was complete as judged by thin layer chromatography. The volatiles were concentrated *in vacuo* and the residue was purified via silica gel flash chromatography (EtOAc/Hexanes) to yield the desired products.

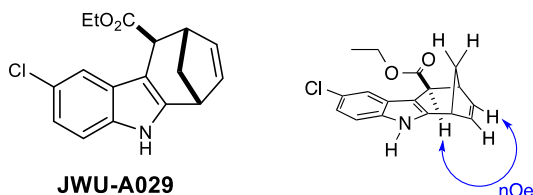
General Procedure B for the Synthesis of Cyclopenta[b]indoles

A round-bottom flask was charged with indole (0.66 mmol, 1 equiv), aldehyde or ketone (1.32 mmol, 2 equiv), and styrene (3.30 mmol, 5 equiv). Then, dichloroethane (2.0 mL) was added followed by TfOH (0.13 mmol, 0.2 equiv). The reaction was stirred at room temperature until it was complete as judged by thin layer chromatography. The volatiles were concentrated *in vacuo* and the residue was purified via silica gel flash chromatography (EtOAc/Hexanes) to yield the desired products.

Characterization of Cyclohepta[b]indole products

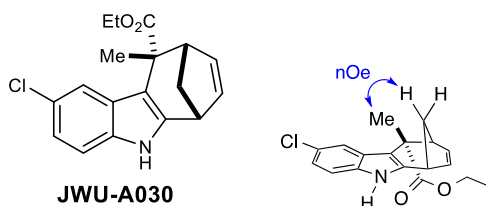
The preparation of **JWU-A001** through **JWU-A021** were carried out as previously described.¹ All characterization data were identical to those previously reported.¹

FIG. S1



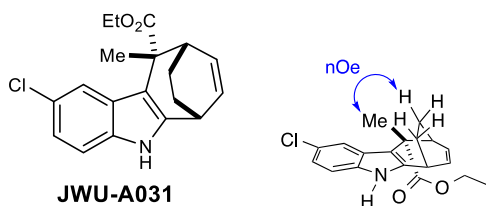
By following the general procedure **A** described above, **JWU-A029** was prepared in 43% yield. ¹H NMR (CD₂Cl₂, 600 MHz): δ, ppm 8.04 (1H, s), 7.40 (1H, d, J = 1.5 Hz), 7.14 (1H, d, J = 8.8 Hz), 6.93 (1H, dd, J = 2.5, 9.0 Hz), 6.34 (1H, dd, J = 3.0, 5.6 Hz), 5.85 (1H, dd, J = 3.0, 6.3 Hz), 4.13 (2H, q, J = 7.4 Hz), 3.47 (1H, d, J = 1.0 Hz), 3.40 (1H, dd, J = 3.3, 4.8 Hz), 3.19 (1H, t, J = 4.2 Hz), 2.28 (1H, d, J = 10.4 Hz), 2.13–2.09 (1H, m), 1.23 (3H, t, J = 8.3 Hz); ¹³C NMR (CD₂Cl₂, 150 MHz): δ 173.6, 142.4, 140.5, 133.0, 131.6, 129.5, 125.2, 120.5, 117.9, 111.6, 101.6, 60.8, 42.3, 41.3, 39.6, 38.8, 14.0; IR (film, cm⁻¹): 3401, 2957, 2846, 1713, 1644, 1468, 1259, 732; HRMS (ESI) calcd. for C₁₇H₁₆ClNO₂ (m/z M+H⁺): 302.0948, found: 302.0950.

FIG. S2



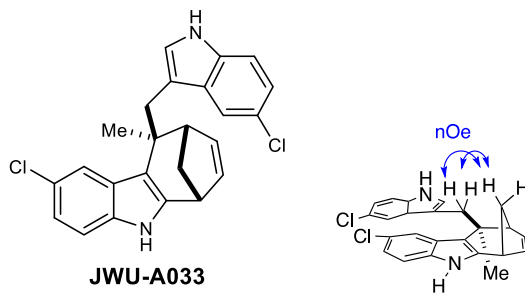
By following the general procedure **A** described above, **JWU-A030** was prepared in 57% yield. **¹H NMR** (CD₂Cl₂, 600 MHz): δ, ppm 8.01 (1H, s), 7.29 (1H, d, J = 2.1 Hz), 7.13 (1H, d, J = 9.0 Hz), 6.91 (1H, dd, J = 1.7, 8.0 Hz), 6.36 (1H, dd, J = 3.0, 5.4 Hz), 5.70 (1H, dd, J = 3.2, 5.2 Hz), 4.17–4.11 (1H, m), 4.06–3.98 (1H, m), 3.29 (1H, t, J = 3.7 Hz), 3.01 (1H, dd, J = 3.0, 4.8 Hz), 2.24 (2H, m, J = 4.9 Hz), 2.07 (1H, d, J = 9.9 Hz), 1.63 (3H, s), 1.16 (2H, t, J = 6.7 Hz); **¹³C NMR** (CD₂Cl₂, 150 MHz): δ 175.2, 140.7, 140.4, 132.9, 131.5, 129.0, 124.7, 120.1, 119.0, 111.7, 108.0, 60.5, 49.9, 46.1, 40.9, 39.0, 25.7, 14.0; **IR** (film, cm⁻¹): 3455, 3048, 2981, 1720, 1637, 1451, 1262, 736; **HRMS (ESI) calcd.** for C₁₈H₁₈ClNO₂ (m/z M+H⁺): 316.1104, found: 316.1104.

FIG. S3



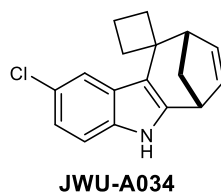
By following the general procedure **A** described above, **JWU-A031** was prepared in 11% yield. **¹H NMR** (CD₂Cl₂, 600 MHz): δ, ppm 7.84 (1H, s), 7.31 (1H, d, J = 2.0 Hz), 7.13 (1H, d, J = 9.4 Hz), 6.93 (1H, dd, J = 2.2, 8.6 Hz), 6.45 (1H, dd, J = 8.0, 8.0 Hz), 6.00 (1H, t, J = 8.0 Hz), 4.11–4.05 (1H, m), 4.02–3.96 (1H, m), 3.24 (1H, t, J = 4.4 Hz), 2.87 (1H, t, J = 7.6 Hz), 2.08–1.96 (2H, m), 1.85–1.78 (1H, m), 1.71–1.65 (1H, m), 1.64 (3H, s), 1.12 (3H, t, J = 7.8 Hz); **¹³C NMR** (CD₂Cl₂, 150 MHz): δ 175.6, 139.3, 135.9, 132.7, 130.9, 130.4, 124.6, 120.7, 120.6, 119.9, 110.6, 60.7, 42.2, 34.2, 30.2, 24.3, 19.0, 14.1, 14.0; **IR** (film, cm⁻¹): 3399, 2923, 2853, 1720, 1637, 796; **HRMS (ESI) calcd.** for C₁₉H₂₀ClNO₂ (m/z M+H⁺): 330.1261, found: 330.1254.

FIG. S4



By following the general procedure **A** described above, **JWU-A033** was prepared in 25% yield. $^1\text{H NMR}$ (CD_2Cl_2 , 600 MHz): δ , ppm 8.18 (1H, s), 7.95 (1H, s), 7.38 (1H, d, $J = 1.6$ Hz), 7.24 (1H, d, $J = 8.1$ Hz), 7.14 (2H, d, $J = 8.9$ Hz), 7.01 (1H, dd, $J = 2.8, 8.9$ Hz), 6.94 (1H, d, $J = 2.8$ Hz), 6.88 (1H, dd, $J = 2.0, 8.1$ Hz), 6.32 (1H, dd, $J = 3.1, 5.1$ Hz), 5.71 (1H, dd, $J = 3.4, 5.5$ Hz), 3.29 (1H, d, $J = 15.7$ Hz), 3.27 (1H, dd, $J = 3.3, 3.3$ Hz), 3.11 (1H, d, $J = 14.2$ Hz), 2.70 (1H, dd, $J = 3.3, 4.8$ Hz), 2.25 (1H, d, $J = 8.4$ Hz), 2.12–2.08 (1H, m), 1.19 (3H, d, $J = 11.3$ Hz); $^{13}\text{C NMR}$ (CD_2Cl_2 , 150 MHz): δ 140.9, 139.6, 134.4, 133.1, 132.8, 130.2, 128.7, 125.4, 124.8, 124.4, 121.6, 119.7, 118.7, 118.6, 113.0, 112.1, 112.0, 111.6, 48.8, 40.2, 40.1, 39.0, 37.0, 21.7; **IR** (film, cm^{-1}): 3427, 2920, 2853, 1648, 1436, 1098, 737; **HRMS (ESI) calcd.** for $\text{C}_{24}\text{H}_{20}\text{Cl}_2\text{N}_2$ (m/z $\text{M}+\text{H}^+$): 407.1082, found: 407.1074.

FIG. S5

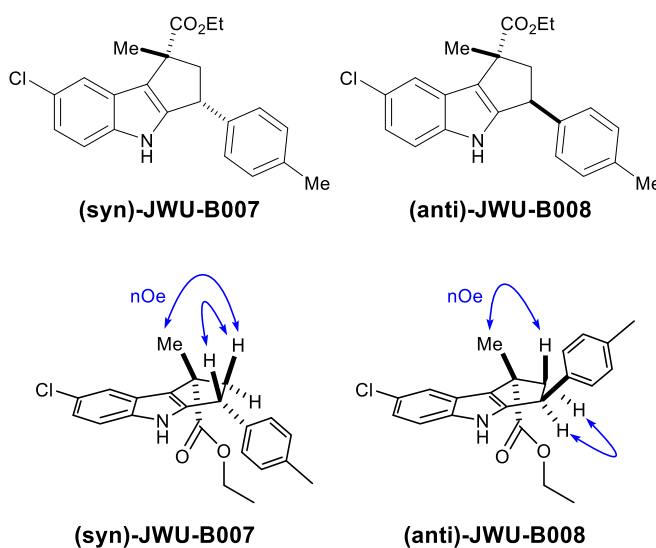


By following the general procedure **A** described above, **JWU-A034** was prepared in 58% yield. $^1\text{H NMR}$ (CD_2Cl_2 , 600 MHz): δ , ppm 7.87 (1H, s), 7.63 (1H, d, $J = 2.5$ Hz), 7.14 (1H, d, $J = 8.6$ Hz), 6.92 (1H, dd, $J = 2.7, 8.4$ Hz), 6.43 (1H, dd, $J = 2.9, 5.9$ Hz), 5.85 (1H, dd, $J = 3.5, 5.3$ Hz), 3.22 (1H, dd, $J = 3.0, 3.9$ Hz), 3.19 (1H, dd, $J = 3.2, 5.2$ Hz), 2.69–2.63

(1H, m), 2.56–2.50 (1H, m), 2.20–2.07 (3H, m), 2.06–1.99 (2H, m), 1.92 (1H, d, J = 10.8 Hz); ^{13}C NMR (CD₂Cl₂, 150 MHz): δ 142.0, 141.3, 133.2, 131.7, 128.9, 124.7, 119.8, 117.6, 111.8, 111.6, 49.8, 41.6, 41.1, 39.1, 35.3, 27.5, 15.0; IR (film, cm⁻¹): 3399, 2923, 2853, 1644, 1467, 1439, 1067, 741; HRMS (ESI) calcd. for C₁₇H₁₆ClN (m/z M+H⁺): 270.1050, found: 270.1050.

Characterization of Cyclopenta[b]indole products

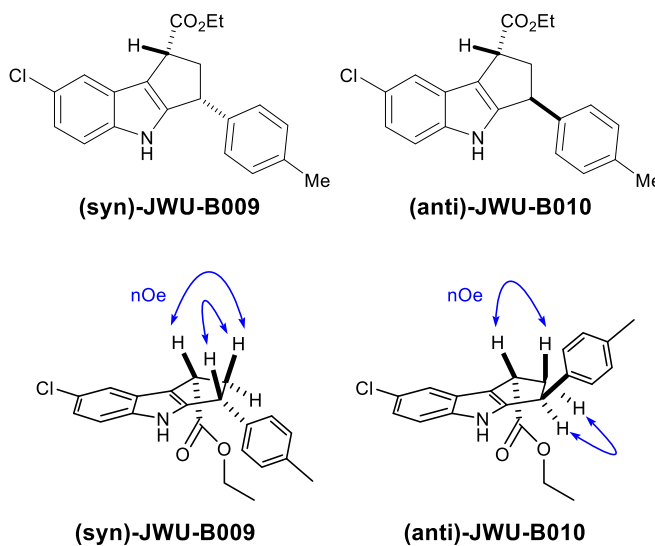
FIG. S6



By following the general procedure **B** described above, a 1:1 diastereomeric mixture (**syn**)-**JWU-B007** and (**anti**)-**JWU-B008** was prepared in 65% combined yield. For (**syn**)-**JWU-B007**, ^1H NMR (CD₂Cl₂, 600 MHz): δ , ppm 7.82 (1H, s), 7.57 (1H, d, J = 2.1 Hz), 7.12 (1H, d, J = 8.8 Hz), 7.04 (2H, d, J = 8.0 Hz), 6.99 (3H, ddd, J = 8.8, 8.8, 3.5 Hz), 4.36 (1H, dd, J = 6.9, 8.0 Hz), 4.12–4.07 (2H, m), 2.94 (1H, dd, J = 7.0, 13.5 Hz), 2.74 (1H, dd, J = 8.6, 13.3 Hz), 2.23 (3H, s), 1.54 (3H, s), 1.20 (3H, t, J = 7.9 Hz); ^{13}C NMR (CD₂Cl₂, 150 MHz): δ 176.0, 146.0, 139.9, 139.4, 136.6, 129.3, 127.4, 125.2, 124.6, 122.7, 121.2, 118.8, 112.5, 60.9, 51.5, 49.3, 43.3, 25.1, 20.7, 14.0; IR (film, cm⁻¹):

3423, 2923, 2860, 1644, 1449, 1289, 1025, 789; **HRMS (ESI) calcd.** for C₂₂H₂₂ClNO₂ (m/z M+H⁺): 368.1417, found: 368.1417; **For (anti)-JWU-B008**, ¹H NMR (CD₂Cl₂, 600 MHz): δ, ppm 7.83 (1H, s), 7.54 (1H, d, J = 1.5 Hz), 7.13 (1H, d, J = 8.9 Hz), 7.06 (2H, d, J = 7.5 Hz), 7.00 (3H, ddd, J = 5.7, 5.7, 13.9 Hz), 4.49 (1H, t, J = 7.9 Hz), 4.06–4.00 (2H, m), 3.54 (1H, dd, J = 9.0, 13.2 Hz), 2.25 (3H, s), 2.11 (1H, dd, J = 8.2, 12.9 Hz), 1.65 (3H, s), 1.15 (3H, t, J = 8.2 Hz); ¹³C NMR (CD₂Cl₂, 150 MHz): δ 175.7, 146.7, 140.2, 139.3, 136.6, 129.4, 127.4, 125.2, 124.7, 122.5, 121.1, 118.3, 112.6, 60.9, 52.7, 49.5, 44.2, 25.2, 20.7, 14.0; **IR** (film, cm⁻¹): 3421, 2918, 2853, 1640, 1374, 1287, 861; **HRMS (ESI) calcd.** for C₂₂H₂₂ClNO₂ (m/z M+H⁺): 368.1417, found: 368.1409.

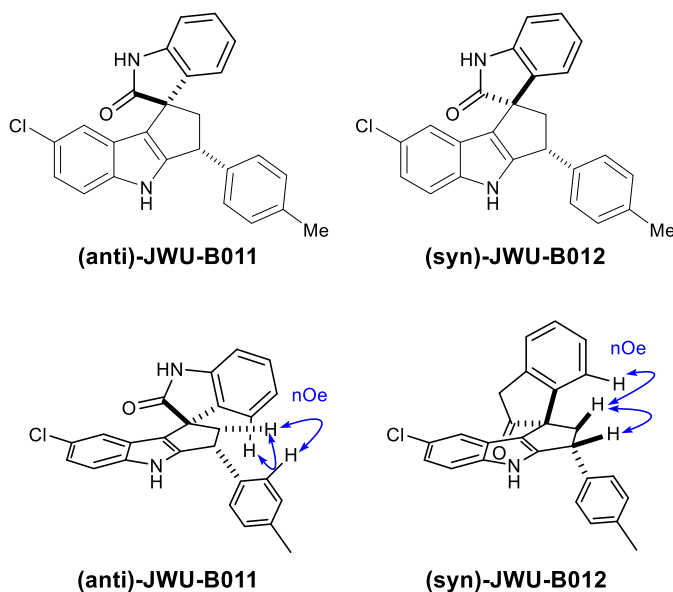
FIG. S7



By following the general procedure **B** described above, a 1:1 diastereomeric mixture **(syn)-JWU-B009** and **(anti)-JWU-B010** as prepared in 44% combined yield. **For (syn)-JWU-B009**, ¹H NMR (CD₂Cl₂, 600 MHz): δ, ppm 7.87 (1H, s), 7.54 (1H, s), 7.13 (1H, d, J = 8.3 Hz), 7.05 (4H, s), 7.00 (1H, d, J = 6.7 Hz), 4.32 (1H, dd, J = 7.6, 7.6 Hz), 4.15 (2H, dd, J = 6.4, 14.6 Hz), 4.03 (1H, dd, J = 7.0, 7.0 Hz), 3.19–3.13 (1H, m), 2.67–2.61 (1H, m), 2.23

(3H, s), 1.25 (3H, t, $J = 7.2$ Hz); $^{13}\text{C-NMR}$ (CD_2Cl_2 , 150 MHz): δ 173.6, 147.5, 140.0, 139.5, 136.7, 129.3, 127.5, 125.3, 125.1, 121.3, 118.8, 117.4, 112.5, 60.9, 44.0, 43.1, 42.7, 20.7, 14.1; **IR** (film, cm^{-1}): 3583, 3357, 2916, 2850, 1713, 1289, 1070, 657; **HRMS (ESI) calcd.** for $\text{C}_{21}\text{H}_{20}\text{ClNO}_2$ (m/z $\text{M}+\text{H}^+$): 354.1261, found: 354.1253; **For (anti)-JWU-B010**, $^1\text{H NMR}$ (CD_2Cl_2 , 600 MHz): δ , ppm 7.89 (1H, s), 7.51 (1H, d, $J = 2.2$ Hz), 7.13 (1H, d, $J = 9.1$ Hz), 7.03 (2H, d, $J = 8.0$ Hz), 6.99 (1H, dd, $J = 2.2, 8.8$ Hz), 6.95 (2H, d, $J = 8.0$ Hz), 4.48 (1H, dd, $J = 7.3, 7.3$ Hz), 4.13–4.07 (3H, m), 3.30–3.24 (1H, m), 2.52–2.47 (1H, m), 2.23 (3H, s), 1.22 (3H, t, $J = 8.1$ Hz); $^{13}\text{C NMR}$ (CD_2Cl_2 , 150 MHz): δ 173.7, 147.9, 140.3, 139.4, 136.6, 129.4, 127.1, 125.3, 125.0, 121.3, 118.6, 117.5, 112.6, 60.9, 43.9, 43.5, 42.9, 20.6, 14.1; **IR**(film, cm^{-1}): 3359, 2919, 2846, 1707, 1640, 1204, 1037, 857, 726; **HRMS (ESI) calcd.** for $\text{C}_{21}\text{H}_{20}\text{ClNO}_2$ (m/z $\text{M}+\text{H}^+$): 354.1261, found: 354.1261.

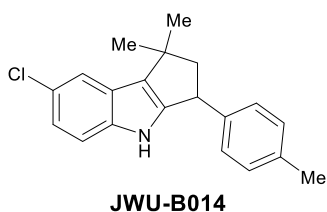
FIG. S8



By following the general procedure **B** described above, a 1:1 diastereomeric mixture of (anti)-JWU-B011 and (syn)-JWU-B012 was prepared in 27% combined yield. **For (anti)-JWU-B011**, $^1\text{H NMR}$ (CD_2Cl_2 , 600 MHz): δ , ppm 8.01 (1H, s), 7.69 (1H, s), 7.25

(2H, d, $J = 8.8$ Hz), 7.18–7.10 (4H, m), 7.01 (1H, d, $J = 7.7$ Hz), 6.94 (1H, dd, $J = 2.1, 8.8$ Hz), 6.90 (2H, dd, $J = 7.0, 7.0$ Hz), 6.85 (1H, s), 4.76 (1H, t, $J = 8.0$ Hz), 3.11 (1H, dd, $J = 8.0, 13.9$ Hz), 2.96 (1H, dd, $J = 8.8, 14.6$ Hz), 2.26 (3H, s); $^{13}\text{C NMR}$ (CD_2Cl_2 , 150 MHz): δ 180.3, 148.9, 139.9, 139.6, 139.5, 137.0, 134.6, 129.4, 128.0, 127.8, 125.4, 123.4, 123.3, 122.7, 121.7, 120.1, 117.1, 112.8, 109.6, 54.0, 52.5, 44.5, 20.7; **IR** (film, cm^{-1}): 3397, 2918, 2360, 1709, 1465, 1290, 1098, 805; **HRMS (ESI) calcd.** for $\text{C}_{25}\text{H}_{19}\text{ClN}_2\text{O}$ (m/z $\text{M}+\text{H}^+$): 399.1261, found: 399.1257; **For (syn)-JWU-B012**, $^1\text{H NMR}$ (CDCl_3 , 600 MHz): δ , ppm 7.92 (1H, s), 7.47 (1H, s), 7.19 (3H, s), 7.11 (2H, ddt, $J = 6.7, 6.7, 6.7$ Hz), 6.99–6.94 (3H, m), 6.90 (2H, d, $J = 7.8$ Hz), 6.69 (1H, d, $J = 1.7$ Hz), 4.86 (1H, t, $J = 8.8$ Hz), 3.38 (1H, ddd, $J = 6.8, 6.8, 6.8$ Hz), 2.63 (1H, dd, $J = 9.6, 14.4$ Hz), 2.30 (3H, s); $^{13}\text{C NMR}$ (CDCl_3 , 150 MHz): δ 180.6, 148.6, 139.7, 139.6, 139.2, 137.1, 134.5, 129.6, 128.1, 127.9, 125.7, 123.6, 123.4, 122.9, 121.9, 120.1, 117.6, 112.6, 109.6, 54.1, 52.6, 44.6, 21.0; **IR** (film, cm^{-1}): 3273, 3186, 2923, 1692, 1619, 1468, 1339, 816; **HRMS (ESI) calcd.** for $\text{C}_{25}\text{H}_{19}\text{ClN}_2\text{O}$ (m/z $\text{M}+\text{H}^+$): 399.1261, found: 399.1249.

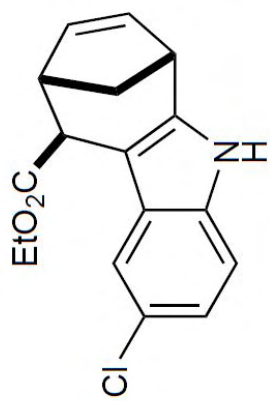
FIG. S9



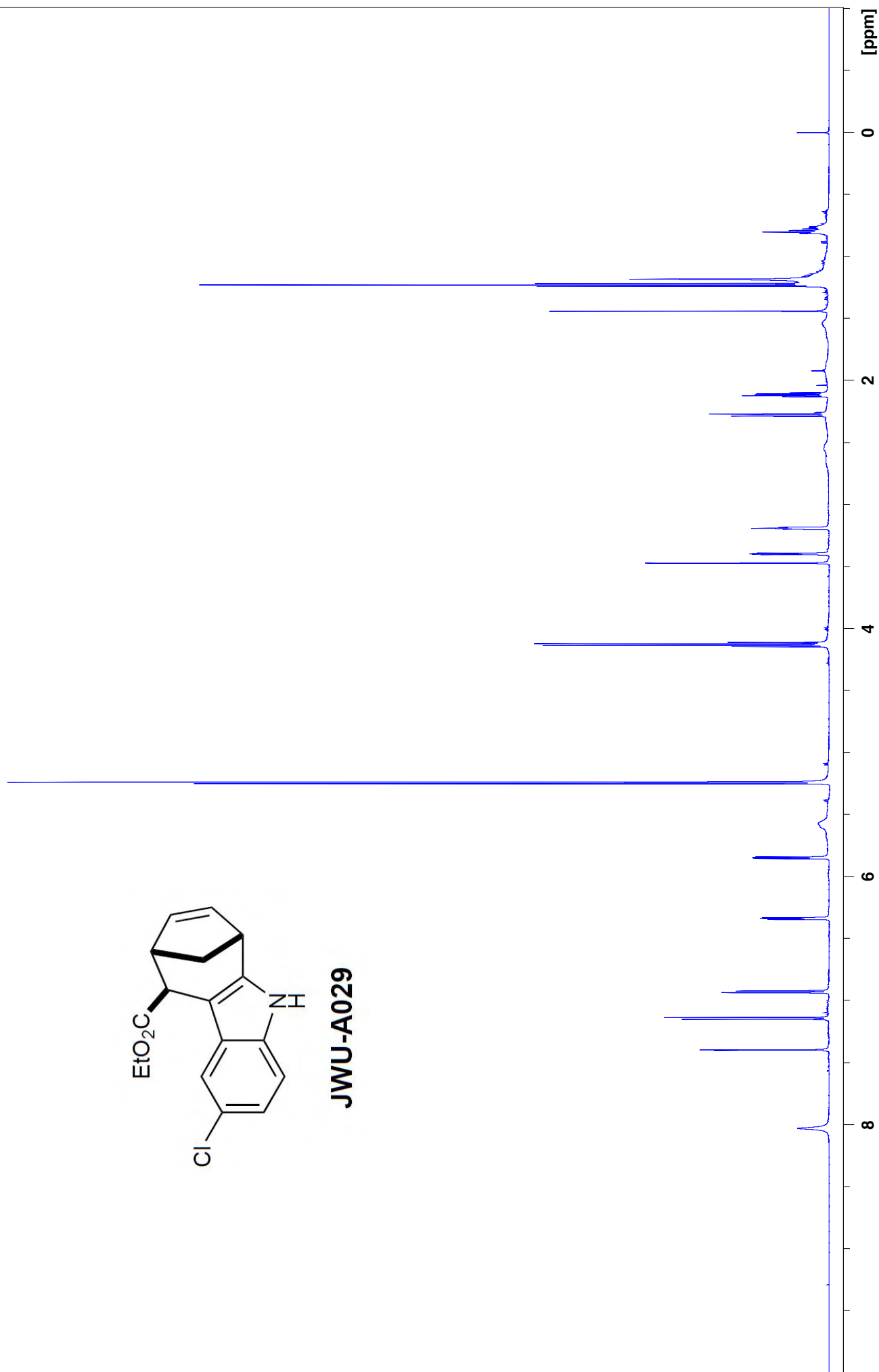
By following the general procedure **B** described above, **JWU-B014** was prepared in 25% yield. $^1\text{H NMR}$ (CDCl_3 , 600 MHz): δ , ppm 7.70 (1H, s), 7.43 (1H, s), 7.12 (1H, d, $J = 7.9$ Hz), 7.03 (4H, dd, $J = 8.3, 22.8$ Hz), 6.96 (1H, dd, $J = 1.4, 8.9$ Hz), 4.39 (1H, t, $J = 7.7$ Hz), 2.71 (1H, dd, $J = 8.8, 12.4$ Hz), 2.23 (3H, s), 2.15 (1H, dd, $J = 7.3, 11.7$ Hz), 1.42 (3H, s), 1.31 (3H, s); $^{13}\text{C NMR}$ (CDCl_3 , 150 MHz): δ 144.7, 140.9, 139.4, 136.3, 129.3, 128.4,

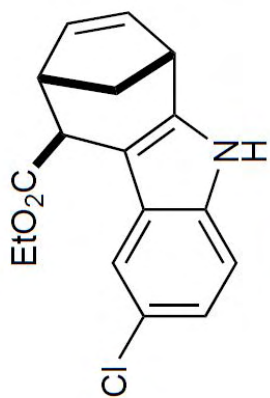
127.7, 124.7, 124.5, 120.6, 117.6, 112.5, 57.2, 44.1, 39.3, 29.4, 28.5, 20.7; **IR** (film, cm^{-1}); 3418, 2923, 2853, 1633, 1443, 1287, 1044, 812; **HRMS (ESI) calcd.** for $\text{C}_{20}\text{H}_{20}\text{ClN}$ (m/z $\text{M}+\text{H}^+$); 310.1363, found: 310.1363.

1. Han, X.; Li, H.; Hughes, R. P.; Wu, J. Gallium(III)-Catalyzed Three-Component (4+3) Cycloaddition Reactions. *Angew. Chem. Int. Ed.* **2012**, *52*, 10390–10393.

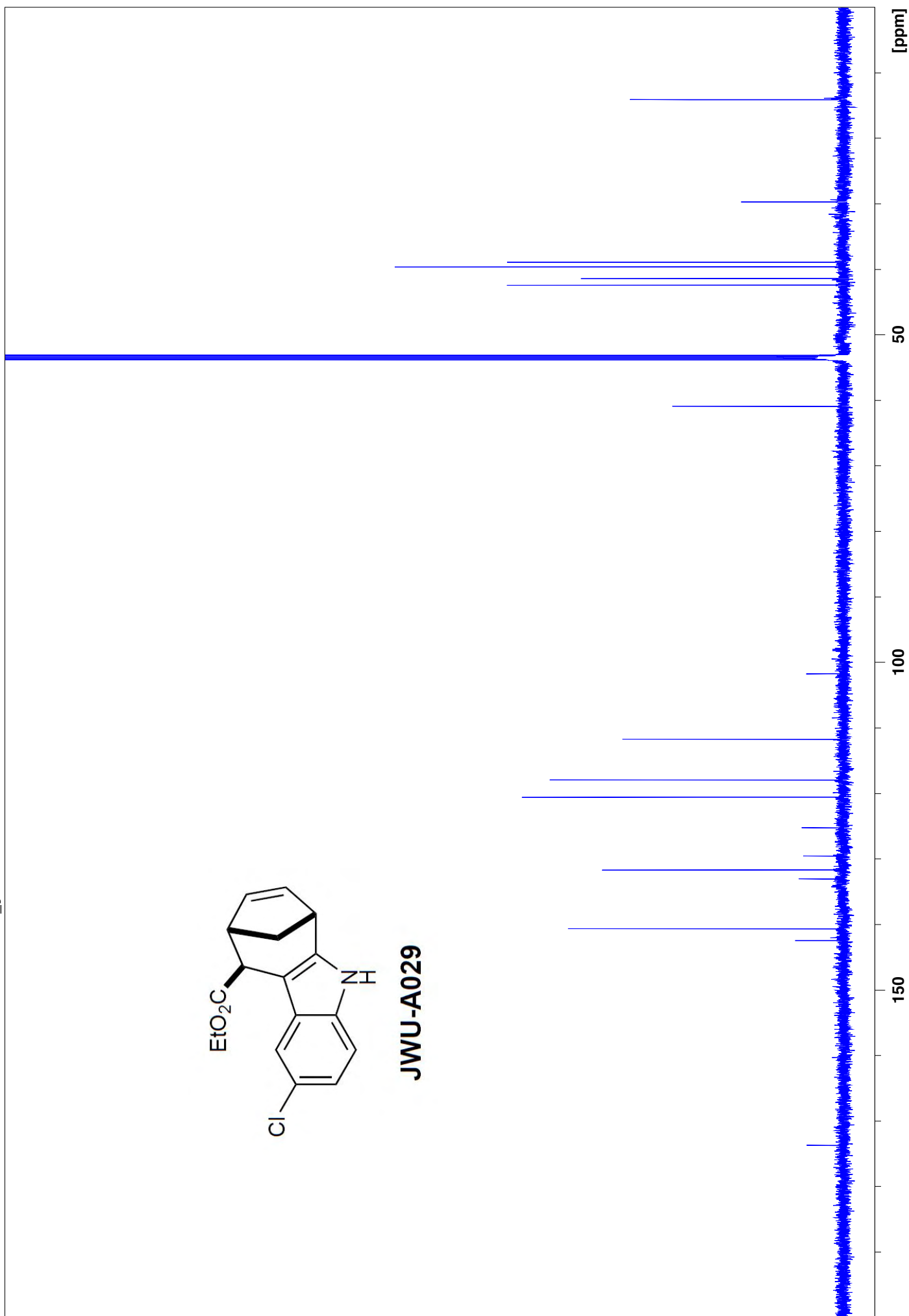


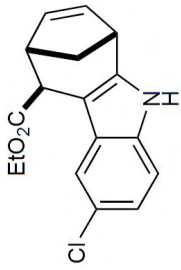
JWU-A029





JWU-A029

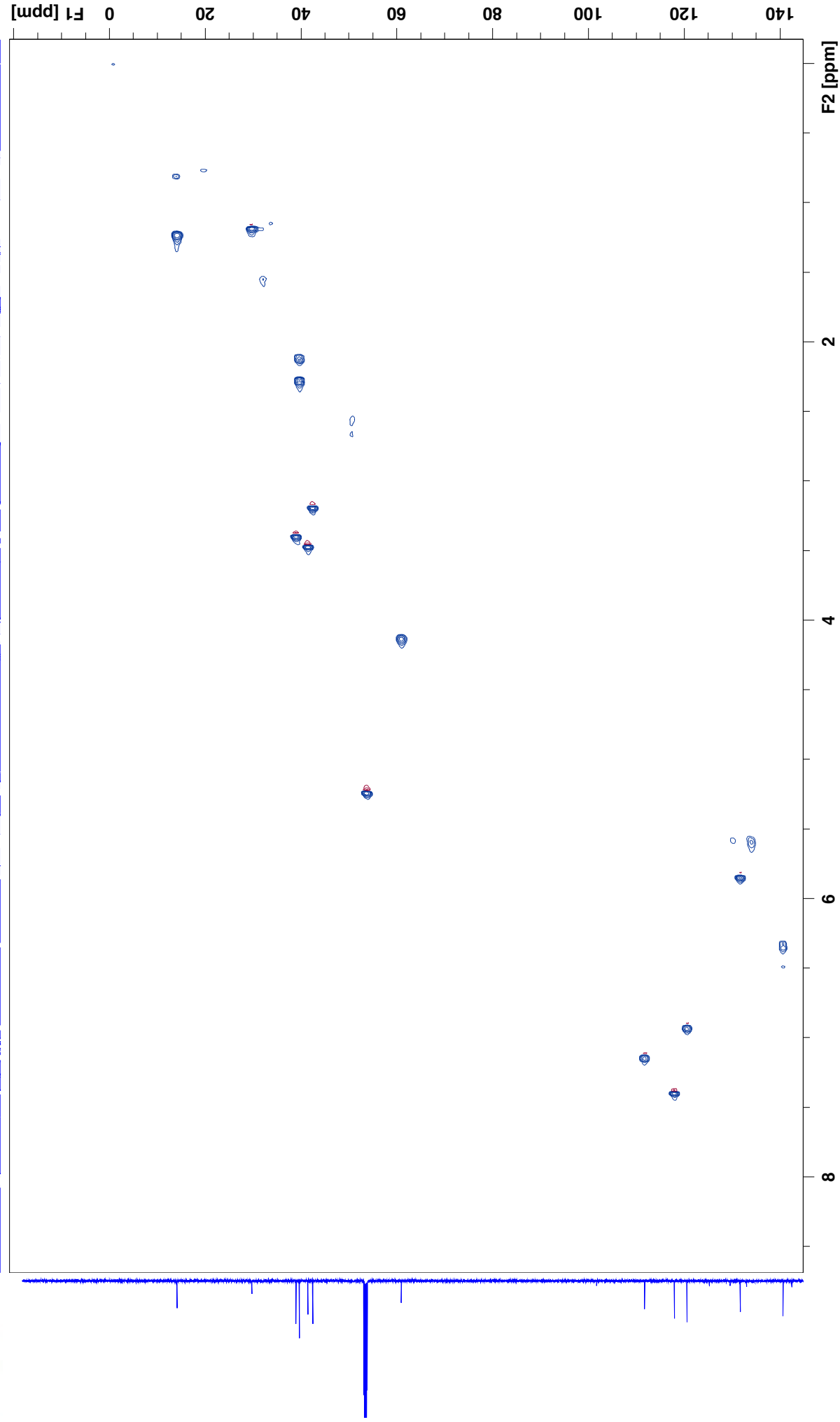




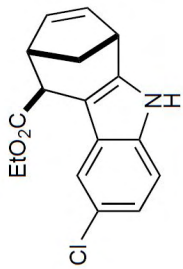
JWU-A029

MT-N3-P106-TT29-8-4-5 12 1 N:\b600\wu\data\wu_guest\nmr

HMQC



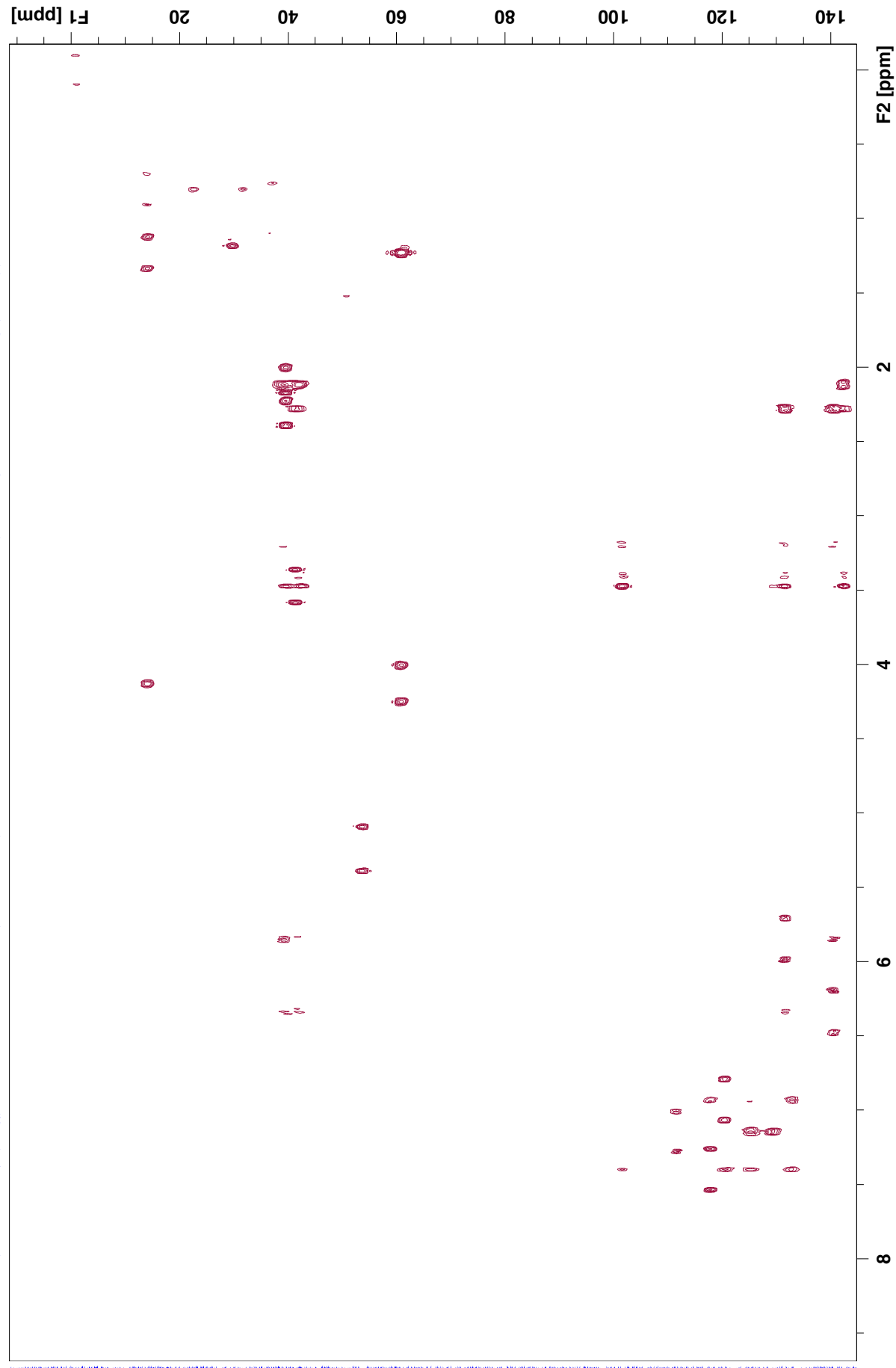
S14



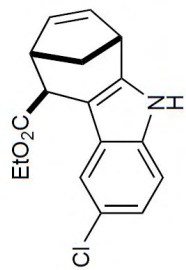
JWU-A029

MT-N3-P106-TT29-8-4-5 I3 1 N:\b600\wu\data\wu_guest\nmr

HMBC



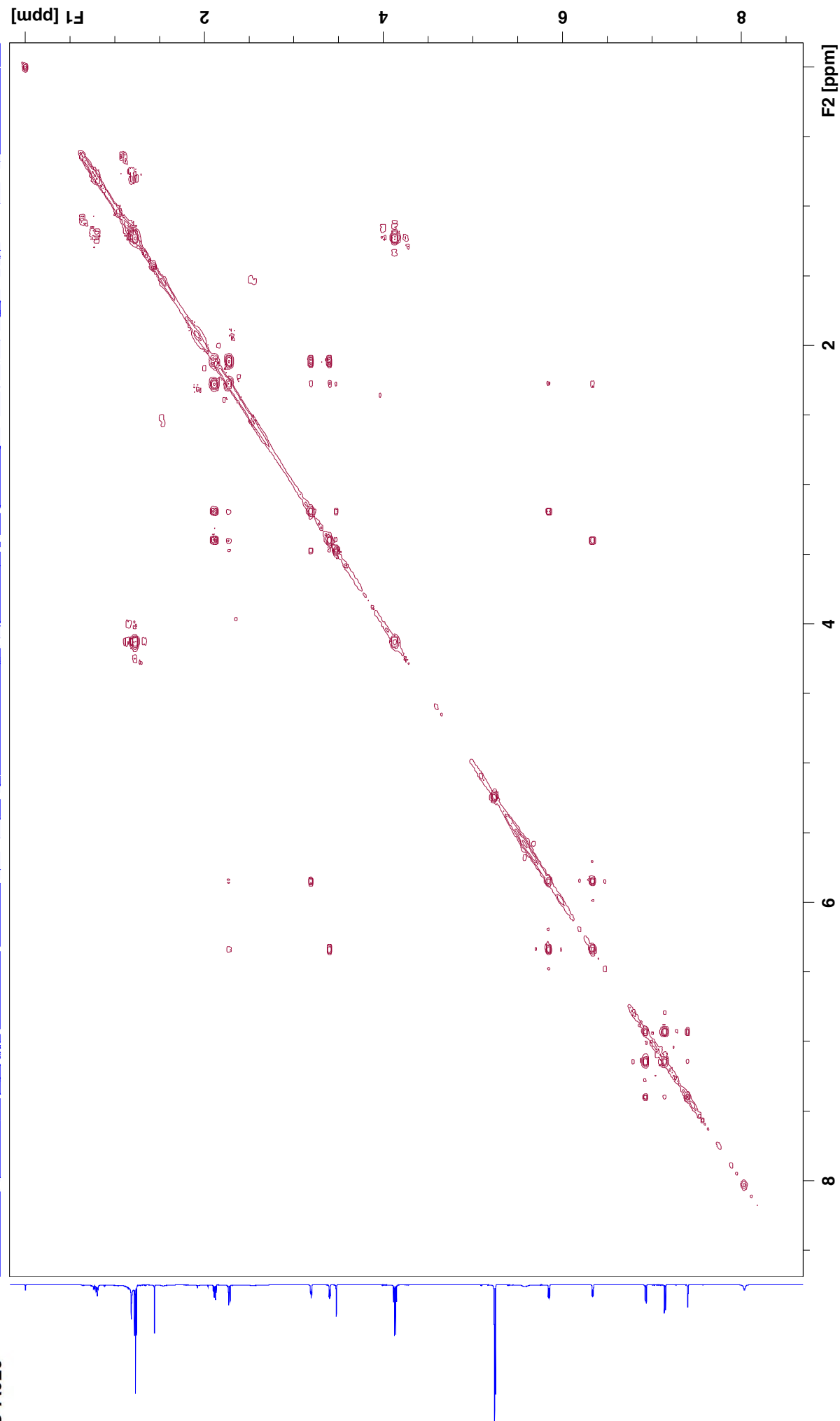
S15

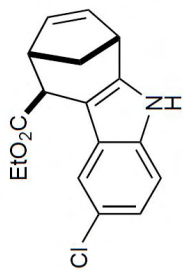


JWU-A029

MT-N3-P106-TT29-8-4-5 14 1 N:\b600\wu\data\wu_guest\nmr

COSY

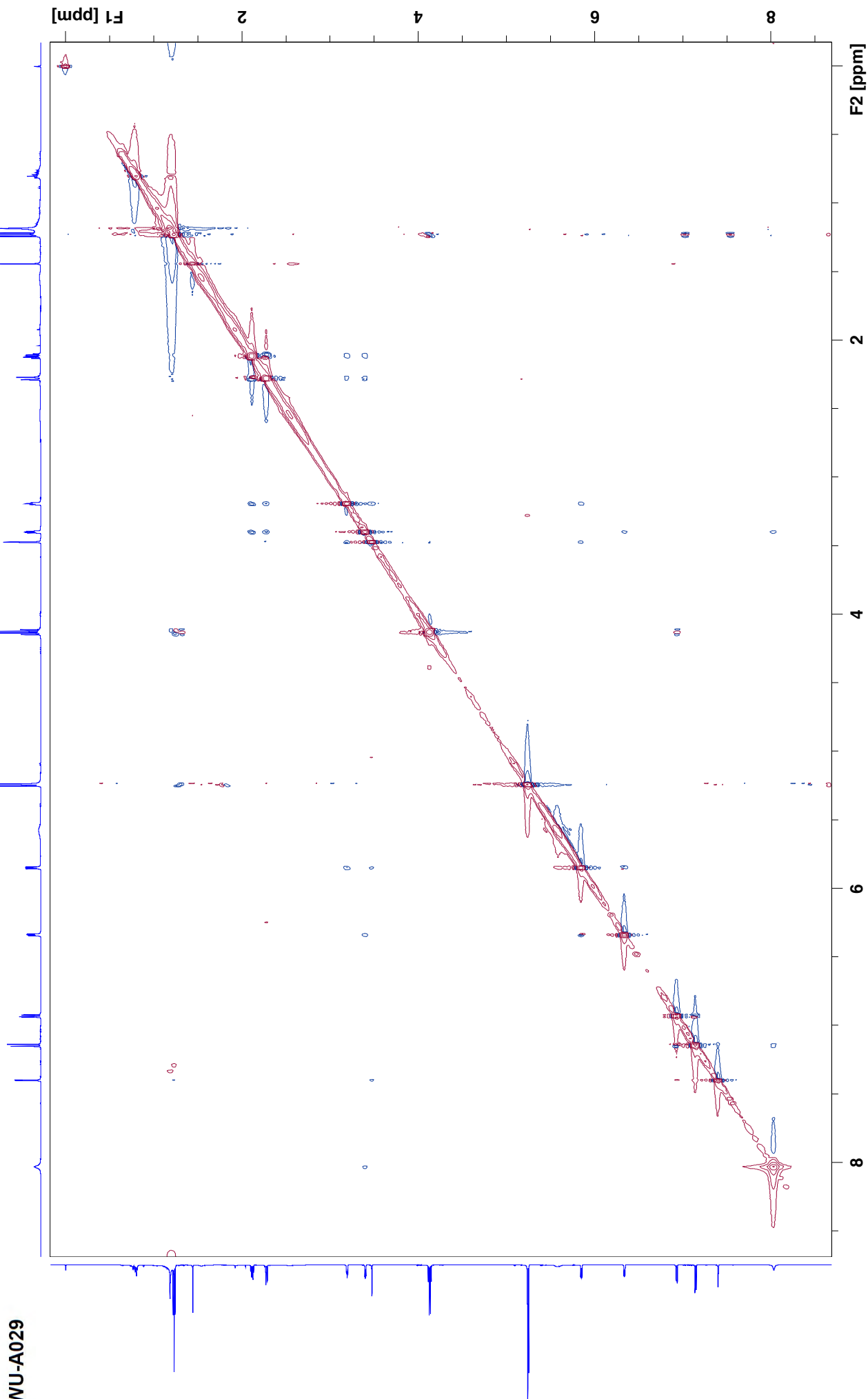


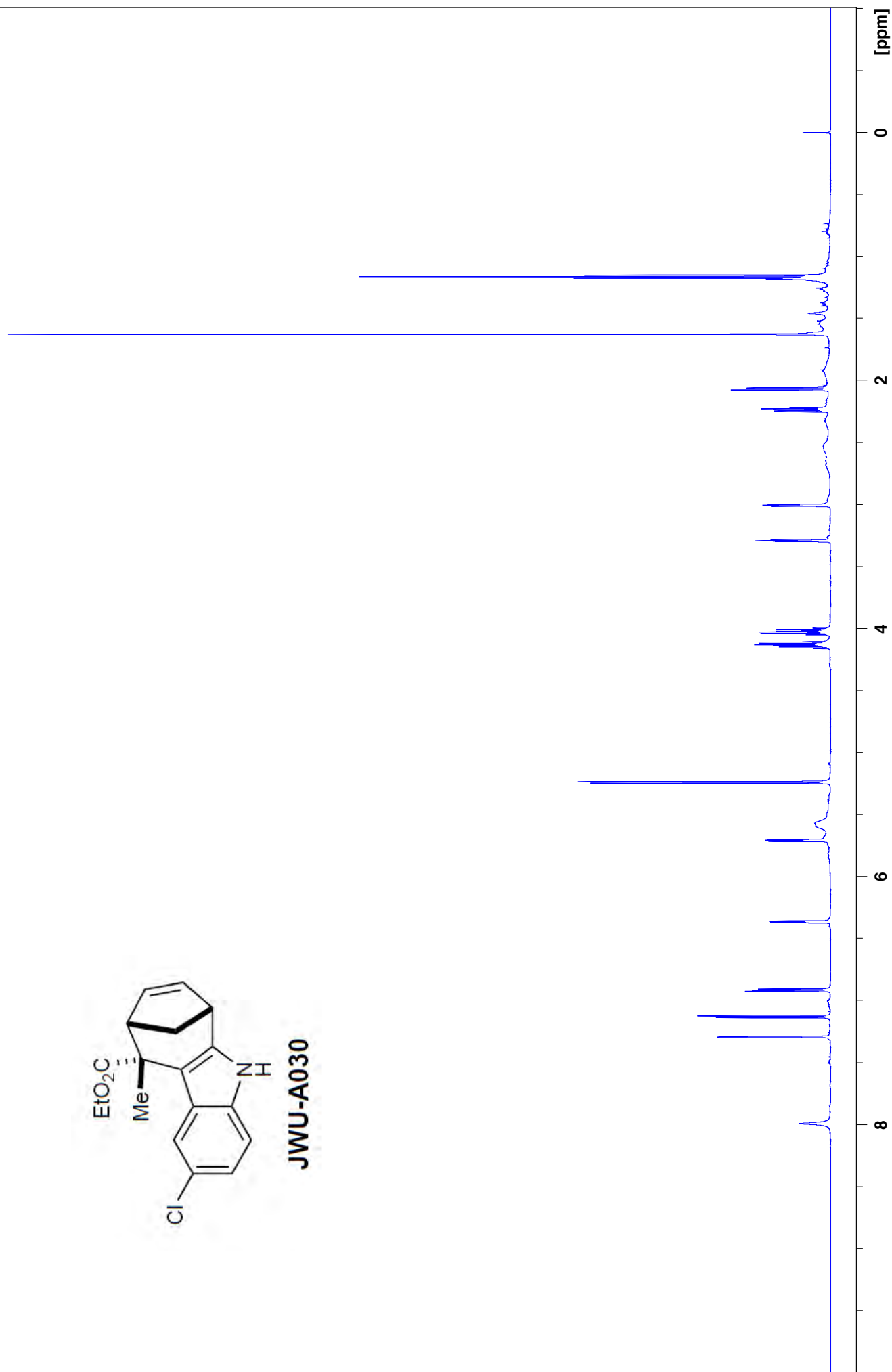
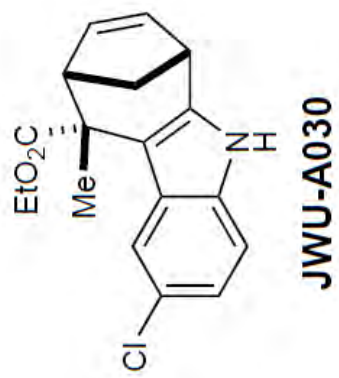


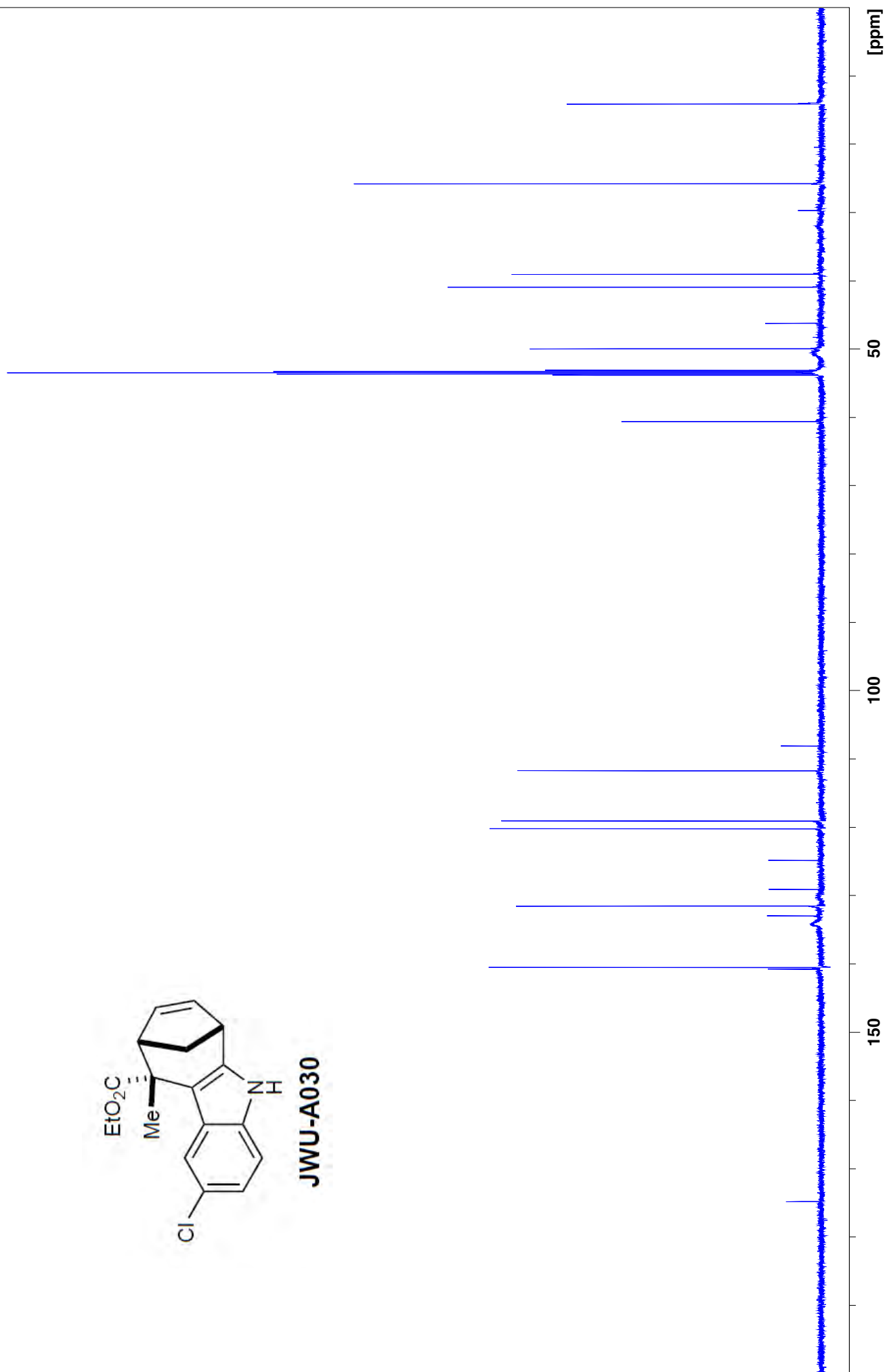
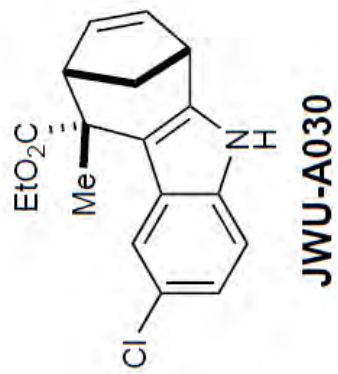
JWU-A029

MT-N3-P106-TR29-8-4-5 15 1 N:\b600\wu\data\wu_guest\nmr

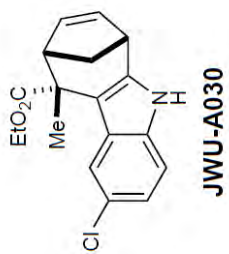
NOESY



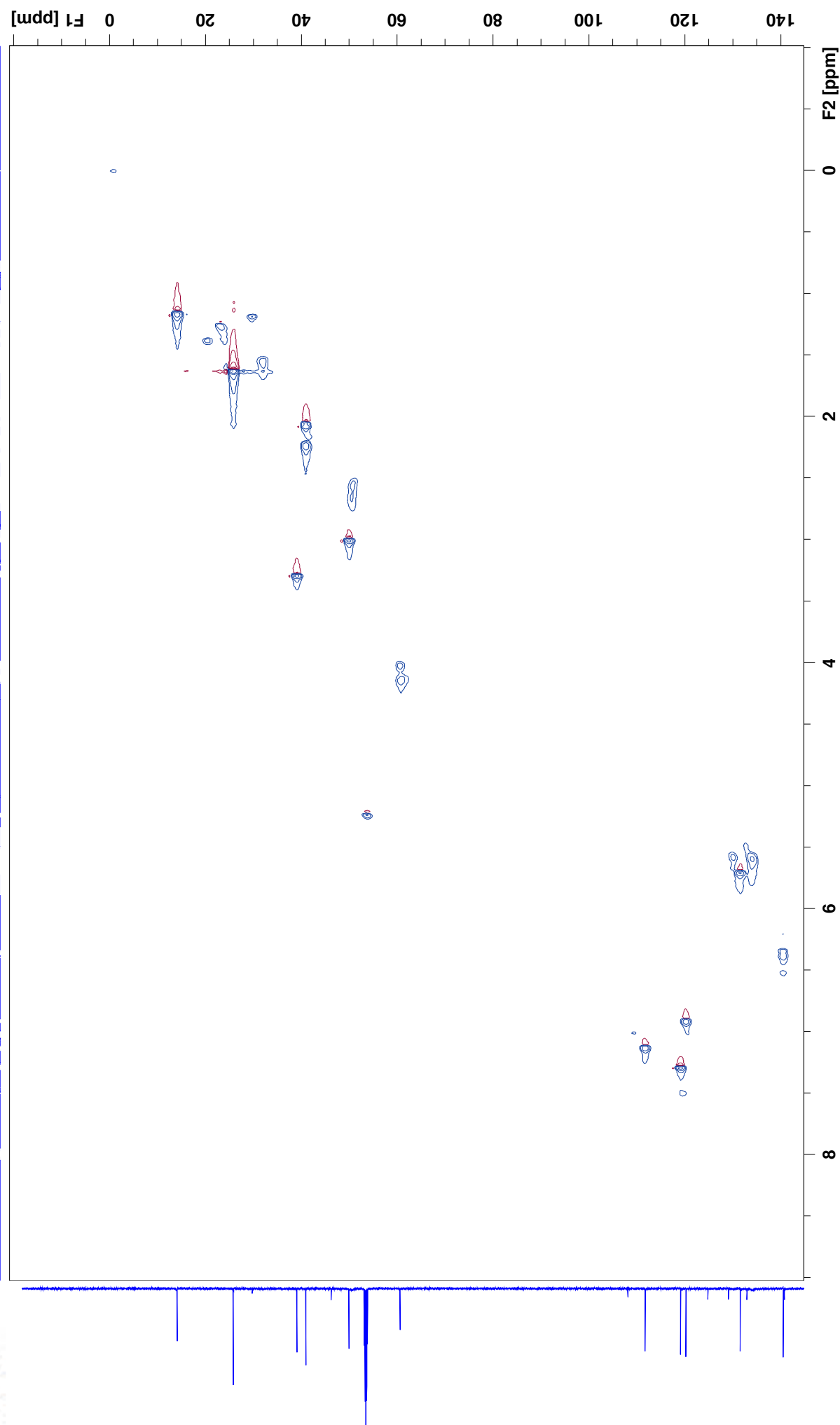




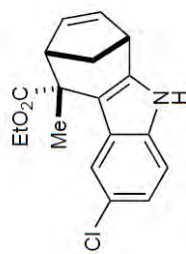
MT-N3-P102-TR26-5-5 13 1 N: \b600\wu\data\wu_guest\hmr



HMQC

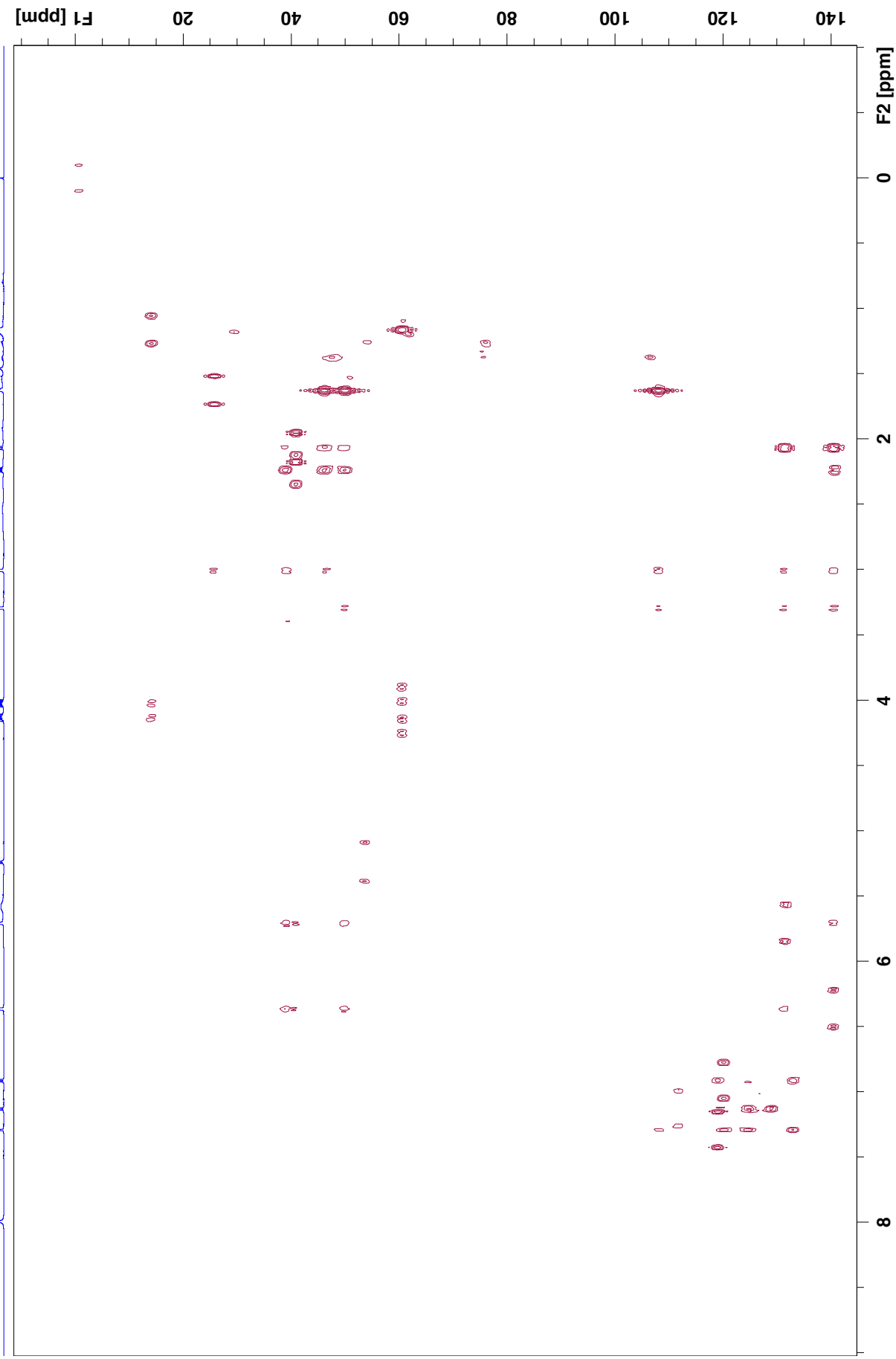


MT-N3-P102-TT26-5-5 14 1 N:\b600\wu\data\wu_guest\hmr

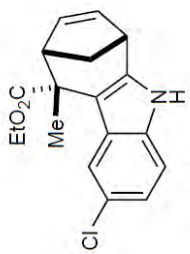


JWU-A030

HMBC

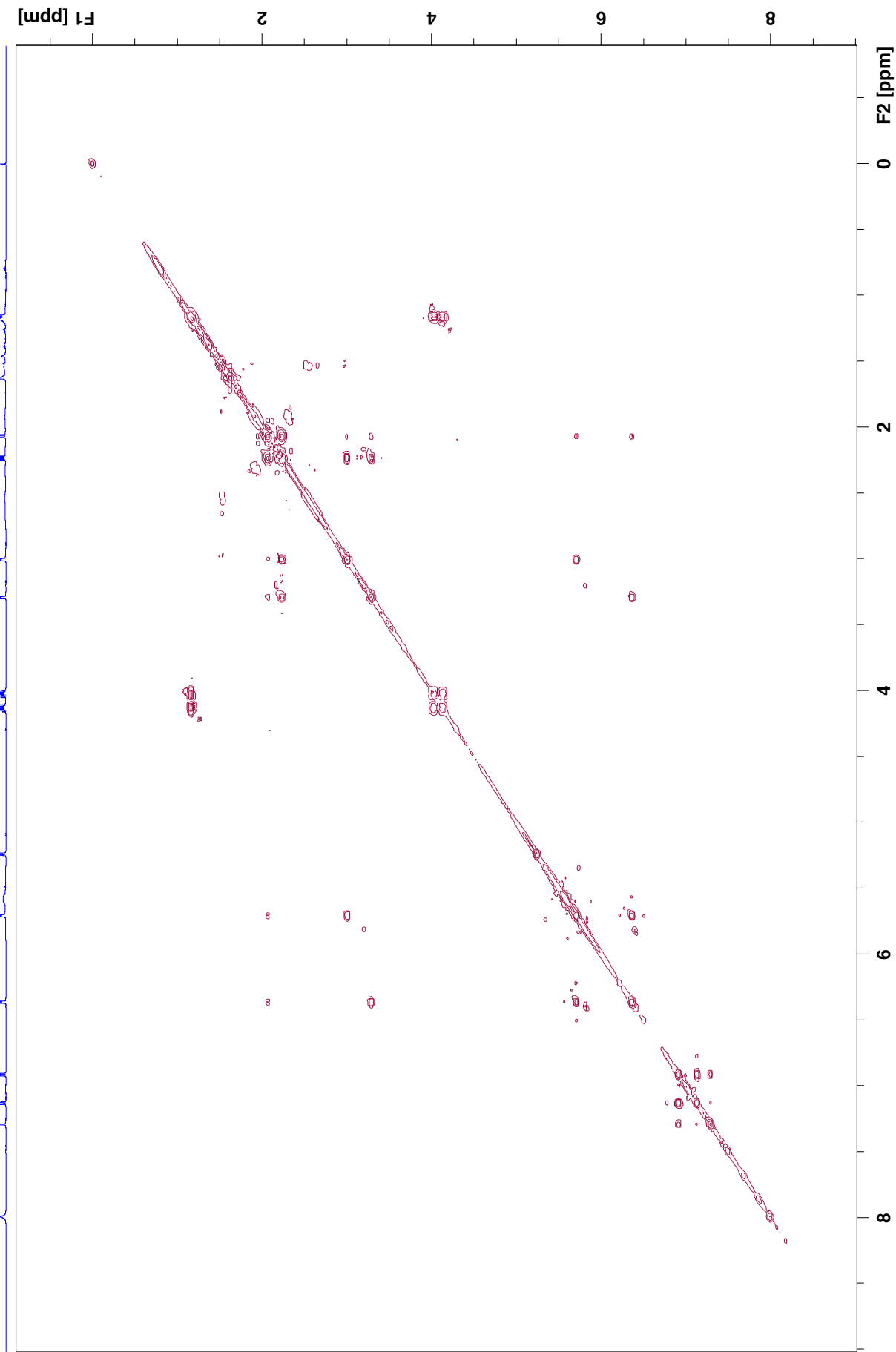


MT-N3-P102-TT26-5-5 16 1 N: \b600\wu\data\wu_guest\nmr

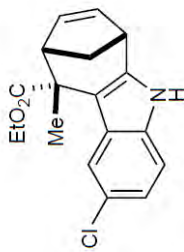


JWU-A030

COSY

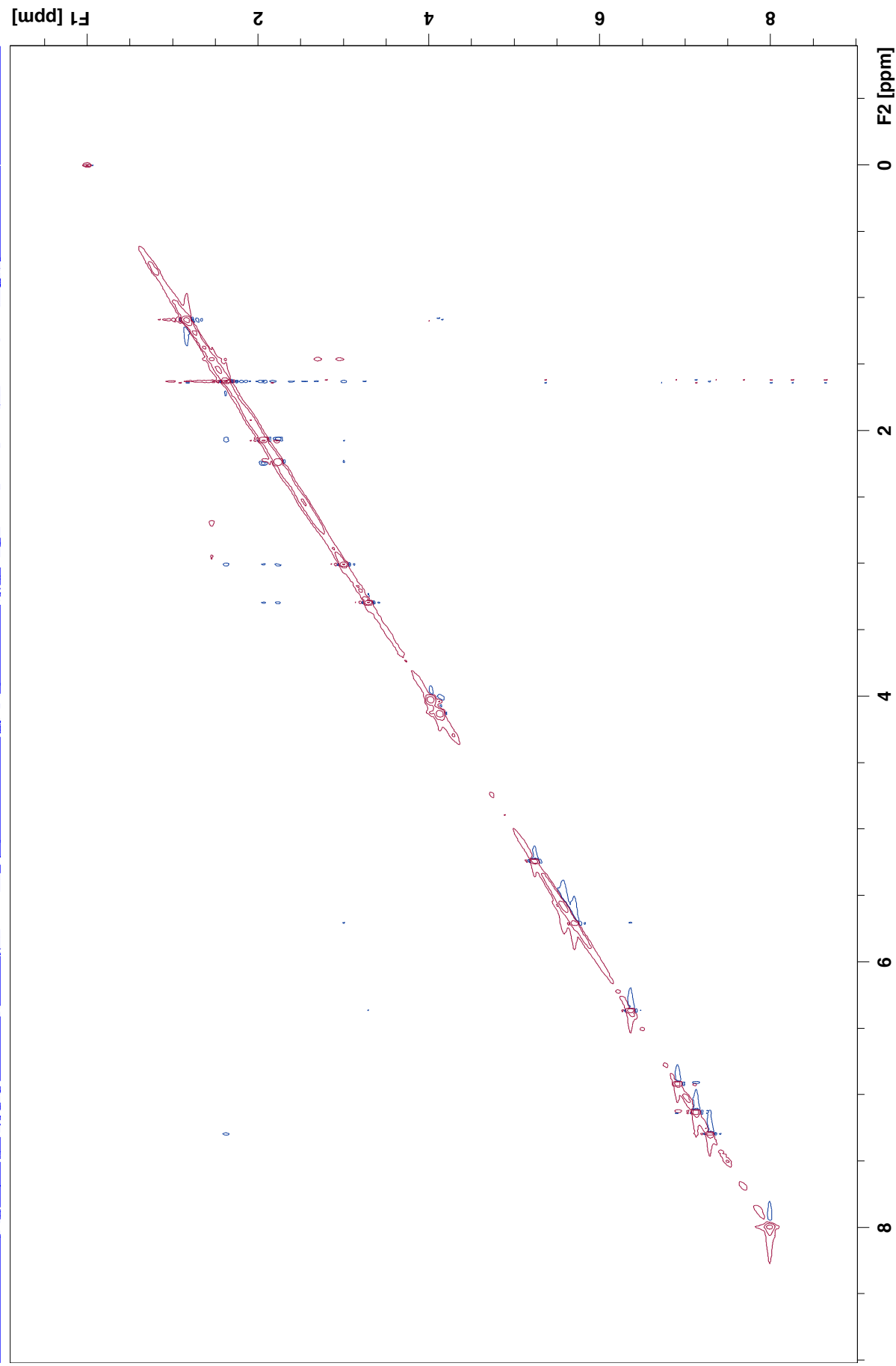


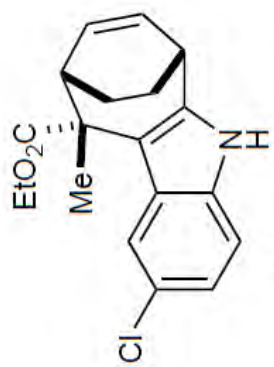
MT-N3-P102-IT26-5-5 15 1 N: \b600\wu\data\wu_guest\hmr



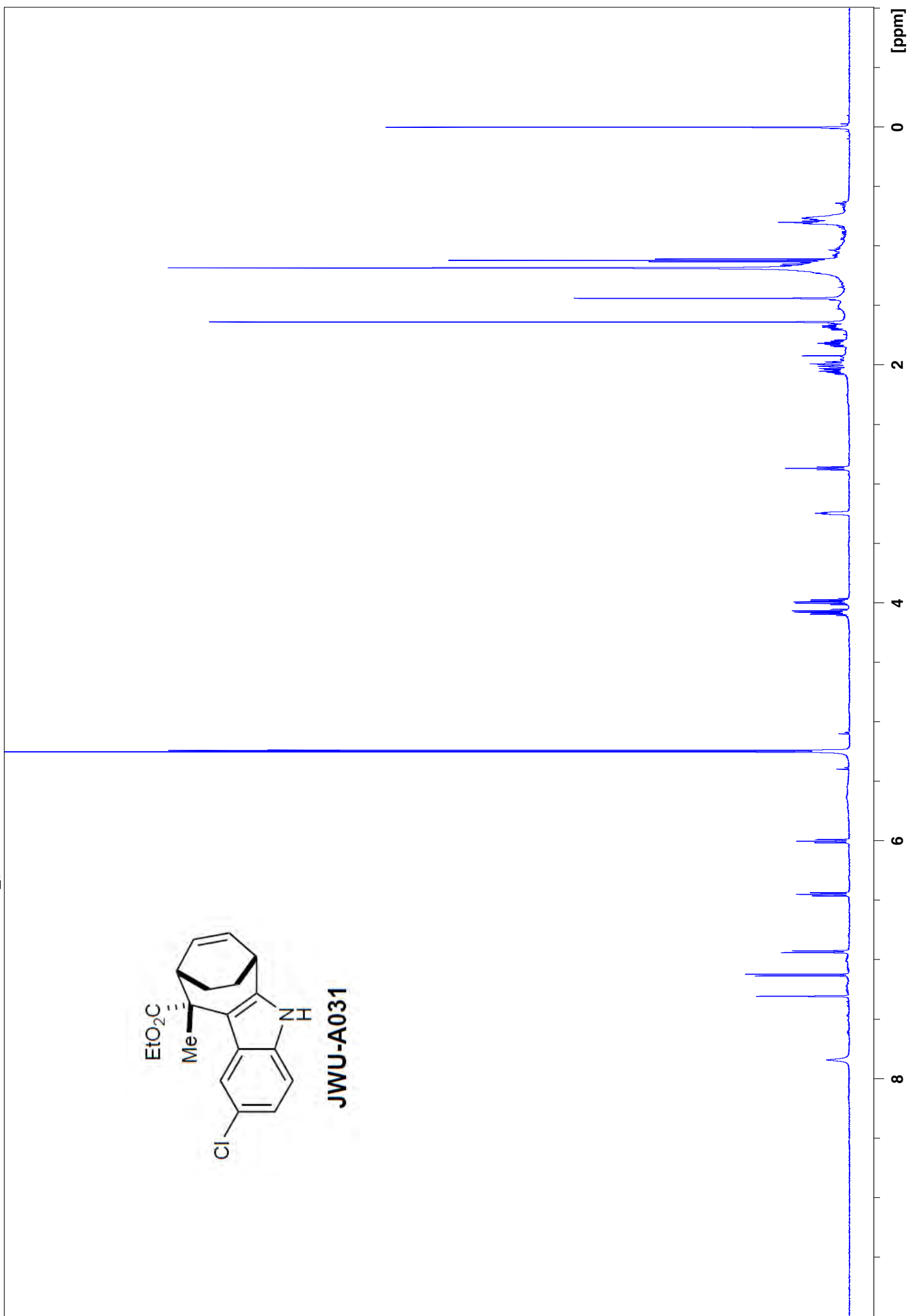
JWU-A030

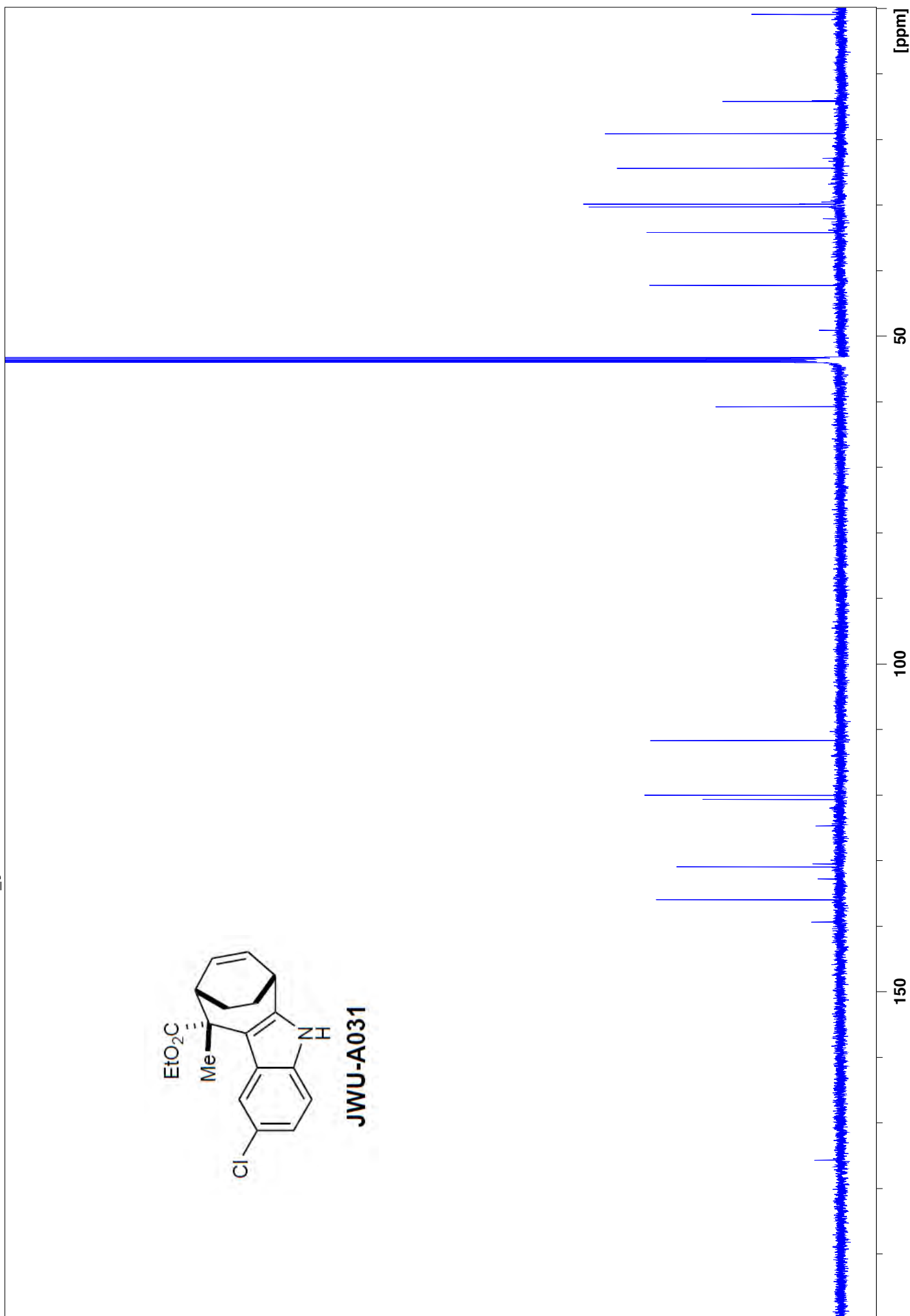
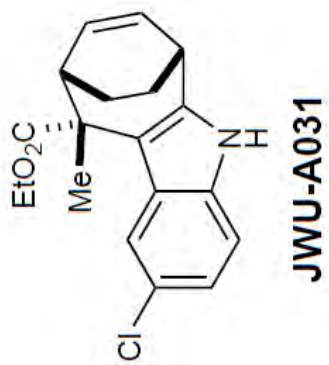
NOESY



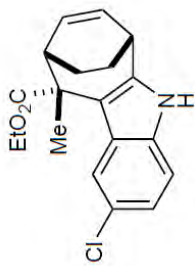


JWU-A031



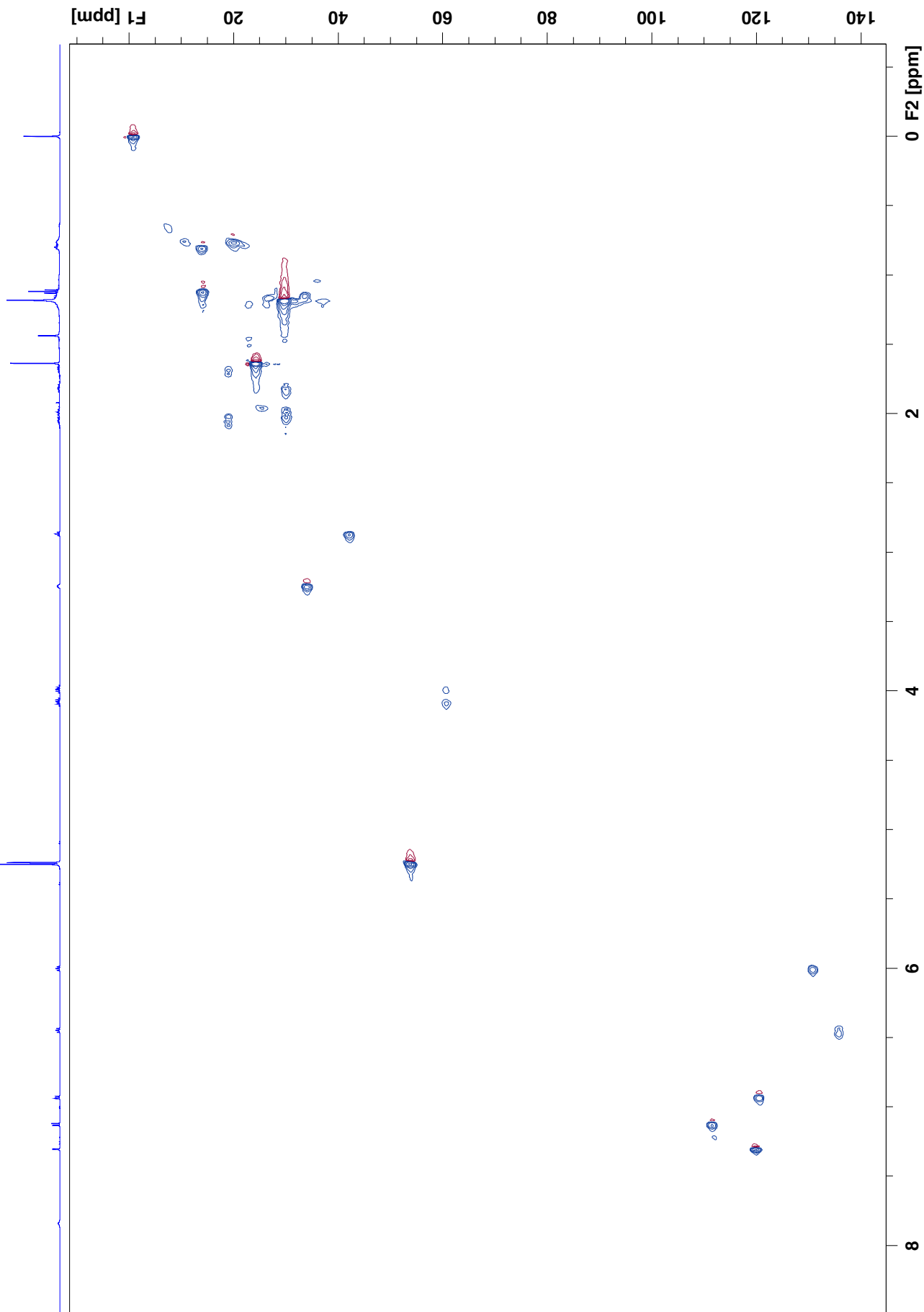


MT-N3-P154-TT14-15-ETOAc-2 12 1 N:\b600\wu\data\wu_guest\nmr



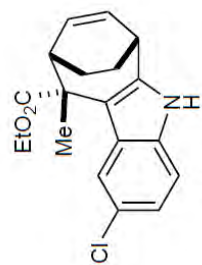
JWU-A031

HMQC



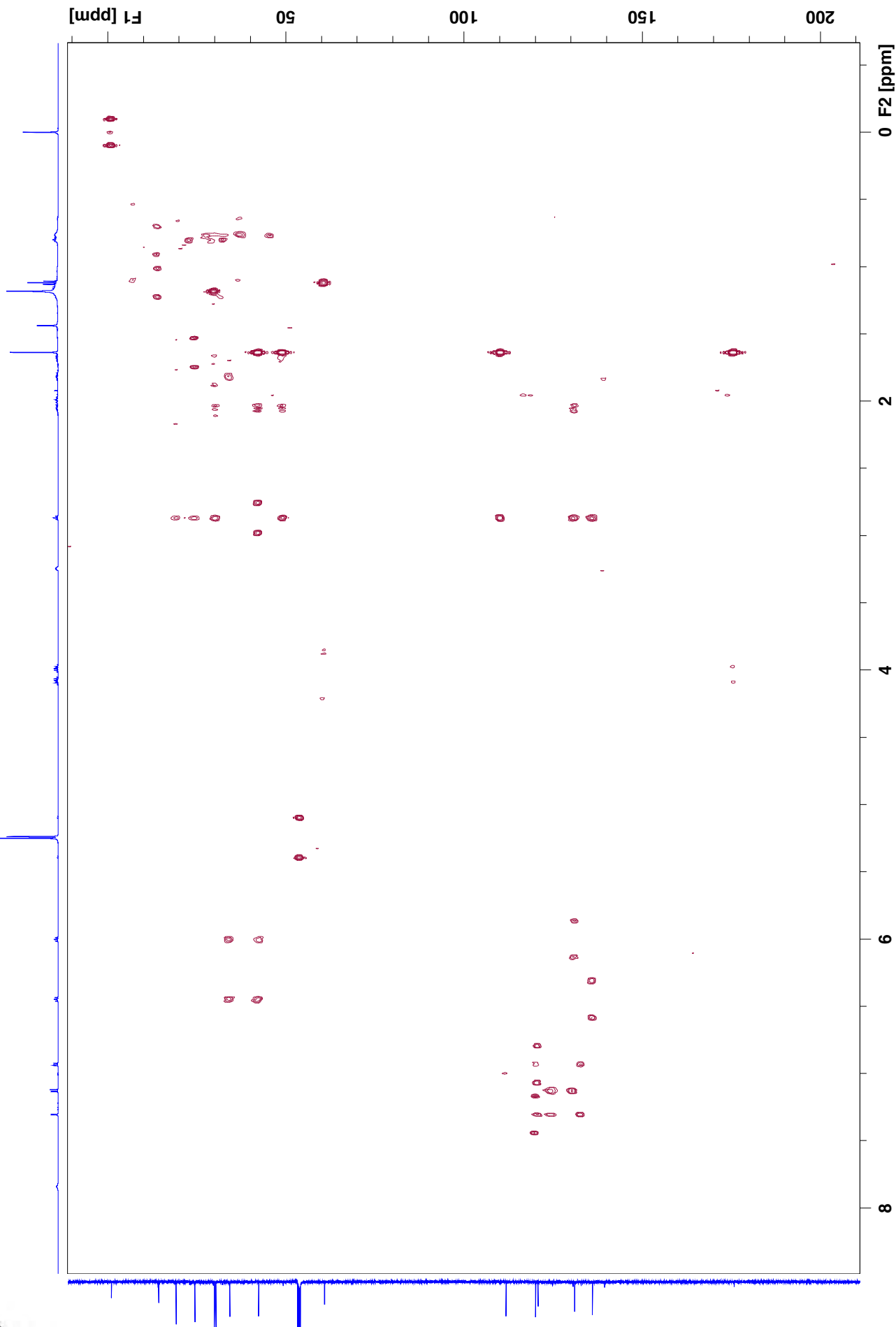
S26

MT-N3-P154-TT14-15-ETOAc-2 I1 1 N:\b600\wu\data\wu_guest\nmr

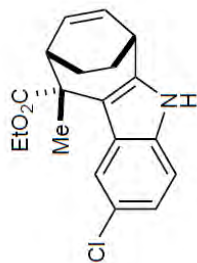


JWU-A031

HMBC

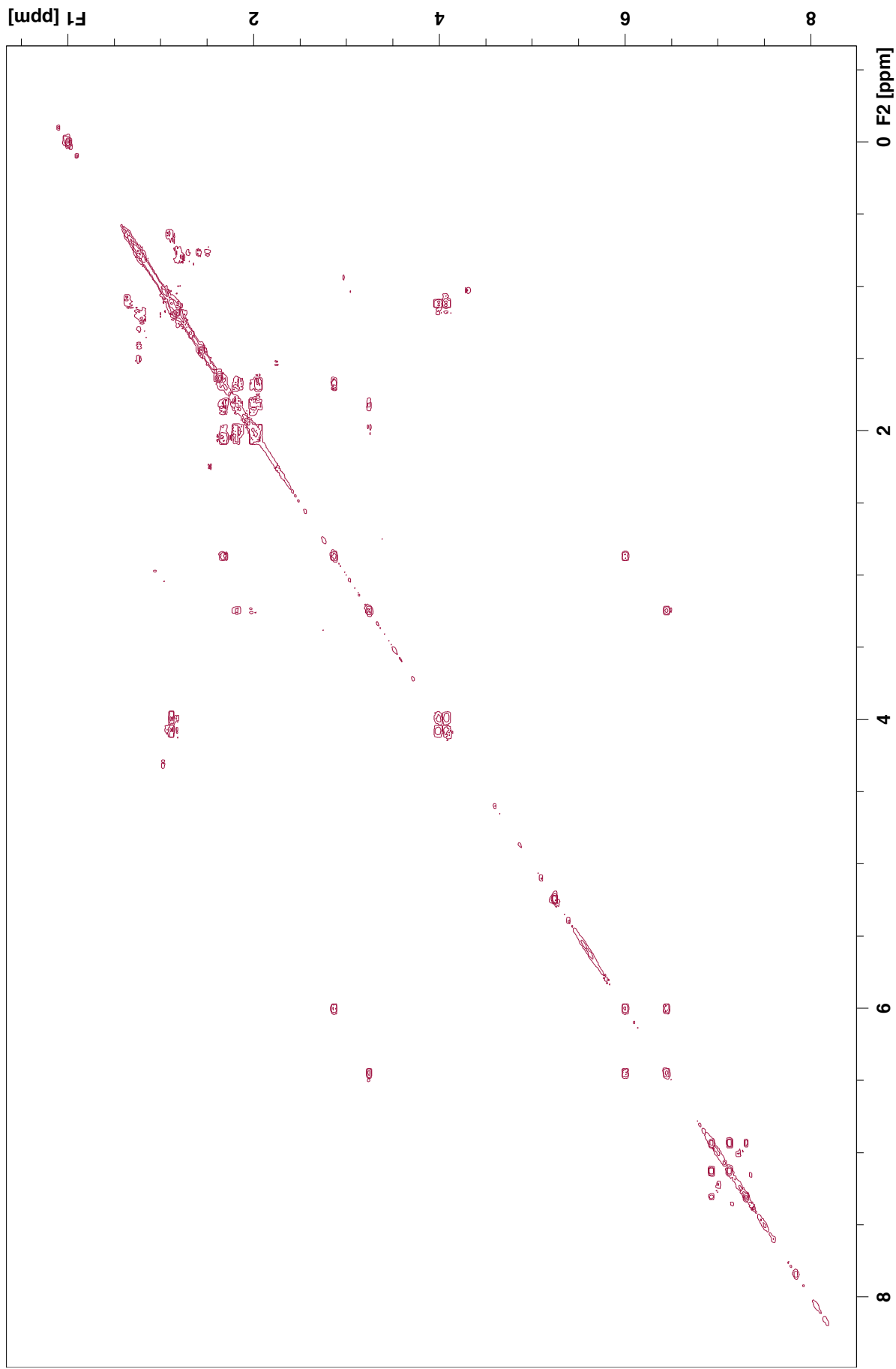


MT-N3-P154-TT14-15-ETOAc-3 I1 1 N:\b600\wu\data\wu_guest\nmr

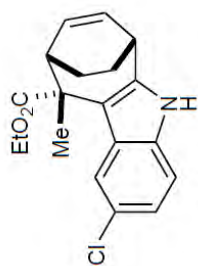


JWU-A031

COSY

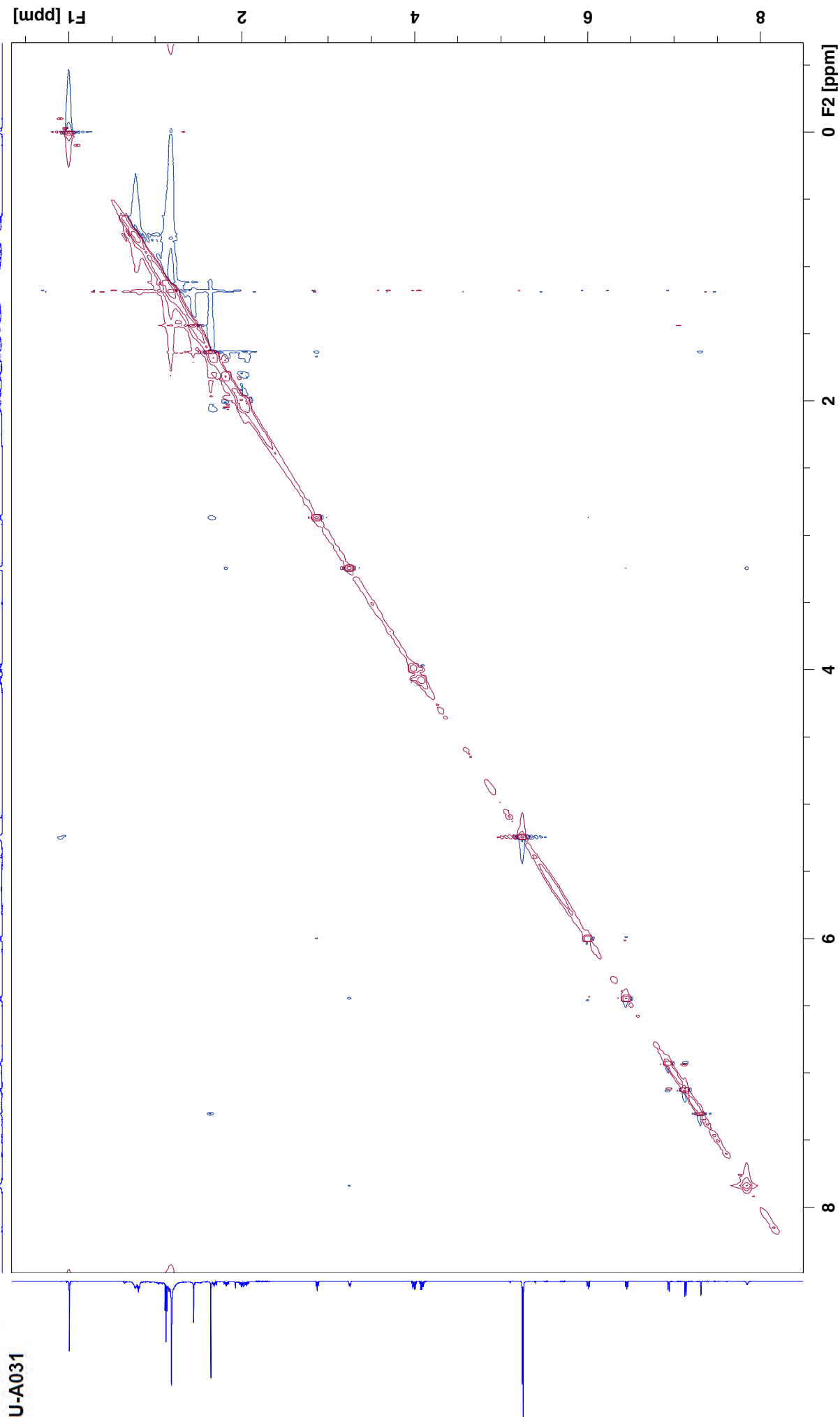


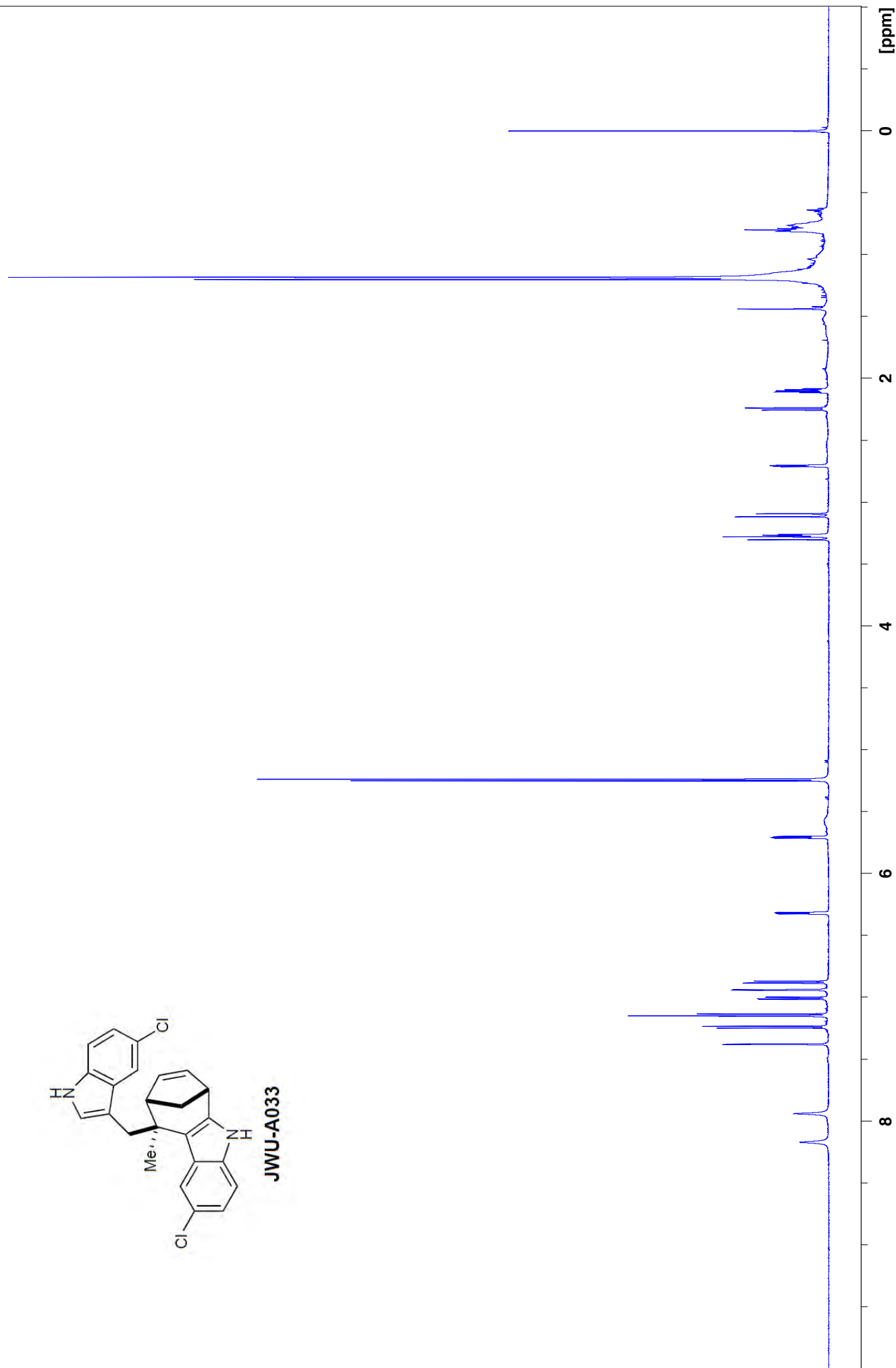
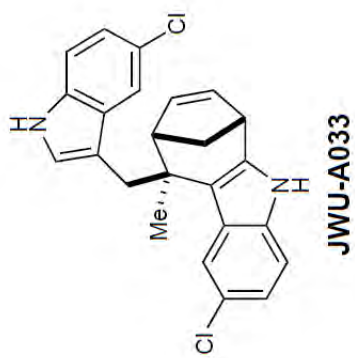
MT-N3-P154-TT14-15-ETOAc-2 13 1 N:\b600\wu\data\wu_guest\nmr

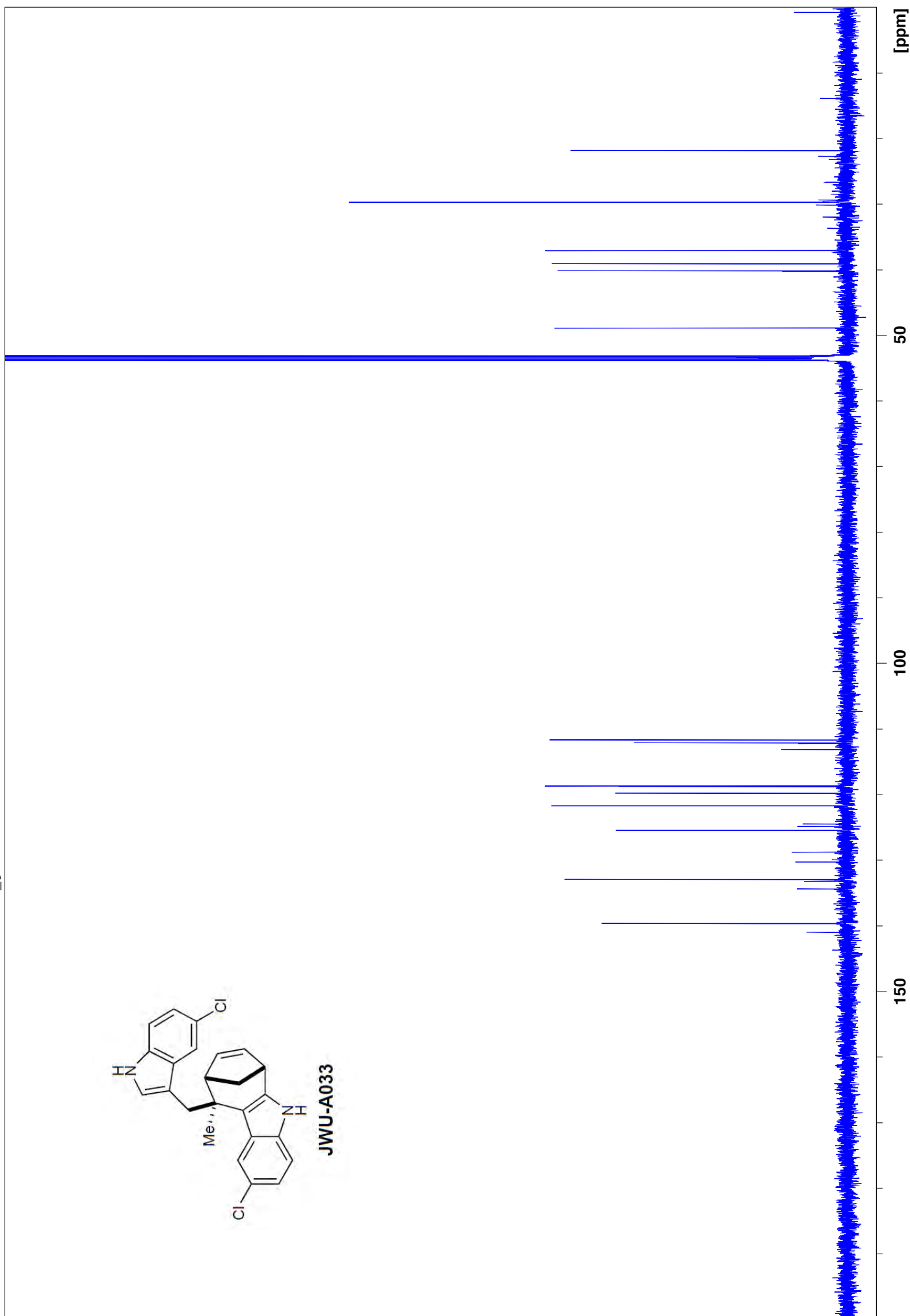
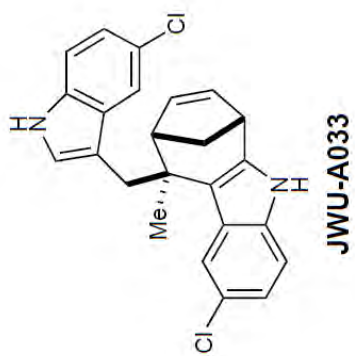


JWU-A031

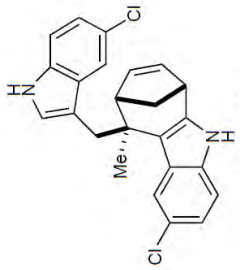
NOESY







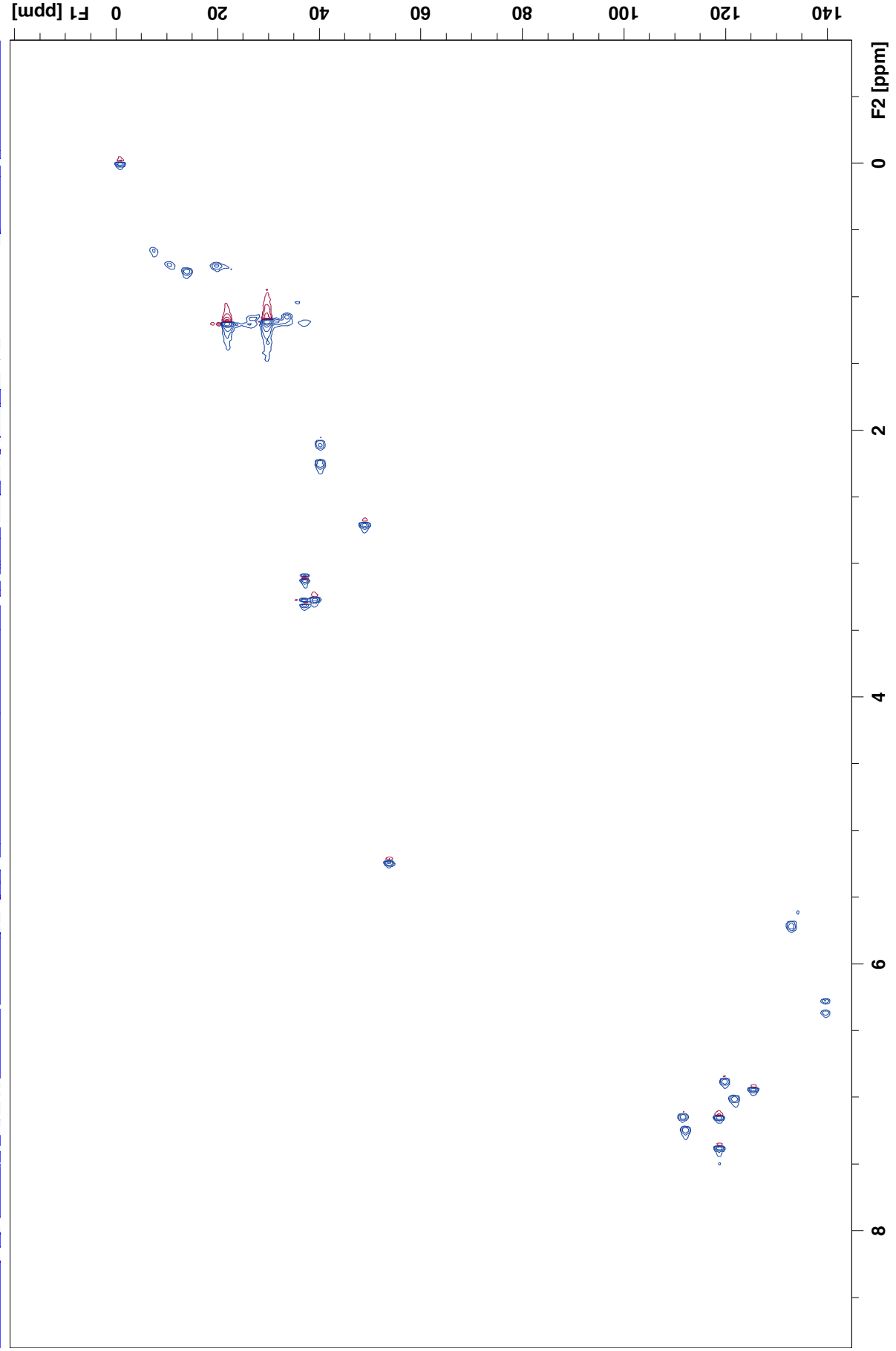
MT-N3-P128-TT22-24-5-6-C 14 1 N:\b600\wu\data\wu_guest\hmr



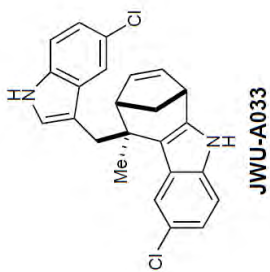
JWU-A033

S32

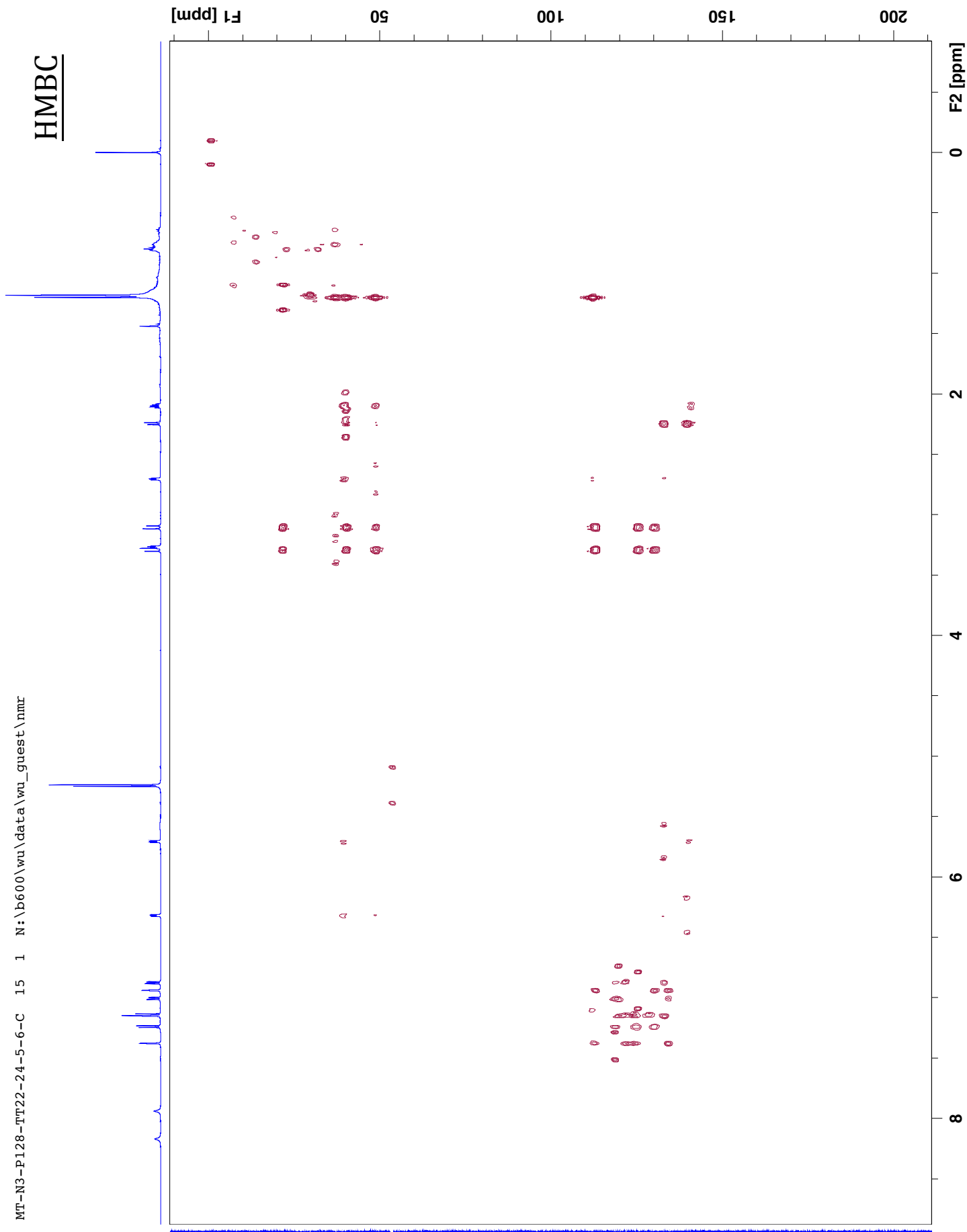
HMQC



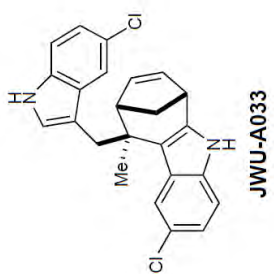
MT-N3-P128-TT22-24-5-6-C 15 1 N:\b600\wu\data\wu_guest\hmr



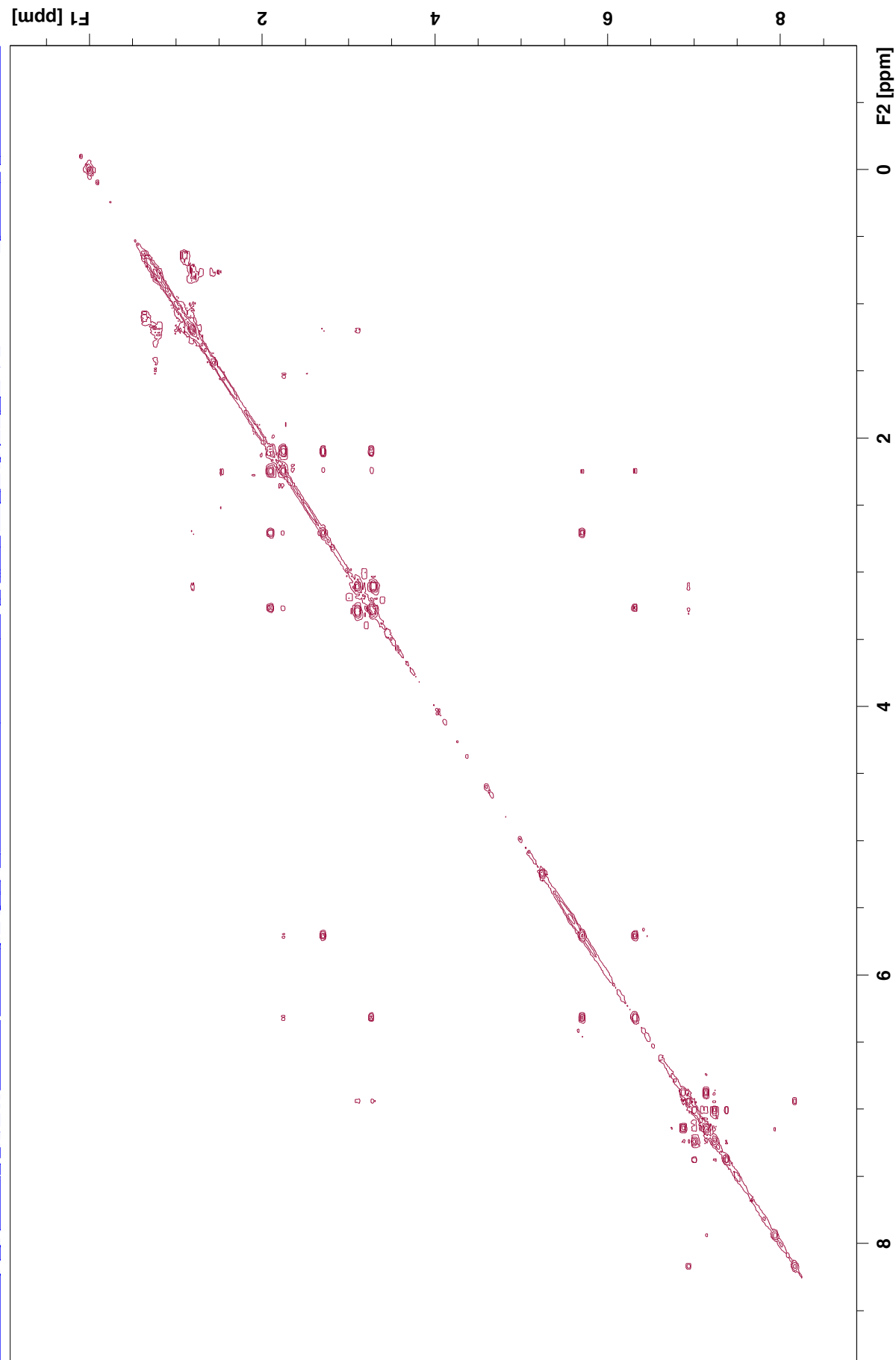
S33



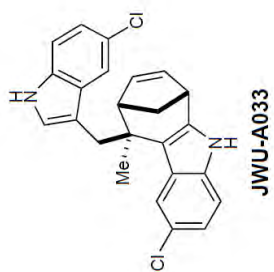
MT-N3-P128-TT22-24-5-6-C 16 1 N:\b600\wu\data\wu_guest\hmr



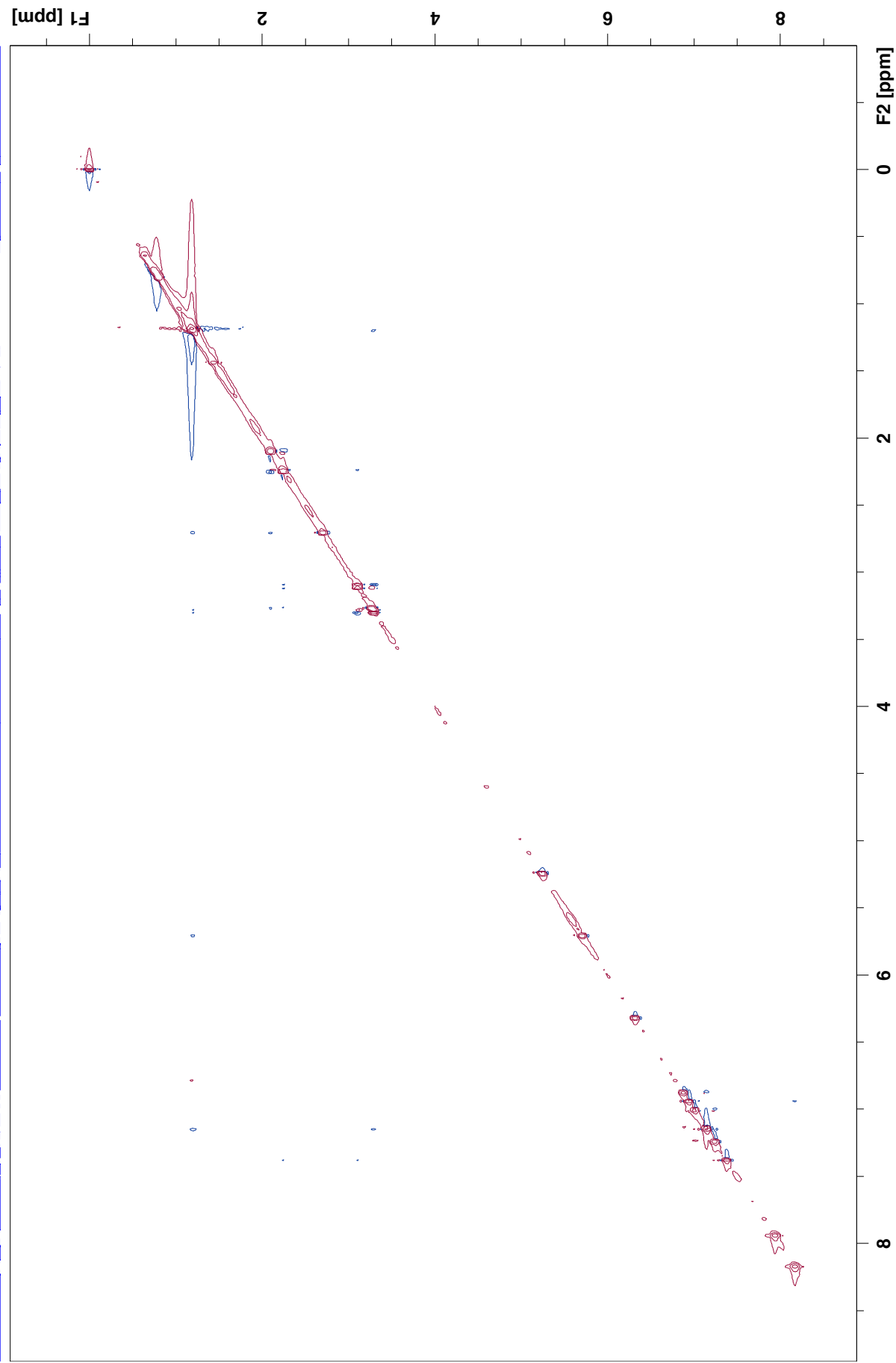
COSY

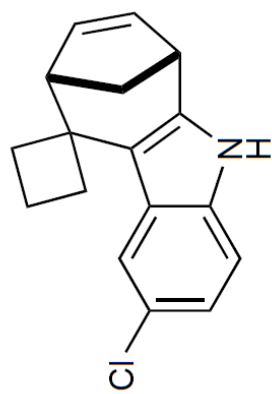


MT-N3-P128-TT22-24-5-6-C 17 1 N:\b600\wu\data\wu_guest\hmr

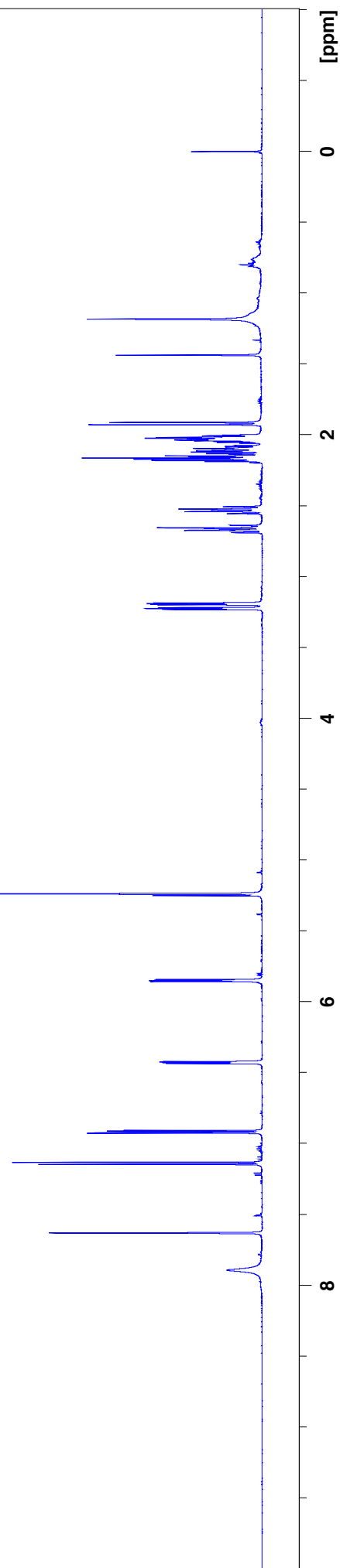


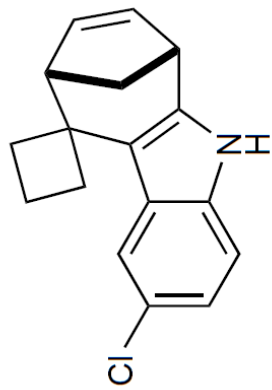
NOESY



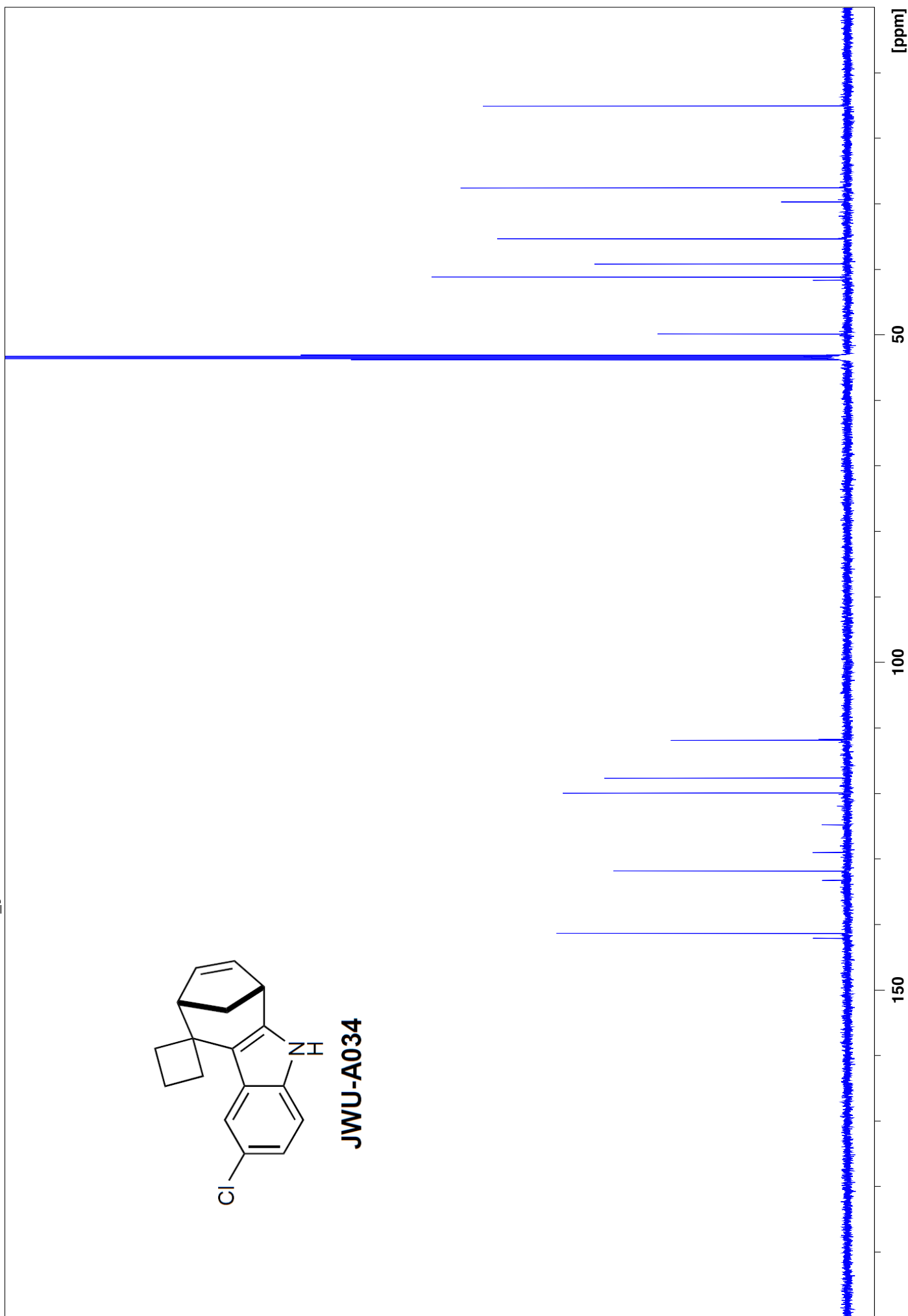


JWU-A034

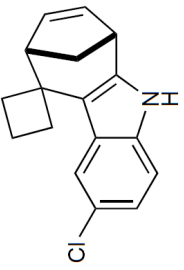




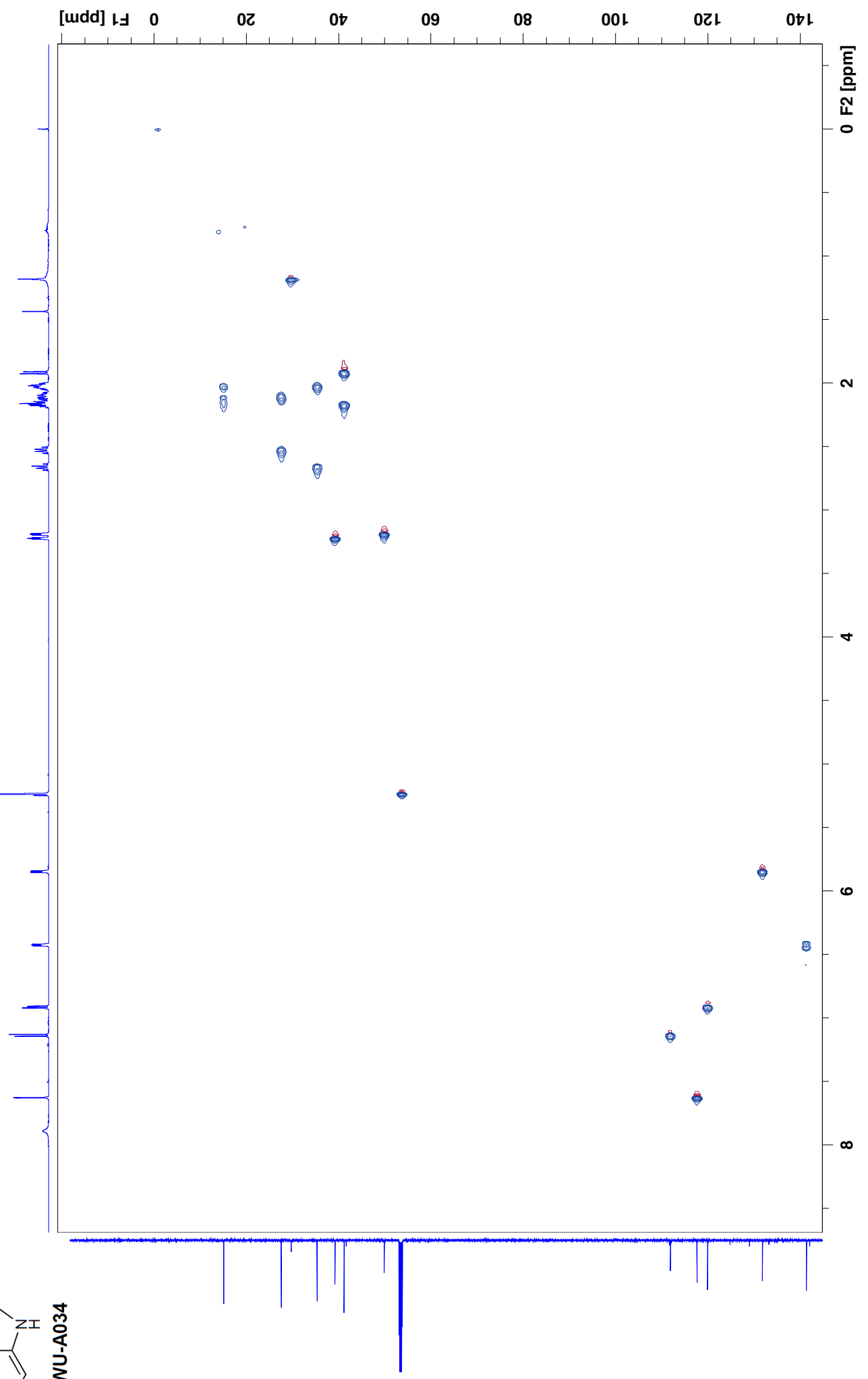
JWU-A034



MT-N3-P114-TT12-17-10 15 1 N:\b600\wu\data\wu_guest\nmr



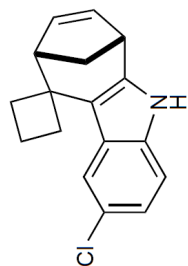
HMQC



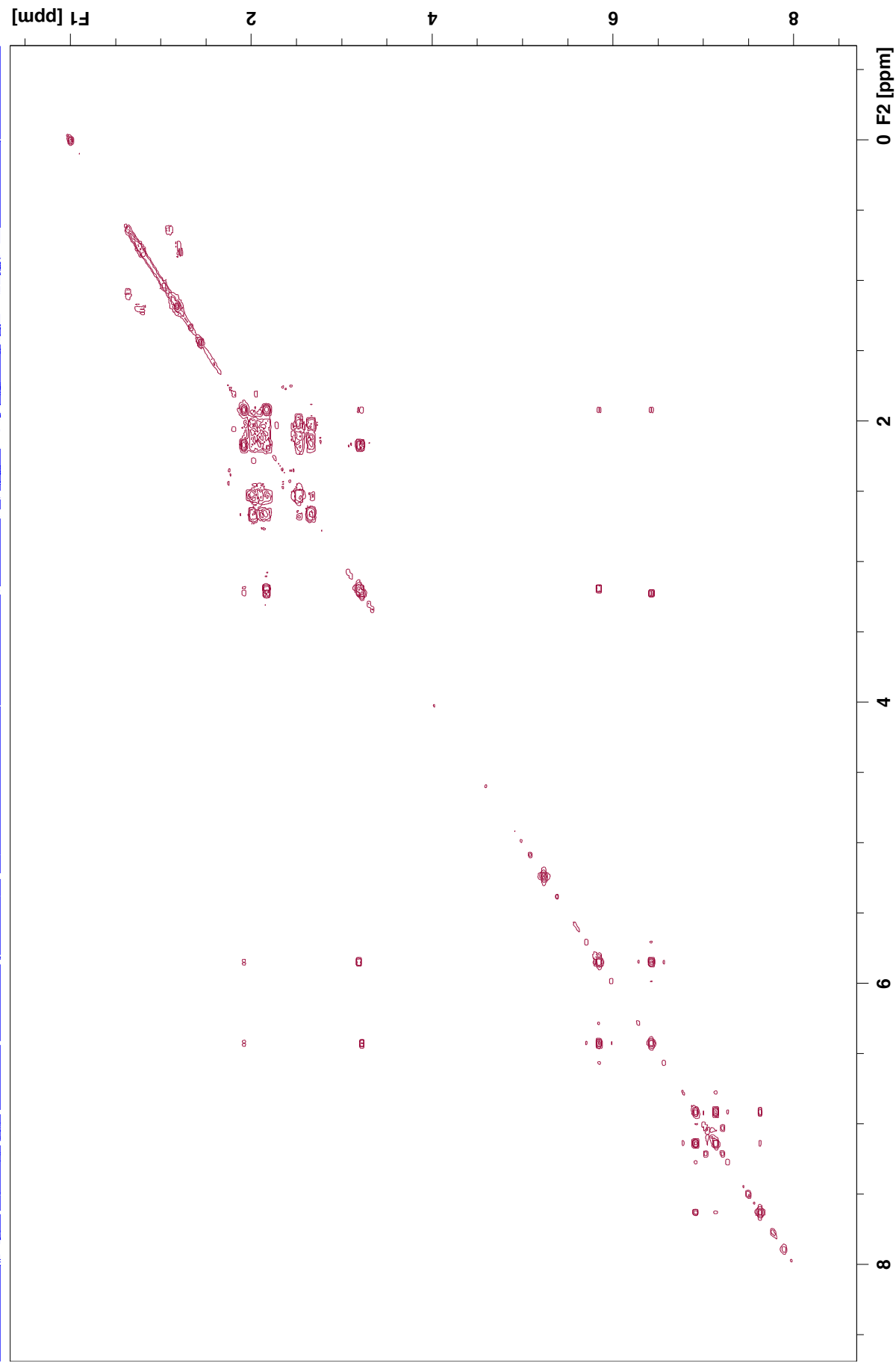
S38

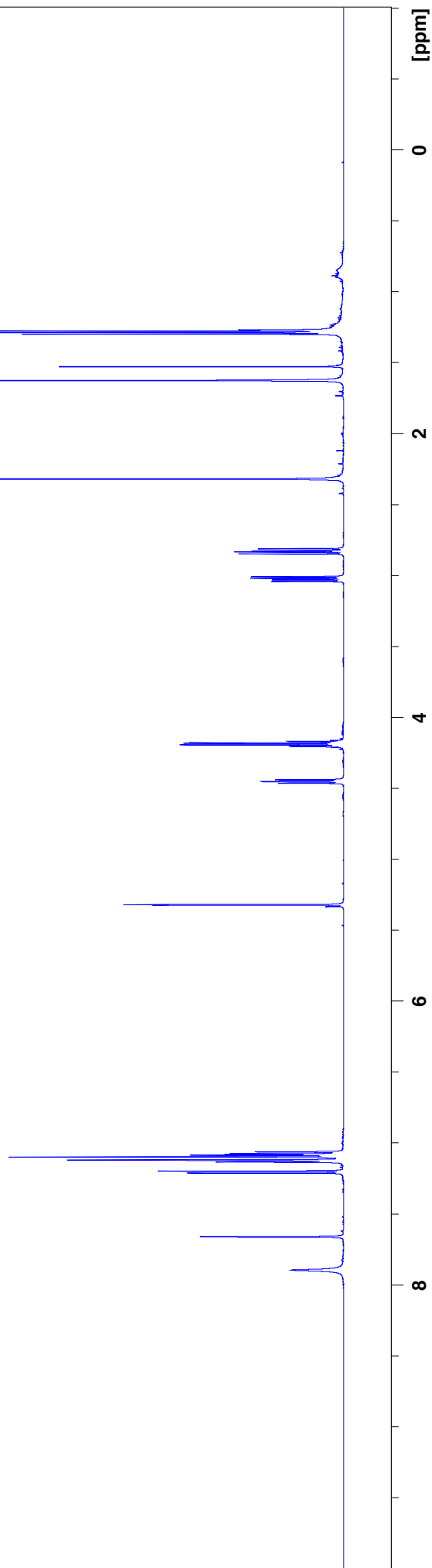
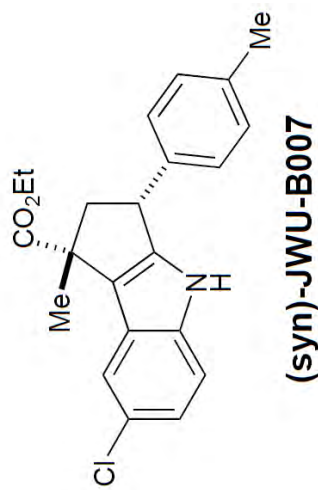
MT-N3-P114-TT12-17-10 16 1 N:\b600\wu\data\wu_guest\nmr

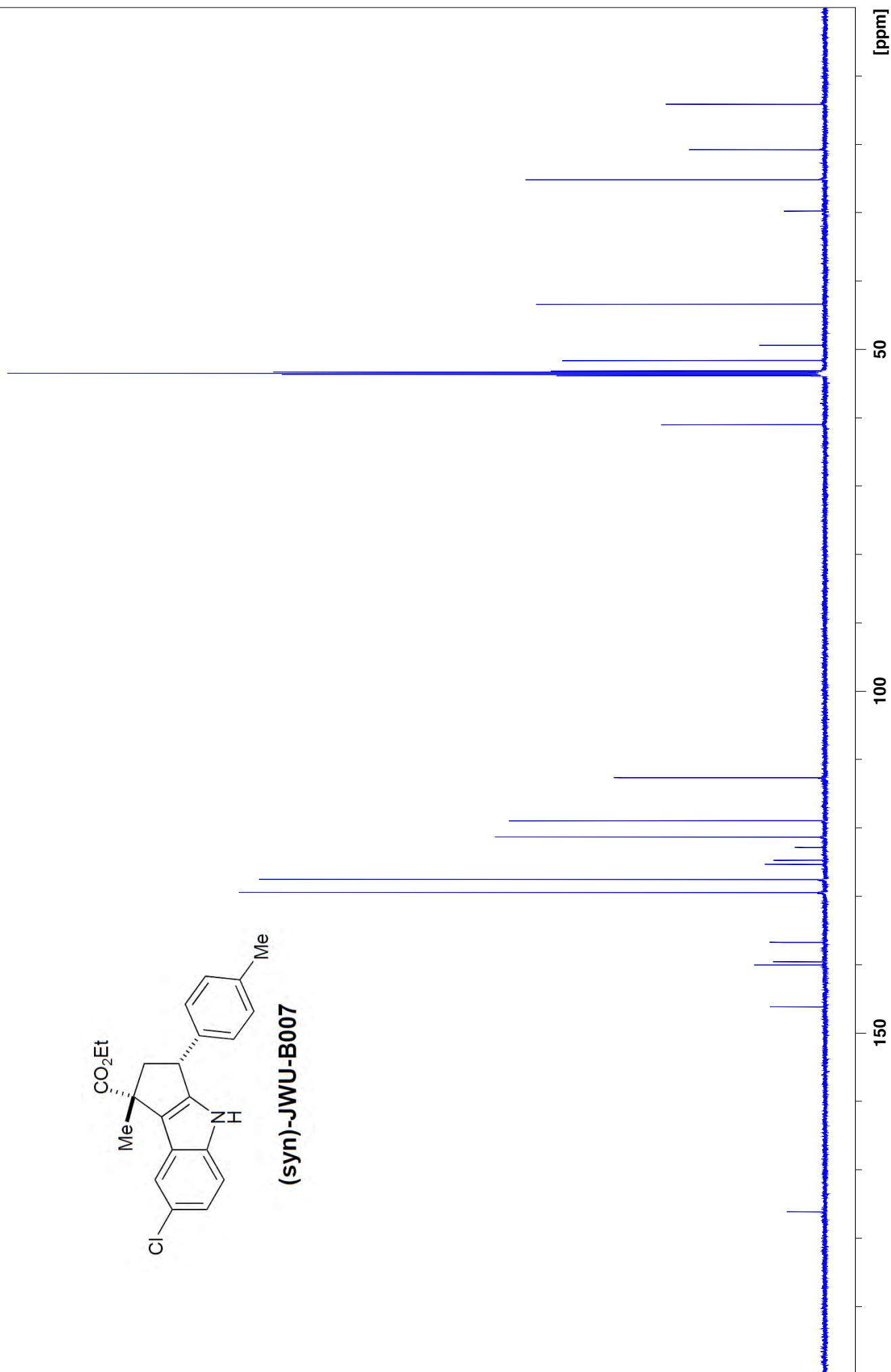
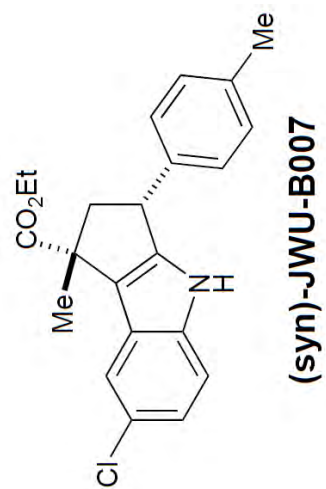
COSY

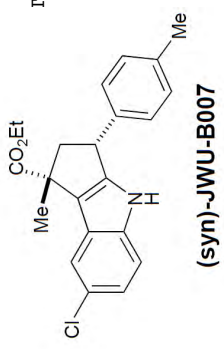


JWU-A034



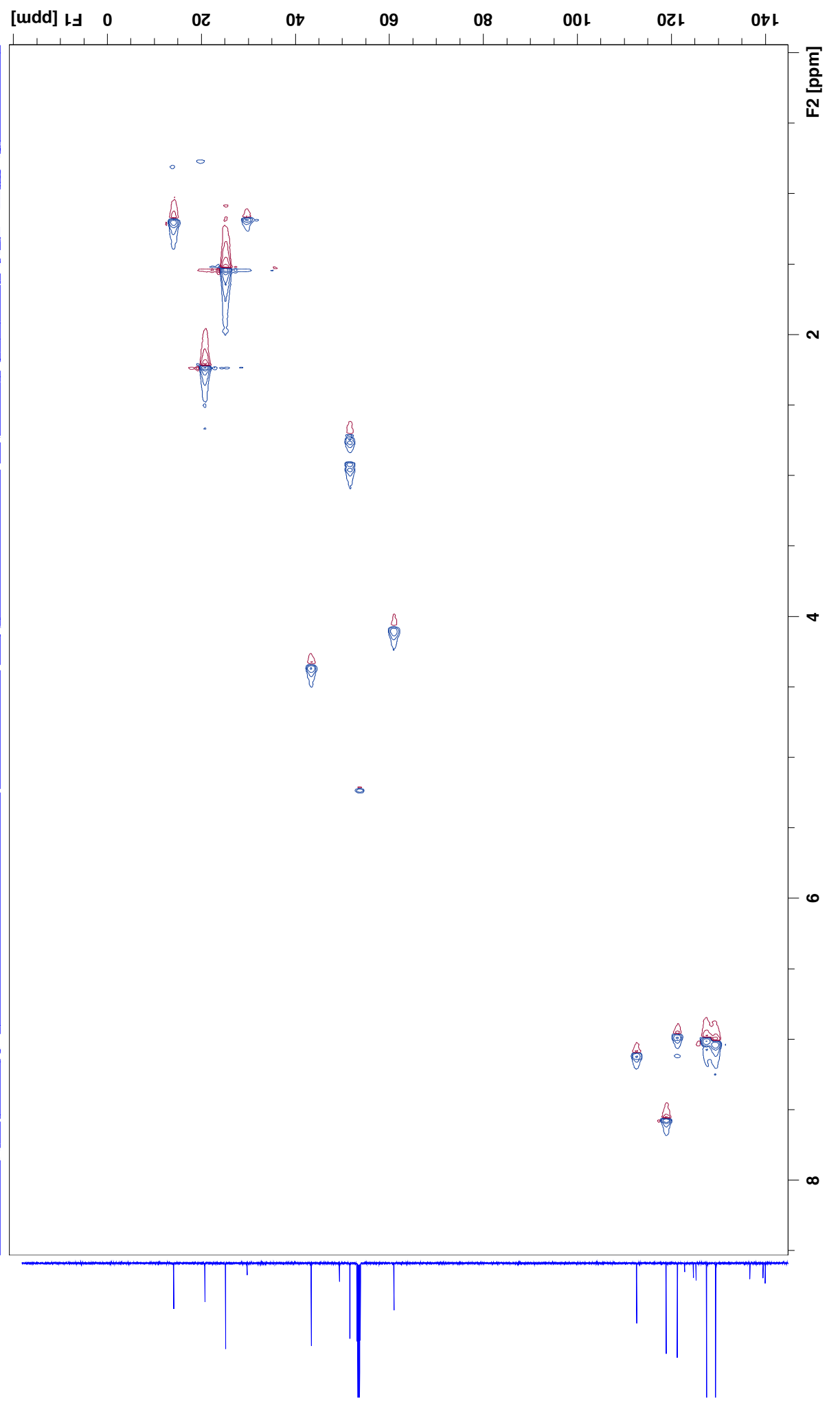


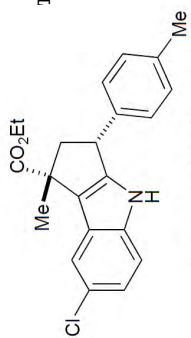




Γ-N3-P30-IT19-7-8 23 1 "I:\3+2 Products"

HMQC

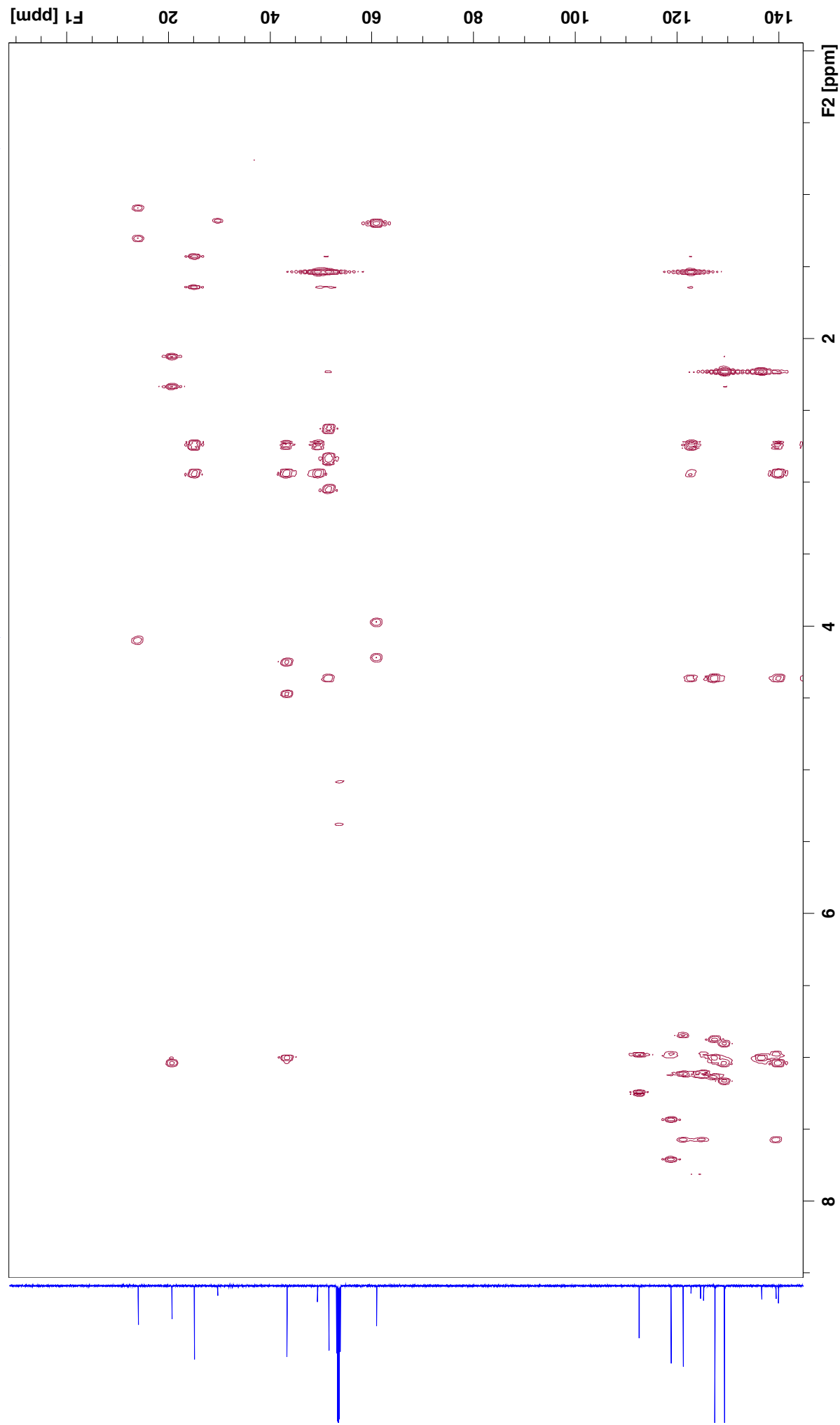




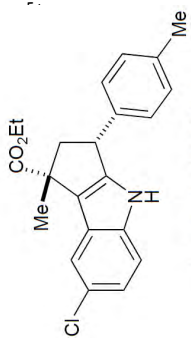
(syn)-JWU-B007

T-N3-P30-TT19-7-8 24 1 "I:\3+2 Products"

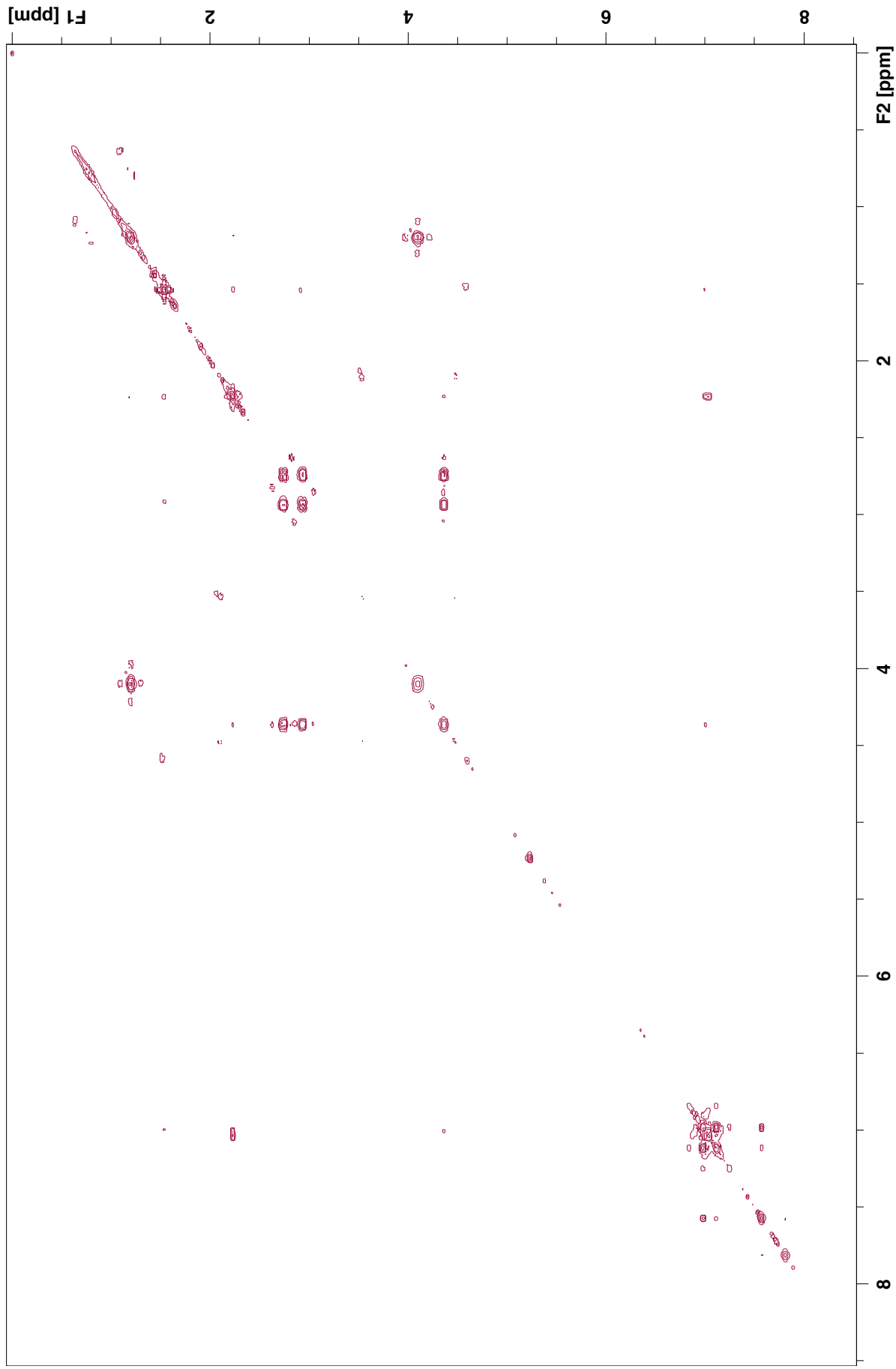
HMBC

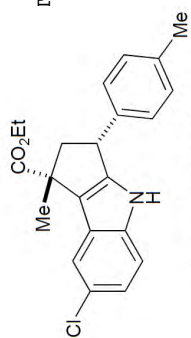


1-N3-P30-TT19-7-8 21 1 "I:\3+2 Products"



COSY

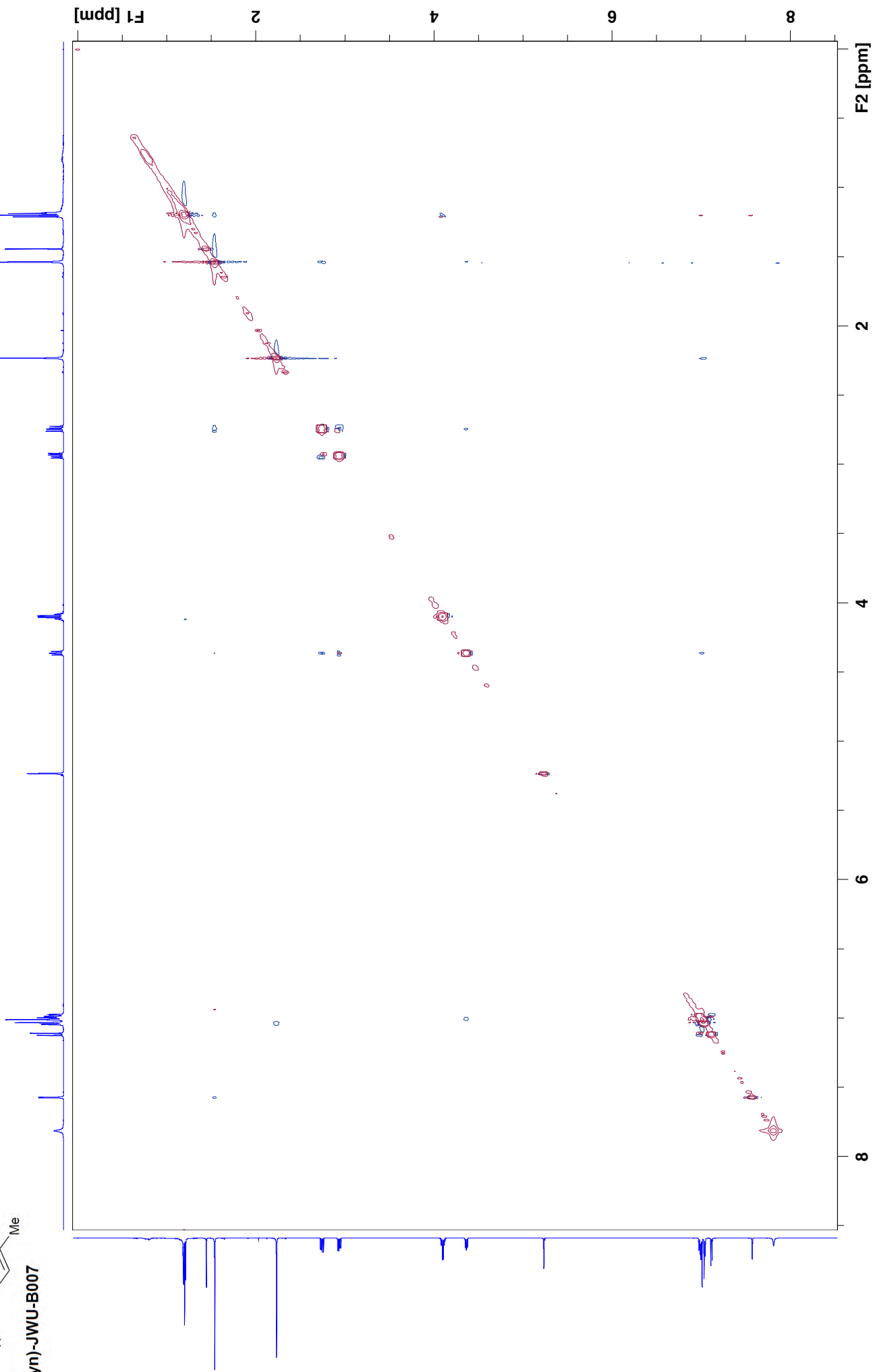


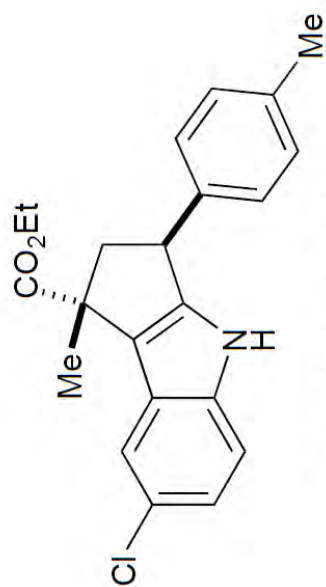


(syn)-JWU-B007

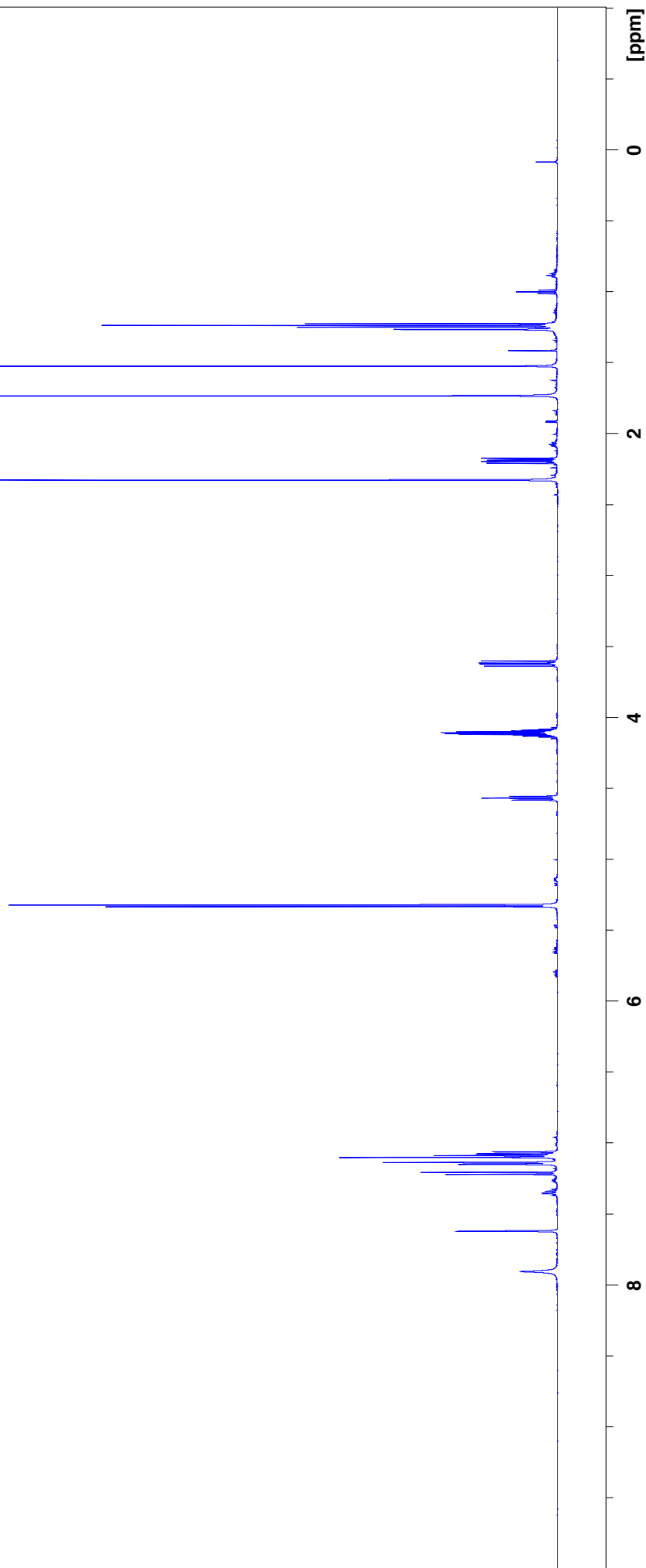
Γ-N3-P30-TT19-7-8 22 1 "I:\3+2 Products"

NOESY

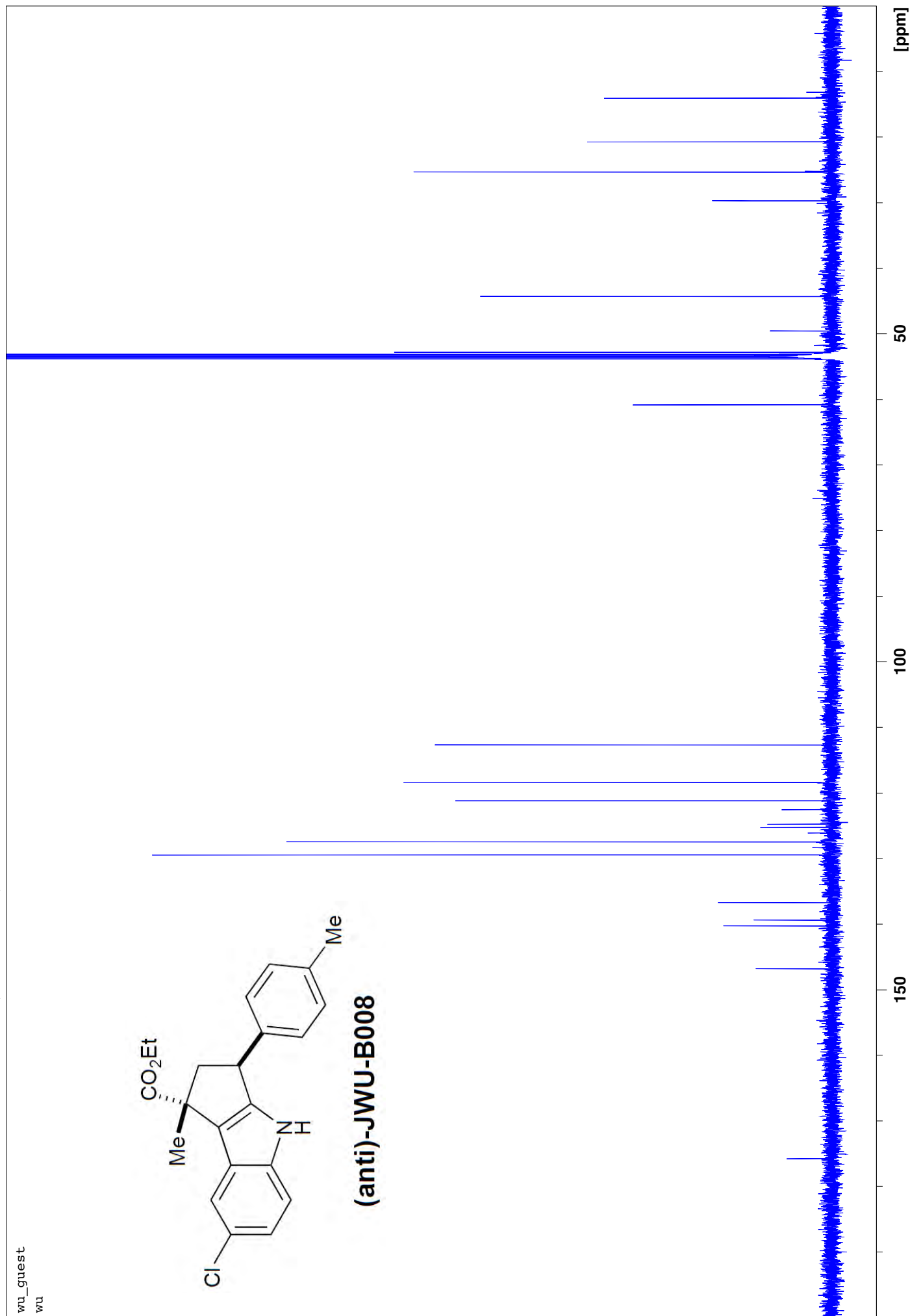
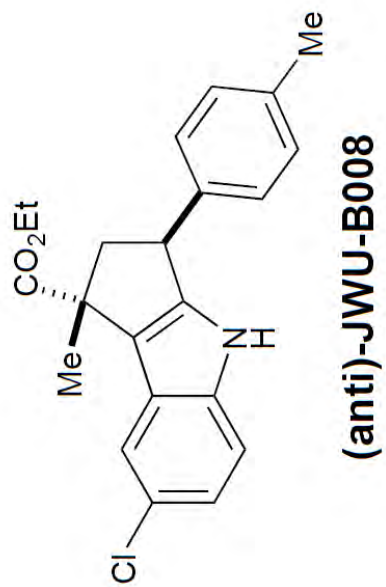


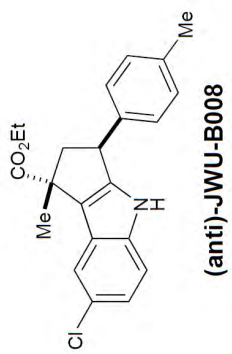


(anti)-JWU-B008



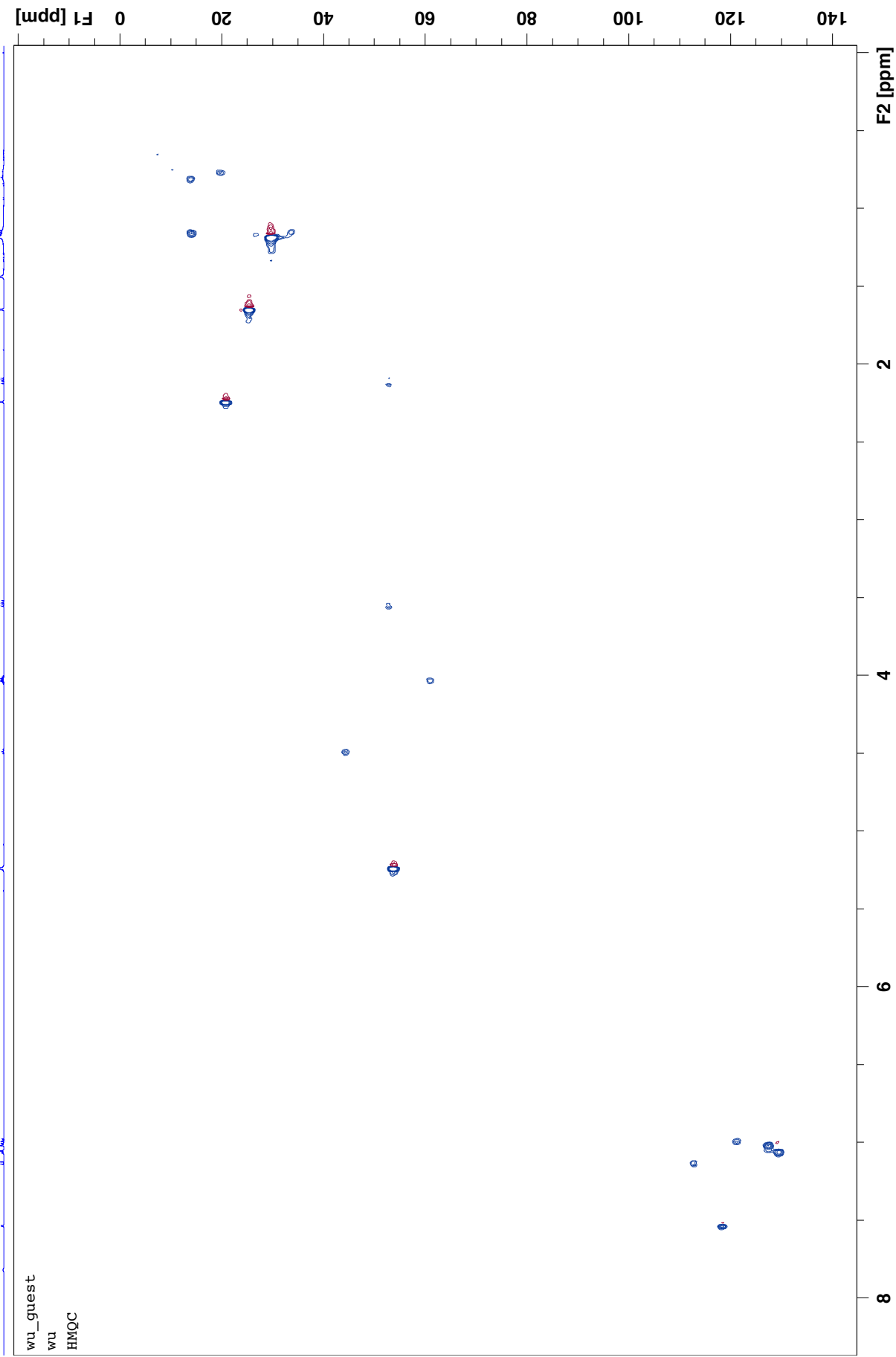
wu_guest
wu





-N3-P30-TT22-RR 1 1 "I:\3+2 Products\MT-N3-P30-TT20-4-5"

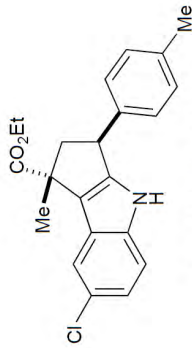
HMQC



wu_guest

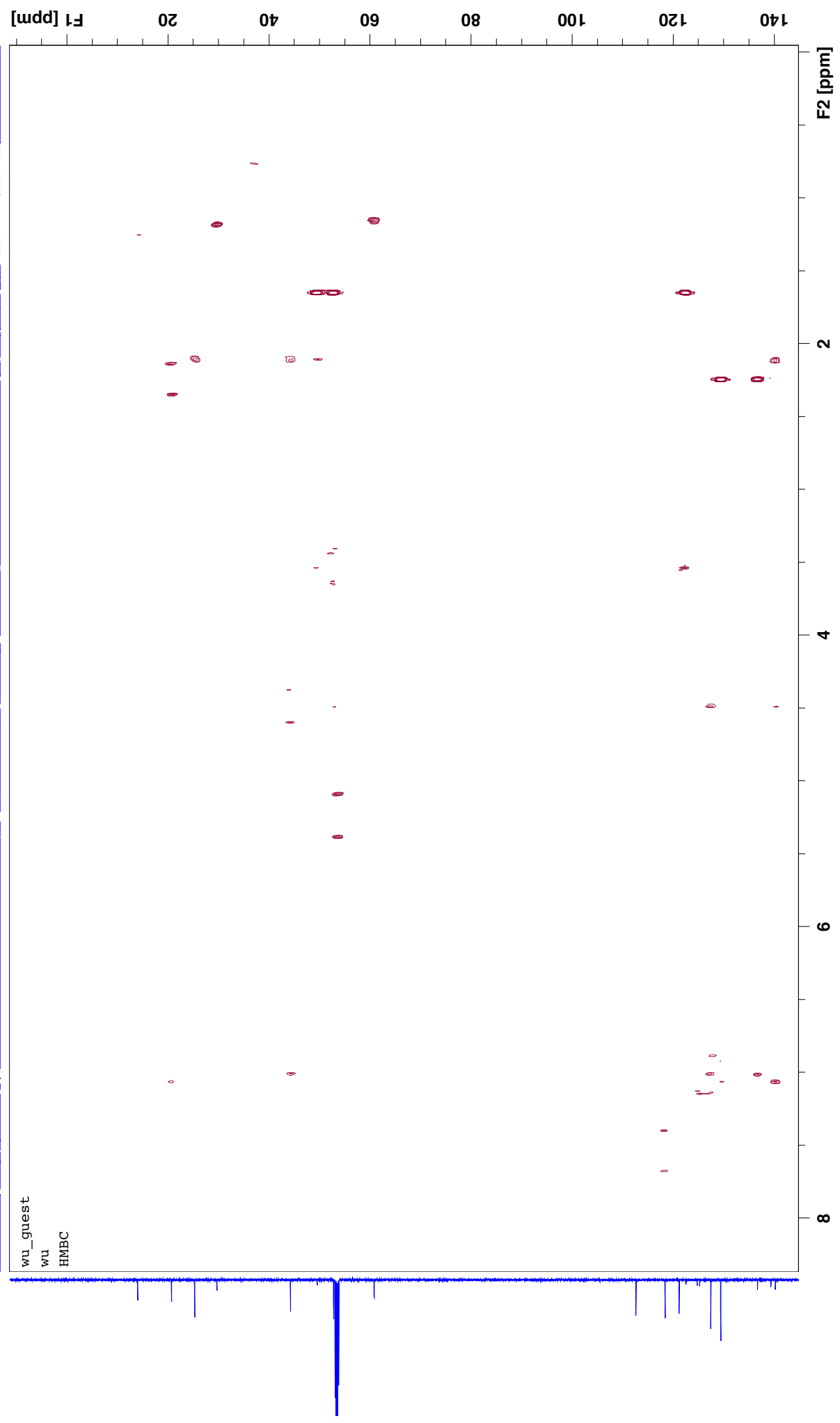
wu

HMQC



I:\3+2 Products\MT-N3-P30-TT20-4-5"

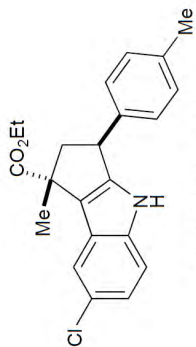
HMBC



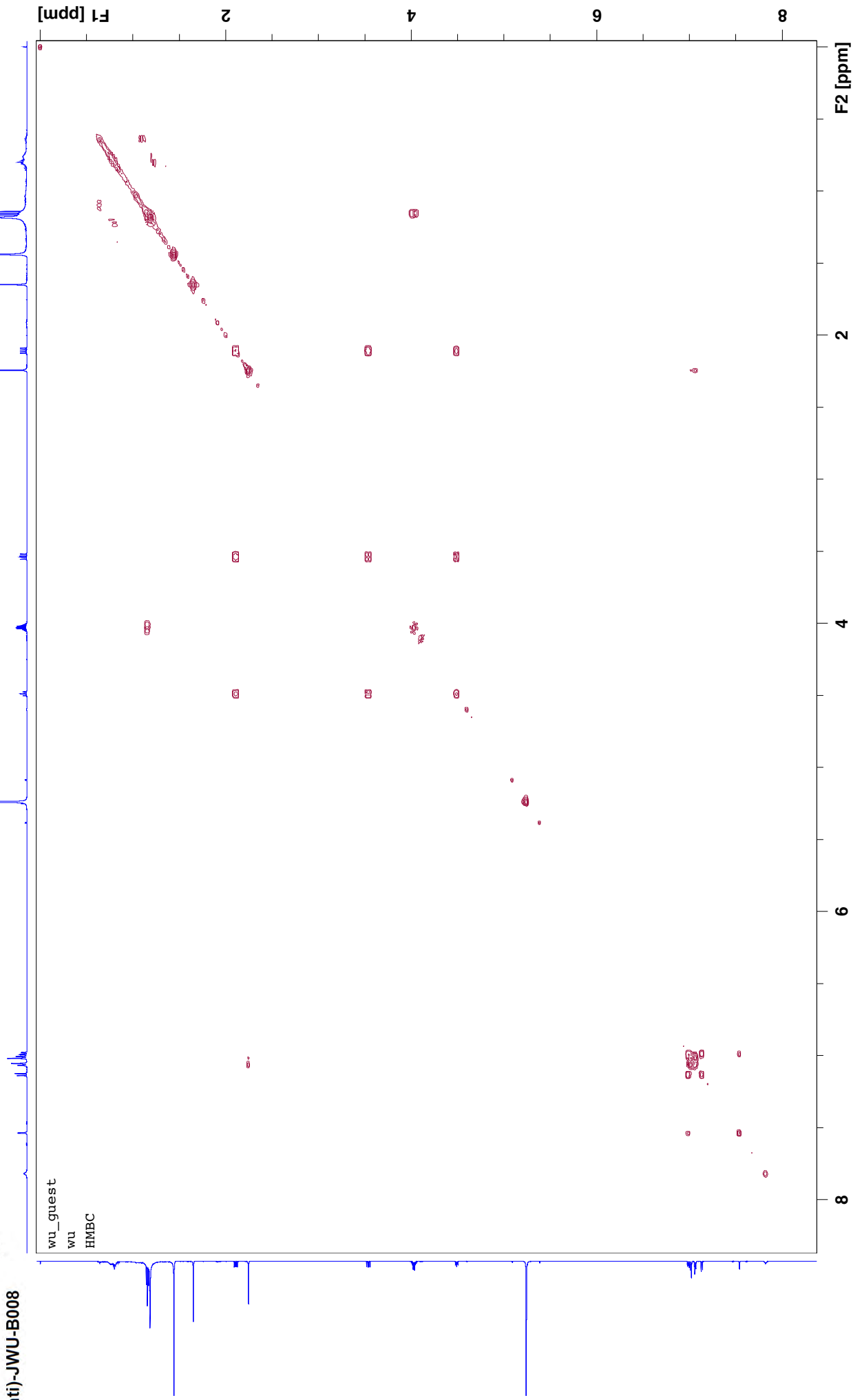
wu_guest
wu
HMBC

S50

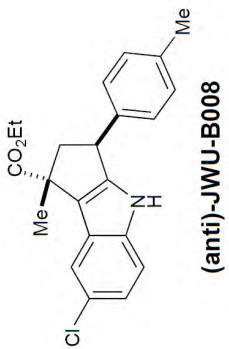
-N3-P30-TT22-RR 13 1 "I:\3+2 Products\MT-N3-P30-TT20-4-5"



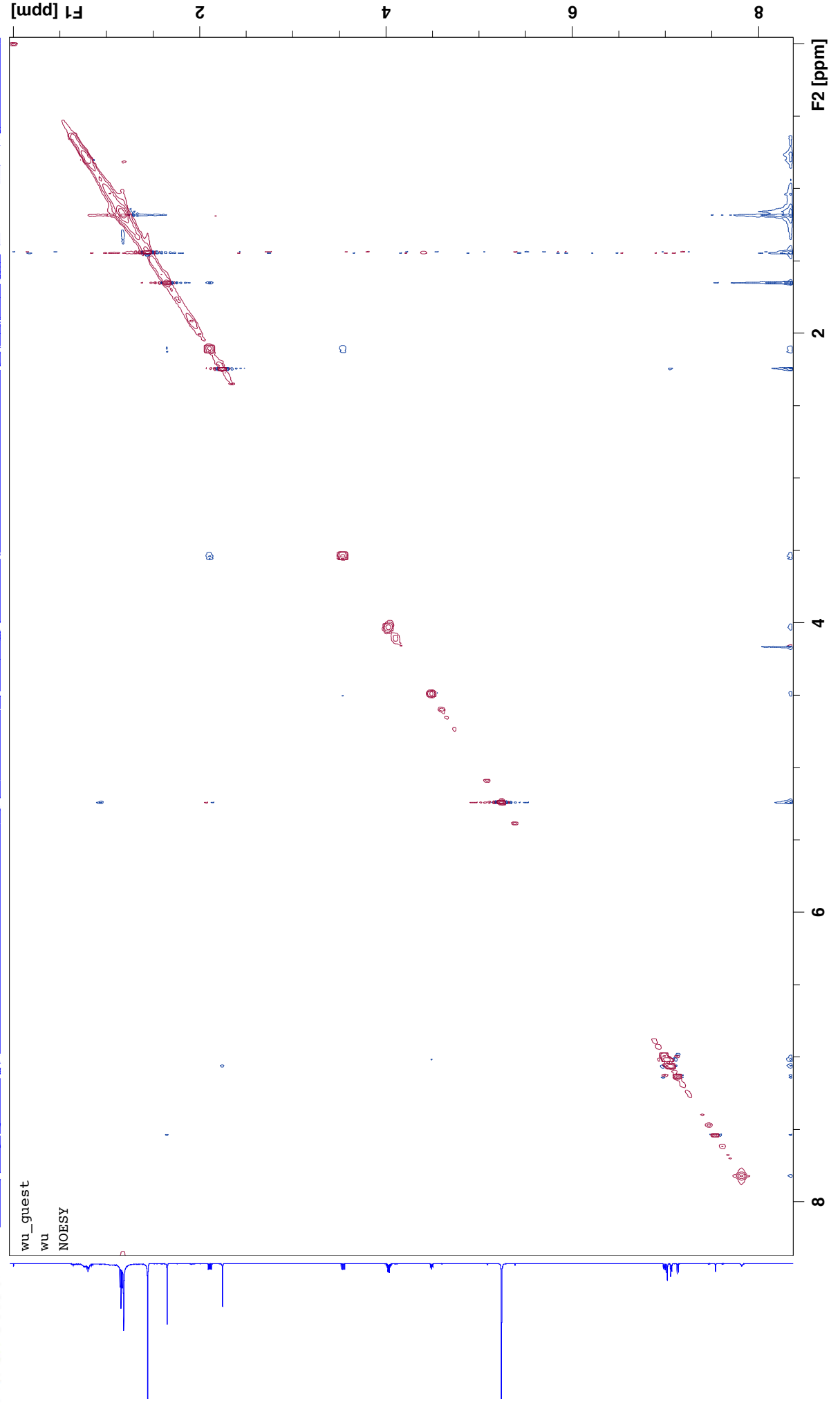
COSY

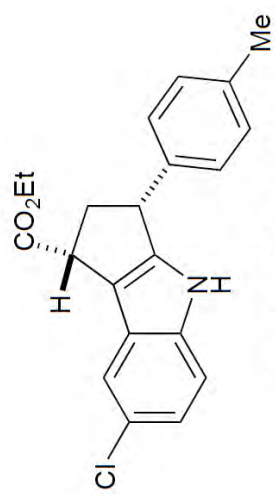


-N3-P30-TT22-RR 14 1 "I:\3+2 Products\MT-N3-P30-TT20-4-5"

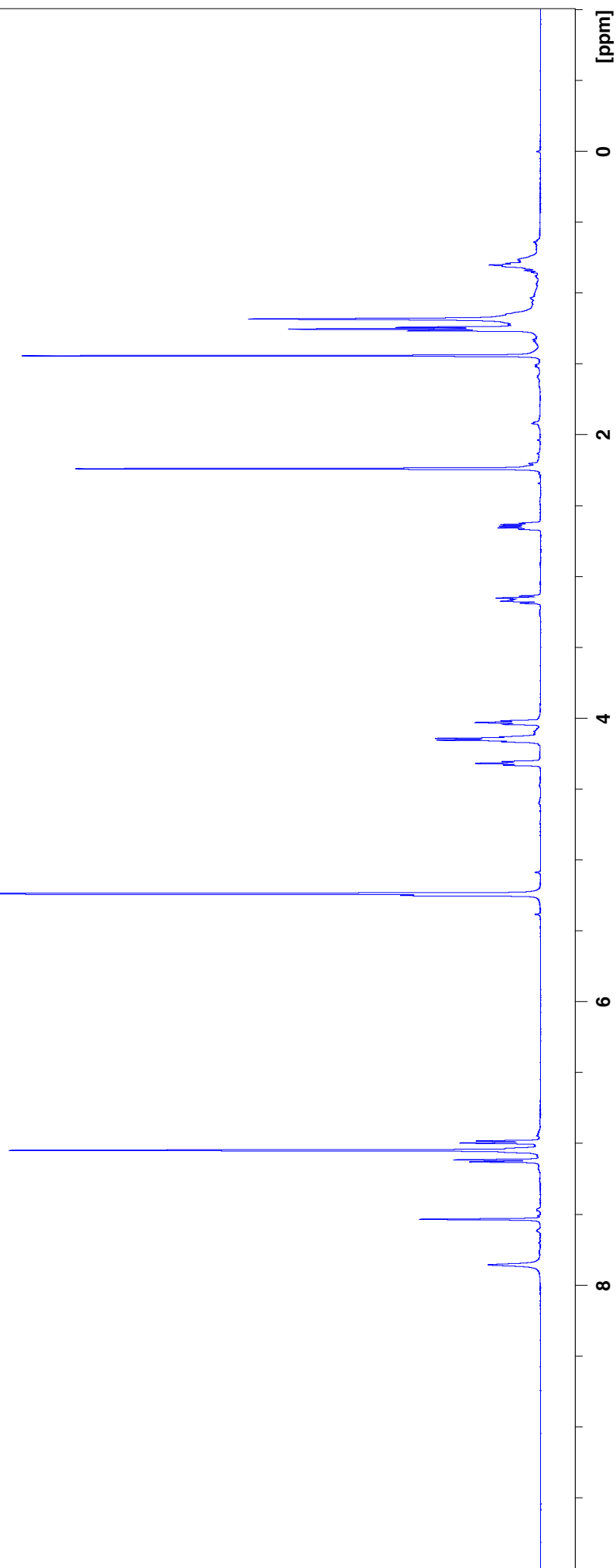


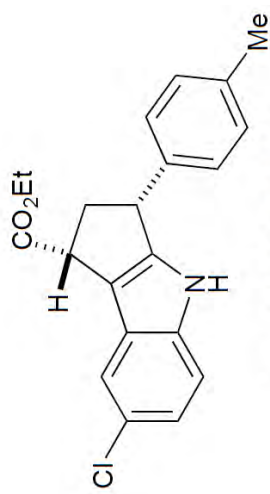
NOESY



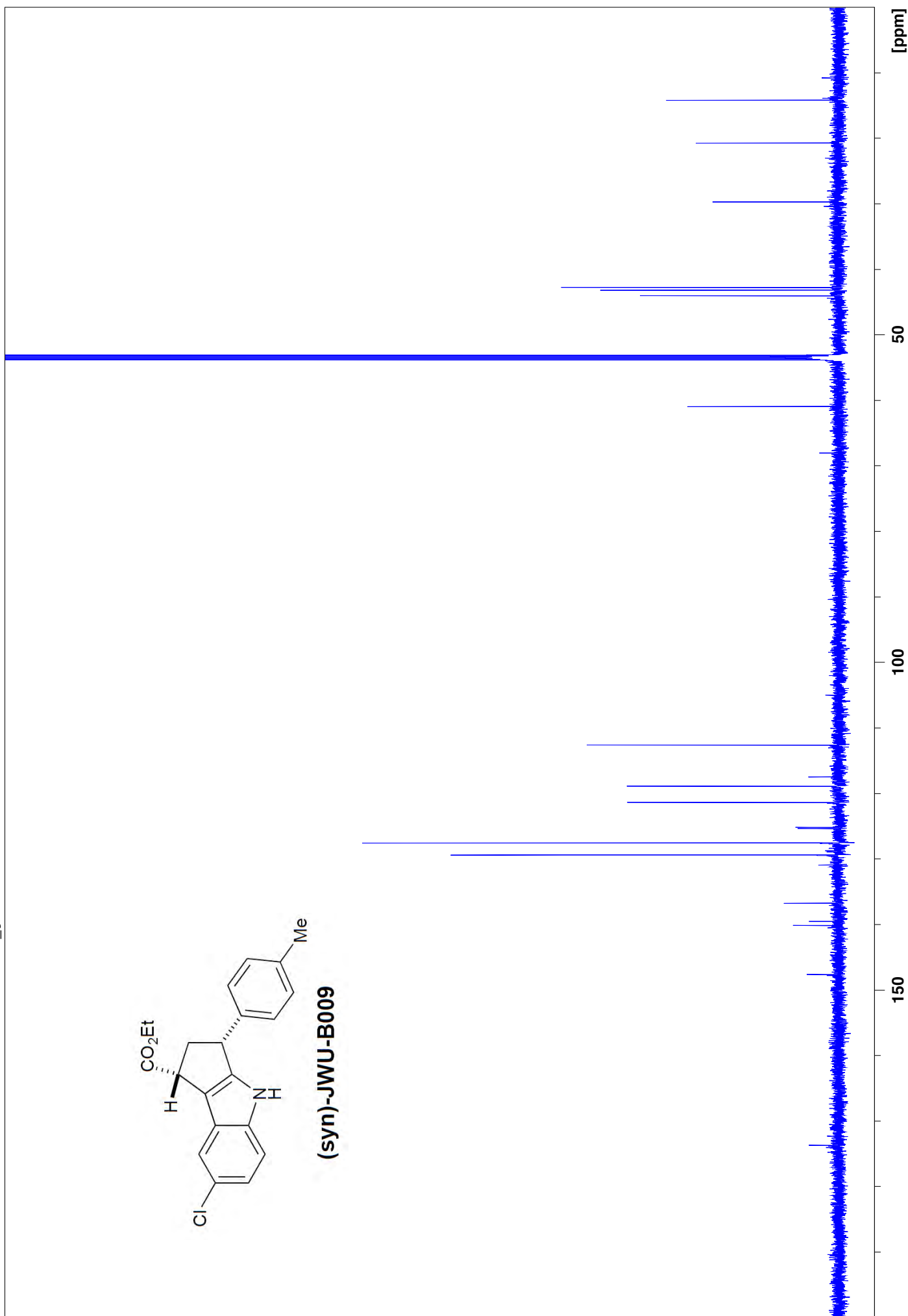


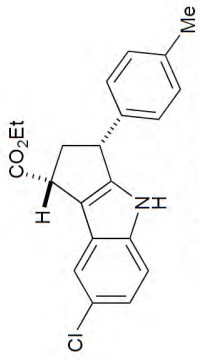
(syn)-JWU-B009





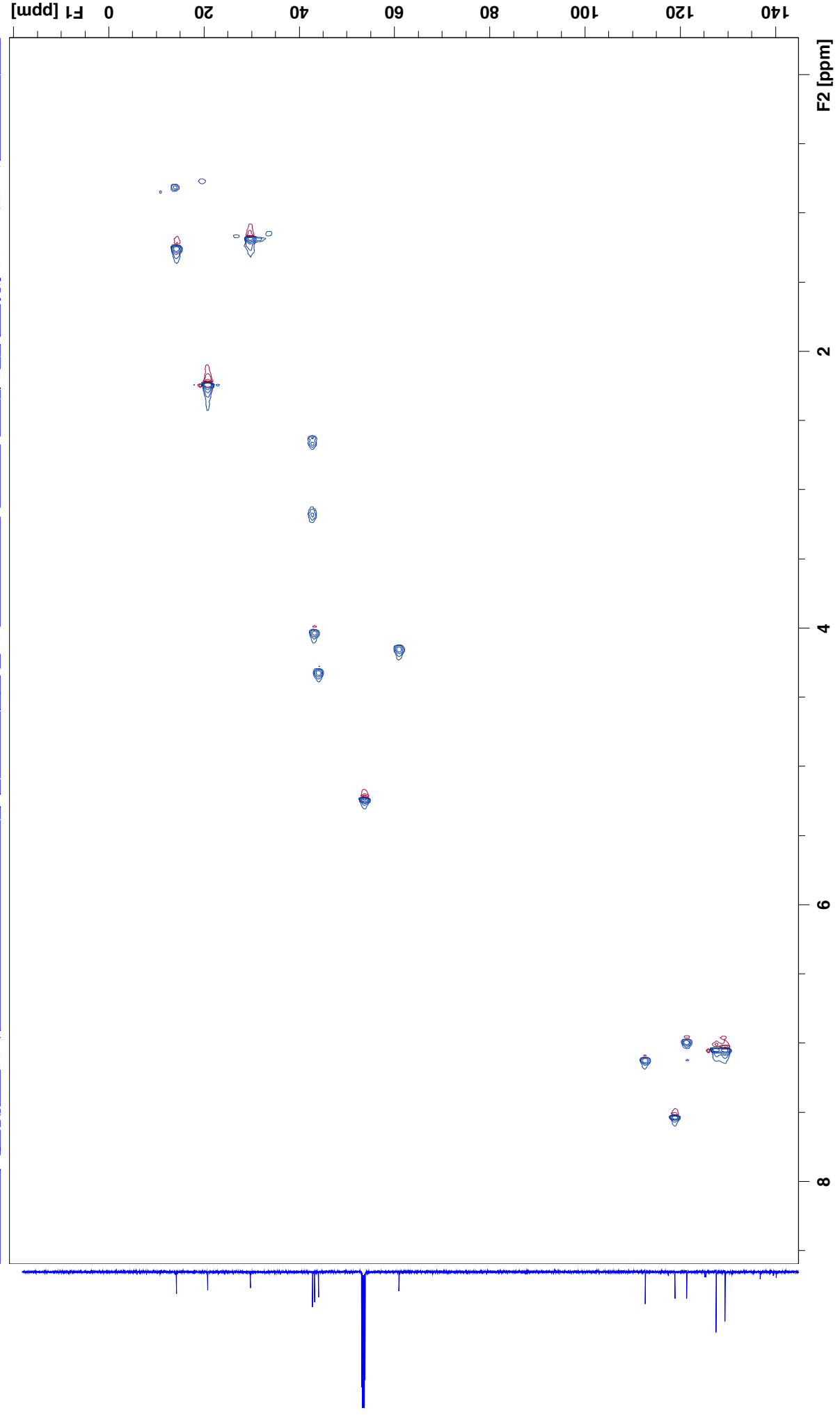
(syn)-JWU-B009



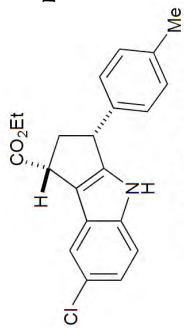


.N3-P48-IT21-5-6 1.1 N:\b600\wu\data\wu_guest\mmr

HMQC



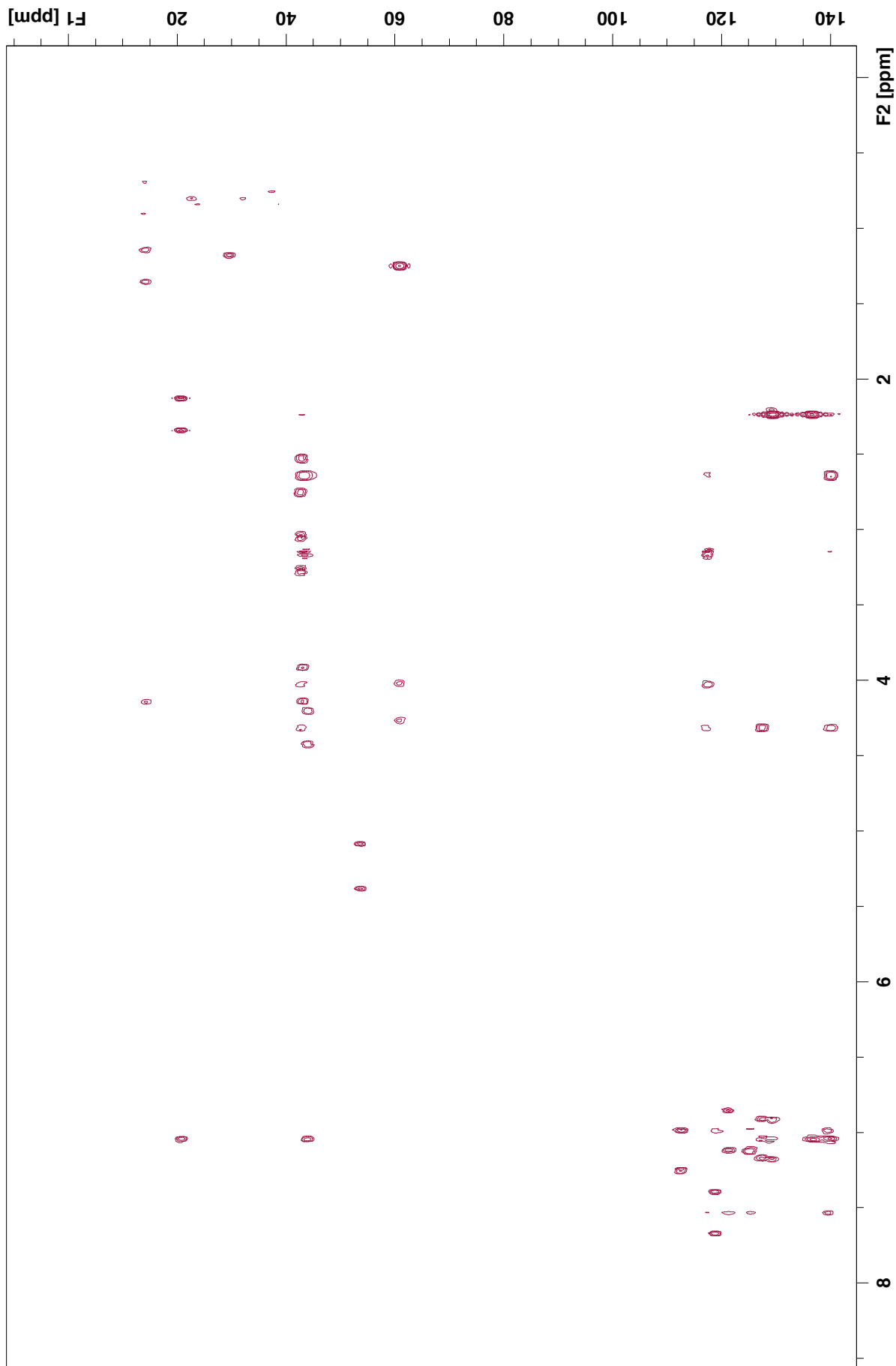
S55

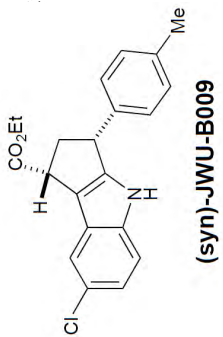


(syn)-JWU-B009

Mt-N3-P48-IT21-5-6 13 1 N:\b600\wu\data\wu_guest\mmr

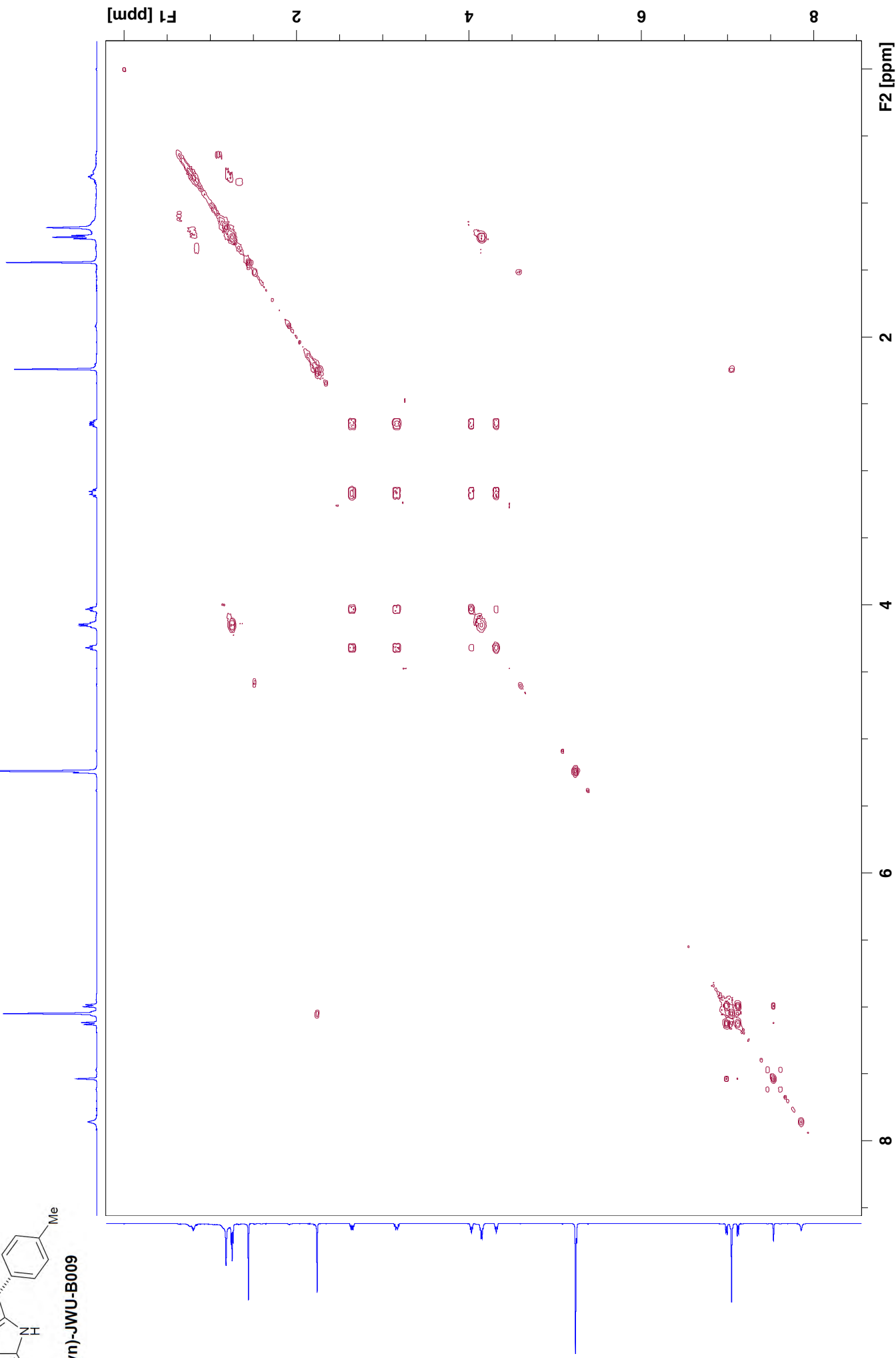
HMBC

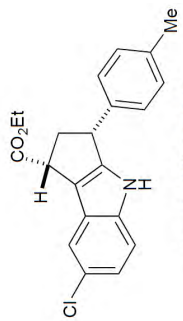




t-N3-P48-TR21-5-6 15 1 N:\b600\wu\data\wu_guest\mmr

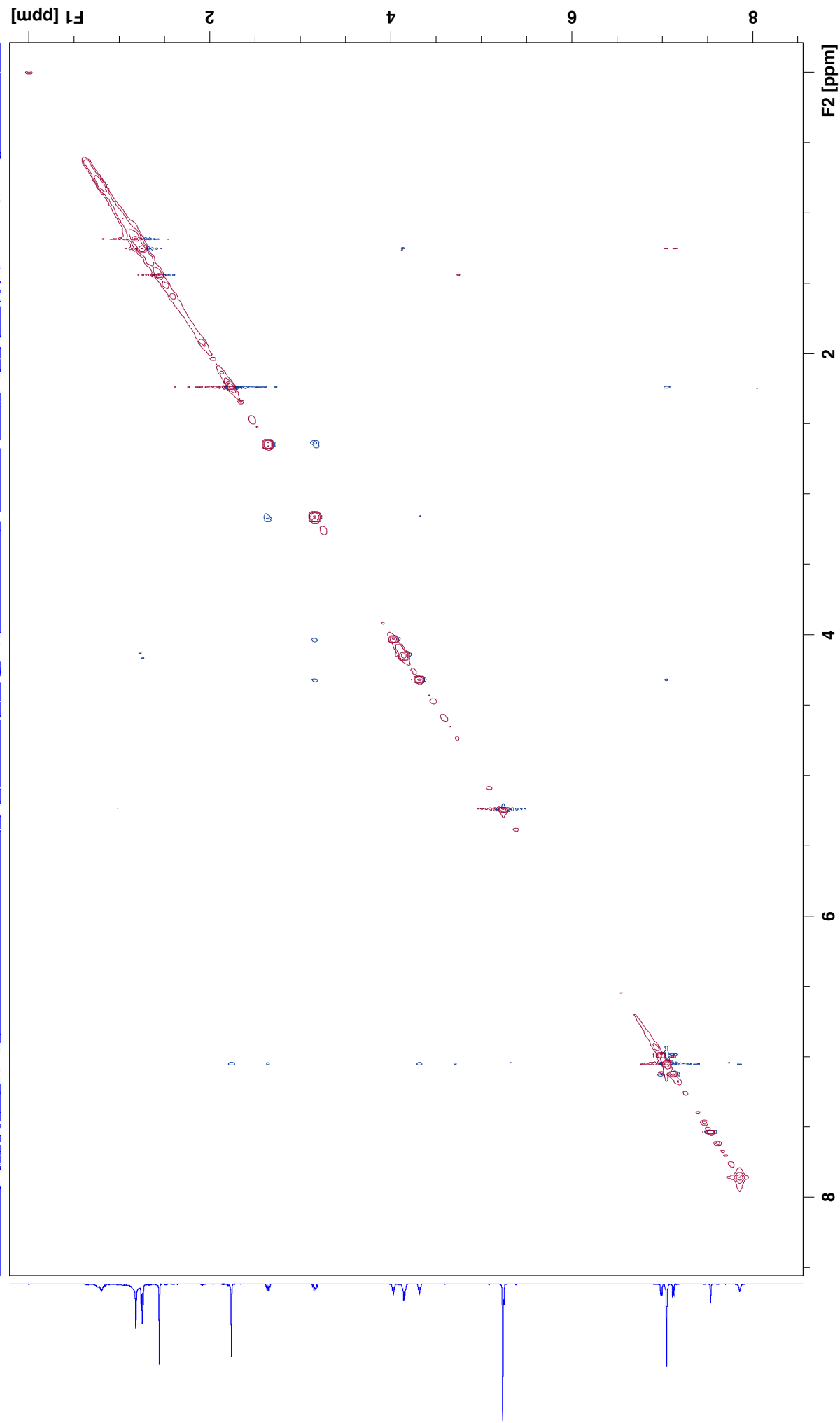
COSY

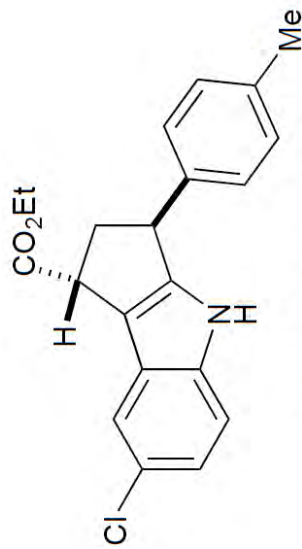




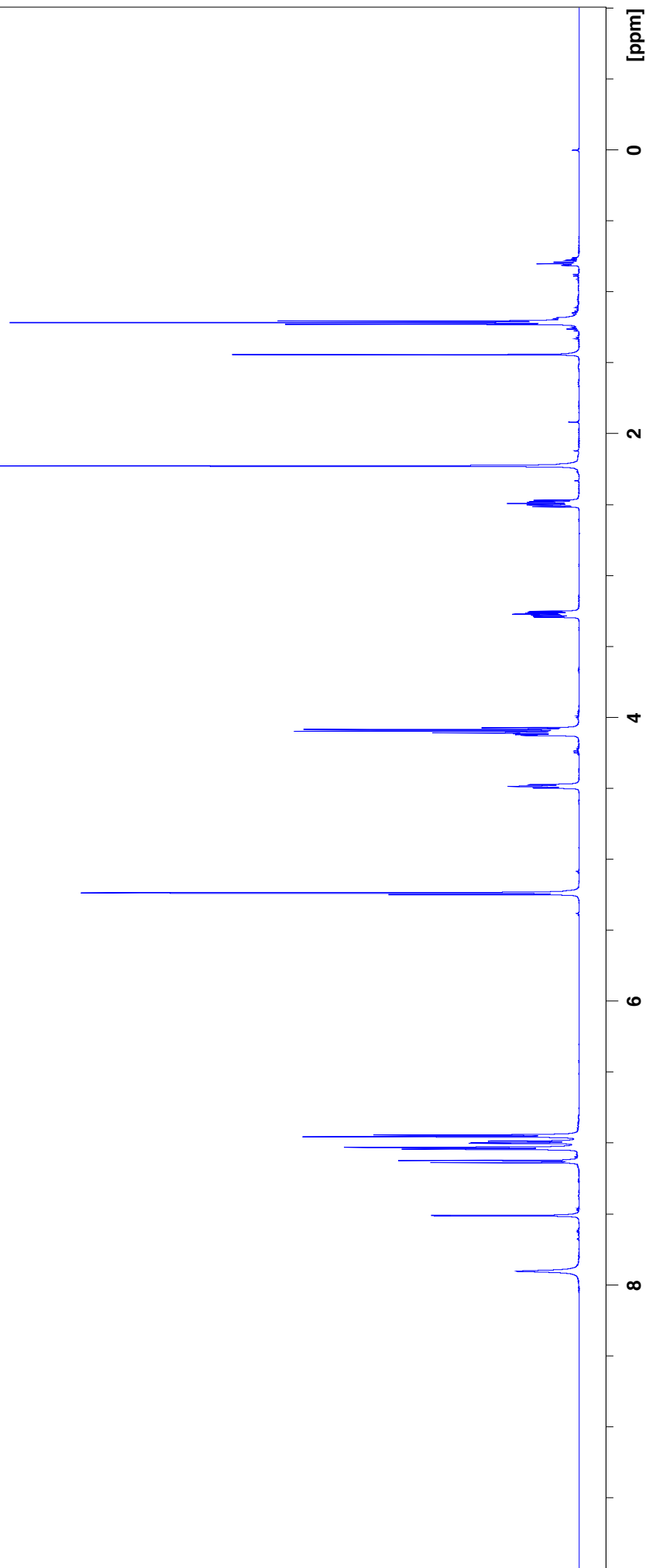
Mt-N3-P48-IT21-5-6 14 1 N:\b600\wu\data\wu_guest\mmr

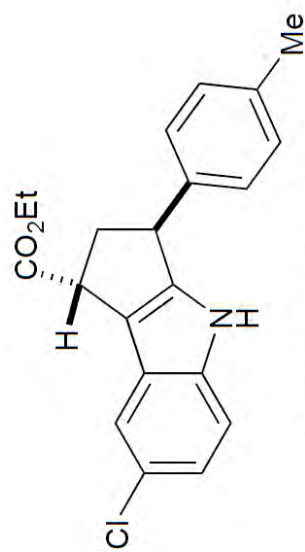
NOESY



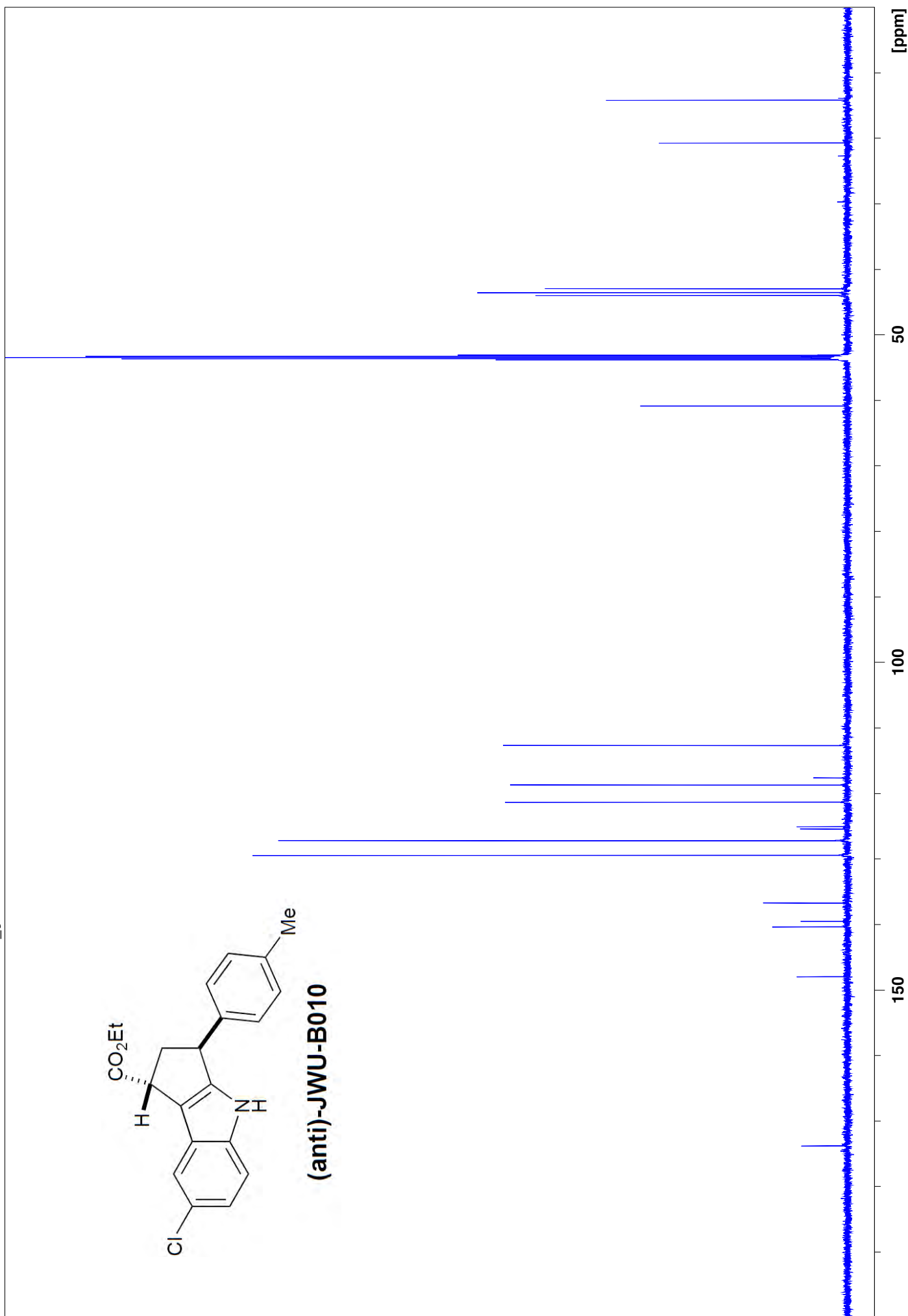


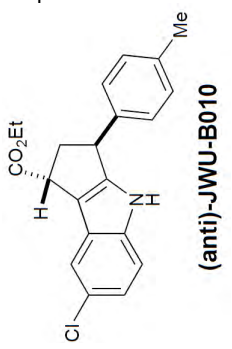
(anti)-JWU-B010





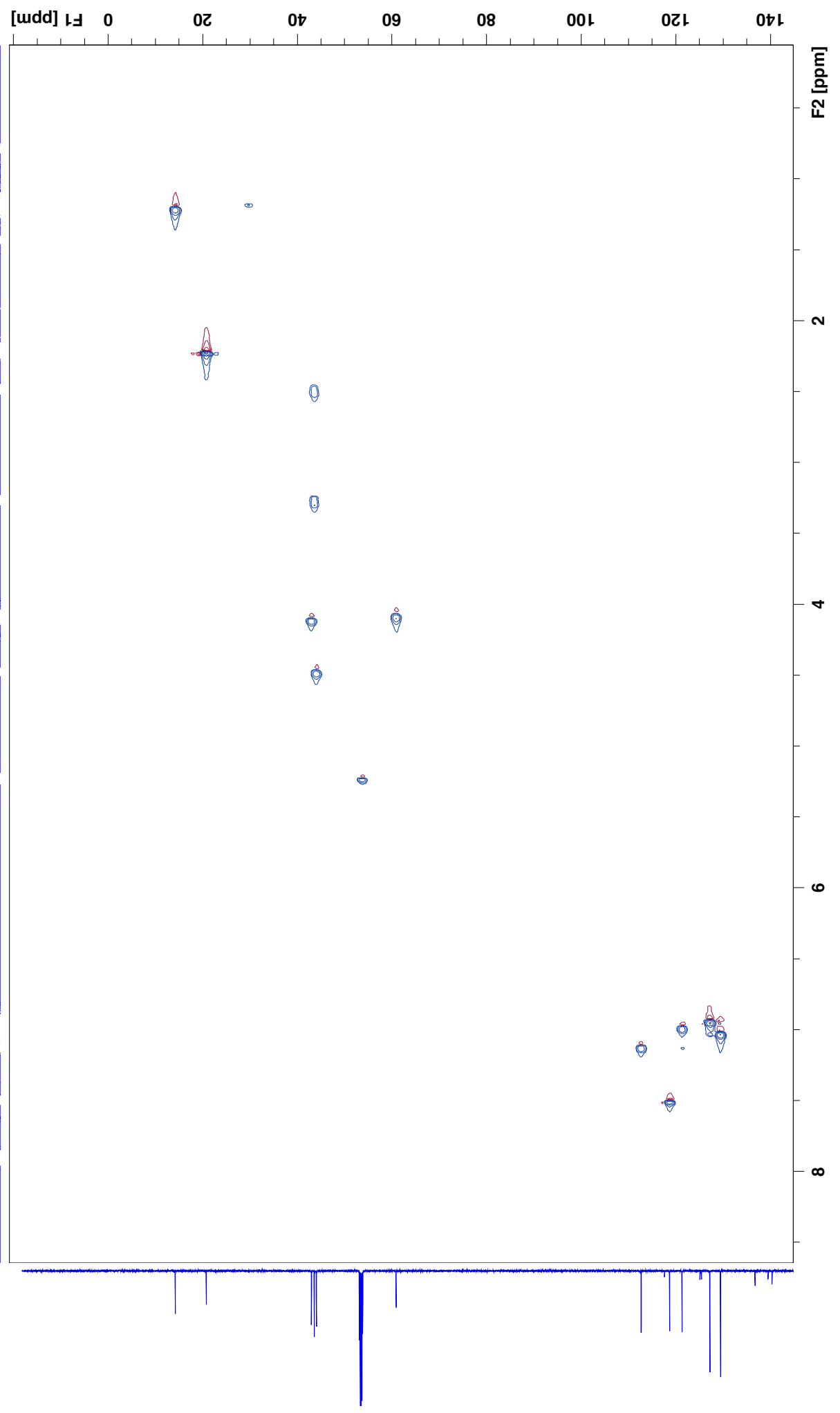
(anti)-JWU-B010



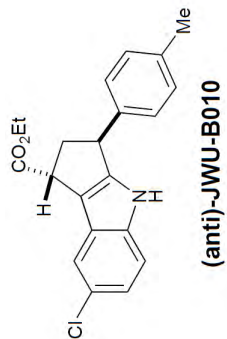


-N3-P48-TT23-3-4 21 1 N:\b600\wu\data\wu_guest\mmr

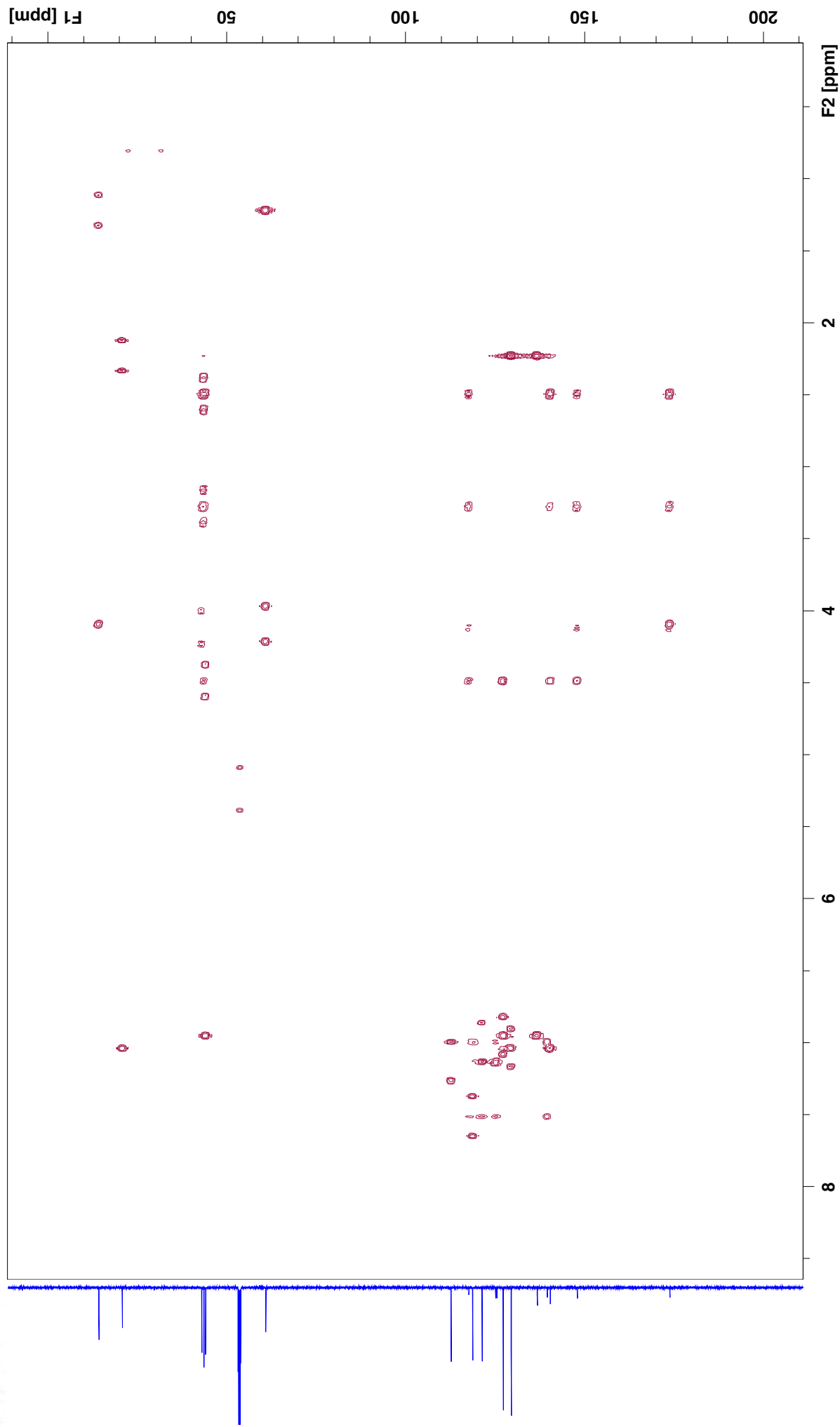
HMQC



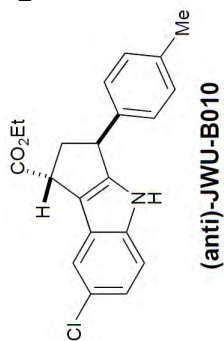
4T-N3-P48-TT23-3-4 22 1 N:\b600\wu\data\wu_guest\mmr



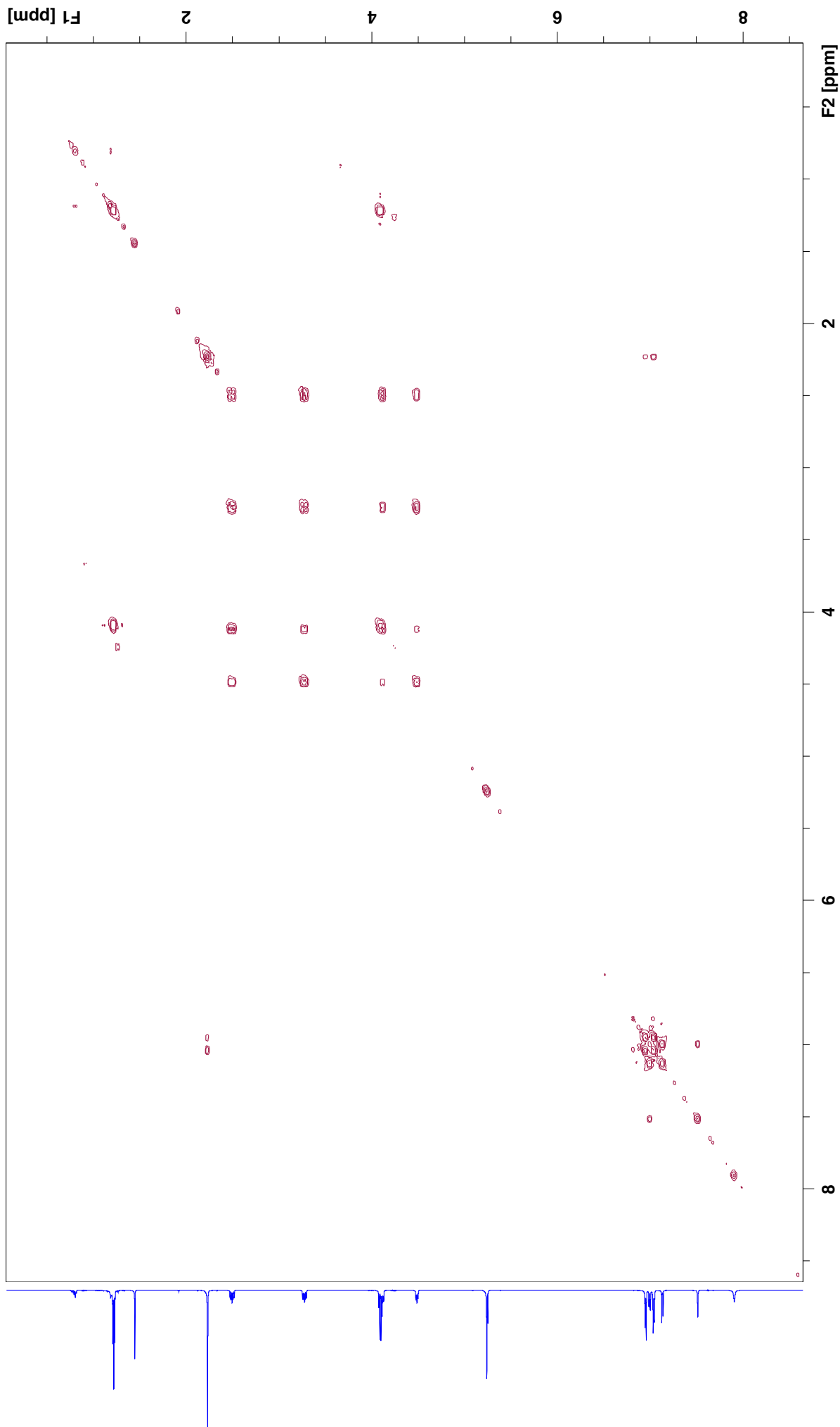
HMBC



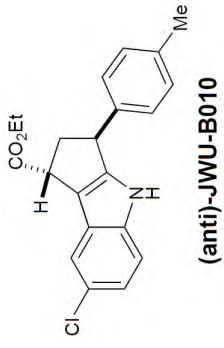
MT-N3-P48-TT23-3-4 24 1 N:\b600\wu\data\wu_guest\mmr



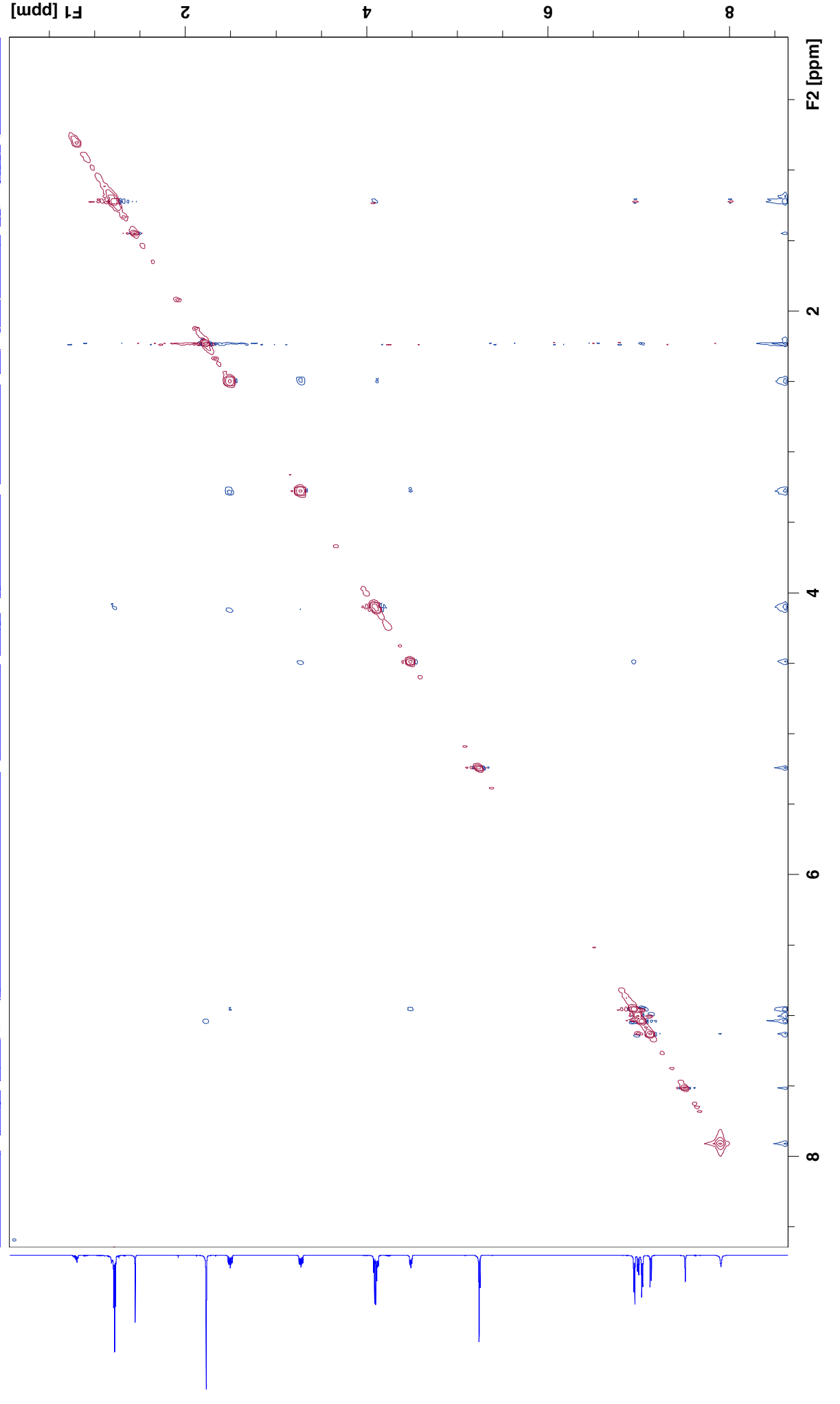
COSY

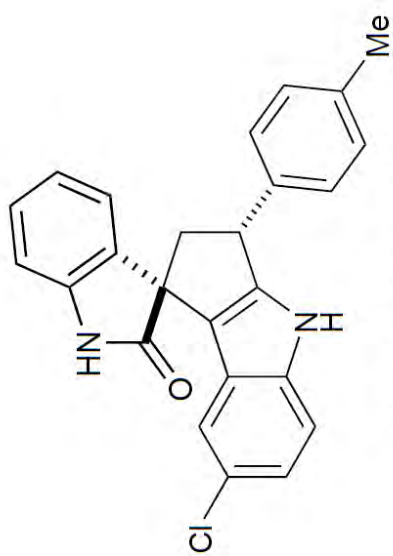


4T-N3-P48-TT23-3-4 23 1 N:\b600\wu\data\wu_guest\mmr

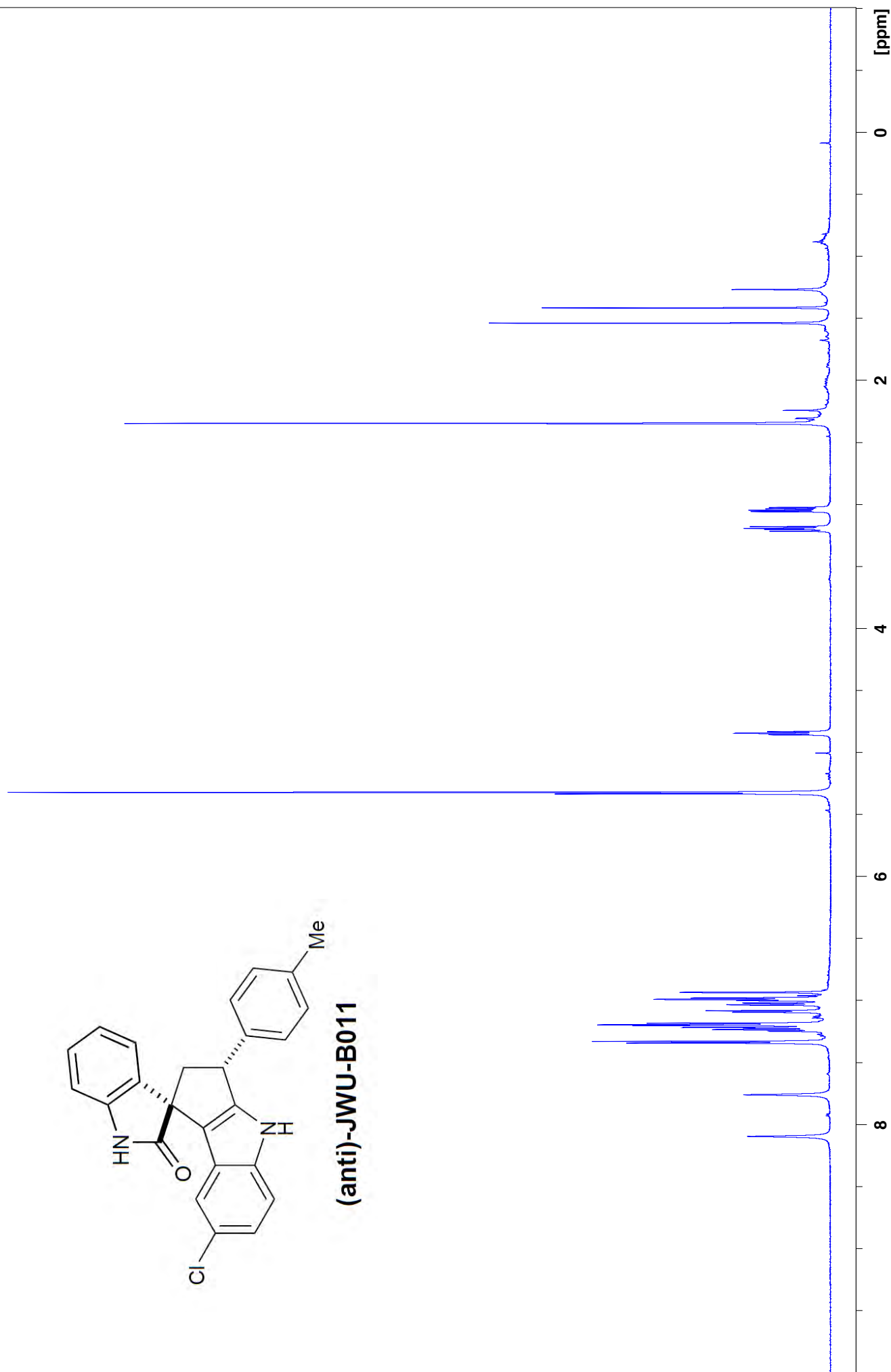


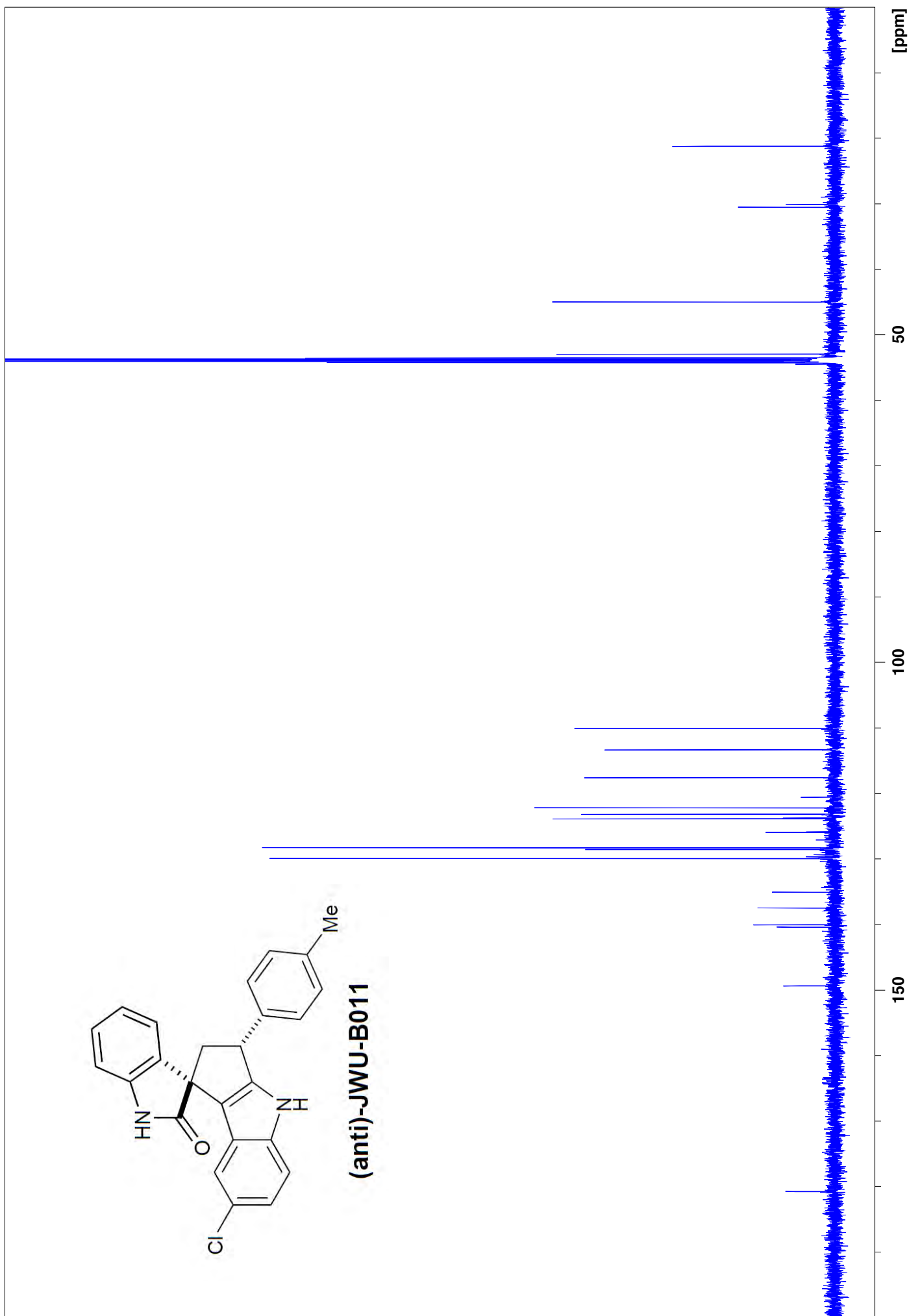
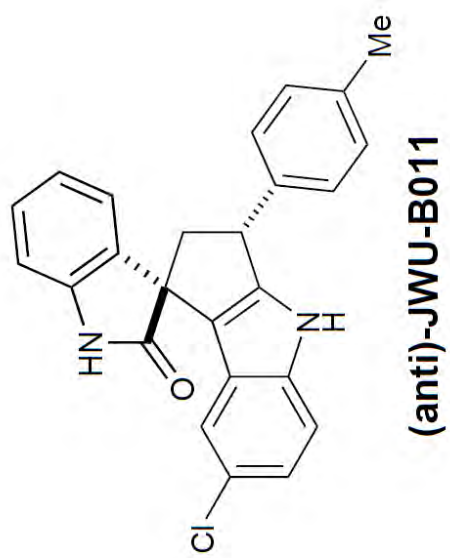
NOESY

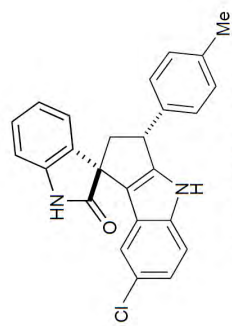




(anti)-JWU-B011



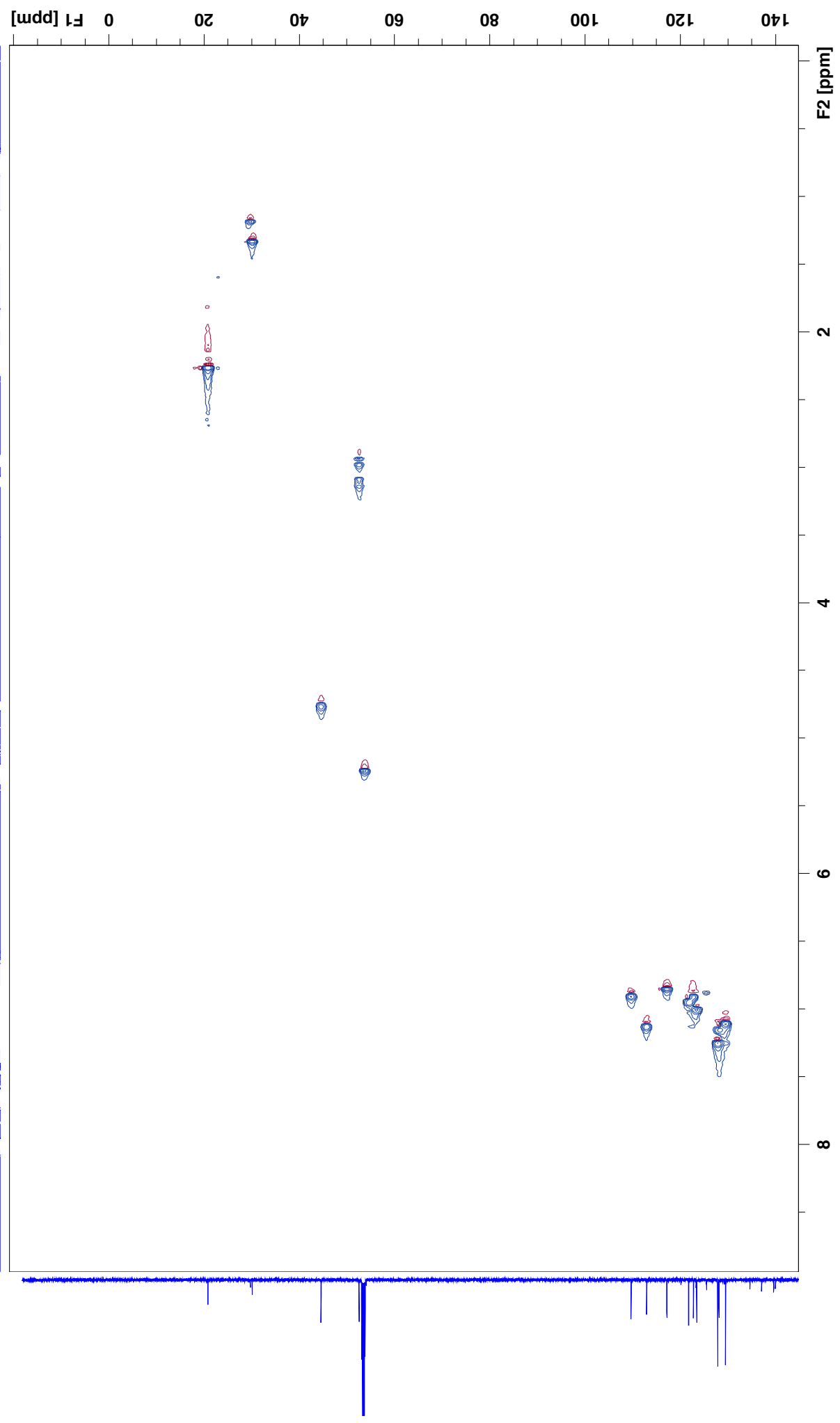


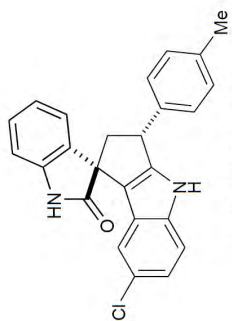


(anti)-JWU-B011

[-N3-P86-46-48-6-7 22 1 "I:\3+2 Products"

HMQC

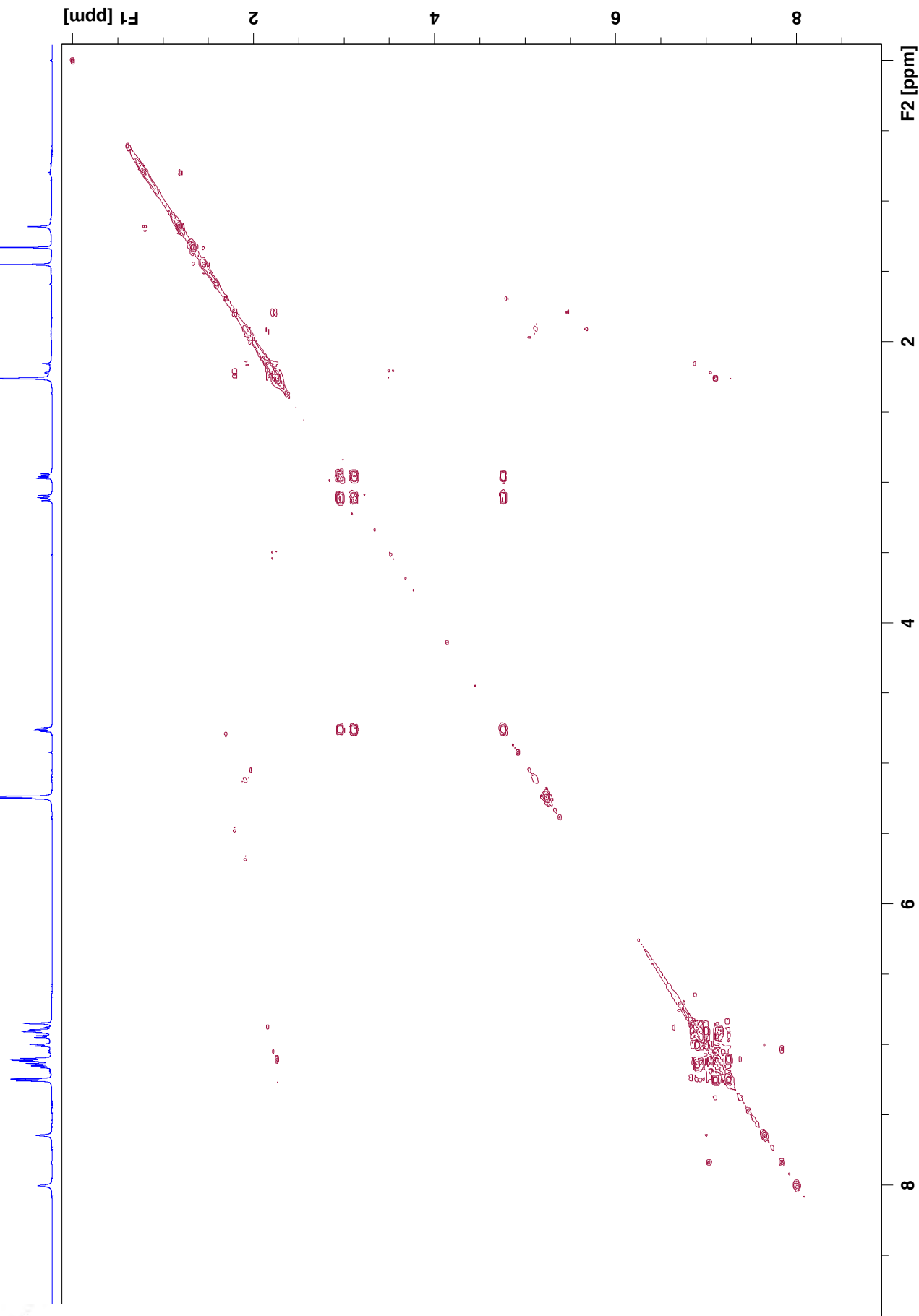


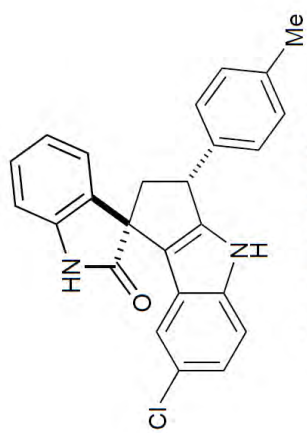


(anti)-JWU-B011

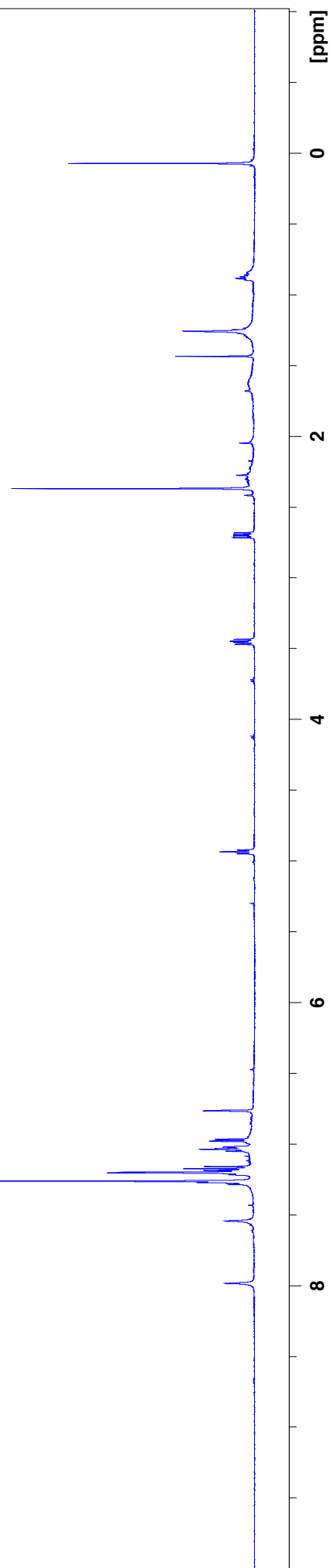
IT-N3-P86-46-48-6-7 24 1 "I:\3+2 Products"

COSY



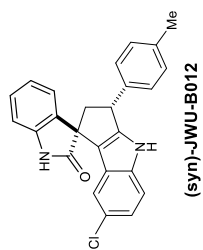


(syn)-JWU-B012

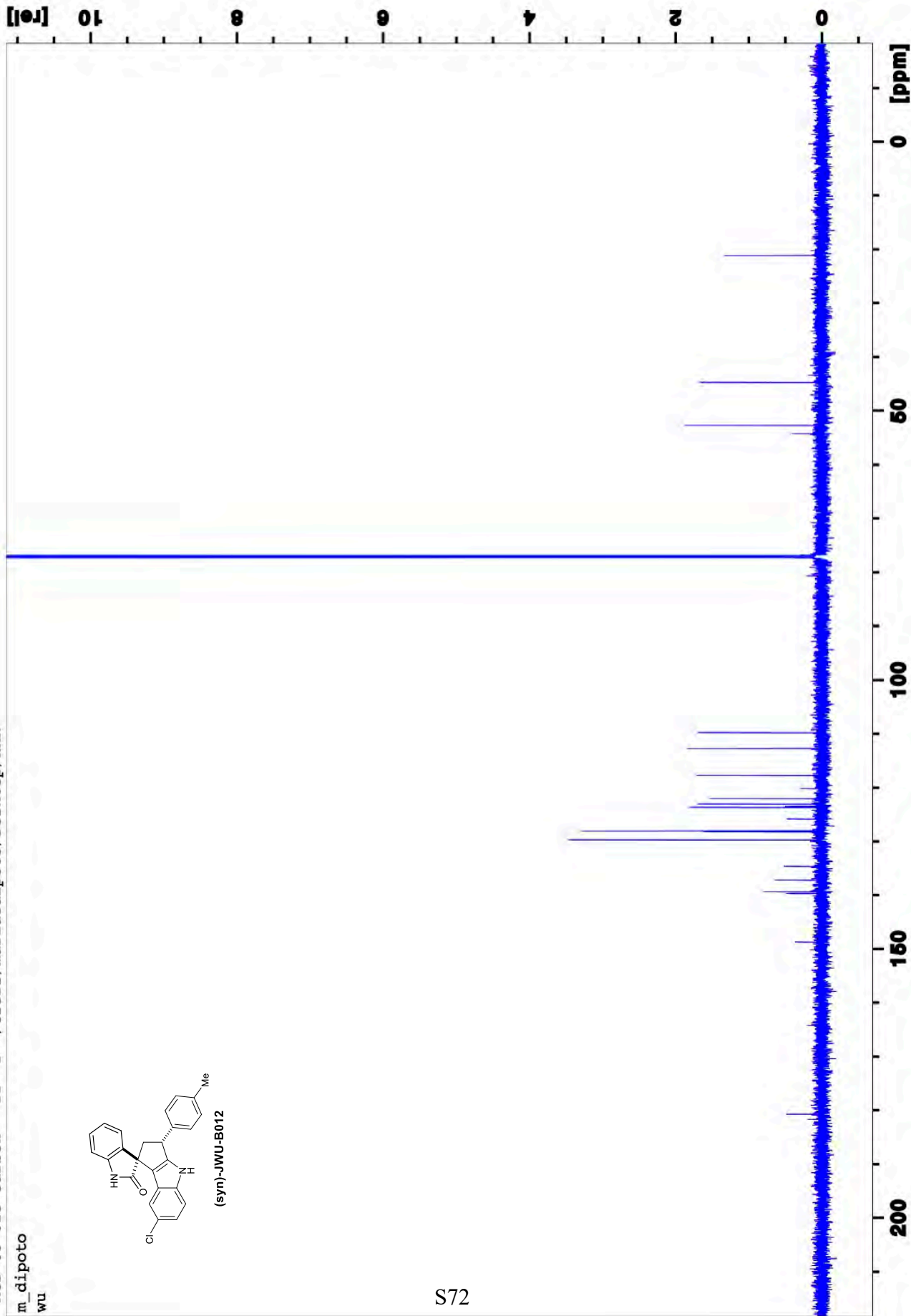


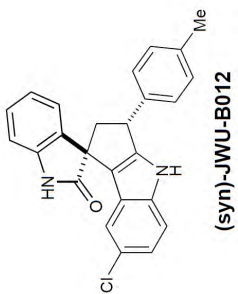
"MCD-06-02c carbon" 11 1 /Users/mariacidipoto/Desktop/NMR

m_dipoto
WU



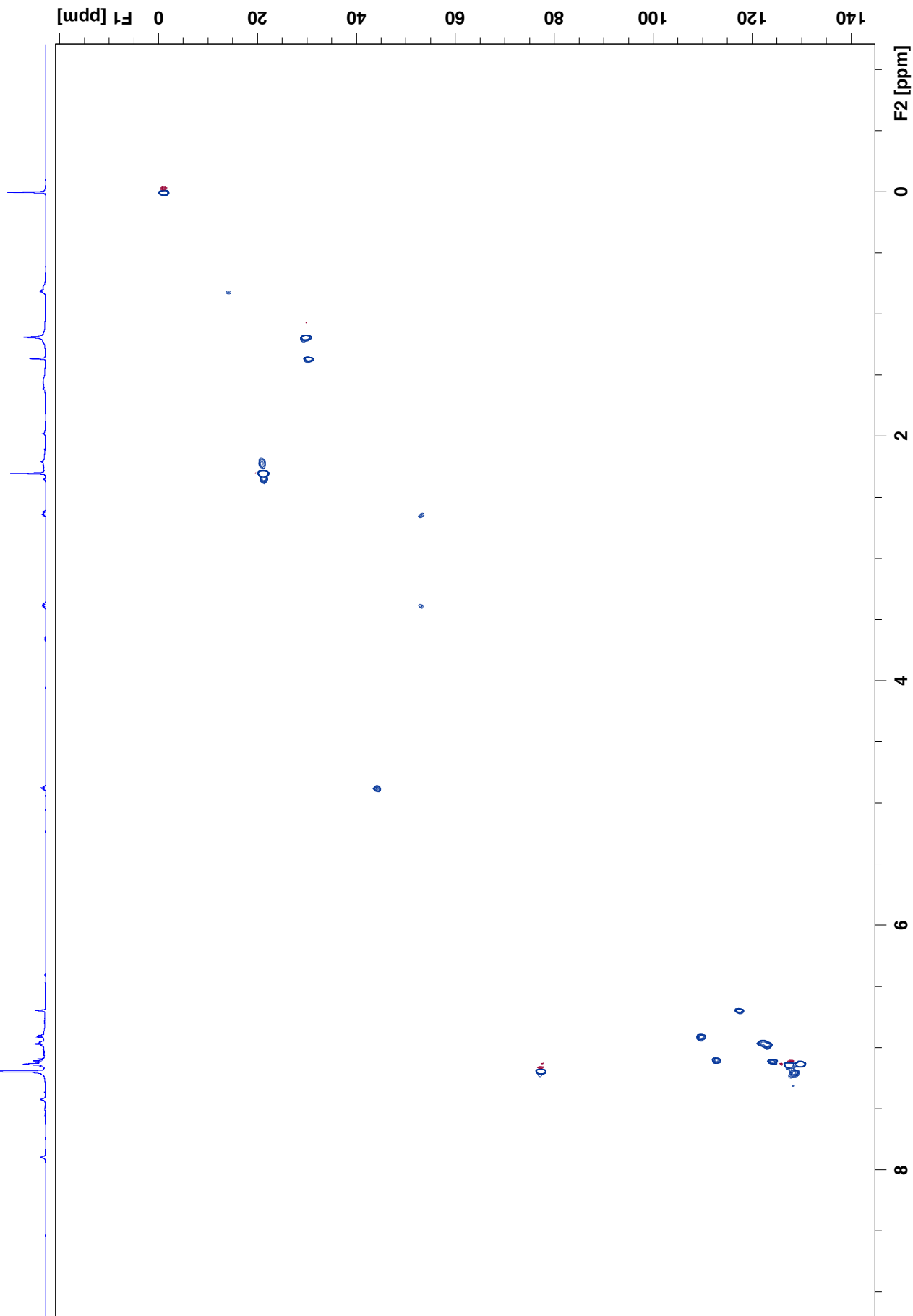
(syn)-JWU-B012

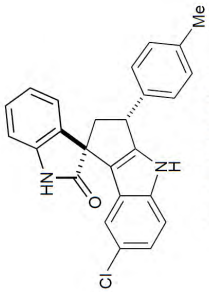




MT-N3-P86-55-59-7-9 13 1 "I:\3+2 Products"

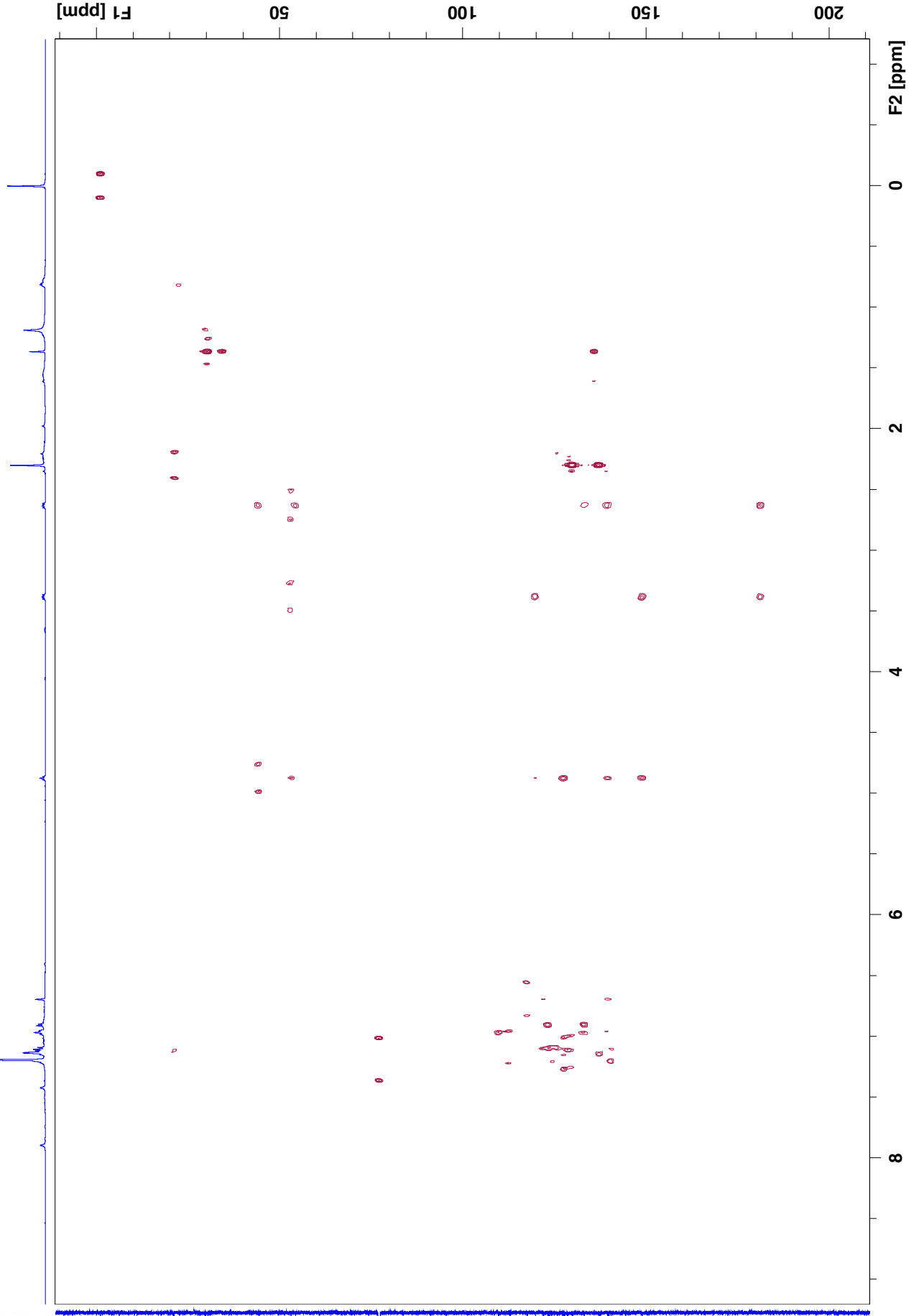
HMQC

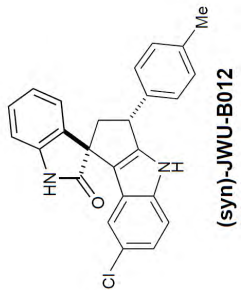




MT-N3-P86-55-59-7-9 14 1 "I:\3+2 Products"

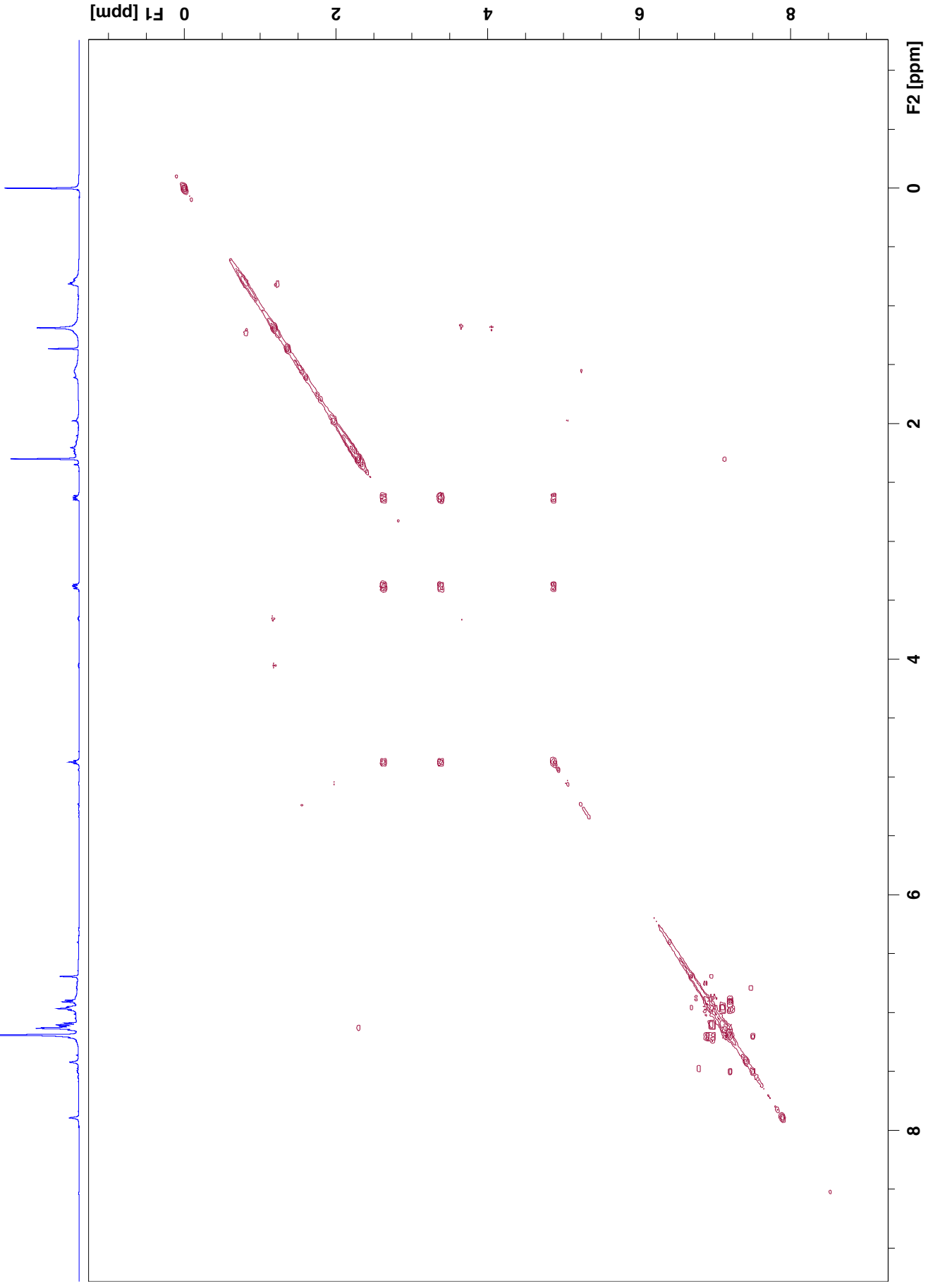
HMBC

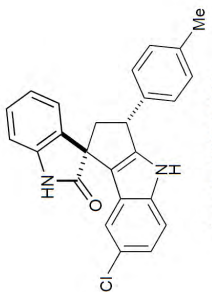




MT-N3-P86-55-59-7-9 15 1 "I:\3+2 Products"

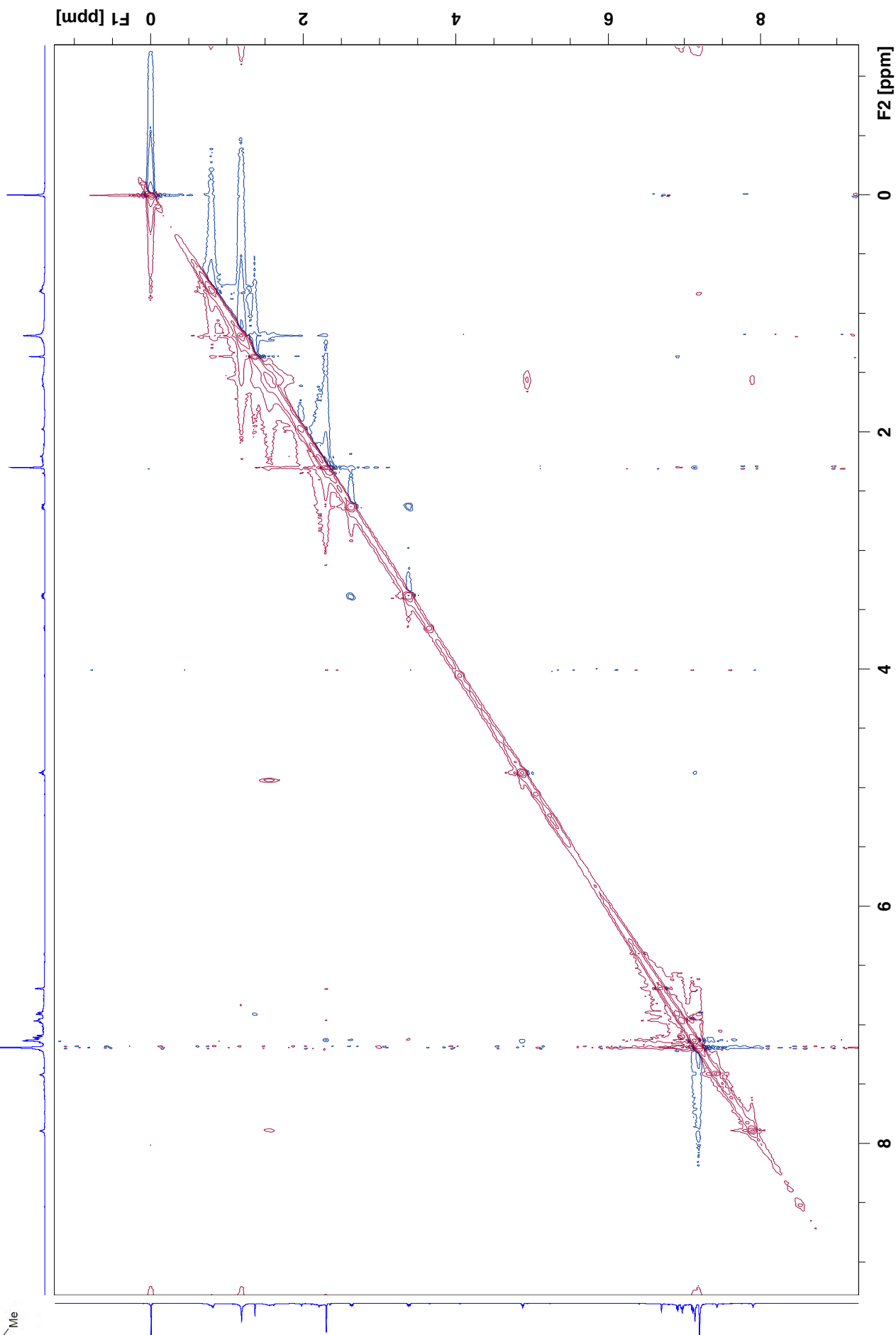
COSY

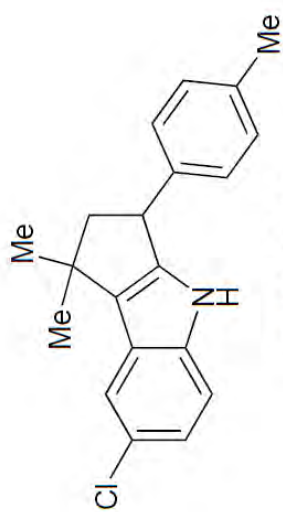




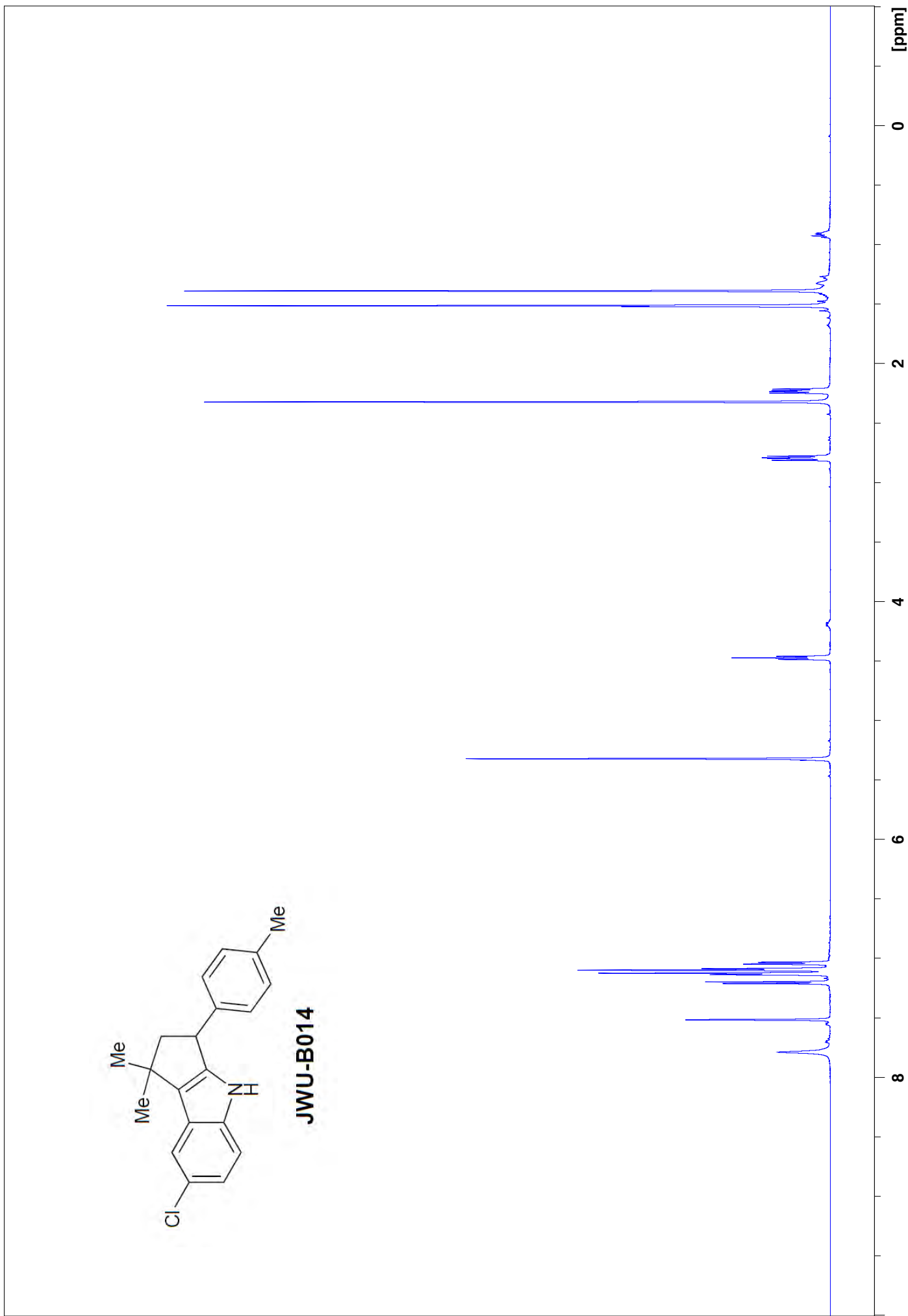
MT-N3-P86-55-59-7-9 16 1 "I:\3+2 Products"

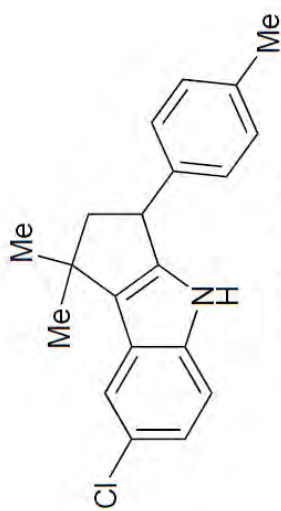
NOESY



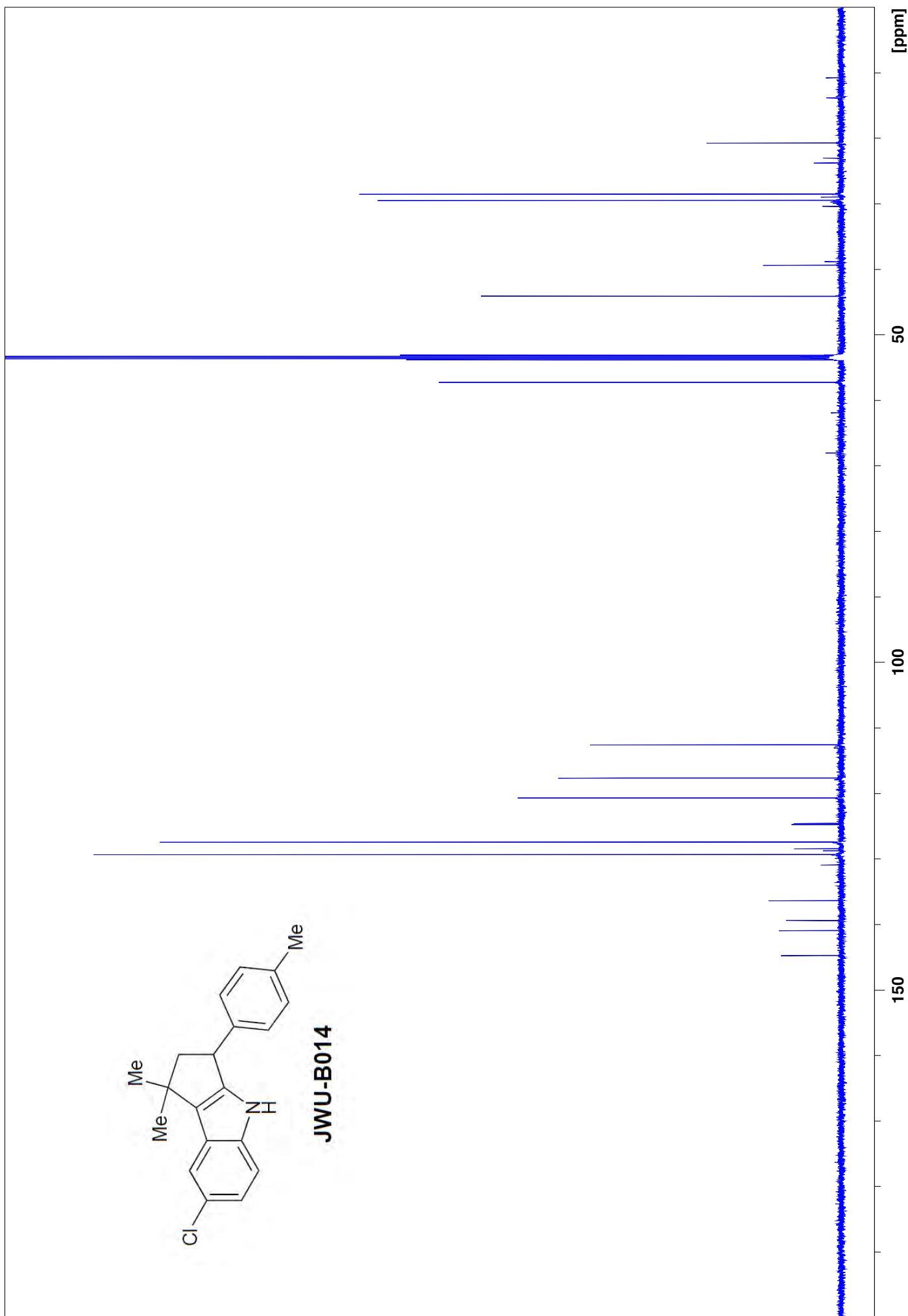


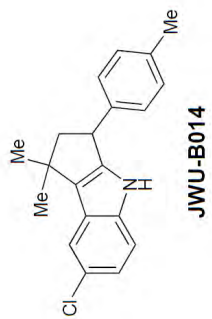
JWU-B014





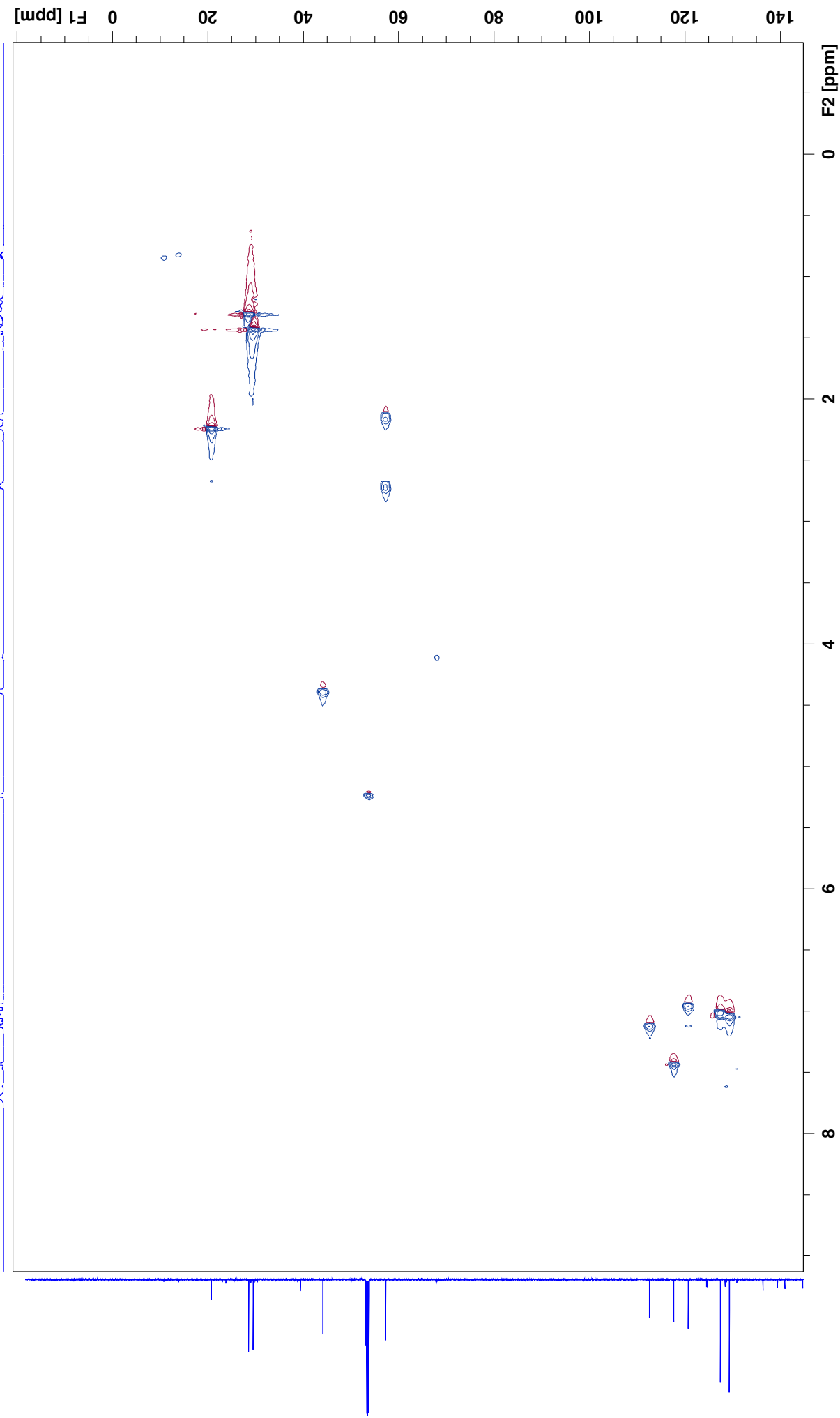
JWU-B014

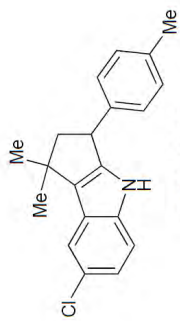




Γ-N3-P42-IT6-8-16-17 13 1 "I:\3+2 Products\MT-N3-P42-IT6-10-16-17"

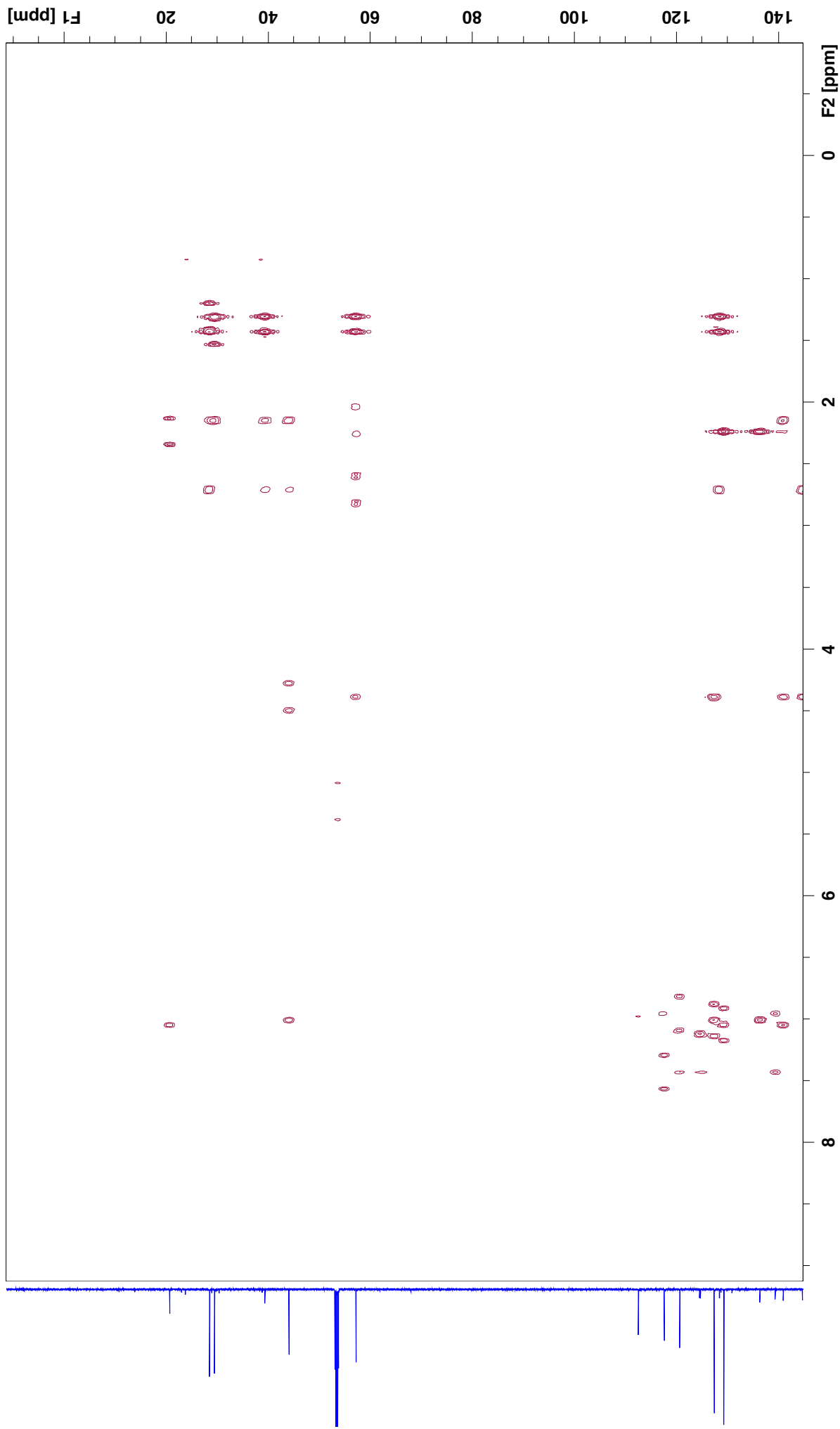
HMQC



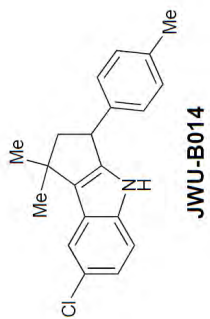


14 1 "I:\3+2 Products\WT-N3-P42-TT6-10-16-17"

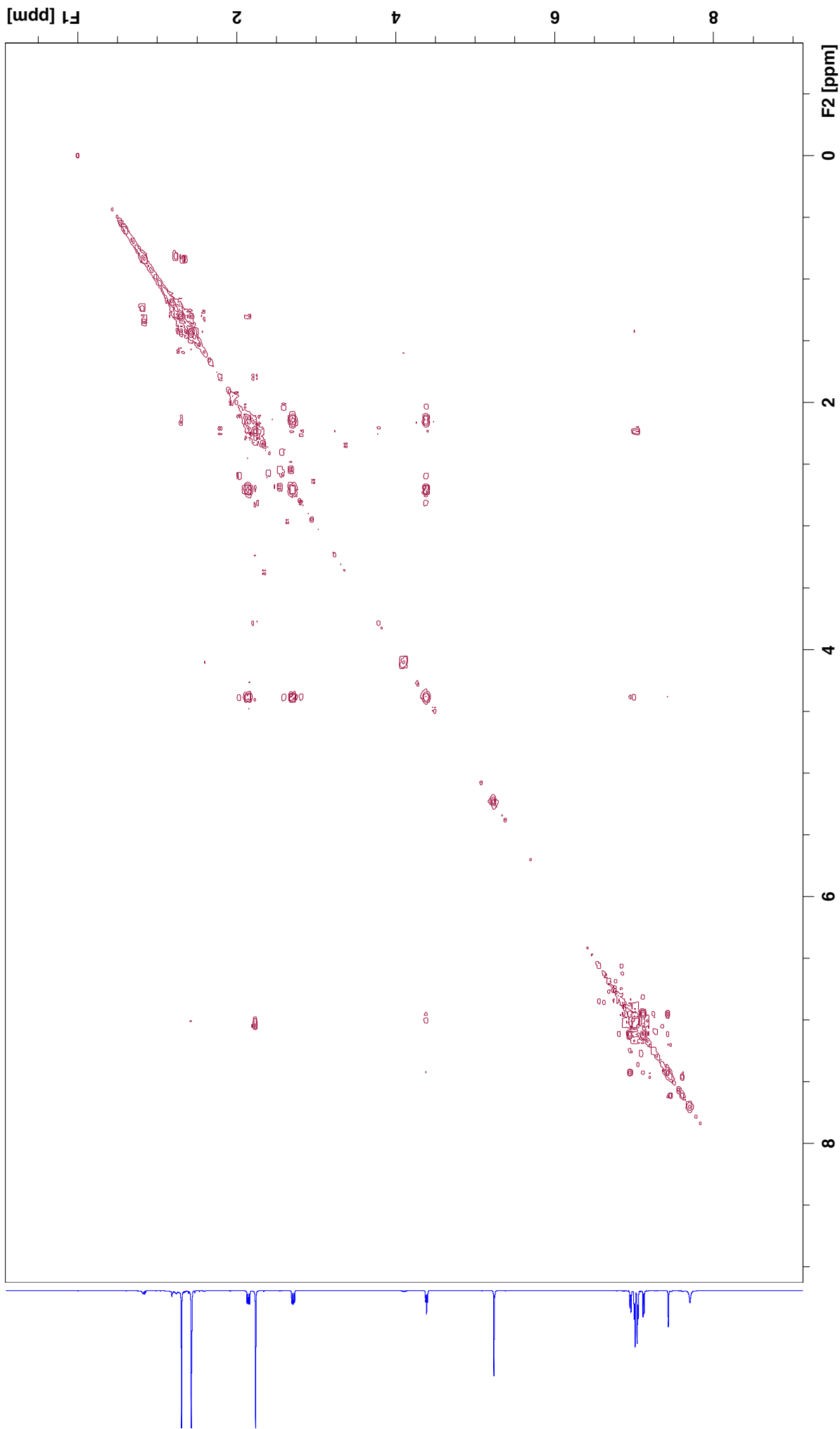
HMBC



Γ-N3-P42-TT6-8-16-17 16 1 "I:\3+2 Products\MT-N3-P42-TT6-10-16-17"



COSY



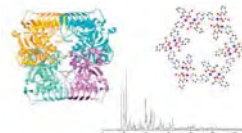
Structural Data

Date: March 17, 2015

Submitter: Jimmy Wu (Dartmouth)

Sample Reference Number: (-)-JWU-A021

X-ray Number: JW315a

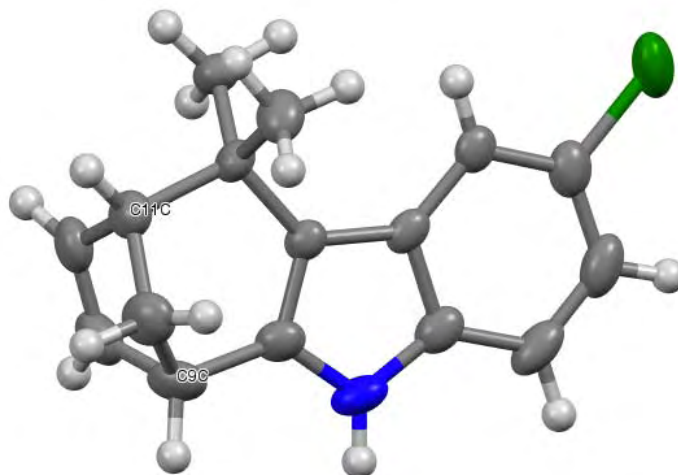


Center Crystallographic for Research
Michigan State University
Department of Chemistry
East Lansing, MI 48824
Dr. Richard J. Staples
staples@chemistry.msu.edu
(Shannon M. Biros, PhD)

Introduction:

Single crystal study to confirm the identity and chirality of the sample submitted. There are eight crystallographically unique molecules of $C_{16}H_{16}ClN$ in the asymmetric unit. Each molecule is labeled with the same atom numbering scheme, but has a different suffix (a-h). One molecule (f) was disordered over two positions with a 60:40 ratio; its counterpart is labeled with the same atom numbering scheme using a z-suffix. Shown below is a drawing of molecule (c) as a representative example.

The chirality of the compound was established by anomalous dispersion techniques using copper radiation with the use of the Flack parameter and Bayesian statistics of Bijvoet differences. Chiral carbons are labeled in the molecule below; C9 = *S*, C11 = *R*.



Experimental Section:

A yellow block crystal with dimensions 0.239 x 0.156 x 0.132 mm was mounted on a Nylon loop using very small amount of paratone oil.

Data were collected using a Bruker CCD (charge coupled device) based diffractometer equipped with an Oxford Cryostream low-temperature apparatus operating at 173 K. Data were measured using omega and phi scans of 1.0° per frame for 10 s. The total number of images was based on results from the program COSMO¹ where redundancy was expected to be 4.0 and completeness of 100% out to 0.83 Å. Cell parameters were retrieved using APEX II software² and refined using SAINT on all observed reflections. Data reduction was performed using the SAINT software³ which corrects for Lp. Scaling and absorption corrections were applied using SADABS⁴ multi-scan technique, supplied by George Sheldrick. The structures are solved by the direct method using the SHELXS-97 program and refined by least squares method on F², SHELXL-97⁵, which are incorporated in OLEX2.⁶

The structure was solved in the space group P2₁ (# 4). All non-hydrogen atoms are refined anisotropically. Hydrogens were calculated by geometrical methods and refined as a riding model. The Flack⁷ parameter is used to determine chirality of the crystal studied, the value should be near zero, a value of one is the other enantiomer and a value of 0.5 is racemic. The Flack parameter was refined to -0.017(9), confirming the absolute stereochemistry. Determination of absolute structure using Bayesian statistics on Bijvoet differences using the program within Platon⁸ also report that we have the correct enantiomer based on this comparison.⁹ The crystal used for the diffraction study showed no decomposition during data collection. All drawings are done at 50% ellipsoids.

Acknowledgement. The CCD based x-ray diffractometer at Michigan State

University were upgraded and/or replaced by departmental funds.

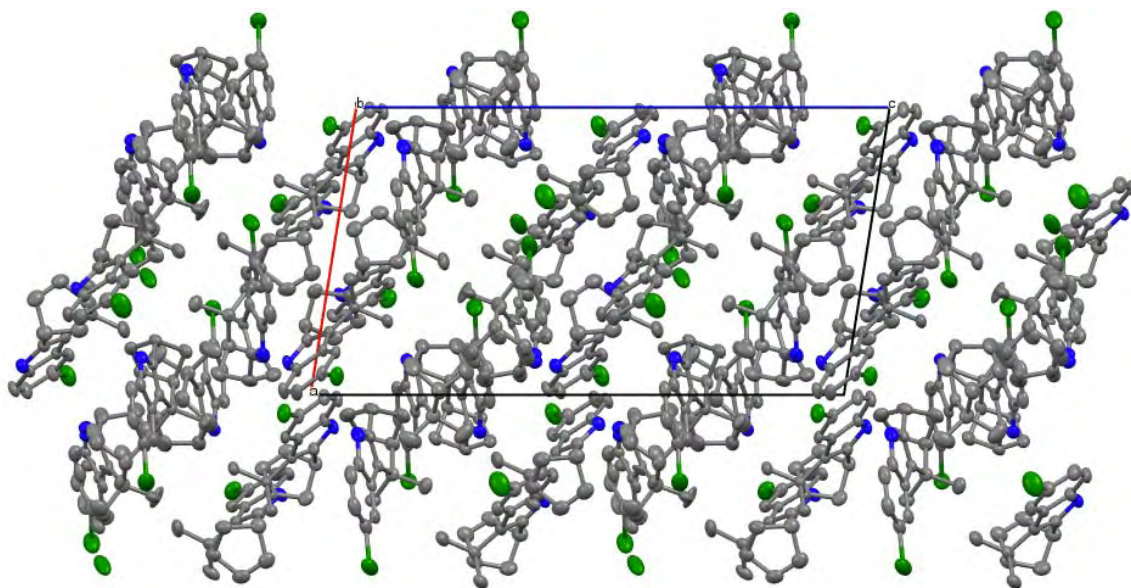
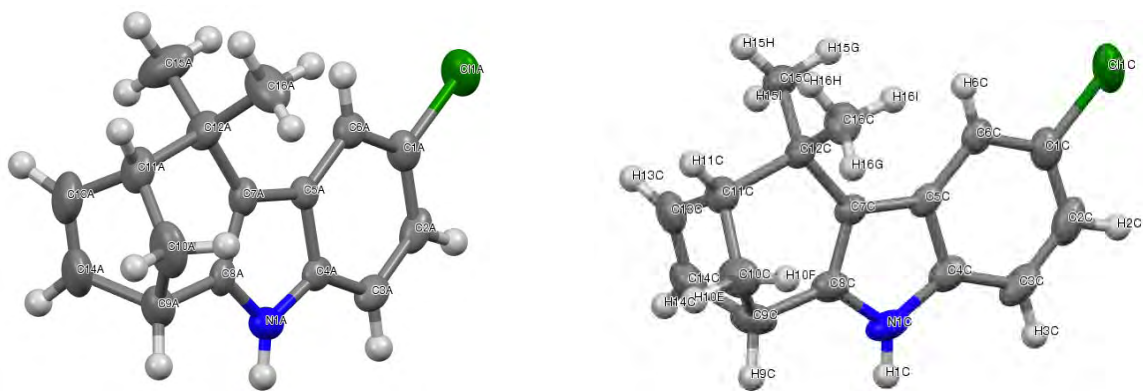
References

1. COSMO V1.61, *Software for the CCD Detector Systems for Determining Data Collection Parameters*. Bruker Analytical X-ray Systems, Madison, WI (2009).
2. APEX2 V2010.11-3. *Software for the CCD Detector System*; Bruker Analytical X-ray Systems, Madison, WI (2010).
3. SAINT V 7.68A *Software for the Integration of CCD Detector System* Bruker Analytical X-ray Systems, Madison, WI (2010).
4. SADABS V2.008/2 Program for absorption corrections using Bruker-AXS CCD based on the method of Robert Blessing; Blessing, R.H. *Acta Cryst.* A51, 1995, 33-38.
5. Sheldrick, G.M. "A short history of SHELX". *Acta Cryst.* **A64**, 2008, 112-122.
6. O. V. Dolomanov, L. J. Bourhis, R. J. Gildea, J. A. K. Howard and H. Puschmann, OLEX2: a complete structure solution, refinement and analysis program. *J. Appl. Cryst.* (2009). 42, 339-341.
7. Flack, H. D. *Acta Cryst.* **A39**, 1983, 876-881.
8. Spek, A.L. (2003), *J. Appl. Cryst.* **36**, 7-13.
9. Hooft, R.W.W.; Straver, L.H. & A. L. Spek, A.L.. *J. Appl. Cryst.* **41**, 2008, 96-103

^a Obtained with graphite monochromated Mo K α ($\lambda = 0.71073 \text{ \AA}$) radiation.

^b $R_1 = \sum \left| |F_o| - |F_c| \right| / \sum |F_o|$ ^c $wR_2 = \left\{ \frac{\sum [w(F_o^2 - F_c^2)^2]}{\sum [w(F_o^2)^2]} \right\}^{1/2}$.

The following are 50% thermal ellipsoidal drawings of one molecule (c) in the asymmetric cell with various amount of labeling.



This is a drawing of the packing along the *b*-axis; hydrogen atoms have been omitted for clarity.

Table 1 Crystal data and structure refinement for JW315a.

Identification code	JW315a
Empirical formula	C ₁₆ H ₁₆ ClN
Formula weight	257.75
Temperature/K	173.0
Crystal system	monoclinic
Space group	P2 ₁
a/Å	12.4101(3)
b/Å	18.9939(3)
c/Å	22.7815(4)
α/°	90
β/°	99.0520(10)
γ/°	90
Volume/Å ³	5303.09(18)
Z	16
ρ _{calc} /cm ³	1.291
μ/mm ⁻¹	2.372
F(000)	2176.0
Crystal size/mm ³	0.239 × 0.156 × 0.132
Radiation	CuKα (λ = 1.54178)
2θ range for data collection/°	3.928 to 144.904
Index ranges	-15 ≤ h ≤ 15, -23 ≤ k ≤ 23, -28 ≤ l ≤ 28
Reflections collected	66305
Independent reflections	20467 [R _{int} = 0.0891, R _{sigma} = 0.0731]
Data/restraints/parameters	20467/522/1477
Goodness-of-fit on F ²	1.009
Final R indexes [I ≥ 2σ (I)]	R ₁ = 0.0522, wR ₂ = 0.1151
Final R indexes [all data]	R ₁ = 0.0758, wR ₂ = 0.1280
Largest diff. peak/hole / e Å ⁻³	0.49/-0.54
Flack parameter	0.017(9)

Table 2 Fractional Atomic Coordinates (×10⁴) and Equivalent Isotropic Displacement Parameters (Å²×10³) for JW315a. U_{eq} is defined as 1/3 of the trace of the orthogonalised U_{ij} tensor.

Atom	x	y	z	U(eq)
Cl1A	3006.9(13)	6780.1(8)	2095.4(7)	49.6(4)
N1A	-1227(3)	5354(2)	1701(2)	36.9(10)
C1A	1708(5)	6368(3)	1963(2)	36.0(12)
C2A	812(5)	6774(3)	1713(2)	36.7(12)

C3A	-212(5)	6477(3)	1609(2)	36.0(12)
C4A	-316(4)	5770(3)	1756(2)	30.3(11)
C5A	588(4)	5359(3)	2012(2)	27.5(10)
C6A	1625(4)	5675(3)	2116(2)	32.6(11)
C7A	167(4)	4664(3)	2104(2)	32.8(11)
C8A	-930(4)	4695(3)	1914(2)	32.3(11)
C9A	-1679(5)	4083(3)	1951(3)	46.9(14)
C10A	-976(6)	3413(4)	1821(3)	63(2)
C11A	-146(5)	3419(3)	2391(3)	47.0(14)
C12A	736(5)	4001(3)	2366(3)	41.9(13)
C13A	-839(6)	3597(4)	2847(3)	66.6(19)
C14A	-1686(6)	3943(4)	2607(3)	67(2)
C15A	1348(7)	4161(4)	2995(3)	68(2)
C16A	1558(6)	3739(3)	1985(4)	61.0(19)
C11B	6660.4(14)	7221.4(8)	1166.4(7)	53.5(4)
N1B	6521(4)	4347(2)	264(2)	37.8(10)
C1B	6680(5)	6365(3)	889(2)	37.2(12)
C2B	7239(4)	6235(3)	415(2)	38.7(13)
C3B	7250(4)	5565(3)	183(2)	37.8(12)
C4B	6676(4)	5040(3)	423(2)	33.0(11)
C5B	6096(4)	5165(3)	902(2)	28.8(10)
C6B	6122(4)	5849(3)	1139(2)	32.7(11)
C7B	5582(4)	4513(3)	1017(2)	30.5(10)
C8B	5860(4)	4042(3)	625(2)	32.7(11)
C9B	5443(5)	3293(3)	588(3)	42.9(13)
C10B	5386(5)	3093(3)	1235(3)	43.0(13)
C11B	4421(4)	3560(3)	1346(3)	40.4(13)
C12B	4795(4)	4346(3)	1447(2)	36.6(12)
C13B	3671(5)	3464(3)	757(3)	46.5(14)
C14B	4234(5)	3305(3)	330(3)	47.4(14)
C15B	3812(5)	4848(3)	1334(3)	48.5(15)
C16B	5354(6)	4429(4)	2096(3)	54.0(16)
C11C	4016.6(14)	3823.9(9)	8376.9(8)	55.4(4)
N1C	8621(4)	4598(3)	8996(2)	42.1(11)
C1C	5417(5)	4010(3)	8569(3)	41.8(13)
C2C	6110(6)	3497(3)	8841(3)	48.7(15)
C3C	7203(6)	3636(3)	9002(3)	47.3(15)
C4C	7589(5)	4309(3)	8885(2)	36.7(12)
C5C	6883(4)	4826(3)	8590(2)	31.0(11)
C6C	5772(4)	4668(3)	8429(2)	32.3(11)
C7C	7539(4)	5439(3)	8525(2)	29.1(10)
C8C	8581(4)	5273(3)	8774(2)	36.5(12)

C9C	9506(5)	5790(4)	8815(3)	48.8(15)
C10C	9284(5)	6197(4)	8222(3)	51.0(16)
C11C	8288(5)	6623(3)	8320(3)	41.1(12)
C12C	7237(4)	6142(3)	8229(2)	33.8(11)
C13C	8615(5)	6835(3)	8961(3)	47.2(14)
C14C	9298(5)	6370(3)	9242(3)	51.5(15)
C15C	6335(4)	6503(3)	8512(3)	41.6(13)
C16C	6831(5)	6042(3)	7572(3)	46.4(14)
C11D	6895(2)	450.6(9)	6189.5(11)	82.8(7)
N1D	6318(4)	3322(3)	5309(2)	40.8(11)
C1D	6716(5)	1308(3)	5902(3)	43.8(14)
C2D	7296(5)	1484(4)	5449(3)	48.1(15)
C3D	7199(5)	2152(4)	5218(2)	44.1(14)
C4D	6539(4)	2628(3)	5455(2)	36.2(12)
C5D	5941(4)	2448(3)	5915(2)	31.7(11)
C6D	6049(5)	1760(3)	6147(2)	39.1(12)
C7D	5330(4)	3061(3)	6029(2)	31.9(11)
C8D	5582(4)	3572(3)	5654(2)	37.1(12)
C9D	5155(5)	4311(3)	5660(3)	47.4(14)
C10D	3967(5)	4229(4)	5774(3)	53.2(16)
C11D	4184(5)	3967(3)	6423(3)	46.0(14)
C12D	4509(4)	3175(3)	6454(3)	37.7(12)
C13D	5137(5)	4429(3)	6675(3)	48.6(14)
C14D	5678(5)	4633(3)	6253(3)	48.7(15)
C15D	4994(5)	2967(3)	7094(3)	47.5(14)
C16D	3495(5)	2721(3)	6252(3)	46.5(15)
C11E	9334.9(17)	9852.4(8)	5388.4(8)	59.8(4)
N1E	8997(4)	6959(2)	4509(2)	36.8(10)
C1E	9243(5)	8986(3)	5105(3)	41.5(13)
C2E	9844(5)	8828(3)	4650(3)	45.6(14)
C3E	9799(5)	8154(3)	4421(3)	40.6(13)
C4E	9173(4)	7656(3)	4655(2)	31.7(11)
C5E	8556(4)	7813(3)	5116(2)	30.5(11)
C6E	8613(4)	8506(3)	5343(2)	33.7(11)
C7E	8002(4)	7183(3)	5232(2)	29.6(10)
C8E	8283(4)	6681(3)	4853(2)	34.6(11)
C9E	7855(5)	5942(3)	4831(3)	46.9(14)
C10E	7746(5)	5767(3)	5476(3)	49.4(15)
C11E	6794(5)	6259(3)	5562(3)	45.3(14)
C12E	7194(4)	7039(3)	5651(3)	39.2(13)
C13E	6058(5)	6152(3)	4972(3)	50.6(15)
C14E	6647(5)	5979(3)	4561(3)	51.1(15)

C15E	6210(5)	7544(3)	5512(3)	48.8(15)
C16E	7728(5)	7147(4)	6303(3)	53.7(16)
C11F	5156(3)	9335.4(17)	6338.3(13)	70.9(9)
N1F	1135(11)	7702(7)	5878(9)	40(3)
C1F	3937(10)	8869(6)	6224(6)	40(2)
C2F	3038(11)	9222(6)	5892(6)	49(3)
C3F	2043(10)	8872(5)	5764(5)	44(2)
C4F	1993(11)	8175(5)	5951(6)	31(3)
C5F	2890(12)	7837(9)	6292(14)	32(3)
C6F	3882(8)	8199(5)	6422(5)	33(2)
C7F	2523(13)	7148(7)	6441(10)	28(4)
C8F	1482(13)	7074(8)	6143(11)	33(3)
C9F	823(11)	6434(7)	6158(7)	37(3)
C10F	1643(14)	5820(9)	6120(8)	48(4)
C11F	2351(13)	5894(8)	6736(8)	46(3)
C12F	3141(13)	6536(8)	6759(9)	40(4)
C13F	1466(16)	6017(13)	7103(8)	46(4)
C14F	611(16)	6326(9)	6793(8)	42(4)
C15F	3560(20)	6730(15)	7419(8)	67(7)
C16F	4123(18)	6338(11)	6446(12)	55(5)
C11Z	5933(4)	8893(3)	6606(2)	69.1(14)
N1Z	1442(14)	7916(9)	5918(11)	36(4)
C1Z	4560(12)	8643(8)	6401(7)	45(3)
C2Z	3807(17)	9122(9)	6083(10)	48(4)
C3Z	2733(16)	8935(8)	5909(8)	42(4)
C4Z	2441(15)	8245(9)	6047(11)	36(4)
C5Z	3192(16)	7782(12)	6372(19)	29(4)
C6Z	4272(13)	7982(8)	6547(9)	41(4)
C7Z	2625(18)	7123(11)	6388(18)	33(6)
C8Z	1564(18)	7245(11)	6158(19)	33(5)
C9Z	720(19)	6693(11)	6139(12)	50(6)
C10Z	1310(20)	5996(12)	6052(11)	52(6)
C11Z	2052(19)	5930(14)	6657(13)	57(6)
C12Z	3039(19)	6441(12)	6691(12)	37(5)
C13Z	1270(30)	6160(20)	7059(14)	62(8)
C14Z	520(30)	6573(14)	6776(15)	54(7)
C15Z	3550(20)	6590(20)	7343(12)	52(7)
C16Z	3940(30)	6137(16)	6362(18)	53(7)
C11G	3039.4(14)	1003.8(9)	7182.2(8)	61.1(4)
N1G	-1298(3)	2261(2)	6715.6(19)	33.9(10)
C1G	1712(5)	1354(3)	7035(3)	42.4(14)
C2G	885(5)	923(3)	6759(3)	44.8(14)

C3G	-170(5)	1188(3)	6634(2)	40.6(13)
C4G	-353(4)	1881(3)	6787(2)	33.4(12)
C5G	495(4)	2324(3)	7072(2)	29.2(10)
C6G	1560(5)	2043(3)	7199(2)	35.8(12)
C7G	2(4)	2983(3)	7166(2)	28.8(10)
C8G	-1082(4)	2918(3)	6949(2)	30.5(11)
C9G	-1893(4)	3507(3)	6938(2)	36.8(12)
C10G	-1518(5)	3900(3)	7528(3)	41.8(13)
C11G	-449(5)	4228(3)	7395(2)	36.7(12)
C12G	477(4)	3666(3)	7444(2)	31.5(11)
C13G	-806(4)	4463(3)	6754(3)	38.0(12)
C14G	-1617(4)	4055(3)	6497(2)	36.4(11)
C15G	1415(4)	3929(3)	7135(2)	38.2(12)
C16G	926(5)	3545(3)	8109(2)	45.1(13)
C11H	644.6(13)	2852.4(7)	9559.9(6)	45.4(3)
N1H	1106(4)	5702(2)	10517.4(19)	33.8(10)
C1H	743(4)	3712(3)	9848(2)	31.4(11)
C2H	86(5)	3883(3)	10263(2)	39.3(13)
C3H	143(5)	4551(3)	10515(2)	38.4(13)
C4H	876(4)	5024(3)	10333(2)	31.3(11)
C5H	1540(4)	4860(3)	9899(2)	27.9(10)
C6H	1474(4)	4181(3)	9654(2)	29.8(10)
C7H	2180(4)	5479(3)	9836(2)	28.2(10)
C8H	1891(4)	5964(3)	10224(2)	32.4(11)
C9H	2393(5)	6686(3)	10296(3)	36.9(12)
C10H	3596(5)	6580(3)	10223(3)	42.9(13)
C11H	3439(4)	6410(3)	9552(3)	36.4(12)
C12H	3037(4)	5629(3)	9437(2)	30.8(11)
C13H	2555(5)	6937(3)	9324(3)	43.1(13)
C14H	1975(5)	7100(3)	9732(3)	45.0(14)
C15H	2562(4)	5532(3)	8778(2)	37.6(12)
C16H	4023(4)	5134(3)	9599(2)	37.4(12)

Table 3 Anisotropic Displacement Parameters ($\text{\AA}^2 \times 10^3$) for JW315a. The Anisotropic displacement factor exponent takes the form: $-2\pi^2[h^2a^*^2U_{11}+2hka^*b^*U_{12}+\dots]$.

Atom	U_{11}	U_{22}	U_{33}	U_{23}	U_{13}	U_{12}
C11A	55.0(8)	39.7(7)	54.4(9)	-4.5(6)	9.6(7)	-21.8(6)
N1A	32(2)	47(3)	32(2)	0(2)	4.5(18)	2(2)
C1A	46(3)	34(3)	30(3)	-10(2)	11(2)	-7(2)
C2A	66(4)	20(2)	26(3)	-3(2)	13(2)	0(2)
C3A	46(3)	34(3)	30(3)	-1(2)	10(2)	12(2)
C4A	37(3)	35(3)	19(2)	-2(2)	8(2)	5(2)

C5A	31(2)	30(3)	23(2)	-3.5(19)	8.8(19)	0.1(19)
C6A	40(3)	30(3)	29(3)	-3(2)	8(2)	1(2)
C7A	43(3)	30(3)	28(3)	0(2)	10(2)	-6(2)
C8A	42(3)	35(3)	21(2)	1(2)	11(2)	-4(2)
C9A	45(3)	56(4)	41(3)	2(3)	10(3)	-14(3)
C10A	75(5)	51(4)	65(4)	-5(3)	23(4)	-35(4)
C11A	62(4)	35(3)	47(3)	8(3)	14(3)	-7(3)
C12A	49(3)	30(3)	45(3)	9(2)	4(3)	-5(2)
C13A	75(5)	73(5)	55(4)	24(4)	23(4)	-13(4)
C14A	58(4)	90(6)	56(4)	22(4)	18(3)	-23(4)
C15A	82(5)	46(4)	66(5)	12(3)	-24(4)	-1(3)
C16A	57(4)	33(3)	99(6)	9(3)	29(4)	6(3)
C11B	70.3(10)	29.7(7)	57.5(9)	-2.9(6)	0.4(7)	-8.5(6)
N1B	40(2)	36(2)	41(3)	-3(2)	17(2)	2.9(19)
C1B	45(3)	32(3)	33(3)	1(2)	-2(2)	-4(2)
C2B	37(3)	41(3)	38(3)	10(2)	3(2)	-9(2)
C3B	36(3)	45(3)	34(3)	5(2)	12(2)	-8(2)
C4B	34(3)	38(3)	28(3)	0(2)	5(2)	1(2)
C5B	27(2)	33(3)	26(2)	3(2)	2.9(19)	0.0(19)
C6B	32(2)	34(3)	32(3)	-3(2)	4(2)	-1(2)
C7B	28(2)	33(3)	30(3)	1(2)	4.7(19)	-2(2)
C8B	31(2)	30(3)	38(3)	-3(2)	6(2)	1(2)
C9B	50(3)	28(3)	51(3)	-5(2)	9(3)	5(2)
C10B	39(3)	33(3)	58(4)	10(3)	8(3)	-1(2)
C11B	37(3)	36(3)	49(3)	9(2)	11(2)	-6(2)
C12B	34(3)	40(3)	37(3)	0(2)	11(2)	-5(2)
C13B	38(3)	35(3)	64(4)	8(3)	3(3)	-9(2)
C14B	53(3)	32(3)	54(4)	-5(2)	1(3)	-7(2)
C15B	46(3)	39(3)	68(4)	1(3)	32(3)	0(3)
C16B	64(4)	69(4)	32(3)	-2(3)	17(3)	-14(3)
C11C	58.3(9)	49.5(9)	62.4(10)	-19.5(8)	22.0(8)	-20.7(7)
N1C	47(3)	42(3)	39(3)	11(2)	12(2)	19(2)
C1C	52(3)	40(3)	37(3)	-9(2)	19(3)	-9(3)
C2C	78(4)	31(3)	42(3)	-5(2)	25(3)	-6(3)
C3C	77(4)	31(3)	37(3)	7(2)	20(3)	13(3)
C4C	50(3)	35(3)	29(3)	3(2)	16(2)	8(2)
C5C	44(3)	27(2)	25(2)	0(2)	14(2)	6(2)
C6C	43(3)	30(3)	26(2)	-7(2)	12(2)	1(2)
C7C	33(2)	29(2)	27(2)	3(2)	12(2)	3(2)
C8C	36(3)	41(3)	35(3)	3(2)	13(2)	8(2)
C9C	30(3)	62(4)	56(4)	14(3)	11(2)	8(2)
C10C	44(3)	55(4)	59(4)	11(3)	22(3)	-5(3)

C11C	41(3)	35(3)	48(3)	8(2)	10(2)	-5(2)
C12C	39(3)	25(2)	38(3)	4(2)	7(2)	2(2)
C13C	46(3)	41(3)	54(4)	-4(3)	7(3)	-17(3)
C14C	40(3)	61(4)	52(4)	2(3)	1(3)	-16(3)
C15C	37(3)	35(3)	51(3)	-1(2)	4(2)	7(2)
C16C	58(4)	42(3)	37(3)	10(3)	2(3)	-5(3)
C11D	125.0(18)	33.8(9)	97.8(16)	8.2(9)	43.2(14)	12.2(10)
N1D	41(2)	50(3)	34(2)	10(2)	15(2)	3(2)
C1D	51(3)	32(3)	47(3)	-1(3)	4(3)	1(3)
C2D	56(4)	50(4)	39(3)	-8(3)	7(3)	14(3)
C3D	48(3)	59(4)	27(3)	2(3)	11(2)	8(3)
C4D	38(3)	40(3)	31(3)	0(2)	8(2)	3(2)
C5D	29(2)	38(3)	29(3)	-4(2)	6(2)	-2(2)
C6D	45(3)	39(3)	33(3)	-6(2)	6(2)	-6(2)
C7D	32(2)	34(3)	30(3)	-1(2)	6(2)	-4(2)
C8D	33(3)	42(3)	36(3)	-3(2)	4(2)	2(2)
C9D	48(3)	41(3)	55(4)	8(3)	10(3)	6(3)
C10D	43(3)	48(4)	67(4)	2(3)	4(3)	12(3)
C11D	37(3)	47(3)	57(4)	-11(3)	16(3)	-1(2)
C12D	37(3)	41(3)	38(3)	-9(2)	14(2)	-2(2)
C13D	51(3)	35(3)	62(4)	-16(3)	17(3)	1(2)
C14D	46(3)	33(3)	69(4)	-4(3)	15(3)	3(2)
C15D	46(3)	59(4)	41(3)	-12(3)	16(2)	-3(3)
C16D	41(3)	54(4)	47(3)	-12(3)	17(3)	-9(3)
C11E	90.9(12)	31.5(7)	63.9(10)	-7.1(7)	33.5(9)	-3.4(8)
N1E	43(2)	35(2)	35(2)	-4.7(19)	12(2)	3.0(19)
C1E	57(3)	32(3)	38(3)	-1(2)	15(3)	-4(3)
C2E	61(4)	40(3)	40(3)	2(3)	23(3)	-8(3)
C3E	50(3)	42(3)	34(3)	-1(2)	22(3)	-5(3)
C4E	33(3)	33(3)	30(3)	-2(2)	8(2)	2(2)
C5E	33(2)	33(3)	25(2)	3(2)	3.8(19)	0(2)
C6E	40(3)	32(3)	31(3)	-2(2)	11(2)	5(2)
C7E	33(2)	30(3)	25(2)	3(2)	2.1(19)	2(2)
C8E	37(3)	34(3)	33(3)	5(2)	6(2)	0(2)
C9E	51(3)	34(3)	56(4)	1(3)	8(3)	-4(2)
C10E	48(3)	38(3)	61(4)	16(3)	4(3)	-2(3)
C11E	40(3)	45(3)	51(4)	20(3)	9(3)	-6(2)
C12E	38(3)	42(3)	39(3)	10(2)	13(2)	1(2)
C13E	44(3)	44(3)	62(4)	14(3)	1(3)	-10(3)
C14E	57(4)	37(3)	56(4)	5(3)	-2(3)	-12(3)
C15E	39(3)	55(4)	56(4)	12(3)	20(3)	3(3)
C16E	59(4)	70(4)	35(3)	10(3)	18(3)	-3(3)

C11F	85(2)	71.3(19)	59.6(16)	-9.6(14)	21.3(15)	-50.0(17)
N1F	33(6)	48(7)	36(5)	2(6)	1(5)	-2(4)
C1F	59(6)	31(6)	33(7)	-3(5)	16(5)	-12(5)
C2F	75(7)	34(6)	40(6)	7(5)	11(6)	-8(5)
C3F	55(6)	39(5)	38(5)	4(4)	7(5)	10(5)
C4F	32(8)	34(5)	28(6)	1(5)	9(7)	-2(5)
C5F	33(7)	33(6)	29(8)	-1(5)	6(7)	-2(6)
C6F	34(5)	40(6)	25(5)	4(4)	4(4)	-11(4)
C7F	40(7)	30(6)	14(5)	0(5)	5(6)	-6(5)
C8F	39(6)	39(7)	21(6)	3(7)	3(4)	-3(5)
C9F	39(6)	38(7)	32(5)	-2(6)	-3(4)	-14(5)
C10F	64(9)	38(7)	45(7)	-4(6)	14(6)	-7(6)
C11F	59(8)	38(6)	41(7)	8(5)	7(5)	3(5)
C12F	45(7)	36(7)	38(9)	11(6)	5(5)	-2(5)
C13F	58(8)	39(9)	41(6)	15(5)	8(5)	-10(7)
C14F	39(7)	54(11)	33(6)	4(7)	7(5)	-19(7)
C15F	91(14)	72(11)	27(7)	15(7)	-24(7)	6(10)
C16F	60(9)	39(11)	69(11)	9(8)	16(8)	15(7)
C11Z	81(3)	67(3)	67(3)	-30(2)	36(2)	-49(3)
N1Z	28(10)	40(11)	39(9)	17(11)	9(10)	10(6)
C1Z	54(8)	39(8)	47(9)	-8(7)	20(7)	-6(7)
C2Z	86(9)	21(8)	40(10)	-2(7)	22(7)	-14(7)
C3Z	70(10)	26(8)	35(8)	5(8)	21(9)	9(8)
C4Z	34(10)	31(7)	42(11)	-4(6)	4(9)	-2(7)
C5Z	36(10)	28(7)	25(12)	-4(6)	12(10)	7(7)
C6Z	46(8)	31(8)	42(10)	1(7)	-1(8)	-7(6)
C7Z	24(7)	35(8)	45(14)	-4(8)	22(7)	11(5)
C8Z	40(9)	25(9)	37(11)	-1(9)	12(8)	0(6)
C9Z	54(10)	53(13)	45(9)	-1(11)	13(7)	-18(9)
C10Z	67(15)	43(12)	49(10)	-4(10)	19(10)	-40(11)
C11Z	62(12)	52(11)	61(14)	17(10)	21(10)	-11(8)
C12Z	46(10)	35(9)	27(10)	0(7)	-1(7)	9(8)
C13Z	82(17)	57(19)	55(12)	18(11)	32(13)	3(13)
C14Z	45(10)	54(17)	64(11)	3(11)	14(9)	-16(10)
C15Z	29(10)	80(18)	50(11)	5(10)	15(8)	0(9)
C16Z	55(13)	35(16)	73(14)	7(12)	18(12)	17(11)
C11G	65.2(10)	61(1)	57.4(9)	16.0(8)	10.5(8)	32.6(8)
N1G	35(2)	32(2)	36(2)	-3.2(19)	7.0(18)	-10.9(18)
C1G	50(3)	42(3)	37(3)	11(2)	11(3)	14(3)
C2G	72(4)	27(3)	39(3)	8(2)	22(3)	6(3)
C3G	67(4)	24(3)	33(3)	2(2)	16(3)	-4(2)
C4G	47(3)	30(3)	26(3)	4(2)	13(2)	-4(2)

C5G	41(3)	27(2)	21(2)	4.5(19)	10.9(19)	0(2)
C6G	44(3)	37(3)	26(3)	7(2)	8(2)	3(2)
C7G	36(3)	29(3)	22(2)	3.9(19)	7.8(19)	-4(2)
C8G	35(3)	31(3)	26(2)	2(2)	9(2)	-5(2)
C9G	31(2)	42(3)	39(3)	-3(2)	11(2)	0(2)
C10G	42(3)	45(3)	41(3)	-11(3)	15(2)	0(2)
C11G	45(3)	32(3)	34(3)	-7(2)	13(2)	-5(2)
C12G	36(3)	34(3)	25(2)	1(2)	5.7(19)	-3(2)
C13G	40(3)	29(3)	44(3)	7(2)	6(2)	7(2)
C14G	36(3)	39(3)	35(3)	1(2)	5(2)	11(2)
C15G	34(3)	39(3)	40(3)	2(2)	2(2)	-7(2)
C16G	56(3)	42(3)	32(3)	-4(2)	-7(2)	-6(3)
C11H	73.0(9)	24.2(6)	39.0(7)	-4.9(5)	8.8(6)	-8.0(6)
N1H	46(2)	30(2)	29(2)	-8.8(18)	16.1(19)	-6.9(19)
C1H	49(3)	22(2)	23(2)	-3.9(19)	3(2)	0(2)
C2H	55(3)	35(3)	29(3)	3(2)	10(2)	-18(2)
C3H	54(3)	38(3)	27(3)	-5(2)	16(2)	-9(3)
C4H	40(3)	33(3)	22(2)	-3(2)	9(2)	-5(2)
C5H	31(2)	33(3)	20(2)	1(2)	5.1(19)	3(2)
C6H	35(2)	35(3)	19(2)	-2(2)	2.6(19)	1(2)
C7H	31(2)	29(2)	24(2)	2.2(19)	4.1(18)	-2.2(19)
C8H	39(3)	32(3)	27(2)	-3(2)	6(2)	-4(2)
C9H	47(3)	26(3)	39(3)	-6(2)	11(2)	-5(2)
C10H	48(3)	31(3)	47(3)	-1(2)	-2(3)	-12(2)
C11H	31(3)	38(3)	42(3)	7(2)	10(2)	-7(2)
C12H	29(2)	38(3)	27(2)	2(2)	7.5(19)	0(2)
C13H	43(3)	35(3)	50(3)	14(2)	3(3)	-8(2)
C14H	45(3)	25(3)	64(4)	7(2)	6(3)	-1(2)
C15H	39(3)	48(3)	27(3)	1(2)	10(2)	-5(2)
C16H	34(3)	41(3)	38(3)	-1(2)	8(2)	2(2)

Table 4 Bond Lengths for JW315a.

Atom Atom Length/Å		Atom Atom Length/Å			
C11A	C1A	1.774(5)	C7E	C12E	1.514(7)
N1A	C4A	1.370(7)	C8E	C9E	1.499(8)
N1A	C8A	1.372(7)	C9E	C10E	1.535(9)
C1A	C2A	1.399(8)	C9E	C14E	1.530(9)
C1A	C6A	1.370(7)	C10E	C11E	1.543(9)
C2A	C3A	1.376(8)	C11E	C12E	1.566(8)
C3A	C4A	1.395(7)	C11E	C13E	1.514(9)
C4A	C5A	1.415(7)	C12E	C15E	1.547(8)
C5A	C6A	1.406(7)	C12E	C16E	1.540(8)

C5A	C7A	1.448(7)	C13E	C14E	1.318(9)
C7A	C8A	1.363(7)	C11F	C1F	1.737(11)
C7A	C12A	1.518(7)	N1F	C4F	1.382(13)
C8A	C9A	1.498(7)	N1F	C8F	1.375(13)
C9A	C10A	1.598(9)	C1F	C2F	1.416(16)
C9A	C14A	1.519(8)	C1F	C6F	1.355(13)
C10A	C11A	1.524(9)	C2F	C3F	1.391(15)
C11A	C12A	1.563(7)	C3F	C4F	1.396(12)
C11A	C13A	1.489(9)	C4F	C5F	1.408(14)
C12A	C15A	1.544(8)	C5F	C6F	1.401(13)
C12A	C16A	1.523(8)	C5F	C7F	1.443(12)
C13A	C14A	1.286(10)	C7F	C8F	1.368(13)
C11B	C1B	1.747(6)	C7F	C12F	1.514(13)
N1B	C4B	1.371(7)	C8F	C9F	1.469(13)
N1B	C8B	1.376(7)	C9F	C10F	1.558(14)
C1B	C2B	1.396(8)	C9F	C14F	1.526(13)
C1B	C6B	1.374(8)	C10F	C11F	1.540(14)
C2B	C3B	1.378(8)	C11F	C12F	1.561(14)
C3B	C4B	1.388(7)	C11F	C13F	1.499(14)
C4B	C5B	1.418(7)	C12F	C15F	1.555(15)
C5B	C6B	1.405(7)	C12F	C16F	1.552(14)
C5B	C7B	1.437(7)	C13F	C14F	1.316(15)
C7B	C8B	1.347(7)	C11Z	C1Z	1.759(14)
C7B	C12B	1.521(7)	N1Z	C4Z	1.378(17)
C8B	C9B	1.512(7)	N1Z	C8Z	1.386(17)
C9B	C10B	1.536(8)	C1Z	C2Z	1.419(19)
C9B	C14B	1.523(8)	C1Z	C6Z	1.360(17)
C10B	C11B	1.543(8)	C2Z	C3Z	1.38(2)
C11B	C12B	1.569(8)	C3Z	C4Z	1.408(17)
C11B	C13B	1.520(9)	C4Z	C5Z	1.405(17)
C12B	C15B	1.537(8)	C5Z	C6Z	1.391(17)
C12B	C16B	1.540(8)	C5Z	C7Z	1.439(17)
C13B	C14B	1.319(9)	C7Z	C8Z	1.358(17)
C11C	C1C	1.760(6)	C7Z	C12Z	1.520(17)
N1C	C4C	1.379(8)	C8Z	C9Z	1.478(18)
N1C	C8C	1.377(7)	C9Z	C10Z	1.539(19)
C1C	C2C	1.381(9)	C9Z	C14Z	1.525(19)
C1C	C6C	1.379(8)	C10Z	C11Z	1.54(2)
C2C	C3C	1.375(10)	C11Z	C12Z	1.555(18)
C3C	C4C	1.406(8)	C11Z	C13Z	1.505(19)
C4C	C5C	1.415(7)	C12Z	C15Z	1.546(18)
C5C	C6C	1.402(8)	C12Z	C16Z	1.548(18)

C5C	C7C	1.440(7)	C13Z	C14Z	1.30(2)
C7C	C8C	1.365(8)	C11G	C1G	1.759(6)
C7C	C12C	1.516(7)	N1G	C4G	1.365(7)
C8C	C9C	1.503(8)	N1G	C8G	1.366(7)
C9C	C10C	1.544(9)	C1G	C2G	1.385(9)
C9C	C14C	1.518(9)	C1G	C6G	1.382(8)
C10C	C11C	1.523(8)	C2G	C3G	1.389(9)
C11C	C12C	1.579(7)	C3G	C4G	1.390(7)
C11C	C13C	1.507(9)	C4G	C5G	1.421(8)
C12C	C15C	1.537(7)	C5G	C6G	1.412(8)
C12C	C16C	1.514(8)	C5G	C7G	1.426(7)
C13C	C14C	1.317(9)	C7G	C8G	1.364(7)
C11D	C1D	1.757(6)	C7G	C12G	1.521(7)
N1D	C4D	1.376(7)	C8G	C9G	1.502(7)
N1D	C8D	1.381(7)	C9G	C10G	1.544(8)
C1D	C2D	1.387(9)	C9G	C14G	1.522(8)
C1D	C6D	1.372(8)	C10G	C11G	1.539(7)
C2D	C3D	1.372(9)	C11G	C12G	1.560(8)
C3D	C4D	1.386(8)	C11G	C13G	1.524(8)
C4D	C5D	1.419(7)	C12G	C15G	1.535(7)
C5D	C6D	1.408(8)	C12G	C16G	1.547(7)
C5D	C7D	1.435(7)	C13G	C14G	1.331(8)
C7D	C8D	1.359(8)	C11H	C1H	1.757(5)
C7D	C12D	1.528(7)	N1H	C4H	1.371(7)
C8D	C9D	1.501(8)	N1H	C8H	1.360(7)
C9D	C10D	1.545(8)	C1H	C2H	1.380(8)
C9D	C14D	1.532(9)	C1H	C6H	1.392(7)
C10D	C11D	1.542(9)	C2H	C3H	1.389(8)
C11D	C12D	1.558(8)	C3H	C4H	1.386(7)
C11D	C13D	1.511(8)	C4H	C5H	1.418(7)
C12D	C15D	1.539(8)	C5H	C6H	1.402(7)
C12D	C16D	1.534(8)	C5H	C7H	1.439(7)
C13D	C14D	1.315(9)	C7H	C8H	1.364(7)
C11E	C1E	1.765(6)	C7H	C12H	1.530(6)
N1E	C4E	1.375(7)	C8H	C9H	1.505(7)
N1E	C8E	1.377(7)	C9H	C10H	1.541(8)
C1E	C2E	1.402(8)	C9H	C14H	1.526(8)
C1E	C6E	1.368(8)	C10H	C11H	1.545(8)
C2E	C3E	1.381(8)	C11H	C12H	1.573(7)
C3E	C4E	1.384(8)	C11H	C13H	1.515(8)
C4E	C5E	1.424(7)	C12H	C15H	1.535(7)
C5E	C6E	1.413(8)	C12H	C16H	1.542(7)

C5E C7E 1.426(7) C13HC14H 1.300(8)
 C7E C8E 1.368(7)

Table 5 Bond Angles for JW315a.

Atom	Atom	Atom	Angle/°	Atom	Atom	Atom	Angle/°
C4A	N1A	C8A	108.8(4)	C7E	C8E	N1E	110.1(5)
C2A	C1A	C11A	118.0(4)	C7E	C8E	C9E	123.3(5)
C6A	C1A	C11A	118.9(4)	C8E	C9E	C10E	104.8(5)
C6A	C1A	C2A	123.1(5)	C8E	C9E	C14E	106.9(5)
C3A	C2A	C1A	119.8(5)	C14E	C9E	C10E	99.6(5)
C2A	C3A	C4A	118.1(5)	C9E	C10E	C11E	100.1(5)
N1A	C4A	C3A	129.8(5)	C10E	C11E	C12E	110.8(5)
N1A	C4A	C5A	108.0(4)	C13E	C11E	C10E	100.0(5)
C3A	C4A	C5A	122.2(5)	C13E	C11E	C12E	112.1(5)
C4A	C5A	C7A	106.4(4)	C7E	C12E	C11E	108.5(5)
C6A	C5A	C4A	118.7(5)	C7E	C12E	C15E	109.7(4)
C6A	C5A	C7A	134.9(5)	C7E	C12E	C16E	110.9(5)
C1A	C6A	C5A	118.1(5)	C15E	C12E	C11E	109.6(5)
C5A	C7A	C12A	131.1(5)	C16E	C12E	C11E	109.3(5)
C8A	C7A	C5A	106.2(4)	C16E	C12E	C15E	108.8(5)
C8A	C7A	C12A	122.7(5)	C14E	C13E	C11E	109.9(6)
N1A	C8A	C9A	126.3(5)	C13E	C14E	C9E	110.0(6)
C7A	C8A	N1A	110.6(5)	C8F	N1F	C4F	109.2(10)
C7A	C8A	C9A	123.1(5)	C2F	C1F	C11F	115.7(9)
C8A	C9A	C10A	104.2(4)	C6F	C1F	C11F	121.2(10)
C8A	C9A	C14A	106.9(5)	C6F	C1F	C2F	123.1(10)
C14A	C9A	C10A	97.5(5)	C3F	C2F	C1F	119.0(10)
C11A	C10A	C9A	98.7(5)	C2F	C3F	C4F	118.0(10)
C10A	C11A	C12A	110.9(5)	N1F	C4F	C3F	130.5(12)
C13A	C11A	C10A	102.1(6)	N1F	C4F	C5F	107.3(9)
C13A	C11A	C12A	110.5(5)	C3F	C4F	C5F	122.1(11)
C7A	C12A	C11A	108.4(5)	C4F	C5F	C7F	106.9(9)
C7A	C12A	C15A	109.4(5)	C6F	C5F	C4F	119.0(10)
C7A	C12A	C16A	111.1(5)	C6F	C5F	C7F	134.1(11)
C15A	C12A	C11A	110.5(5)	C1F	C6F	C5F	118.6(10)
C16A	C12A	C11A	109.0(5)	C5F	C7F	C12F	130.8(11)
C16A	C12A	C15A	108.6(6)	C8F	C7F	C5F	106.6(10)
C14A	C13A	C11A	110.1(6)	C8F	C7F	C12F	121.8(11)
C13A	C14A	C9A	112.1(7)	N1F	C8F	C9F	126.2(11)
C4B	N1B	C8B	108.5(4)	C7F	C8F	N1F	109.5(10)
C2B	C1B	C11B	118.8(4)	C7F	C8F	C9F	124.0(11)
C6B	C1B	C11B	118.6(4)	C8F	C9F	C10F	104.3(11)

C6B C1B C2B 122.6(5) C8F C9F C14F 108.2(12)
 C3B C2B C1B 119.8(5) C14F C9F C10F 99.3(10)
 C2B C3B C4B 118.3(5) C11F C10F C9F 99.6(9)
 N1B C4B C3B 130.2(5) C10F C11F C12F 111.6(11)
 N1B C4B C5B 107.3(5) C13F C11F C10F 99.1(11)
 C3B C4B C5B 122.5(5) C13F C11F C12F 111.8(12)
 C4B C5B C7B 106.8(4) C7F C12F C11F 108.3(11)
 C6B C5B C4B 117.9(5) C7F C12F C15F 110.4(13)
 C6B C5B C7B 135.3(5) C7F C12F C16F 110.0(13)
 C1B C6B C5B 118.8(5) C15F C12F C11F 109.3(13)
 C5B C7B C12B 130.2(5) C16F C12F C11F 109.3(12)
 C8B C7B C5B 106.5(4) C16F C12F C15F 109.5(13)
 C8B C7B C12B 123.1(5) C14F C13F C11F 111.7(11)
 N1B C8B C9B 126.4(5) C13F C14F C9F 108.9(11)
 C7B C8B N1B 110.9(5) C4Z N1Z C8Z 107.1(13)
 C7B C8B C9B 122.7(5) C2Z C1Z C11Z 119.6(12)
 C8B C9B C10B 104.2(5) C6Z C1Z C11Z 117.7(13)
 C8B C9B C14B 108.4(4) C6Z C1Z C2Z 122.7(14)
 C14B C9B C10B 100.6(5) C3Z C2Z C1Z 120.8(14)
 C9B C10B C11B 99.7(5) C2Z C3Z C4Z 116.6(15)
 C10B C11B C12B 110.6(4) N1Z C4Z C3Z 129.0(16)
 C13B C11B C10B 99.8(5) N1Z C4Z C5Z 109.1(12)
 C13B C11B C12B 111.7(5) C5Z C4Z C3Z 121.8(15)
 C7B C12B C11B 108.0(4) C4Z C5Z C7Z 105.8(13)
 C7B C12B C15B 109.6(5) C6Z C5Z C4Z 120.7(14)
 C7B C12B C16B 111.1(4) C6Z C5Z C7Z 133.1(16)
 C15B C12B C11B 110.9(5) C1Z C6Z C5Z 117.4(15)
 C15B C12B C16B 108.9(5) C5Z C7Z C12Z 128.5(16)
 C16B C12B C11B 108.4(5) C8Z C7Z C5Z 106.9(14)
 C14B C13B C11B 110.9(5) C8Z C7Z C12Z 124.0(15)
 C13B C14B C9B 108.8(5) N1Z C8Z C9Z 127.5(17)
 C8C N1C C4C 108.8(5) C7Z C8Z N1Z 110.4(15)
 C2C C1C C11C 119.4(5) C7Z C8Z C9Z 122.0(16)
 C6C C1C C11C 117.6(5) C8Z C9Z C10Z 105.4(16)
 C6C C1C C2C 123.0(6) C8Z C9Z C14Z 107(2)
 C3C C2C C1C 120.2(6) C14Z C9Z C10Z 98.3(15)
 C2C C3C C4C 118.4(6) C11Z C10Z C9Z 100.7(14)
 N1C C4C C3C 131.3(5) C10Z C11Z C12Z 110.6(16)
 N1C C4C C5C 107.5(5) C13Z C11Z C10Z 99.5(16)
 C3C C4C C5C 121.2(5) C13Z C11Z C12Z 112(2)
 C4C C5C C7C 106.9(5) C7Z C12Z C11Z 107.6(15)
 C6C C5C C4C 119.1(5) C7Z C12Z C15Z 110(2)

C6C C5C C7C 134.0(5) C7Z C12Z C16Z 108.3(19)
C1C C6C C5C 118.1(5) C15Z C12Z C11Z 111.3(17)
C5C C7C C12C 130.8(5) C15Z C12Z C16Z 108.5(18)
C8C C7C C5C 106.5(5) C16Z C12Z C11Z 111.3(17)
C8C C7C C12C 122.7(5) C14Z C13Z C11Z 110.5(17)
N1C C8C C9C 127.1(5) C13Z C14Z C9Z 110.6(17)
C7C C8C N1C 110.2(5) C4G N1G C8G 108.9(4)
C7C C8C C9C 122.6(5) C2G C1G C11G 117.9(5)
C8C C9C C10C 104.1(5) C6G C1G C11G 118.1(5)
C8C C9C C14C 108.0(4) C6G C1G C2G 124.0(5)
C14C C9C C10C 100.0(5) C1G C2G C3G 119.1(5)
C11C C10C C9C 100.0(5) C2G C3G C4G 118.5(6)
C10C C11C C12C 110.2(5) N1G C4G C3G 130.0(5)
C13C C11C C10C 100.6(5) N1G C4G C5G 107.6(5)
C13C C11C C12C 111.9(4) C3G C4G C5G 122.4(5)
C7C C12C C11C 108.1(4) C4G C5G C7G 106.5(4)
C7C C12C C15C 110.6(4) C6G C5G C4G 118.2(5)
C15C C12C C11C 109.1(4) C6G C5G C7G 135.3(5)
C16C C12C C7C 110.4(4) C1G C6G C5G 117.7(5)
C16C C12C C11C 110.0(4) C5G C7G C12G 131.7(5)
C16C C12C C15C 108.6(5) C8G C7G C5G 106.7(5)
C14C C13C C11C 110.3(6) C8G C7G C12G 121.6(5)
C13C C14C C9C 109.6(6) N1G C8G C9G 125.7(5)
C4D N1D C8D 108.4(5) C7G C8G N1G 110.2(5)
C2D C1D C11D 116.8(5) C7G C8G C9G 123.9(5)
C6D C1D C11D 118.4(5) C8G C9G C10G 103.6(5)
C6D C1D C2D 124.7(6) C8G C9G C14G 107.4(4)
C3D C2D C1D 119.0(6) C14G C9G C10G 100.2(5)
C2D C3D C4D 118.3(5) C11G C10G C9G 100.1(4)
N1D C4D C3D 129.6(5) C10G C11G C12G 110.9(5)
N1D C4D C5D 107.6(5) C13G C11G C10G 100.2(5)
C3D C4D C5D 122.7(5) C13G C11G C12G 111.6(4)
C4D C5D C7D 106.8(5) C7G C12G C11G 108.7(4)
C6D C5D C4D 118.2(5) C7G C12G C15G 111.0(4)
C6D C5D C7D 135.0(5) C7G C12G C16G 109.7(4)
C1D C6D C5D 117.0(5) C15G C12G C11G 110.4(4)
C5D C7D C12D 130.7(5) C15G C12G C16G 108.4(4)
C8D C7D C5D 106.6(4) C16G C12G C11G 108.6(4)
C8D C7D C12D 122.6(5) C14G C13G C11G 109.7(5)
N1D C8D C9D 126.2(5) C13G C14G C9G 109.9(5)
C7D C8D N1D 110.5(5) C8H N1H C4H 108.9(4)
C7D C8D C9D 123.1(5) C2H C1H C11H 117.5(4)

C8D C9D C10D 104.7(5) C2H C1H C6H 123.4(5)
 C8D C9D C14D 106.3(5) C6H C1H C11H 119.1(4)
 C14DC9D C10D 100.0(5) C1H C2H C3H 120.0(5)
 C11DC10DC9D 99.6(5) C4H C3H C2H 117.4(5)
 C10DC11DC12D 111.0(5) N1H C4H C3H 129.1(5)
 C13DC11DC10D 100.7(5) N1H C4H C5H 107.8(4)
 C13DC11DC12D 111.2(5) C3H C4H C5H 123.2(5)
 C7D C12DC11D 107.6(5) C4H C5H C7H 106.3(4)
 C7D C12DC15D 111.3(5) C6H C5H C4H 118.4(5)
 C7D C12DC16D 109.1(4) C6H C5H C7H 135.3(4)
 C15DC12DC11D 110.5(5) C1H C6H C5H 117.6(4)
 C16DC12DC11D 109.6(5) C5H C7H C12H 131.1(4)
 C16DC12DC15D 108.7(5) C8H C7H C5H 106.4(4)
 C14DC13DC11D 110.6(6) C8H C7H C12H 122.5(5)
 C13DC14DC9D 109.5(6) N1H C8H C7H 110.7(5)
 C4E N1E C8E 108.8(4) N1H C8H C9H 126.6(5)
 C2E C1E C11E 117.3(4) C7H C8H C9H 122.7(5)
 C6E C1E C11E 119.0(4) C8H C9H C10H 105.0(4)
 C6E C1E C2E 123.7(5) C8H C9H C14H 107.2(5)
 C3E C2E C1E 118.9(5) C14HC9H C10H 100.6(4)
 C2E C3E C4E 118.7(5) C9H C10HC11H 99.3(4)
 N1E C4E C3E 129.9(5) C10HC11HC12H 110.4(4)
 N1E C4E C5E 107.3(5) C13HC11HC10H 100.0(5)
 C3E C4E C5E 122.7(5) C13HC11HC12H 111.9(4)
 C4E C5E C7E 107.0(5) C7H C12HC11H 108.0(4)
 C6E C5E C4E 117.6(5) C7H C12HC15H 111.3(4)
 C6E C5E C7E 135.4(5) C7H C12HC16H 110.1(4)
 C1E C6E C5E 118.3(5) C15HC12HC11H 109.8(4)
 C5E C7E C12E 130.9(5) C15HC12HC16H 109.2(4)
 C8E C7E C5E 106.8(4) C16HC12HC11H 108.4(4)
 C8E C7E C12E 122.2(5) C14HC13HC11H 111.4(5)
 N1E C8E C9E 126.6(5) C13HC14HC9H 109.1(5)

Table 6 Torsion Angles for JW315a.

A	B	C	D	Angle/°	A	B	C	D	Angle/°
C11A	C1A	C2A	C3A	-179.3(4)	C7E	C5E	C6E	C1E	-179.0(6)
C11A	C1A	C6A	C5A	179.6(4)	C7E	C8E	C9E	C10E	-34.8(7)
N1A	C4A	C5A	C6A	-179.7(4)	C7E	C8E	C9E	C14E	70.4(7)
N1A	C4A	C5A	C7A	0.6(5)	C8E	N1E	C4E	C3E	-178.2(6)
N1A	C8A	C9A	C10A	145.1(5)	C8E	N1E	C4E	C5E	1.0(6)
N1A	C8A	C9A	C14A	-112.3(6)	C8E	C7E	C12E	C11E	0.1(7)
C1A	C2A	C3A	C4A	-0.5(8)	C8E	C7E	C12E	C15E	-119.6(6)

C2A C1A C6A C5A 0.3(8) C8E C7E C12E C16E 120.1(6)
C2A C3A C4A N1A 179.7(5) C8E C9E C10E C11E 69.0(6)
C2A C3A C4A C5A 0.8(7) C8E C9E C14E C13E -82.1(6)
C3A C4A C5A C6A -0.5(7) C9E C10E C11E C12E -76.4(6)
C3A C4A C5A C7A 179.7(5) C9E C10E C11E C13E 42.1(5)
C4A N1A C8A C7A -0.7(6) C10E C9E C14E C13E 26.7(6)
C4A N1A C8A C9A 178.4(5) C10E C11E C12E C7E 40.0(6)
C4A C5A C6A C1A -0.1(7) C10E C11E C12E C15E 159.8(5)
C4A C5A C7A C8A -1.0(5) C10E C11E C12E C16E -81.1(6)
C4A C5A C7A C12A -179.5(5) C10E C11E C13E C14E -27.5(6)
C5A C7A C8A N1A 1.0(6) C11E C13E C14E C9E 0.6(7)
C5A C7A C8A C9A -178.1(5) C12E C7E C8E N1E 177.8(5)
C5A C7A C12A C11A 176.4(5) C12E C7E C8E C9E -2.2(8)
C5A C7A C12A C15A 55.8(8) C12E C11E C13E C14E 90.0(6)
C5A C7A C12A C16A -64.0(8) C13E C11E C12E C7E -70.8(6)
C6A C1A C2A C3A -0.1(8) C13E C11E C12E C15E 49.0(7)
C6A C5A C7A C8A 179.3(5) C13E C11E C12E C16E 168.1(5)
C6A C5A C7A C12A 0.8(10) C14E C9E C10E C11E -41.4(6)
C7A C5A C6A C1A 179.6(5) C11F C1F C2F C3F 177.7(11)
C7A C8A C9A C10A -35.9(7) C11F C1F C6F C5F -176.9(18)
C7A C8A C9A C14A 66.7(7) N1F C4F C5F C6F 179(2)
C8A N1A C4A C3A -179.0(5) N1F C4F C5F C7F -2(3)
C8A N1A C4A C5A 0.1(5) N1F C8F C9F C10F 145(2)
C8A C7A C12A C11A -2.0(7) N1F C8F C9F C14F -110(2)
C8A C7A C12A C15A -122.5(6) C1F C2F C3F C4F -2.5(19)
C8A C7A C12A C16A 117.7(6) C2F C1F C6F C5F 0(3)
C8A C9A C10A C11A 69.4(5) C2F C3F C4F N1F -178.6(17)
C8A C9A C14A C13A -79.4(8) C2F C3F C4F C5F 4(2)
C9A C10A C11A C12A -77.2(6) C3F C4F C5F C6F -3(4)
C9A C10A C11A C13A 40.5(5) C3F C4F C5F C7F 175.8(18)
C10A C9A C14A C13A 28.0(8) C4F N1F C8F C7F 6(3)
C10A C11A C12A C7A 42.7(7) C4F N1F C8F C9F -179(2)
C10A C11A C12A C15A 162.6(6) C4F C5F C6F C1F 1(4)
C10A C11A C12A C16A -78.2(7) C4F C5F C7F C8F 6(3)
C10A C11A C13A C14A -25.8(8) C4F C5F C7F C12F 175(2)
C11A C13A C14A C9A -2.5(9) C5F C7F C8F N1F -7(3)
C12A C7A C8A N1A 179.7(5) C5F C7F C8F C9F 178(2)
C12A C7A C8A C9A 0.6(8) C5F C7F C12F C11F -174(3)
C12A C11A C13A C14A 92.2(7) C5F C7F C12F C15F 66(3)
C13A C11A C12A C7A -69.7(6) C5F C7F C12F C16F -55(3)
C13A C11A C12A C15A 50.2(7) C6F C1F C2F C3F 1(2)
C13A C11A C12A C16A 169.3(6) C6F C5F C7F C8F -175(3)

C14A C9A C10A C11A -40.2(5) C6F C5F C7F C12F -6(6)
C11B C1B C2B C3B -178.9(4) C7F C5F C6F C1F -178(3)
C11B C1B C6B C5B 177.3(4) C7F C8F C9F C10F -41(3)
N1B C4B C5B C6B -179.3(5) C7F C8F C9F C14F 64(3)
N1B C4B C5B C7B -0.4(6) C8F N1F C4F C3F -179.9(18)
N1B C8B C9B C10B 146.8(5) C8F N1F C4F C5F -2(3)
N1B C8B C9B C14B -106.7(6) C8F C7F C12F C11F -6(3)
C1B C2B C3B C4B 1.5(8) C8F C7F C12F C15F -126(2)
C2B C1B C6B C5B -1.2(8) C8F C7F C12F C16F 113(3)
C2B C3B C4B N1B 177.3(5) C8F C9F C10F C11F 69.4(14)
C2B C3B C4B C5B -1.0(8) C8F C9F C14F C13F -82.0(18)
C3B C4B C5B C6B -0.6(8) C9F C10F C11F C12F -75.2(14)
C3B C4B C5B C7B 178.3(5) C9F C10F C11F C13F 42.8(14)
C4B N1B C8B C7B -0.3(6) C10F C9F C14F C13F 26.5(18)
C4B N1B C8B C9B 177.3(5) C10F C11F C12F C7F 42.0(16)
C4B C5B C6B C1B 1.7(7) C10F C11F C12F C15F 162.3(14)
C4B C5B C7B C8B 0.2(6) C10F C11F C12F C16F -77.8(16)
C4B C5B C7B C12B -175.1(5) C10F C11F C13F C14F -29(2)
C5B C7B C8B N1B 0.0(6) C11F C13F C14F C9F 1(2)
C5B C7B C8B C9B -177.7(5) C12F C7F C8F N1F -178(2)
C5B C7B C12B C11B 175.4(5) C12F C7F C8F C9F 7(4)
C5B C7B C12B C15B 54.5(7) C12F C11F C13F C14F 89(2)
C5B C7B C12B C16B -65.9(7) C13F C11F C12F C7F -68.1(16)
C6B C1B C2B C3B -0.4(8) C13F C11F C12F C15F 52.3(17)
C6B C5B C7B C8B 178.8(6) C13F C11F C12F C16F 172.2(15)
C6B C5B C7B C12B 3.5(10) C14F C9F C10F C11F -42.2(13)
C7B C5B C6B C1B -176.8(5) C11Z C1Z C2Z C3Z 178.9(15)
C7B C8B C9B C10B -35.8(7) C11Z C1Z C6Z C5Z -179(2)
C7B C8B C9B C14B 70.6(7) N1Z C4Z C5Z C6Z 179(3)
C8B N1B C4B C3B -178.1(6) N1Z C4Z C5Z C7Z 5(4)
C8B N1B C4B C5B 0.4(6) N1Z C8Z C9Z C10Z 142(4)
C8B C7B C12B C11B 0.7(7) N1Z C8Z C9Z C14Z -114(4)
C8B C7B C12B C15B -120.1(6) C1Z C2Z C3Z C4Z -2(3)
C8B C7B C12B C16B 119.5(6) C2Z C1Z C6Z C5Z 0(4)
C8B C9B C10B C11B 70.2(5) C2Z C3Z C4Z N1Z -179(2)
C8B C9B C14B C13B -80.9(6) C2Z C3Z C4Z C5Z 3(4)
C9B C10B C11B C12B -76.8(6) C3Z C4Z C5Z C6Z -3(6)
C9B C10B C11B C13B 41.0(5) C3Z C4Z C5Z C7Z -176(3)
C10B C9B C14B C13B 28.1(6) C4Z N1Z C8Z C7Z -5(4)
C10B C11B C12B C7B 39.4(6) C4Z N1Z C8Z C9Z 180(3)
C10B C11B C12B C15B 159.5(5) C4Z C5Z C6Z C1Z 1(5)
C10B C11B C12B C16B -81.0(6) C4Z C5Z C7Z C8Z -8(5)

C10B C11B C13B C14B -25.9(6) C4Z C5Z C7Z C12Z -179(3)
C11B C13B C14B C9B -1.3(7) C5Z C7Z C8Z N1Z 8(5)
C12B C7B C8B N1B 175.7(5) C5Z C7Z C8Z C9Z -176(4)
C12B C7B C8B C9B -2.0(8) C5Z C7Z C12Z C11Z 171(4)
C12B C11B C13B C14B 91.0(6) C5Z C7Z C12Z C15Z 50(5)
C13B C11B C12B C7B -70.7(6) C5Z C7Z C12Z C16Z -68(5)
C13B C11B C12B C15B 49.4(6) C6Z C1Z C2Z C3Z 0(3)
C13B C11B C12B C16B 168.9(5) C6Z C5Z C7Z C8Z 180(5)
C14B C9B C10B C11B -42.1(5) C6Z C5Z C7Z C12Z 9(8)
C11C C1C C2C C3C -179.1(4) C7Z C5Z C6Z C1Z 172(4)
C11C C1C C6C C5C 178.9(4) C7Z C8Z C9Z C10Z -33(4)
N1C C4C C5C C6C -179.4(4) C7Z C8Z C9Z C14Z 71(4)
N1C C4C C5C C7C 0.3(6) C8Z N1Z C4Z C3Z -179(3)
N1C C8C C9C C10C 144.8(6) C8Z N1Z C4Z C5Z 0(4)
N1C C8C C9C C14C -109.5(6) C8Z C7Z C12Z C11Z 2(5)
C1C C2C C3C C4C 0.4(8) C8Z C7Z C12Z C15Z -119(4)
C2C C1C C6C C5C -2.1(8) C8Z C7Z C12Z C16Z 123(4)
C2C C3C C4C N1C 179.6(6) C8Z C9Z C10Z C11Z 69(2)
C2C C3C C4C C5C -2.4(8) C8Z C9Z C14Z C13Z -81(3)
C3C C4C C5C C6C 2.2(8) C9Z C10Z C11Z C12Z -76.0(19)
C3C C4C C5C C7C -178.1(5) C9Z C10Z C11Z C13Z 42(2)
C4C N1C C8C C7C 0.8(6) C10Z C9Z C14Z C13Z 28(3)
C4C N1C C8C C9C 177.6(5) C10Z C11Z C12Z C7Z 39(3)
C4C C5C C6C C1C 0.1(7) C10Z C11Z C12Z C15Z 159(2)
C4C C5C C7C C8C 0.1(6) C10Z C11Z C12Z C16Z -80(3)
C4C C5C C7C C12C 177.9(5) C10Z C11Z C13Z C14Z -26(4)
C5C C7C C8C N1C -0.6(6) C11Z C13Z C14Z C9Z -1(4)
C5C C7C C8C C9C -177.6(5) C12Z C7Z C8Z N1Z 179(3)
C5C C7C C12C C11C 177.7(5) C12Z C7Z C8Z C9Z -5(6)
C5C C7C C12C C15C 58.3(7) C12Z C11Z C13Z C14Z 91(3)
C5C C7C C12C C16C -62.0(7) C13Z C11Z C12Z C7Z -71(3)
C6C C1C C2C C3C 1.9(9) C13Z C11Z C12Z C15Z 49(2)
C6C C5C C7C C8C 179.8(5) C13Z C11Z C12Z C16Z 170(2)
C6C C5C C7C C12C -2.4(9) C14Z C9Z C10Z C11Z -41.8(18)
C7C C5C C6C C1C -179.6(5) C11G C1G C2G C3G -179.6(4)
C7C C8C C9C C10C -38.7(7) C11G C1G C6G C5G 179.1(4)
C7C C8C C9C C14C 67.0(7) N1G C4G C5G C6G 179.5(4)
C8C N1C C4C C3C 177.5(5) N1G C4G C5G C7G 0.2(5)
C8C N1C C4C C5C -0.7(6) N1G C8G C9G C10G 146.2(5)
C8C C7C C12C C11C -4.9(7) N1G C8G C9G C14G -108.3(6)
C8C C7C C12C C15C -124.3(5) C1G C2G C3G C4G 0.5(8)
C8C C7C C12C C16C 115.5(6) C2G C1G C6G C5G -0.5(8)

C8C C9C C10C C11C	70.7(6)	C2G C3G C4G N1G	-179.9(5)
C8C C9C C14C C13C	-82.1(6)	C2G C3G C4G C5G	-0.7(8)
C9C C10C C11C C12C	-77.2(6)	C3G C4G C5G C6G	0.2(7)
C9C C10C C11C C13C	41.0(6)	C3G C4G C5G C7G	-179.1(5)
C10C C9C C14C C13C	26.4(6)	C4G N1G C8G C7G	1.0(6)
C10C C11C C12C C7C	42.4(6)	C4G N1G C8G C9G	177.5(5)
C10C C11C C12C C15C	162.7(5)	C4G C5G C6G C1G	0.4(7)
C10C C11C C12C C16C	-78.2(6)	C4G C5G C7G C8G	0.4(5)
C10C C11C C13C C14C	-26.9(6)	C4G C5G C7G C12G	-179.5(5)
C11C C13C C14C C9C	0.0(7)	C5G C7G C8G N1G	-0.9(6)
C12C C7C C8C N1C	-178.6(5)	C5G C7G C8G C9G	-177.4(4)
C12C C7C C8C C9C	4.4(8)	C5G C7G C12G C11G	176.9(5)
C12C C11C C13C C14C	90.1(6)	C5G C7G C12G C15G	55.4(7)
C13C C11C C12C C7C	-68.7(6)	C5G C7G C12G C16G	-64.4(7)
C13C C11C C12C C15C	51.7(6)	C6G C1G C2G C3G	0.0(9)
C13C C11C C12C C16C	170.7(5)	C6G C5G C7G C8G	-178.7(5)
C14C C9C C10C C11C	-40.9(6)	C6G C5G C7G C12G	1.4(9)
C11D C1D C2D C3D	-178.8(5)	C7G C5G C6G C1G	179.5(5)
C11D C1D C6D C5D	178.7(4)	C7G C8G C9G C10G	-37.8(6)
N1D C4D C5D C6D	-179.1(5)	C7G C8G C9G C14G	67.7(6)
N1D C4D C5D C7D	1.4(6)	C8G N1G C4G C3G	178.5(5)
N1D C8D C9D C10D	146.0(6)	C8G N1G C4G C5G	-0.8(5)
N1D C8D C9D C14D	-108.7(6)	C8G C7G C12G C11G	-2.9(6)
C1D C2D C3D C4D	1.2(9)	C8G C7G C12G C15G	-124.5(5)
C2D C1D C6D C5D	0.8(9)	C8G C7G C12G C16G	115.7(5)
C2D C3D C4D N1D	179.1(6)	C8G C9G C10G C11G	69.7(5)
C2D C3D C4D C5D	-1.6(9)	C8G C9G C14G C13G	-81.4(5)
C3D C4D C5D C6D	1.5(8)	C9G C10G C11G C12G	-76.6(5)
C3D C4D C5D C7D	-178.0(5)	C9G C10G C11G C13G	41.4(5)
C4D N1D C8D C7D	1.0(6)	C10G C9G C14G C13G	26.5(5)
C4D N1D C8D C9D	177.1(5)	C10G C11G C12G C7G	41.0(6)
C4D C5D C6D C1D	-1.0(8)	C10G C11G C12G C15G	163.0(4)
C4D C5D C7D C8D	-0.8(6)	C10G C11G C12G C16G	-78.3(5)
C4D C5D C7D C12D	177.1(5)	C10G C11G C13G C14G	-27.1(6)
C5D C7D C8D N1D	-0.1(6)	C11G C13G C14G C9G	0.3(6)
C5D C7D C8D C9D	-176.4(5)	C12G C7G C8G N1G	179.0(4)
C5D C7D C12D C11D	175.3(5)	C12G C7G C8G C9G	2.6(8)
C5D C7D C12D C15D	54.1(7)	C12G C11G C13G C14G	90.4(5)
C5D C7D C12D C16D	-65.9(7)	C13G C11G C12G C7G	-69.9(5)
C6D C1D C2D C3D	-0.8(10)	C13G C11G C12G C15G	52.1(6)
C6D C5D C7D C8D	179.8(6)	C13G C11G C12G C16G	170.8(4)
C6D C5D C7D C12D	-2.3(10)	C14G C9G C10G C11G	-41.3(5)

C7D	C5D	C6D	C1D	178.3(6)	C11H	C1H	C2H	C3H	178.8(5)
C7D	C8D	C9D	C10D	-38.3(8)	C11H	C1H	C6H	C5H	-179.3(4)
C7D	C8D	C9D	C14D	67.0(7)	N1H	C4H	C5H	C6H	178.1(5)
C8D	N1D	C4D	C3D	177.9(6)	N1H	C4H	C5H	C7H	0.1(6)
C8D	N1D	C4D	C5D	-1.5(6)	N1H	C8H	C9H	C10H	144.5(5)
C8D	C7D	C12D	C11D	-7.1(7)	N1H	C8H	C9H	C14H	-109.1(6)
C8D	C7D	C12D	C15D	-128.4(6)	C1H	C2H	C3H	C4H	-0.1(9)
C8D	C7D	C12D	C16D	111.7(6)	C2H	C1H	C6H	C5H	0.3(8)
C8D	C9D	C10D	C11D	68.8(6)	C2H	C3H	C4H	N1H	-178.6(6)
C8D	C9D	C14D	C13D	-80.9(6)	C2H	C3H	C4H	C5H	1.4(9)
C9D	C10D	C11D	C12D	-77.3(6)	C3H	C4H	C5H	C6H	-1.9(8)
C9D	C10D	C11D	C13D	40.5(6)	C3H	C4H	C5H	C7H	-179.9(5)
C10D	C9D	C14D	C13D	27.7(6)	C4H	N1H	C8H	C7H	1.2(6)
C10D	C11D	C12D	C7D	44.3(6)	C4H	N1H	C8H	C9H	-179.3(5)
C10D	C11D	C12D	C15D	166.0(5)	C4H	C5H	C6H	C1H	1.0(7)
C10D	C11D	C12D	C16D	-74.3(6)	C4H	C5H	C7H	C8H	0.6(6)
C10D	C11D	C13D	C14D	-25.6(6)	C4H	C5H	C7H	C12H	-179.7(5)
C11D	C13D	C14D	C9D	-1.4(7)	C5H	C7H	C8H	N1H	-1.1(6)
C12D	C7D	C8D	N1D	-178.2(5)	C5H	C7H	C8H	C9H	179.3(5)
C12D	C7D	C8D	C9D	5.5(8)	C5H	C7H	C12H	C11H	178.6(5)
C12D	C11D	C13D	C14D	92.1(6)	C5H	C7H	C12H	C15H	58.0(7)
C13D	C11D	C12D	C7D	-67.1(6)	C5H	C7H	C12H	C16H	-63.2(7)
C13D	C11D	C12D	C15D	54.7(6)	C6H	C1H	C2H	C3H	-0.7(9)
C13D	C11D	C12D	C16D	174.4(5)	C6H	C5H	C7H	C8H	-176.9(6)
C14D	C9D	C10D	C11D	-41.1(6)	C6H	C5H	C7H	C12H	2.7(10)
C11E	C1E	C2E	C3E	179.4(5)	C7H	C5H	C6H	C1H	178.3(5)
C11E	C1E	C6E	C5E	-179.4(4)	C7H	C8H	C9H	C10H	-36.0(7)
N1E	C4E	C5E	C6E	179.7(5)	C7H	C8H	C9H	C14H	70.4(7)
N1E	C4E	C5E	C7E	-0.5(6)	C8H	N1H	C4H	C3H	179.2(6)
N1E	C8E	C9E	C10E	145.3(6)	C8H	N1H	C4H	C5H	-0.8(6)
N1E	C8E	C9E	C14E	-109.6(6)	C8H	C7H	C12H	C11H	-1.9(7)
C1E	C2E	C3E	C4E	-0.8(10)	C8H	C7H	C12H	C15H	-122.4(5)
C2E	C1E	C6E	C5E	-0.5(9)	C8H	C7H	C12H	C16H	116.4(5)
C2E	C3E	C4E	N1E	-179.9(6)	C8H	C9H	C10H	C11H	70.0(5)
C2E	C3E	C4E	C5E	1.1(9)	C8H	C9H	C14H	C13H	-82.0(6)
C3E	C4E	C5E	C6E	-1.0(8)	C9H	C10H	C11H	C12H	-77.4(5)
C3E	C4E	C5E	C7E	178.7(5)	C9H	C10H	C11H	C13H	40.6(5)
C4E	N1E	C8E	C7E	-1.1(6)	C10H	C9H	C14H	C13H	27.5(6)
C4E	N1E	C8E	C9E	178.9(5)	C10H	C11H	C12H	C7H	41.8(6)
C4E	C5E	C6E	C1E	0.7(8)	C10H	C11H	C12H	C15H	163.2(4)
C4E	C5E	C7E	C8E	-0.1(6)	C10H	C11H	C12H	C16H	-77.6(5)
C4E	C5E	C7E	C12E	-176.8(5)	C10H	C11H	C13H	C14H	-26.2(6)

C5E C7E C8E N1E 0.7(6) C11HC13HC14HC9H -0.8(6)
 C5E C7E C8E C9E -179.2(5) C12HC7H C8H N1H 179.2(4)
 C5E C7E C12E C11E 176.3(5) C12HC7H C8H C9H -0.3(8)
 C5E C7E C12E C15E 56.6(8) C12HC11HC13HC14H90.7(6)
 C5E C7E C12E C16E -63.6(7) C13HC11HC12HC7H -68.6(6)
 C6E C1E C2E C3E 0.5(10) C13HC11HC12HC15H52.8(6)
 C6E C5E C7E C8E 179.5(6) C13HC11HC12HC16H172.1(5)
 C6E C5E C7E C12E 2.9(10) C14HC9H C10HC11H-41.3(5)

Table 7 Hydrogen Atom Coordinates ($\text{\AA} \times 10^4$) and Isotropic Displacement Parameters ($\text{\AA}^2 \times 10^3$) for JW315a.

Atom	x	y	z	U(eq)
H1A	-1894	5487	1554	44
H2A	910	7253	1614	44
H3A	-830	6746	1442	43
H6A	2250	5416	2288	39
H9A	-2414	4122	1701	56
H10A	-1417	2976	1780	75
H10B	-626	3479	1463	75
H11A	200	2946	2469	56
H13A	-679	3474	3255	80
H14A	-2250	4093	2816	81
H15A	1926	4505	2970	102
H15B	1670	3726	3176	102
H15C	835	4353	3240	102
H16A	1176	3615	1588	92
H16B	1933	3322	2171	92
H16C	2093	4109	1951	92
H1B	6797	4133	-21	45
H2B	7611	6606	252	46
H3B	7642	5465	-134	45
H6B	5761	5952	1467	39
H9B	5886	2963	381	51
H10C	6067	3217	1504	52
H10D	5227	2587	1277	52
H11B	4078	3380	1685	48
H13B	2900	3512	703	56
H14B	3934	3213	-73	57
H15D	4055	5330	1432	73
H15E	3271	4709	1582	73
H15F	3483	4824	914	73
H16D	5886	4050	2196	81

H16E	4804	4406	2361	81
H16F	5728	4885	2145	81
H1C	9210	4385	9180	51
H2C	5830	3046	8917	58
H3C	7687	3285	9187	57
H6C	5279	5005	8230	39
H9C	10248	5574	8903	59
H10E	9904	6505	8167	61
H10F	9117	5876	7877	61
H11C	8188	7045	8054	49
H13C	8365	7245	9137	57
H14C	9613	6394	9650	62
H15G	5662	6225	8428	62
H15H	6203	6976	8344	62
H15I	6564	6537	8942	62
H16G	7417	5843	7381	70
H16H	6608	6498	7391	70
H16I	6206	5720	7520	70
H1D	6599	3565	5041	49
H2D	7753	1148	5302	58
H3D	7576	2285	4903	53
H6D	5675	1615	6460	47
H9D	5240	4597	5301	57
H10G	3570	4683	5737	64
H10H	3559	3877	5505	64
H11D	3540	4055	6627	55
H13D	5320	4554	7083	58
H14D	6297	4934	6308	58
H15J	5154	2461	7110	71
H15K	4469	3075	7360	71
H15L	5669	3232	7219	71
H16J	3228	2809	5830	70
H16K	2925	2841	6487	70
H16L	3686	2222	6309	70
H1E	9292	6728	4239	44
H2E	10274	9180	4501	55
H3E	10191	8034	4109	49
H6E	8223	8636	5654	40
H9E	8292	5596	4636	56
H10I	8419	5883	5754	59
H10J	7559	5266	5524	59
H11E	6430	6098	5900	54

H13E	5287	6203	4909	61
H14E	6363	5891	4155	61
H15M	6452	8029	5602	73
H15N	5654	7416	5754	73
H15O	5900	7507	5090	73
H16M	8253	6767	6421	81
H16N	7164	7140	6559	81
H16O	8107	7601	6342	81
H1F	473	7789	5691	48
H2F	3112	9690	5757	59
H3F	1417	9101	5555	53
H6F	4504	7980	6645	40
H9F	154	6417	5849	45
H10K	1270	5358	6072	58
H10L	2073	5892	5795	58
H11F	2758	5449	6855	55
H13F	1516	5887	7509	55
H14F	-33	6460	6942	50
H15P	4178	7055	7439	101
H15Q	3795	6301	7643	101
H15R	2971	6955	7591	101
H16P	3855	6180	6040	83
H16Q	4542	5959	6667	83
H16R	4593	6751	6434	83
H1Z	840	8098	5720	43
H2Z	4048	9578	5990	57
H3Z	2215	9255	5707	51
H6Z	4790	7669	6760	49
H9Z	45	6779	5845	60
H10M	789	5598	5981	62
H10N	1735	6027	5721	62
H11Z	2296	5433	6739	68
H13Z	1305	6022	7463	75
H14Z	-65	6771	6942	64
H15S	4170	6911	7351	78
H15T	3798	6148	7540	78
H15U	3001	6808	7552	78
H16S	3627	6044	5946	80
H16T	4216	5697	6553	80
H16U	4533	6478	6378	80
H1G	-1941	2108	6547	41
H2G	1037	453	6656	54

H3G	-753	901	6448	49
H6G	2151	2319	7391	43
H9G	-2674	3354	6875	44
H10O	-2050	4264	7604	50
H10P	-1388	3572	7870	50
H11G	-227	4639	7660	44
H13G	-497	4843	6567	46
H14G	-1971	4099	6097	44
H15V	2029	3601	7214	57
H15W	1649	4396	7289	57
H15X	1166	3960	6706	57
H16V	330	3397	8317	68
H16W	1245	3983	8285	68
H16X	1486	3177	8147	68
H1H	795	5930	10783	41
H2H	-405	3545	10377	47
H3H	-303	4680	10800	46
H6H	1912	4045	9367	36
H9H	2291	6931	10672	44
H10Q	3936	6183	10467	52
H10R	4034	7012	10320	52
H11H	4121	6501	9382	44
H13H	2440	7125	8932	52
H14H	1385	7424	9686	54
H15Y	2356	5038	8704	56
H	3111	5665	8533	56
HA	1916	5831	8677	56
H16Y	4336	5200	10018	56
HB	4576	5243	9349	56
HC	3786	4644	9533	56

Table 8 Atomic Occupancy for JW315a.

<i>Atom Occupancy</i>	<i>Atom Occupancy</i>	<i>Atom Occupancy</i>
C11F 0.6	N1F 0.6	H1F 0.6
C1F 0.6	C2F 0.6	H2F 0.6
C3F 0.6	H3F 0.6	C4F 0.6
C5F 0.6	C6F 0.6	H6F 0.6
C7F 0.6	C8F 0.6	C9F 0.6
H9F 0.6	C10F 0.6	H10K 0.6
H10L 0.6	C11F 0.6	H11F 0.6
C12F 0.6	C13F 0.6	H13F 0.6
C14F 0.6	H14F 0.6	C15F 0.6

H15P 0.6	H15Q 0.6	H15R 0.6
C16F 0.6	H16P 0.6	H16Q 0.6
H16R 0.6	C11Z 0.4	N1Z 0.4
H1Z 0.4	C1Z 0.4	C2Z 0.4
H2Z 0.4	C3Z 0.4	H3Z 0.4
C4Z 0.4	C5Z 0.4	C6Z 0.4
H6Z 0.4	C7Z 0.4	C8Z 0.4
C9Z 0.4	H9Z 0.4	C10Z 0.4
H10M 0.4	H10N 0.4	C11Z 0.4
H11Z 0.4	C12Z 0.4	C13Z 0.4
H13Z 0.4	C14Z 0.4	H14Z 0.4
C15Z 0.4	H15S 0.4	H15T 0.4
H15U 0.4	C16Z 0.4	H16S 0.4
H16T 0.4	H16U 0.4	

Experimental

Single crystals of C₁₆H₁₆CIN [JW315a] were used as received. A suitable crystal was selected and mounted on a nylon loop using a small amount of paratone oil on a 'Bruker APEX-II CCD' diffractometer. The crystal was kept at 173.0 K during data collection. Using Olex2 [1], the structure was solved with the ShelXS [2] structure solution program using Direct Methods and refined with the ShelXL [3] refinement package using Least Squares minimization.

1. Dolomanov, O.V., Bourhis, L.J., Gildea, R.J., Howard, J.A.K. & Puschmann, H. (2009), *J. Appl. Cryst.* 42, 339-341.
2. Sheldrick, G.M. (2008). *Acta Cryst.* A64, 112-122.
3. Sheldrick, G.M. (2008). *Acta Cryst.* A64, 112-122.

Crystal structure determination of [JW315a]

Crystal Data for C₁₆H₁₆CIN (*M* = 257.75 g/mol): monoclinic, space group P2₁ (no. 4), *a* = 12.4101(3) Å, *b* = 18.9939(3) Å, *c* = 22.7815(4) Å, β = 99.0520(10)°, *V* = 5303.09(18) Å³, *Z* = 16, *T* = 173.0 K, μ (CuK α) = 2.372 mm⁻¹, *D*_{calc} = 1.291 g/cm³, 66305 reflections measured (3.928° ≤ 2 θ ≤ 144.904°), 20467 unique (*R*_{int} = 0.0891, *R*_{sigma} = 0.0731) which were used in all calculations. The final *R*₁ was 0.0522 (*I* > 2 σ (*I*)) and *wR*₂ was 0.1280 (all data).

Refinement model description

Number of restraints - 522, number of constraints - unknown.

Details:

1. Fixed Uiso

At 1.2 times of:

All C(H) groups, All C(H,H) groups, All N(H) groups

At 1.5 times of:

All C(H,H,H) groups

2. Rigid bond restraints

C11F, N1F, C1F, C2F, C3F, C4F, C5F, C6F, C7F, C8F, C9F, C10F, C11F, C12F,
C13F, C14F, C15F, C16F

with sigma for 1-2 distances of 0.01 and sigma for 1-3 distances of 0.01

C11Z, N1Z, C1Z, C2Z, C3Z, C4Z, C5Z, C6Z, C7Z, C8Z, C9Z, C10Z, C11Z, C12Z,
C13Z, C14Z, C15Z, C16Z

with sigma for 1-2 distances of 0.01 and sigma for 1-3 distances of 0.01

3. Uiso/Uanis restraints and constraints

C11F \approx N1F \approx C1F \approx C2F \approx C3F \approx C4F \approx C5F \approx C6F

\approx C7F \approx C8F \approx C9F \approx C10F \approx C11F \approx C12F \approx C13F \approx

C14F \approx C15F \approx C16F: within 1.7Å with sigma of 0.04 and sigma for
terminal atoms of 0.08

C11Z \approx N1Z \approx C1Z \approx C2Z \approx C3Z \approx C4Z \approx C5Z \approx C6Z

\approx C7Z \approx C8Z \approx C9Z \approx C10Z \approx C11Z \approx C12Z \approx C13Z \approx

C14Z \approx C15Z \approx C16Z: within 1.7Å with sigma of 0.04 and sigma for
terminal atoms of 0.08

Uanis(C2Z) \approx Ueq: with sigma of 0.01 and sigma for terminal atoms of 0.02

4. Same fragment restrains

{C11A, N1A, C1A, C2A, C3A, C4A, C5A, C6A, C7A, C8A, C9A, C10A, C11A, C12A,
C13A, C14A, C15A, C16A} sigma for 1-2: 0.02, 1-3: 0.04

as

{C11F, N1F, C1F, C2F, C3F, C4F, C5F, C6F, C7F, C8F, C9F, C10F, C11F, C12F,
C13F, C14F, C15F, C16F}

{C11A, N1A, C1A, C2A, C3A, C4A, C5A, C6A, C7A, C8A, C9A, C10A, C11A, C12A,
C13A, C14A, C15A, C16A} sigma for 1-2: 0.02, 1-3: 0.04

as

{C11Z, N1Z, C1Z, C2Z, C3Z, C4Z, C5Z, C6Z, C7Z, C8Z, C9Z, C10Z, C11Z, C12Z,
C13Z, C14Z, C15Z, C16Z}

5. Others

Fixed Sof: C11F(0.6) N1F(0.6) H1F(0.6) C1F(0.6) C2F(0.6) H2F(0.6) C3F(0.6)
H3F(0.6) C4F(0.6) C5F(0.6) C6F(0.6) H6F(0.6) C7F(0.6) C8F(0.6) C9F(0.6)
H9F(0.6) C10F(0.6) H10K(0.6) H10L(0.6) C11F(0.6) H11F(0.6) C12F(0.6) C13F(0.6)
H13F(0.6) C14F(0.6) H14F(0.6) C15F(0.6) H15P(0.6) H15Q(0.6) H15R(0.6)
C16F(0.6) H16P(0.6) H16Q(0.6) H16R(0.6) C11Z(0.4) N1Z(0.4) H1Z(0.4) C1Z(0.4)
C2Z(0.4) H2Z(0.4) C3Z(0.4) H3Z(0.4) C4Z(0.4) C5Z(0.4) C6Z(0.4) H6Z(0.4)
C7Z(0.4) C8Z(0.4) C9Z(0.4) H9Z(0.4) C10Z(0.4) H10M(0.4) H10N(0.4) C11Z(0.4)
H11Z(0.4) C12Z(0.4) C13Z(0.4) H13Z(0.4) C14Z(0.4) H14Z(0.4) C15Z(0.4)
H15S(0.4) H15T(0.4) H15U(0.4) C16Z(0.4) H16S(0.4) H16T(0.4) H16U(0.4)

6.a Ternary CH refined with riding coordinates:

C9A(H9A), C11A(H11A), C9B(H9B), C11B(H11B), C9C(H9C), C11C(H11C),
C9D(H9D),

C11D(H11D), C9E(H9E), C11E(H11E), C9F(H9F), C11F(H11F), C9Z(H9Z),
C11Z(H11Z),

C9G(H9G), C11G(H11G), C9H(H9H), C11H(H11H)

6.b Secondary CH2 refined with riding coordinates:

C10A(H10A,H10B), C10B(H10C,H10D), C10C(H10E,H10F), C10D(H10G,H10H),
C10E(H10I),

H10J), C10F(H10K,H10L), C10Z(H10M,H10N), C10G(H10O,H10P),

C10H(H10Q,H10R)

6.c Aromatic/amide H refined with riding coordinates:

N1A(H1A), C2A(H2A), C3A(H3A), C6A(H6A), C13A(H13A), C14A(H14A),
N1B(H1B),
C2B(H2B), C3B(H3B), C6B(H6B), C13B(H13B), C14B(H14B), N1C(H1C),
C2C(H2C),
C3C(H3C), C6C(H6C), C13C(H13C), C14C(H14C), N1D(H1D), C2D(H2D),
C3D(H3D),
C6D(H6D), C13D(H13D), C14D(H14D), N1E(H1E), C2E(H2E), C3E(H3E),
C6E(H6E),
C13E(H13E), C14E(H14E), N1F(H1F), C2F(H2F), C3F(H3F), C6F(H6F), C13F(H13F),
C14F(H14F), N1Z(H1Z), C2Z(H2Z), C3Z(H3Z), C6Z(H6Z), C13Z(H13Z),
C14Z(H14Z),
N1G(H1G), C2G(H2G), C3G(H3G), C6G(H6G), C13G(H13G), C14G(H14G),
N1H(H1H),
C2H(H2H), C3H(H3H), C6H(H6H), C13H(H13H), C14H(H14H)

6.d Idealised Me refined as rotating group:

C15A(H15A,H15B,H15C), C16A(H16A,H16B,H16C), C15B(H15D,H15E,H15F),
C16B(H16D,
H16E,H16F), C15C(H15G,H15H,H15I), C16C(H16G,H16H,H16I),
C15D(H15J,H15K,H15L),
C16D(H16J,H16K,H16L), C15E(H15M,H15N,H15O), C16E(H16M,H16N,H16O),
C15F(H15P,
H15Q,H15R), C16F(H16P,H16Q,H16R), C15Z(H15S,H15T,H15U),
C16Z(H16S,H16T,H16U),
C15G(H15V,H15W,H15X), C16G(H16V,H16W,H16X), C15H(H15Y,H,HA),
C16H(H16Y,HB,HC)

This report has been created with Olex2, compiled on 2015.01.26 svn.r3151 for OlexSys.
Please [let us know](#) if there are any errors or if you would like to have additional features.